

**An investigation of the role of *C-terminal tensin-like*
(*Cten*) gene in colorectal cancer**

Abdulkader Albasri, MBBCh

Under supervision of

Professor Mohammad Ilyas

Thesis submitted to the University of Nottingham
for the degree of Doctor of Philosophy

August, 2010

Abstract

The C-terminal tensin-like (*Cten*) gene is a member of the tensin family and is localised at the cytoplasmic tail of β -integrin. It is involved in various biological events although the role of in the development of colorectal cancer (CRC) is uncertain. In order to study this, the expression of *Cten* during the development of CRC was initially evaluated using immunohistochemistry (IHC) on colorectal adenomas and carcinomas. Positive immunoreactivity for *Cten* was observed in 317/342 (92.6%) of CRC and 19/20 (90%) of colorectal adenoma. High *Cten* expression was significantly associated with advance Dukes stage ($p=0.001$), lymph node metastasis ($p<0.001$), extra-mural vascular invasion ($p=0.001$) and distant metastases ($p=0.008$). Survival analysis demonstrated that patients with high *Cten* expression had significantly shorter disease free survival (DFS) on univariate analysis ($p<0.001$) a trend towards *Cten* expression as an independent predictor of DFS on multivariate analysis ($p=0.071$). To further test the association with metastasis, the role of *Cten* in metastasis was tested by (a) intrasplenic injection of CRC cells stably transfected with Green Fluorescent Protein (GFP) tagged *Cten* into nude mice and (b) testing a series of primary CRCs and their metastases by IHC. Compared with control mice (injected with cells transfected with GFP empty vector), mice injected with cells expressing *Cten* developed larger tumours in the spleen ($p=0.03$) and liver ($p=0.05$). Compared with primary tumours, the metastatic deposits had a significantly higher frequency of nuclear localisation of *Cten* ($p=0.002$). To further investigate the potential role of *Cten* in metastasis, *in-vitro* models were used to investigate *Cten* function. Ectopic expression of *Cten* in the HCT116 CRC cell line (which expresses low levels of *Cten*) caused changes in cell morphology and increased cell motility (both migration and invasion). Conversely, the reciprocal *Cten* knock-down experiments in SW620 CRC cell line (which expresses high levels of *Cten*) resulted in inhibition of both cell migration and invasion. Since *Cten* is in complex with integrins at focal adhesions, its interaction with integrin-linked kinase (ILK), focal adhesion kinase (FAK) and CD24 were tested. *Cten* was shown to regulate ILK, FAK and CD24. Moreover, inhibition of CD24 after forced expression of *Cten* abrogated the *Cten*-mediated effects on both cell motility and protein levels of ILK and FAK. The studies were expanded and *Cten* expression was tested by IHC in another cancer model i.e. breast cancer (BC). Consistent with the data from CRC, increased *Cten* expression in BC was found to be associated with poor prognostic variables and shorter disease free survival.

In conclusion, *Cten* expression is associated with poor prognosis in CRC and BC. This may be consequent to an ability to enhance metastasis which is related to promotion of cell motility. The activities of *Cten* are probably consistent across different tumour models.

List of published papers

Albasri A, Seth R, Jackson D, Benhasouna A, Crook S, Nateri AS, Roger C and Ilyas M. C-terminal tensin-like (CTEN) is an oncogene which alters cell motility possibly through repression of E-cadherin in CRC. *Journal of Pathology*. 2009; 218(1):57-65.

Albasri A, Aleskandarany M, Benhasouna A, Powe DG, Ellis IO, Ilyas M, Andrew R. Green. CTEN (C-terminal tensin-like), a novel oncogene overexpressed in invasive breast carcinoma of poor prognosis. *Breast cancer Res Treat*. 2011; 126(1):47-54.

Abdulkader Albasri, Saleh Al-Ghamdi, Salih Ibrahim, Wakkas Fadhil, Julien Cachat, Yi-Chun Liao, Darryl Jackson, Dileep Lobo, Abed Zaitoun, Abdolrahman Nateri, Su Hao Lo, Sue Watson, Rajendra Kumari, Lindy Durrant, Karin Kindle and Mohammad Ilyas. Cten signals through Integrin-linked Kinase (ILK) and may promote metastasis in colorectal cancer. *Oncogene*. 2011 Feb 21. [Epub ahead of print]

Submitted papers

Abdulkader Albasri, Mohammed Aleskandarany, Wakkas Fadhil, John H Scholefield, Hany Habashy, Abed Zaitoun, Dileep N Lobo, Lindy G Durrant and Mohammad Ilyas. The prognostic significant of phosphorylated-focal adhesion kinase (Y397) expression in colorectal cancer.

Saleh Al-Ghamdi, Julien Cachat, **Abdulkader Albasri**, Mohammed A H Ahmed, Darryl Jackson, Abed Zaitoun, Naomi Guppy, William R. Otto, Malcolm R Alison, Karin B. Kindle and Mohammad Ilyas. Cten is oncogenic and promotes cell motility in pancreatic cancer.

Saleh Al-Ghamdi, **Abdulkader Albasri**, Julien Cachat, Salih Ibrahim, Darryl Jackson, Abdolrahman S. Nateri, Karin B. Kindle and Mohammad Ilyas. Cten is targeted by Kras signalling to regulate cell motility in the colon and pancreas.

Acknowledgements

I would like to take the opportunity to send my special thanks to everyone who has assisted me and paid efforts to make me able to reach the goal by completing this thesis.

Firstly, and before everyone I must express my deepest gratitude and thanks to **ALLAH** who protects and helps me during my life and blessing me with great family who backed me up during my study.

I want to express my sincere thanks and appreciation to my supervisor, Professor Mohammad Ilyas, for his support, advice, patience and time. I am proud to be one of his students and I hope that he is satisfied with me. Also I want to specially thank Dr Mohammed Aleskandarany for helping with the statistical analysis, Dr Su Hao Lo and Dr Yi-Chun Liao for kindly donating expression constructs and antibodies and Professor Adrian Robins for helping with the cell sorting and flow cytometry. I want to extend my deep thanks to Professor Ian Ellis and Professor Lindy Durrant for kindly providing tissue microarray sets of colorectal and breast cancer cases.

Finally, I would like to thank my colleagues and members of our group for continuous support and wise advices during the practical work.

Declaration

I declare that no part of this work has been presented, whether in the same or a different form, to this or any other university in support of an application for any degree. The studies described and presented in this thesis are the original work of the author except where otherwise stated in the text.

Abdulkader Albasri, MBBCh

TABLE OF CONTENTS

Chapter 1. Literature review	1
1.1 <i>Tensin</i> gene family	1
1.1.1 Introduction	1
1.1.2 Genomic structure	2
1.1.3 Protein structure	4
1.1.4 Tissue expression	9
1.1.5 Biological function	10
1.1.6 Role in human tumours	14
1.1.7 Medical applications	16
1.2 Focal adhesions	18
1.3 Focal adhesion molecules	21
1.3.1 Integrins	21
1.3.2 FAK	22
1.3.3 ILK	22
1.3.4 CD24	32
1.4 Colorectal Cancer	40
Chapter 2. Aims of the thesis	42
Chapter 3. Materials and methods	44
3.1 Cell culture and transfection	44
3.2 Gene knock-down	44
3.3 Forced gene expression	45
3.4 RNA extraction	46
3.5 Complementary DNA (cDNA) preparation and reverse transcriptase	47
3.6 Quantitative real time polymerase chain reaction (Q-RT-PCR)	47
3.7 Polymerase chain reaction (PCR)	48
3.8 Agarose gel electrophoresis	49
3.9 DNA extraction from agarose gel	50
3.10 DNA/RNA quantification by spectrophotometry	50
3.11 TA cloning and ligation of plasmids vectors and inserts	50
3.12 Plasmid transfection	51
3.13 Plasmid Miniprep and Midiprep production	52
3.14 Glycerol stock preparation of bacterial cultures	53
3.15 Enzyme restriction digests	54
3.16 Cloning <i>Cten</i> coding sequence into an expression vector	54
3.17 Sequencing	55
3.18 Protein extraction and quantitation	55
3.19 Western Blotting (WB)	56
3.20 Epifluorescence Microscopy	58
3.21 Proliferation Assay	58
3.22 Staurosporine induced apoptosis	58
3.23 Cell Migration / Invasion Assays	59
3.24 Construction of Tissue Micro Arrays (TMA) sets	60
3.25 Immunohistochemistry (IHC)	61
3.26 <i>In vivo</i> tumourigenesis study	63
3.27 Statistical analysis	65
Results	66
Chapter 4. Evaluation of expression of <i>Cten</i> in benign colorectal diseases and CRC	66
4.1 Introduction	66
4.2 Evaluation of expression of <i>Cten</i> in non-neoplastic colorectal diseases (normal and IBDs)	67
4.3 Evaluation of expression of <i>Cten</i> in benign colorectal diseases	69
4.4 Evaluation of expression and role of <i>Cten</i> in CRC	70
4.4.1 <i>Cten</i> expression in CRC	70
4.4.2 Association of <i>Cten</i> cytoplasmic expression with clinicopathological parameters	72
4.4.3 Association of <i>Cten</i> cytoplasmic expression with patients' outcome	74
4.4.4 Association of <i>Cten</i> nuclear expression with clinicopathological parameters and patient outcome	76
4.5 Evaluation of expression of <i>Cten</i> in metastatic tumours	77
4.6 Discussion	79

Chapter 5. Evaluation of the function of <i>Cten</i> in CRC	82
5.1 Introduction.....	82
5.2 Quantification of <i>Cten</i> in CRC cell lines	83
5.2.1 Cloning of hypoxanthine-guanine phosphoribosyltransferase (HPRT) into pCR2.1 vector ..	83
5.2.2 Cloning of <i>Cten</i> into pCR2.1 vector	85
5.2.3 Evaluating the <i>HPRT</i> mRNA expression in CRC cell lines.....	88
5.2.4 Evaluating the <i>Cten</i> mRNA expression in CRC cell lines	91
5.3 Establishment of stable <i>Cten</i> -stably expressing cell lines	96
5.4 Role of <i>Cten</i> in regulating cell proliferation	98
5.5 Role of <i>Cten</i> in resisting apoptotic stress	100
5.6 Role of <i>Cten</i> in regulating cell motility.....	102
5.6.1 Effects of <i>Cten</i> forced expression on cell migration and invasion.....	102
5.6.2 Effects of <i>Cten</i> knock-down on cell migration and invasion	107
5.7 Role of <i>Cten</i> in metastasis.....	111
5.8 Discussion.....	115
Chapter 6. Evaluation of <i>Cten</i> targets in CRC.....	118
6.1 Introduction.....	118
6.2 Cloning of <i>Cten</i> into an expression vector	119
6.3 <i>Cten</i> and E-cadherin (<i>CDH1</i>) expression.....	126
6.4 <i>Cten</i> and ILK (ILK) expression	129
6.5 <i>Cten</i> and FAK (FAK) expression.....	131
6.5.1 Evaluation of expression and role of FAK in CRC.....	131
6.5.1.1 P-FAK expression in CRC cases.....	132
6.5.1.2 Association of P-FAK expression with clinicopathological parameters	134
6.5.1.3 Association of P-FAK expression with patients' outcome.....	136
6.5.2 <i>Cten</i> and FAK interaction	139
6.6 <i>Cten</i> and CD24 expression.....	142
6.7 Analysis of <i>Cten</i> and P-FAK expression in metastatic CRC	147
6.8 Discussion.....	149
Chapter 7. <i>Cten</i> expression in other tumour types.....	154
7.1 Introduction.....	154
7.2 Evaluating the expression and the role of <i>Cten</i> in breast cancer.....	155
7.2.1 <i>Cten</i> expression in breast cancer.....	155
7.2.2 Association of <i>Cten</i> expression with clinicopathological parameters.....	157
7.2.3 Association of <i>Cten</i> expression with patients' outcome	160
7.3 Evaluating the expression of <i>Cten</i> in pancreatic cancer.....	163
7.4 Discussion.....	165
Chapter 8. General discussion and future outlook	169
References	181
Chapter 9. Appendix.....	198

LIST OF TABLES

Table 1. CRC cell lines and their characteristics	199
Table 2. Characterisation of PCR primers.	47
Table 3. BC patient and tumour characteristics (n = 1,409)	201
Table 4. CRC patient and tumour characteristics (n = 462).....	202
Table 5. Clinical and pathological correlates of <i>Cten</i> expression.	73
Table 6. Cox-proportional hazard analysis for predictors of DFS and <i>Cten</i> expression.	74
Table 7. Expression of <i>Cten</i> in CRC cell lines assessed by Q-RT-PCR.....	93
Table 8. Association of P-FAK cytoplasmic and nuclear expressions with clinicopathological features	135
Table 9. Cox-proportional hazard analysis for predictors of DFS and P-FAK cytoplasmic and nuclear expression.	138
Table 10. Association between <i>Cten</i> expression and P-FAK expression in hepatic metastases cases...	148
Table 11. Correlations between <i>Cten</i> expression and clinicopathological parameters.	158
Table 12. Correlations between <i>Cten</i> expression and other biomarkers.	159
Table 13. Cox-proportional hazard analysis for predictors of BCSS, DFI and <i>Cten</i> expression.	162

LIST OF FIGURES

Figure 1. Schematic structure of tensin.	6
Figure 2. Alignment of functional domains of tensin family members.	6
Figure 3. Alignment of amino acids sequences of tensin family members.....	7
Figure 4. <i>Cten</i> mRNA expression in the human total RNA master panel.	9
Figure 5. A model representing the role of TNS3- <i>Cten</i> expression switch in promoting EGF-induced cell migration.	11
Figure 6. Schematic structure of FAK.	25
Figure 7. Schematic illustration of binding interactions between β -integrins, FAK, Src and p130Cas proteins.	27
Figure 8. Schematic diagram of FAK downstream signalling pathways.	31
Figure 9. Schematic structure of ILK.	34
Figure 10. Schematic diagram of ILK downstream signalling pathways.	37
Figure 11. <i>Cten</i> immunostaining in normal colonic tissue.	67
Figure 12. <i>Cten</i> immunostaining in non-neoplastic colorectal diseases.	68
Figure 13. <i>Cten</i> immunostaining in colorectal adenomas.	69
Figure 14. <i>Cten</i> protein expression in CRC.	71
Figure 15. <i>Cten</i> immunostaining in CRC.	71
Figure 16. Kaplan-Meier plot for DFS in relation to expression of cytoplasmic <i>Cten</i>	74
Figure 17. Kaplan-Meier plot for DFS in relation to expression of nuclear <i>Cten</i>	76
Figure 18. <i>Cten</i> protein expression in primary tumour samples and their corresponding liver metastasis.	78
Figure 19. HPRT PCR product amplification for cloning into pCR2.1 vector.	78
Figure 20. Real time PCR dissociation curves of pCR2.1-HPRT cloning samples.	84
Figure 21. <i>Cten</i> PCR product amplification for cloning into pCR2.1 vector.	84
Figure 22. The map of the linearised vector, pCR2.1.	85
Figure 23. EcoRI enzyme restriction digests of pCR2.1- <i>Cten</i> plasmid in tested samples.	86
Figure 24. <i>Cten</i> PCR product amplification using pCR2.1- <i>Cten</i> plasmid.	86
Figure 25. HPRT Q-RT-PCR standard curve of 29 human CRC cell lines.	87
Figure 26. HPRT Q-RT-PCR amplification plots of 16 human CRC cell lines.	88
Figure 27. HPRT Q-RT-PCR amplification plots of 13 human CRC cell lines.	89
Figure 28. HPRT Q-RT-PCR dissociation curves of 29 human CRC cell lines.	90
Figure 29. <i>Cten</i> Q-RT-PCR standard curve of 29 human CRC cell lines.	91
Figure 30. <i>Cten</i> Q-RT-PCR amplification plots of 9 human CRC cell lines.	92
Figure 31. <i>Cten</i> Q-RT-PCR amplification plots of 20 human CRC cell lines.	93
Figure 32. <i>Cten</i> Q-RT-PCR dissociation curves of 29 human CRC cell lines.	97
Figure 33. Bar chart of <i>Cten</i> levels in CRC cell lines as measured by Q-RT-PCR.	97
Figure 34. Immunoblotting for <i>Cten</i> using whole cell extracts from HCT116-GFP or HCT116-GFP- <i>Cten</i>	99
Figure 35. SW480 cell line FACS sorting.	97
Figure 36. Effect of <i>Cten</i> forced expression on cell proliferation.	99
Figure 37. <i>Cten</i> conferred resistance to staurosporine-induced apoptosis in both SW480 and HCT116 cells.	105
Figure 38. Epifluorescence microscopy to assess the localisation of GFP and <i>Cten</i> in transfected cells.	105
Figure 39. Effect of <i>Cten</i> forced expression on cell migration using a transwell migration assay.	106
Figure 40. Effect of <i>Cten</i> forced expression on cell migration using a cell wounding assay.	108
Figure 41. Effect of <i>Cten</i> forced expression on cell invasion.	110
Figure 42. <i>Cten</i> knock-down in SW620 cells.	110
Figure 43. Effect of <i>Cten</i> knock-down on cell migration.	112
Figure 44. Effect of <i>Cten</i> knock-down on cell invasion.	113
Figure 45. Average intra-splenic tumour volume from the mice injected with HCT116-GFP or HCT116-GFP- <i>Cten</i> cells.	114
Figure 46. Average liver tumour volume from the mice injected with HCT116-GFP or HCT116-GFP- <i>Cten</i> cells.	114
Figure 47. Kaplan-Meier plot for survival in mice injected with HCT116-GFP or HCT116-GFP- <i>Cten</i> cells.	120
Figure 48. pCR2.1 vector map.	121
Figure 49. Gel purification and sequential digestion of pCR2.1- <i>Cten</i> plasmid.	122

Figure 50. pCMV-Tag3B expression vector map.....	123
Figure 51. Gel purification and sequential digestion of pCMV-Tag3B vector.....	123
Figure 52. Diagram shows XhoI and SacI enzymes restriction sites in pCMVTag3B-Cten plasmid....	125
Figure 53. Agarose gel of potential pCMVTag3B-Cten clones after analytical enzyme digestions.....	127
Figure 54. Agarose gel of potential pCMVTag3B-Cten clones after analytical digestion with SacI and XhoI enzymes.....	127
Figure 55. Cten and E-cadherin protein expression.....	128
Figure 56. Cten and <i>CDHI</i> mRNA expression.....	130
Figure 57. Effect of Cten knock-down on E-cadherin protein expression.....	133
Figure 58. Effect of Cten forced expression and knock-down on ILK protein expression.....	137
Figure 59. P-FAK protein expression in CRC.....	140
Figure 60. Kaplan-Meier plot for DFS in relation to expression of nuclear and cytoplasmic P-FAK...	141
Figure 61. Effect of Cten forced expression on FAK and P-FAK protein expression levels.....	143
Figure 62. Effect of Cten knock-down on FAK and P-FAK protein expression levels.....	145
Figure 63. Cten and CD24 protein expression.....	146
Figure 64. Cten functional relationship with CD24 protein.....	148
Figure 65. CD24 involvement in Cten signalling pathway.	153
Figure 66. P-FAK protein expression in primary tumour samples and their corresponding liver metastasis.....	156
Figure 67. A model representing the role of Cten in cancer metastasis.....	161
Figure 68. Cten protein expression in normal and BC TMA cores.	164
Figure 69. Kaplan-Meier plot for BCSS and DFI in relation to expression of cytoplasmic Cten.....	164
Figure 70. Cten immunostaining non-neoplastic pancreatic diseases and pancreatic cancer.	164

LIST OF ABBREVIATIONS

Tensin1 (TNS1)
Tensin2 (TNS2)
Tensin3 (TNS3)
C-terminal tensin-like (*Cten*)
Focal adhesion kinase (FAK)
Phosphatidylinositol 3-kinase (PI3K)
Crk-associated substrate (p130Cas)
Extracellular matrix (ECM)
Platelet-derived growth factor (PDGF)
Actin-binding domain (ABD)
Src-homology 2 (SH2)
Phosphotyrosine-binding (PTB)
Cyclin G associated kinase (GAK)
Putative transmembrane tyrosine phosphatase (TPTE)
Mutated in multiple advanced cancers1 (MMAC1)
Focal adhesion-binding (FAB)
Protein kinase C (PKC)
Actin-capping domain (ACD)
Knockout (KO)
ICR-derived glomerulonephritis (ICGN)
Epidermal growth factor (EGF)
Wild-type (WT)
C-Jun N-terminal kinase (JNK)
Mitogen-activated protein kinase (MAPK)
Deleted in liver cancer 1 (DLC1)
Hepatocellular carcinoma (HCC)
Rho GTPases-activating protein (RhoGAP)
Immunohistochemistry (IHC)
Silver–Russell syndrome (SRS)
Maternal uniparental disomy (UPD)
Inflammatory breast cancer (IBC)
Epidermal growth factor receptor (EGFR)
Epidermal growth factor receptor phospholoration (P-EGFR)
Phosphatidylinositol–4,5– biphosphate (PIP2)
Receptor tyrosine kinases (RTKs)
Vascular endothelial growth factor receptor 2 (VEGFR2)
Protein tyrosine kinase (PTK)
4.1, ezrin, radixin, and moesin (FERM)

Focal adhesion targeting (FAT)
Src-homology 3 (SH3)
GTPase regulator associated with FAK (Graf)
Arf GTPase-activating protein (ASAP1)
Growth factor receptor bound protein 7 (Grb7)
Phospholipase C γ (PLC γ)
Growth factor receptor bound protein 2 (Grb2)
Son of sevenless (SOS)
Apoptosis proteins (IAPs)
FAK interacting protein 200 kDa (FIP200)
Epithelial-to-mesenchymal transition (EMT)
Extracellular signal regulated kinase 2 (ERK-2)
Mitogen activated protein kinase kinase 1 (MEK1)
Vascular endothelial growth factor (VEGF)
Integrin-linked kinase (ILK)
Ankyrin repeats (ANK)
Particularly interesting Cys-His-rich protein (PINCH)
NCK adaptor protein-2 (Nck2)
Pleckstrin homology (PH)
Phosphatidylinositol (3, 4, 5)-trisphosphate (PIP3)
Nuclear factor B (NF- κ B)
Activator protein 1 (AP1)
Glycogen synthase kinase 3 (GSK-3)
PAK-interactive exchange factor (PIX)
Guanine-nucleotide exchange factor (GEF)
Myosin light chain (MLC)
Mammalian target of rapamycin (mTOR)
Hypoxia inducible factor-1 alpha (HIF1 α)
ILK-associated protein (ILKAP)
Phosphatase and tensin homolog deleted on chromosome 10 (PTEN)
Colorectal cancer (CRC)
Inflammatory bowel disease (IBD)
Quantitative real time polymerase chain reaction (Q-RT-PCR)
Phosphorylated FAK (P-FAK)
Breast cancer (BC)
Tissue microarray (TMA)
Dulbecco's modified eagle medium (DMEM)
Foetal calf serum (FCS)
Phosphate buffered saline (PBS)
RNA interference (RNAi)

Post-transcriptional gene silencing (PTGS)
Double stranded RNA (dsRNA)
Short interfering RNAs (siRNAs)
RNA-induced silencing complex (RISC)
Green fluorescent protein (GFP)
Fluorescence associated cell sorting (FACS)
Complementary DNA (cDNA)
Cadherin-1(CDH1)
Homo sapiens hypoxanthine phosphoribosyltransferase (HPRT)
Molecular biology core facilities (MBCF)
Polymerase chain reaction (PCR)
Tris Borate EDTA (TBE)
5-bromo-4-chloro-3-indolyl- β -D-galactopyranoside (X-GAL)
Isopropyl β -D-1-thiogalactopyranoside (IPTG)
Bovine serum albumin (BSA)
Paraformaldehyde (PFA)
Charge coupled device camera (CCD)
Lymph nodes (LN)
Nottingham prognostic index (NPI)
Vascular invasion (VI)
Distant metastases (DM)
Breast cancer specific survival (BCSS)
Disease-free interval (DFI)
Estrogen receptor (ER)
Progesterone receptor (PR)
Androgen receptor (AR)
Cytokeratins (CKs)
Normal swine serum (NSS)
Diaminobenzidine (DAB)
UK Co-ordinating Committee for Cancer Research (UKCCCR)
Nanozoomer digital pathology image (NDPI)
Crohn's disease (CD)
Ulcerative colitis (UC)
Adenomatous polyps (AP)
Disease-free survival (DFS)
Messenger RNA (mRNA)
Glycosyl-phosphatidylinositol (GPI)
Phosphorylated-Akt (P-Akt)
Human epidermal growth factor receptor 2 (HER2)
Mindbomb homolog 1 (MIB1)

Breast cancer1, early onset (BRCA1)

Immunoprecipitation (IP)

Two-dimensional gel electrophoresis (2D PAGE)

LITERATURE REVIEW

Chapter 1. Literature review

1.1 *Tensin* gene family

1.1.1 Introduction

The *tensin* gene family consists of four members: *tensin1* (*TNS1*), *tensin2* (*TNS2*), *tensin3* (*TNS3*) and *C-terminal tensin-like* (*Cten*) encoding proteins which are localised to the cytoplasmic tail of β integrins at focal adhesions (1). These genes are highly homologous and encode multi-domain proteins that can bind to several structural and signalling molecules including vinculin, paxillin, Src, focal adhesion kinase (FAK), phosphatidylinositol 3-kinase (PI3K) and Crk-associated substrate (p130Cas). Tensin binds to the actin cytoskeleton at multiple sites, enabling tensin both to cap the barbed ends and to cross-link actin stress fibers (2, 3). In addition, it is phosphorylated in response to several factors, such as extracellular matrix (ECM), platelet-derived growth factor (PDGF), angiotensin, thrombin, and by certain oncogenes like v-Src or BCR/ABL on its tyrosine, serine and threonine residues (4-7). Tensin appears to be critical in controlling cell adhesion and migration, but is also thought to participate in regulating other crucial biological events such as proliferation, differentiation and apoptosis (8). Therefore, it is believed that tensin can be an essential component linking the ECM to the actin cytoskeleton and thereby mediating signalling for cell shape and motility associated with cytoskeletal reorganisation (9).

1.1.2 Genomic structure

A search of the available human genomic sequence databases using the human *TNS1* (OMIM ref. no. 600076) cDNA shows that the length of human *TNS1* is about 150 kb and is localised at 2q35-q36. The total composed cDNA is 10,276 bp which encodes a 1,735 amino acid protein. It has 33 exons; the putative start codon is in exon 6, whereas the stop codon is in exon 33. Exon 33 is the largest exon with 4,815 bp, but only 145 bp comprise the coding sequence, whereas the rest is the 3' untranslated region. Exon 21 is the smallest exon with 24 bp (10).

Compared to *TNS1*, *TNS2* gene (OMIM ref. no. 607717) is shorter, it is about 12,5 kb in length and maps to chromosome 12. The total composed cDNA is 5,009 bp which encodes 1,285 amino acid protein. It has 29 exons; the putative start codon is in exon 7, whereas stop codon is in exon 28. Exon 18 is the largest exon with 1,212 bp, while exon 28 is the smallest exon with 30 bp. Exons 5-15 in *TNS2* are similar in size to exons 6-16 in *TNS1*. These exons encode the actin-binding domain (ABD). In addition, Exons 21-28 in *TNS2* are identical in size to exons 25-32 in *TNS1*. These exons encode the Src-homology 2 (SH2) and phosphotyrosine-binding (PTB) domains. These conserved genomic structures of human *TNS1* and *TNS2* confirm that they represent a single gene family (10).

The *TNS3* gene (OMIM ref. no. 606825) is about 264 kb in length and is localised at 7p12.3. It is composed of 4,415 bp cDNA which encode 1,445 amino acid protein, and has 31 exons. The putative start codon is in exon 6, whereas stop codon is in exon 31. Exon 31 is the largest exon with 3,067 bp, but only 145 bp comprise the coding sequence, whereas the rest is the 3' untranslated region. Exon 30 is the smallest exon

with 27 bp. In contrast to *TNS1* and *TNS2*, exons 6-15 (encoding the ABD) and exons 23-30 (encoding the SH2 and PTB domains) in *TNS3* are almost identical, supporting the idea that *TNS3* is related to the *tensin* gene family (11).

The *Cten* gene (OMIM ref. no. 608385) is about 21 kb in length and is localised at 17q21.2. It is composed of 4,090 bp cDNA which encode 715 amino acid protein, and has 13 exons. The putative start codon is in exon 2, whereas stop codon is in exon 13. Exon 13 is the largest exon with 1,900 bp, but only 141 bp comprise the coding sequence, whereas the rest is the 3' untranslated region. Exon 12 is the smallest exon with 27 bp. Exons 5–12 encode the SH2 and PTB domains are identical to other *tensin* genes, confirming the fact that they represent a single gene family (8).

1.1.3 Protein structure

Generally, tensin proteins are composed of three regions that are each involved in mediating protein-protein interactions, the C-terminal regions, middle and the N-terminal regions (Figure 1) (3, 5).

The C-terminus of tensin contains an SH2 domain, allowing tensin to interact with certain tyrosine-phosphorylated proteins, such as PI3K, FAK and p130Cas (5, 12). This binding is critical for tensin-mediated increased cell migration (13). The C-terminus contains a PTB domain, which allows tensin to bind to the NPXY motif on the cytoplasmic tail of β integrin (Figure 1) (14).

The N-terminus of tensin contains an ABD, which allows tensin to interact with actin filaments (Figure 1) (3). It also contains sequences which share homology with auxilin, a coat protein of brain clathrin coated vesicles, cyclin G associated kinase (GAK), phosphatase and tensin homolog deleted on chromosome 10 (PTEN), putative transmembrane tyrosine phosphatase (TPTE) and mutated in multiple advanced cancers1 (MMAC1). However, the significance of this sequence similarity is not clear, because none of these molecules bind to actin filaments (15-19).

The C-terminal and the N-terminal regions of tensin also contain two focal adhesion-binding (FAB) domains which seem to be crucial for tensin-mediated biological effects, such as cell adhesion and migration (Figure 1) (13).

Analysis of the cDNA and genomic sequences of the tensin family genes shows an extensive homology within the tensin members at their amino and carboxy terminals.

The arrangement and size of exons encoding for the functional domains, such as ABD, SH2 and PTB domains of TNS1, TNS2, TNS3 and *Cten* are almost identical, indicating that these domains have been conserved through evolution (Figure 2, 3) (10, 11). However, during evolution *Cten* has lost its actin-binding ability (8). In contrast to other tensin molecules, TNS2 is the only tensin family member harbouring a protein kinase C (PKC) domain at its amino terminus (Figure 2) (20).

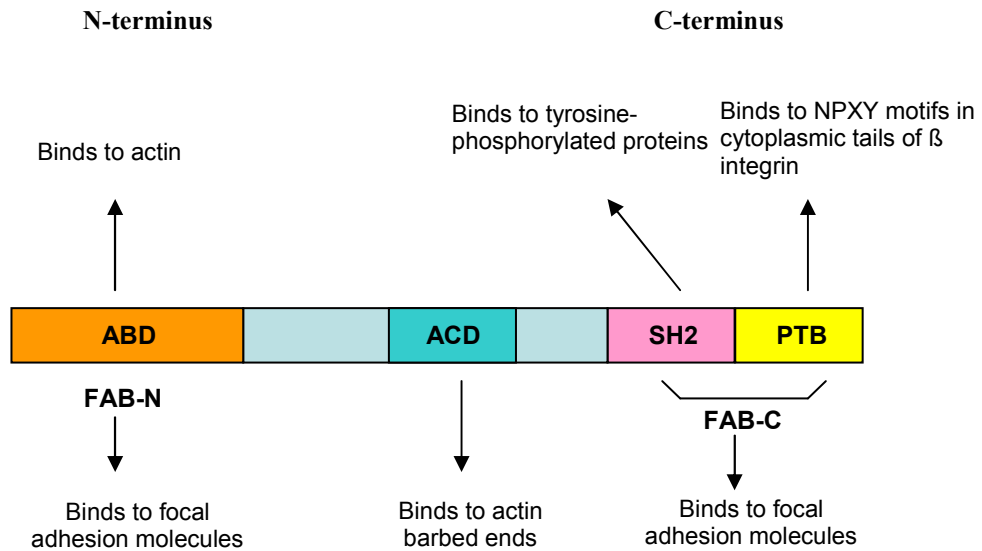


Figure 1. Schematic structure of tensin. The C-terminus of tensin contains SH2 and PTB domains, allowing tensin to interact with tyrosine-phosphorylated proteins and β integrin respectively. Tensin can also bind actin via ABD present in its N-terminus. The central region of tensin contains actin-capping domain (ACD), which allows tensin to regulate the actin polymerization rate. Two FAB domains are present in the C-terminal and the N-terminal regions, and these involved in mediating binding of tensin to other focal adhesion molecules.

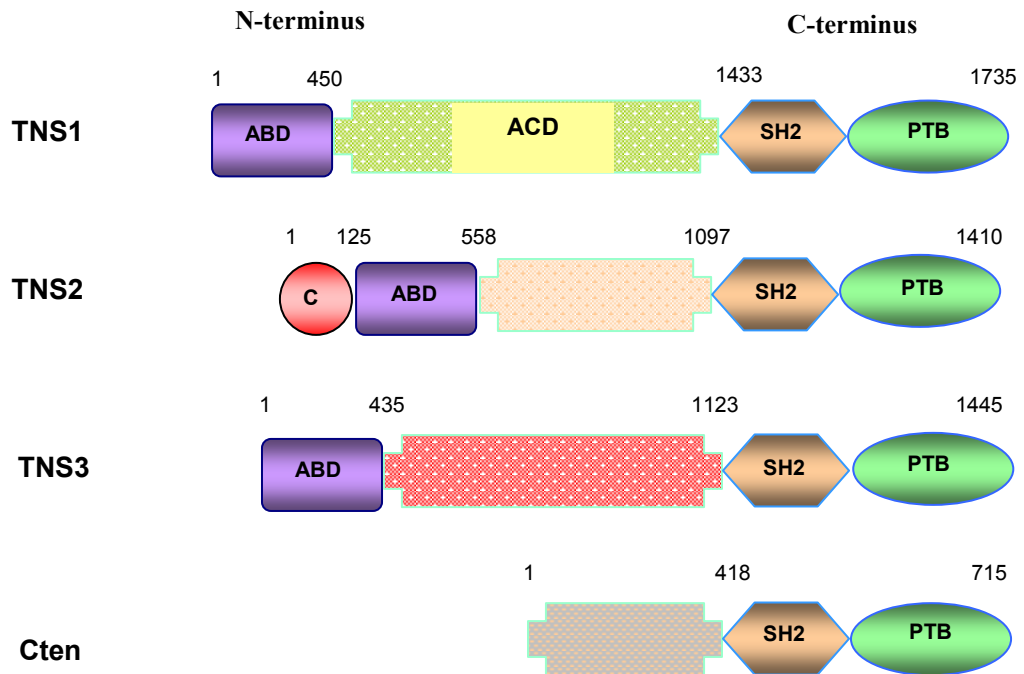


Figure 2. Alignment of functional domains of tensin family members. TNS1, TNS2, TNS3 and *cten* are highly conserved at C- and N-terminal regions although the central regions are very diverse. TNS2 is the only tensin family member contains PKC domain at its amino terminus.

The actin-binding domains

TNS1 MSVSRTMEDSCELDLVYVTERIIAVSFSTANEEENFRSNLREVAQMLKSKHGNYLLFNLSERRPDI TK
TNS2 MERRWDLDTYVTERILAAAFPARPDEQRHRGHLRELAHVLSQSKHRDKYLLFNLSSEKRHDLTR
TNS3 MEEGHGLDLTYITERIIAVSFPAAGCSEESYLHNLQEVTRMLKSKHGDNYLVNLSEKRYDLTK

TNS1 LHAKVLEFGWPDLHTPALEKICSIICKAMDTWLNADPHNVVVLHNKGNRGRIGVVI AAYMHYSN
TNS2 LNPKVQDFGWPELHAPPLDKLCSICKAMETWLSADPQHVVVLYCKGNKKGKLGIVSAYMHYSK
TNS3 LNPKIMDVGWPELHAPPLDKMCTICKAQESWLN SNLQHVVV IHCRRGGKGRIGVVISSYMHFTN

TNS1 ISASADQALDRFAMKRFYEDKIVPIGQPSQRRYVHYFSGLLSGS IKMNNKPLFLLHVMHGIP
TNS2 ISAGADQALATLTMRFKCEDKVATELQPSQRRYISYFSGLLSGSIRMNSSPLFLHYVLI PMLP
TNS3 VSASADQALDRFAMKKFYDDKVSALMQPSQKRYVQFLSGLLSGSVKMNASPLFLHFVILHGTP

TNS1 NFESKGGCRPFLRIYQAMQPVYTSIGIYNI PGDSQTSVCITIEPGLLLKGDILLKCYHKKFRSP
TNS2 AFEPGTGFQPFLLKIYQSMQLVYTSIGVYHIAGPGPQQLCISLEPALLLKGDVMVTCYHKGGRT
TNS3 NFD TGGVCRPFLKLYQAMQPVYTSIGIYNVGPENPSRICIVIEPAQLLKGDVMVKCYHKKYRSA

TNS1 ARDVI FRVQFHTCAI HDLGVVFGKEDLDDAFKDDRFPEYGVKVEFVFSYGP EKI QGMEHLENGP
TNS2 DRTL VFRVQFHTCTIHGPQLTFPKDQLDEAWTDERFPFQASVEFVFSSSPEKIKGSTPR-NDP
TNS3 TRDVI FRLQFHTGAVQGYGLVFGKEDLDNASKDDRFPDYGVKVELVFSATPEKI QGSEHLYNDH

TNS1 SVSVDYNTSDPLIRWDSYDNFSGHRDDGMEEVVGHTQGPLDGSLYA
TNS2 SVSVDYNTTEPAVRWDSYENFNQHHEDSVDGSLTHTRGPLDGS PYA
TNS3 GVIVDYNTTDPLIRWDSYENLSADG-----EVLHTQGPVDGS LYA

The SH2 domains

TNS1 WYKPEISREQAIALLKDQEPGAFIIRDSSHFRGAYGLAMKVSSPPPTIMQQNKK-GDMTHELV
TNS2 WYKPHLSRDQAIALLKDKDPGAF LIRDSSHFRGAYGLALKVATPPPSAQ PWK---GDPVEQLV
TNS3 WYKADISREQAIAMLKDKPEGSFIVRSSHFRGAYGLAMKVATPPPSVLQLNKKAGDLANELV
TNS4 WFKPNITREQAIELLRKEEPGAFVIRDSSSYRGSFGLALKVQEV PASAQSRP---GEDSNDLI

TNS1 RHFLIETGPRGVKLGCPNEPNFGSLSALVYQHSIIP
TNS2 RHFLIETGPKGVKIKGCPSEPYFGSLSALVSQHSISP
TNS3 RHFLIECTPKGVR LKGSNEPYFGSLTALVCQHSITP
TNS4 RHFLIESSAKGVHLKGADEEPYFGSLSAFVCQHSIMA

The PTB domains

TNS1 QGAACNVLFVNSVDMESLTGPQAI SKATSETLAADPTPAATIVHFKVSAQGITLTDNQRKLLFF
TNS2 QGAACS VLYLTSVETESLTGPQAVARASSAALSCSPRPTPAVVHFKVSAQGITLTDNQRKLLFF
TNS3 QGAACNVWYLNSEVEMESLTGHQAIQKALSITLVQEP PPVSTVVHFKVSAQGITLTDNQRKLLFF
TNS4 KSAGCHTLYLSVSVETLTGALAVQKAISTTFERDILPTPTVVHFKVTEQGITLTDVQRKVFF

TNS1 RRHYPLNTVTFCDLDPQERKWMKTEGGAPAKLFGFVARKQGSTTDNACHLFAELDPNQPASAI
TNS2 RRHYPVNSITFSSTDPQDRRTN-PDGTTSKIFGFVAKKPGSPWENVCHLFAELDPDPAGAI
TNS3 RRHYPVNSVIFCALDPQDRKWIK--DGPSSKVFVARKQGSATDNVCHLFAEHDPEQPASAI
TNS4 RRHYPLTTLRFCGMDPEQRKWQK--YCKPSWIFGFVAKSQTEPQENVCHLFAEYDMVQPASQV

TNS1 VNFVSKVMLNAGQKR
TNS2 VTFITKVLGQ-RK
TNS3 VNFVSKVMIGSPKKVN
TNS4 IGLVTALLQDAERM

Figure 3. Alignment of amino acids sequences of tensin family members. Alignment of human tensins amino acids sequences showing conserved functional ABD, SH2 and PTB domains. Red colour indicates similar residues. Non-similar residues are shown in black.

Despite the high sequence similarities at the N and C-terminal regions of tensin family proteins, the center regions show no sequence homology. The central region of TNS1 contains an insertin or actin-capping domain (ACD), which allows TNS1 to regulate actin polymerisation through capping the barbed ends of actin filaments and facilitating the cross-linking of actin filament processes (3). In comparison, TNS2 is lacking this sequence, so, it is not able to interfere with the actin polymerisation process (3). However, its central region is very rich in proline residues, which provides potential binding sites for protein-protein interaction modules Src-homology 3 (SH3) and WW domains (21). This shows that each tensin member may have an additional unique biological role.

1.1.4 Tissue expression

TNS1 is broadly expressed in a wide variety of human tissues, including heart, lung, skeletal muscle, small intestine, colon, liver, kidney, prostate, testis, and ovaries. In contrast, very low expression was observed in thymus, brain and circulating leukocytes (22). The expression pattern of TNS2 is very similar to that of TNS1 (10). This similarity of expression may indicate a potential functional overlap between these tensin family members. In contrast, TNS3 is expressed at high levels in thyroid, kidney and placenta. Very low expression of TNS3 was reported in lung, skeletal muscle, brain, pancreas, liver and heart (11, 23). *Cten* messenger RNA (mRNA) expression in normal tissues was evaluated by K. Sakashita *et al* using the human total RNA master panel and revealed that *Cten* is expressed at high levels in prostate, oesophagus, breast and salivary glands. Moderate *Cten* expression was found in the thyroid and trachea. In contrast, very low expression was reported in colon, lung, small intestine, spleen, kidney, stomach and testis (Figure 4) (24).

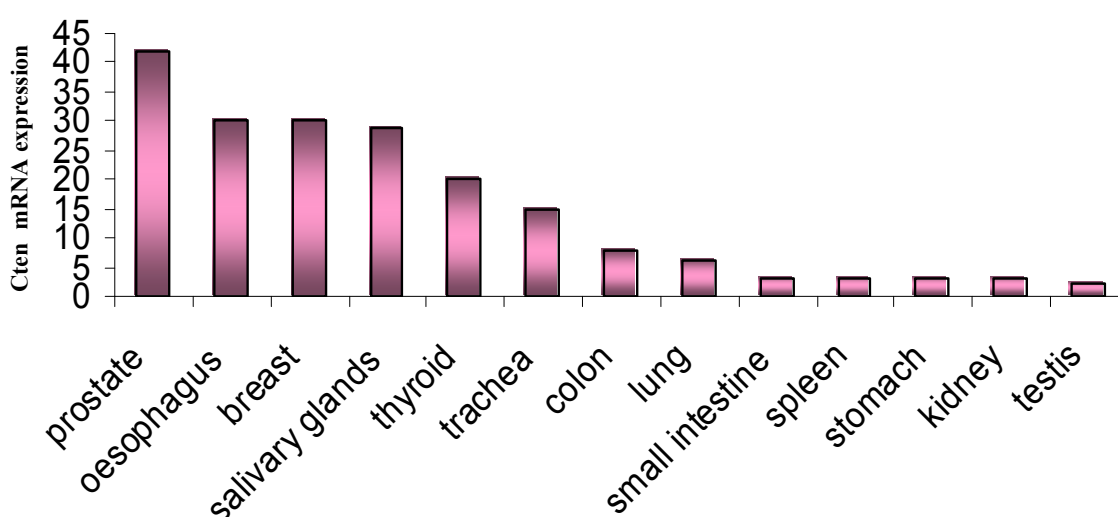


Figure 4. *Cten* mRNA expression in the human total RNA master panel. Evaluation of *Cten* expression in the human total RNA master panel using quantitative real time PCR (Q-RT-PCR) revealed that *Cten* shows different expression patterns for different organs, contributing to adverse biological behaviors in at least some types (24).

1.1.5 Biological function

Focal adhesion localisation is the common feature of all tensin members. Given the extensive homology the tensin family genes share at their C- and N-terminal regions, where the functional domains such as PTB, SH2 and ABD domains are encoded, it is likely that they may have a similar biological role (10). Knockout (KO) mice for TNS1 and TNS3 show cystic kidney disease and renal failure (25, 26). Furthermore, a frameshift mutation of the TNS2 gene in ICR-derived glomerulonephritis (ICGN) mice, a model for human idiopathic nephrotic syndrome, was shown to be responsible for morphologic changes of the glomerulus and proteinuria consistent with features of nephrotic syndrome (27). These data clearly suggest that TNS1, TNS2 and TNS3 expressions are necessary for maintaining normal renal function (26). In addition, KO of TNS3 in mice results in growth retardation and post-natal lethality accompanied with a combination of developmental defects in the small intestine, lung and bone and indicates that TNS3 might regulate normal growth and is essential for normal development and functions of the small intestine, lung and bone (25).

It has been reported that the protein binding activity of the SH2 domain is a critical factor for regulating TNS1-mediated cell migration effects (28). Another important factor is the focal adhesion localisation of TNS1 since non-focal adhesion-localised mutant TNS1 has no effect on cell migration. Isolated fibroblasts from TNS1-KO mice as well as normal mouse embryos were analysed and showed that TNS1-KO cells migrated significantly slower than their normal counterparts (10). Functional analysis also demonstrates that ectopic expression of TNS2 resulted in promoting cell migration on fibronectin in a cell migration assay (10). In comparison with other tensin members, TNS3 up-regulation in the normal human mammary cell line, MCF10A was

coupled to more cytoskeletal stability and consequently, rendering the cell less motile (29). Conversely, stimulation by epidermal growth factor (EGF) appears to induce expression of *Cten*, thereby causing a switch from TNS3 to *Cten* at focal adhesions. This stimulates migration through disruption of the link between integrins and cortical actin fibres (Figure 5) (30).

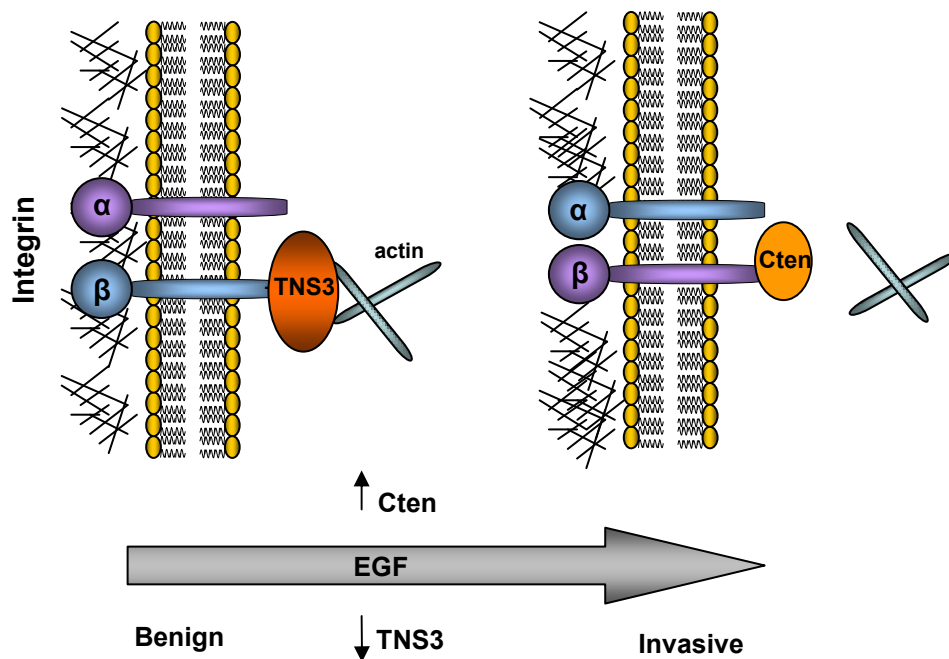


Figure 5. A model representing the role of TNS3-Cten expression switch in promoting EGF-induced cell migration. In normal epithelial cell, the integrity of focal adhesions was maintained, at least in part, via TNS3 which binds integrin through its PTB and cytoskeletal actin filaments through its ABD domain. Upon EGF stimulation, *Cten* is up-regulated and competes with TNS3 at the cytoplasmic site of β integrin. This results in dissociation of TNS3 from focal adhesions and stimulates migration through disruption of the link between integrins and cortical actin fibres.

In addition to focal adhesions, TNS1 is also localised at fibrillar adhesions (or ECM contacts), where it can form a complex with $\alpha 5\beta 1$ integrin, fibronectin fibrils and actin filaments (31). Previous data has demonstrated that integrin can be translocated from focal adhesions to fibrillar adhesions through the interference of TNS1. Therefore, TNS1 is crucial for fibronectin fibrillogenesis, which converts soluble fibronectin into insoluble fibronectin matrix (32). This fibronectin matrix provides positional information for cell migration during early embryogenesis and plays an important role in cell growth, differentiation, survival and oncogenic transformation (33).

The localisation of TNS1 at the dense plaques of smooth muscles as well as at neuromuscular, myotendinous junctions and along the sarcolemma of skeletal muscles, suggest that TNS1 may play a role in the maintenance of normal muscle function (34, 35). Previous data show that TNS1 is not essential for myogenesis, since TNS1-KO mice seemed to develop normal muscle fibers (26). However, the regeneration process in experimentally damaged skeletal muscle fibers was much slower in TNS1-KO mice compared to wild-type (WT) skeletal muscle fibers. Moreover, this regeneration delay was accompanied by an increase in the population of premature skeletal muscle fibers and defects in cell activation, proliferation, differentiation and fusion in TNS1-KO skeletal muscles compared to WT muscle fibers, implying the role of TNS1 in wound healing processes (36).

The close localisation of TNS1 and calpain II at focal adhesion sites raises the possibility that there might be an interaction between these two molecules (37). It has been reported that calpain II, a calcium-dependent cysteine protease, is involved in integrin-mediated signalling pathways and cytoskeletal reorganisation (38). Previous data showed the ability of calpain II to cleave TNS1 into small fragments in a time-

and dose-dependent manner, and this cleavage eventually leads to cell morphological changes, indicating an abnormality in both reorganisation of the actin cytoskeleton and focal adhesion complexes (22).

TNS1 is also cleaved by caspase-3, a member of the caspase family, at the DYPD¹²²⁶G sequence, releasing the C-terminal region containing the SH2 domain away from the N-terminal region containing the actin binding domain. The resultant C-terminal fragment is unable to bind PI3K and transduce cell survival signalling. On the other hand, the released N-terminal fragment can induce disruption of the actin cytoskeleton organisation at focal adhesions. Therefore, caspase-mediated cleavage of TNS1 contributes to the interruption of ECM-mediated survival signals through PI3-K and is considered a critical step for disrupting the structure of focal adhesions during apoptosis (39). *Cten* has also been reported to be a caspase-3 substrate, similarly to TNS1. It has been shown that caspase-3 is able to cleave *Cten* at the DSTD⁵⁷⁰S sequence, thereby releasing a fragment, *Cten* 571–715, which contains the PTB domain and is able to reduce cell growth by inducing apoptosis through binding to the β integrin tails and disruption of the link between integrins and cortical actin fibres. This might lead to disruption of cell adhesions and eventually facilitate cell death (40).

Previous reports have shown that TNS1 over-expression activates both c-Jun N-terminal kinase (JNK) and p38 mitogen-activated protein kinase (MAPK) pathways, and this activation was independent of the activities of the small GTP binding proteins Rac and Cdc42, but was dependent on Sek, a receptor tyrosine kinase involved in the JNK pathway (41).

1.1.6 Role in human tumours

Deleted in liver cancer 1 (*DLC1*) is a recently cloned gene mapped to chromosome 8p21.3-22, a region shown to harbour tumour suppressor genes. It is frequently deleted in various human cancers, such as liver, breast, lung, brain, stomach, colon, and prostate cancers. It is widely expressed in normal human tissues, but frequently down-regulated in human hepatocellular carcinoma (HCC) and various cancer cell lines. Given that, a growing body of evidence suggests that *DLC1* acts as a tumour suppressor gene (42-51).

It has been reported that *TNS2* directly interacts, via its SH2 domain, with *DLC1* *in vitro* and *in vivo*, and the formation of a *DLC1-TNS2* complex brings *DLC1* in close proximity to Rho GTPases and facilitates the inactivation of Rho proteins. The Rho proteins regulate the remodelling of the actin cytoskeleton, focal adhesion turnover and promote cell proliferation and metastasis through the Rho GTPases-activating protein (RhoGAP) activity of *DLC1*. These data, in conjunction with the finding that *TNS2* expression was down-regulated in HCC, clearly demonstrates the tumour suppressor activity of *TNS2* in HCC (52). However, expression of the splice variant of *TNS2* (variant 3) has been shown to be up-regulated in human HCC, and this over-expression was significantly associated with venous invasion, tumour microsatellite formation and tumour non-encapsulation. In addition, forced expression of variant 3 caused significant increase in cell migration, invasion and proliferation of HCC cells, demonstrating the oncogenic role of variant 3 in hepatocarcinogenesis (53).

Evaluation of the expression level of *TNS3* in thyroid tissue has revealed that in addition to normal thyroid tissue, *TNS3* is also up-regulated in benign thyroid lesions,

such as adenomatous goitres and functional follicular adenomas. However, its expression is decreased in papillary and follicular carcinomas and even markedly decreased in anaplastic thyroid carcinomas. These data clearly show that abundant expression of *TNS3* mRNA is observed in tissues that produce thyroid hormone, suggesting that *TNS3* may play a fundamental role in thyroid function and may relate to thyroid diseases (23, 54).

Previously published data suggest that the function of *Cten* is tissue-specific. It has been reported, that *Cten* is down-regulated in prostate cancer compared to normal prostate, and therefore acts as a tumour suppressor in the prostate (8). Moreover, the localisation of *Cten* at chromosome 17q21, a region frequently deleted in prostate cancer, and the interaction of mutant *DLC1* with the *Cten* SH2 domain, which facilitates the recruitment of *DLC1* to focal adhesion sites, and in turn restore its tumour suppression activities, clearly demonstrate the tumour suppressor behaviour of *Cten* in prostate and liver cancers (55). However, in thymomas and lung tumours, *Cten* has been described as an oncogene with progressive up-regulation correlating with increasing tumour stage (56, 57). In addition, evaluation of the expression of *Cten* in gastric cancer cases using immunohistochemistry (IHC) revealed that *Cten* over-expression was significantly associated with histologically poorer grade, deeper invasion into the serosa, lymph node metastasis and peritoneal dissemination. Patients with high *Cten* expression tended to show shorter survival than patients had a lower expression of *Cten* (24).

1.1.7 Medical applications

Several aspects of the function of tensin genes are of medical interest. Evaluation of the renal histology of TNS1 and TNS2-KO mice showed tubular basement membrane disintegration, tubular atrophy with cyst development and interstitial cell infiltration with fibrosis, lesions commonly seen in human nephronophthisis disorders. Thus, TNS1 and TNS2-KO mice could be a useful animal model for human nephronophthisis or similar renal diseases (20).

Silver-Russell dwarfism, also called Silver–Russell syndrome (SRS) is a growth disorder occurring in children, with an incidence of approximately 1:10,000 births. The major phenotypic features are growth retardation, short limbs, and triangular face. Its exact cause is unknown, but previous research shows it is usually caused by a maternal uniparental disomy (UPD) on chromosome 7p11.2–13. Having shown that TNS3 is essential for normal development and functions of the small intestine, lung and bone as its KO in mice results in growth retardation accompanied with a combination of developmental defects in the small intestine, lung and bone. These phenotypes of the TNS3-KO mice are similar to some clinical features of SRS. In addition, the localisation of *TNS3* at chromosome 7p12.3, these data suggesting a potential link between TNS3 and SRS.

Inflammatory breast cancer (IBC) is a subtype of highly aggressive breast cancer (BC) characterised by HER2 over-expression and showing a large degree of lymphovascular invasion (58, 59). Recently, it has been found that *Cten* expression is up-regulated in 56% of IBC patients, and this over-expression is found to be strongly correlated with epidermal growth factor receptor (EGFR) phosphorylation (P-EGFR). Analysis of

Cten expression in tumour biopsies from P-EGFR positive IBC patients prior to and during lapatinib, a dual EGFR/HER2 tyrosine kinase inhibitor (Tykerb), monotherapy revealed that after a 21-day treatment with the drug, Cten expression was significantly down-regulated in most tumours. Similarly P-EGFR, P-HER2 and P-Erk levels were reduced following lapatinib treatment. Taken together, this data demonstrates that Cten expression in BCis highly dependent on EGFR activation, and may predict the response to EGFR/HER2-targeted therapy (30).

Furthermore, evaluation of the Cten expression in prostate cancer (PC-3) and paclitaxel-resistance prostate cancer (PC-3-TxR) cell lines, has revealed that Cten-KO in PC-3 cells and Cten forced expression in PC-3-TxR cells is associated with induced paclitaxel resistance and restored paclitaxel sensitivity respectively, possibly through elevation of F-actin which modifies the cytoskeletal cell structure to confer resistance to paclitaxel. These results strongly suggest that Cten plays an important role in paclitaxel sensitivity in prostate cancer (60).

1.2 Focal adhesions

Adhesive interactions between cells and the ECM play a crucial role regulating a wide variety of dynamic cellular processes, such as cell motility, cell proliferation, cell differentiation, regulation of gene expression and cell survival. Perturbing this coordination can lead to cell transformation and cancer development (61, 62). Focal adhesions are specialised areas of the plasma membrane allowing cells to attach to the ECM through transmembrane receptors of the integrin family that link intracellularly to the actin cytoskeleton (61, 62). In addition to structural molecules which participate in maintaining the integrity of the structural link between membrane receptors and the actin cytoskeleton, focal adhesions also contain several types of signalling molecules, including different protein kinases and phosphatases, their substrates, and various adapter proteins which suggest a considerable functional diversity (63, 64). Upon engagement of integrins with their ECM ligands and subsequent integrin clustering, the cytoplasmic tail of β -integrins triggers signal transduction events such as tyrosine phosphorylation of cytoplasmic tyrosine kinases (e.g. FAK) and serine/threonine kinases (such as those in the MAPK cascade), and induced phosphatidylinositol-4,5-bisphosphate (PIP₂) synthesis (65-67), forming large intracellular protein complexes clustered at the cytoplasmic tails of β -integrins and linked to the actin cytoskeleton. Thus focal adhesions not only provide a structural link between ECM components and actin cytoskeleton, but also play a key role in mediating signal transduction. In addition, focal adhesions play crucial roles in the creation, mediation and sensing of tension (68).

Based on their adhesion maturation state, focal adhesions can be classified into different structural categories including: focal points which are formed at the periphery

of the cells and linked to an F-actin network; focal complexes—mid-size stationary adhesion sites which are linked to the actin meshwork at the leading edge of the cell within lamellipodia; focal adhesions—large elongated adhesions connected to the actin stress fibers; fibrillar adhesions—elongated contact sites that connect extracellular fibronectin fibers to microfilament stress fibers; and podosomes—invasive ring structures composed of adhesion machinery and actin filaments (69).

Cell migration is an emergent process that ultimately derives from a vast diversity of molecular interactions between, ECM components, integrins, adaptor proteins, actin and kinases at focal adhesions. These combine progressively to produce recognisable sub-cellular systems of intermediate complexity which control actin polymerisation, cytoskeletal tension, and focal adhesions organisation and turn-over and eventually produce adhesive and migratory cellular behaviours (69).

Cell migration occurs in response to chemokines and growth factors that are captured by transmembrane receptors on the cell surface. In addition cell migration can also be initiated more directly by focal adhesions and their interaction with ECM components (69). These signalling systems are designed to induce cell shape changes accompanied by formation of actin-dependent cellular protrusions such as filopodia and lamellipodia at the front of the migrating cell that form the molecular scaffold formed by the polymerised actin cytoskeleton to the ECM and required for the initiation and maturation of further focal complexes (70). Once the actin cytoskeleton is linked to the ECM, the newly added actin molecules to the actin cytoskeletal scaffold can serve to push the plasma membrane at the leading edges of filopodia and lamellipodia forward (71). The second phase of cell migration is initiated when focal complexes start to

mature into focal adhesions which results in the compaction of the actin cytoskeleton and integrin receptors, creating a robust link between actin stress fibers and the ECM (68, 72). This is followed by sliding of the focal adhesions in the direction of migration accompanied with dispersion of integrin dependent adhesion sites at the rear and formation of integrin dependent adhesion sites at the proximal edge of sliding focal contacts respectively (73, 74).

1.3 Focal adhesion molecules

1.3.1 Integrins

Among the several proteins involved in cell attachment, is a family of cell surface receptors known as integrins, named for maintaining the integrity of the cytoskeletal-ECM linkage, play a fundamental role in mediating these molecular interactions (75, 76). Whereas the extracellular domain of integrins binds ECM proteins, their cytoplasmic tail anchors to the actin cytoskeleton. This linkage is dynamic - while the integrin binding to ECM changes the composition and morphology of the cell cytoskeleton, the actin networks itself controls avidity and affinity of the integrins extracellular domain, thereby modulating the ECM (77).

A key feature of integrin is that in addition to binding ECM molecules, they bind other proteins including growth factors, cytokines and matrix-degrading proteases. The signals are integrated and adapted to play a critical role in regulating many vital cellular events, including gene expression, tissue development, inflammation, angiogenesis, tumour cell growth and metastasis. Therefore, integrins appear as a cornerstone in many cellular biological processes (78).

Another important feature of integrin is that they are able to coordinate with and regulate the informational outputs of receptor tyrosine kinases (RTKs). For example, in response to integrin $\alpha\beta3$ -ECM binding combined with low concentrations of EGF exposure, EGFR is phosphorylated in a c-Src and p130Cas-dependent fashion leading to downstream signalling for cell survival and proliferation. In the absence of integrin-ECM interactions, the EGF responsiveness of EGFR is significantly reduced (79). Another example is phosphorylation and significant signal enhancement of vascular

endothelial growth factor receptor 2 (VEGFR2) upon its direct interaction with $\alpha\beta3$ integrin (80).

Typically, integrins are obligate heterodimers composed of α and β subunits in close non-covalent association that form structural and functional bridges between the ECM and intracellular cytoskeleton. There are 18 α and 8 β subunits that have been characterised, forming 22 different heterodimeric receptor complexes and despite this high redundancy level, most integrins have unique and specific biological roles (81-83).

Integrins do not themselves possess kinase activity, however, they rely on cytoplasmic proteins such as talin, paxillin, vinculin and alpha-actinin which in turn interact with the actin cytoskeleton (84). At focal adhesions, the cytoplasmic proteins act by regulating cytoplasmic kinases such as FAK and Src family kinases, which in turn bind and phosphorylate adaptor proteins, such as p130Cas, thereby recruiting signalling molecules and activating intracellular signalling pathways. These eventually promote cell migration, proliferation and survival in both normal and tumorigenic cell contexts. Therefore, integrins are not only structural proteins, but also play a key role in mediating signal transduction (85).

The close localisation of *Cten* with integrin-linked kinase (ILK), FAK and CD24 molecules at cytoplasmic tails of integrins and the finding that *Cten* contains an SH2 domain that allows *Cten* to bind phosphotyrosine-containing proteins at focal adhesions, raise the possibility that there might be a potential link between these molecules and prompted us to focus on ILK, FAK and CD24 as secondary downstream targets of *Cten*. These secondary molecules play a key role in various biological functions such as cell adhesion, migration, proliferation, differentiation, apoptosis and

invasion. Their protein structure, downstream signalling pathways and biological role in cancer will be discussed in details in the following sections.

1.3.2 FAK

FAK is a 125 kDa non-receptor and non-membrane associated protein tyrosine kinase (PTK), which was shown to be localised at focal adhesions and involved in many critical cellular events including adhesion, migration, proliferation and survival (86).

FAK contains three different structural domains: the C-terminal, the central and the N-terminal domains (Figure 6). The central tyrosine kinase domain is flanked on the N-terminus by a band 4.1, ezrin, radixin, and moesin (FERM) domain, which may serve as a binding site for growth factors receptors such as EGFR, and PDGFR, ezrin, a cytoskeletal linker and JSAP1, a component of the JNK pathway (87-89), and on its C-terminus by the focal adhesion targeting (FAT) domain. The FAT domain modulates FAK localisation to focal adhesions via interactions with the integrin-associated proteins, such as talin and paxillin (90, 91). It also promotes activation of Rho GTPase via direct interactions with p190Rho GEF (92). The proline-rich regions present in both the C-terminal and N-terminal domains of FAK act as binding sites for a variety of SH3-containing proteins, including p130Cas adaptor protein, GTPase regulator associated with FAK (Graf), Arf GTPase-activating protein (ASAP1) and Trio proteins (93-96).

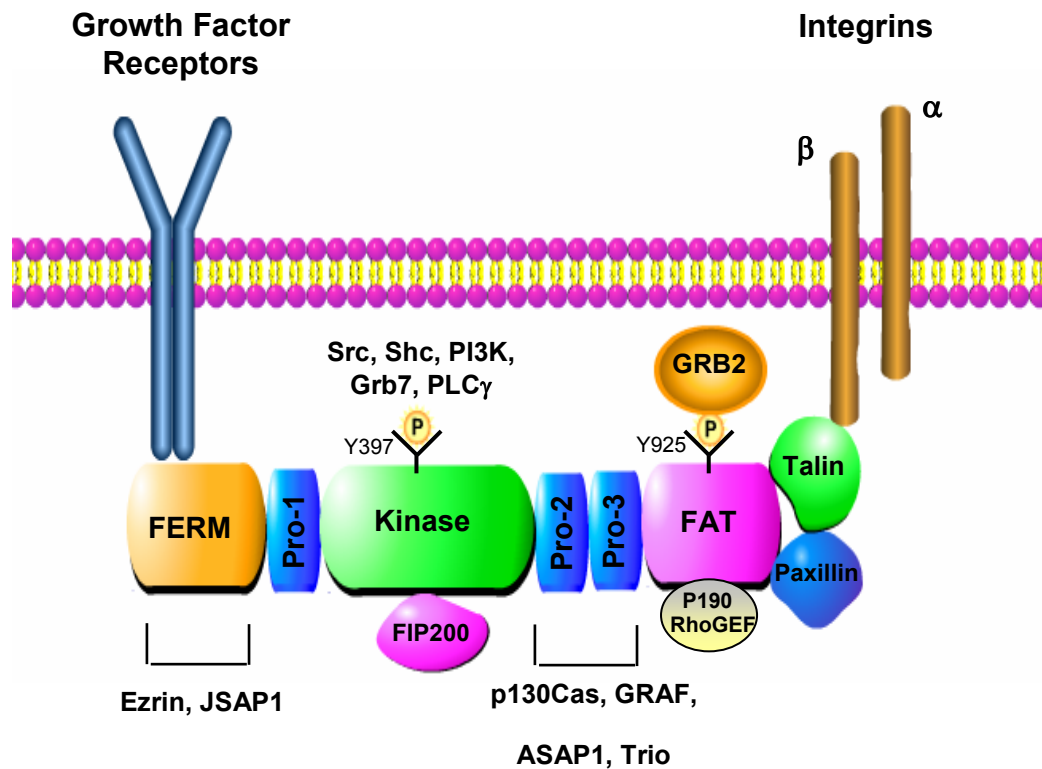


Figure 6. Schematic structure of FAK. FAK contains centrally located tyrosine-kinase domain flanked by the C-terminal domain that consists of a FAT, which modulates FAK interactions with the integrin-associated proteins, including talin and paxillin as well as activation of Rho GTPase via direct interactions with p190Rho GEF and the N-terminal domain that consists of a FERM domain, which facilitates FAK interactions with growth factors receptors, ezrin and JSAP1. Three proline-rich regions are present in both the C-terminal and N-terminal domains of FAK and modulate FAK association with p130Cas, Graf, ASAP1 and Trio proteins. Important tyrosine phosphorylation sites of FAK are shown. Phosphorylation of FAK at Tyr397 serves as a binding site for SH2-containing proteins, including Src, Shc, PI3K, Grb7 and PLC γ . FAK is also phosphorylated by Src at Tyr925 residue, allowing FAK to interact with the adaptor protein Grb2.

Upon engagement of integrins with their ECM ligands, the cytoplasmic tail of β -integrins ($\beta 1$, $\beta 3$ and $\beta 5$) mediates FAK activation and recruitment to focal adhesions possibly via facilitating the interactions between FAK and the integrin-binding proteins such as talin and paxillin (97). This results in phosphorylation of FAK at

Tyr397, which creates a high-affinity binding site for SH2-containing proteins such as Src, Shc, PI3K, growth factor receptor bound protein 7 (Grb7) and phospholipase C γ (PLC γ). The binding of Src to FAK can lead to formation of FAK–Src signalling complex which facilitates tyrosine phosphorylation of p130Cas, enabling it to bind Crk adaptor protein (98-102). Interestingly, it has been reported that up-regulation of Crk is associated with the activation of FAK and this activation is dependent on p130Cas activity (103). Furthermore, over-expression of p130Cas can enhanced tyrosine phosphorylation of FAK and paxillin, suggesting that these multiple feedback interactions between FAK, Src and p130Cas can lead to stabilisation of the FAK–Src signalling complex (Figure 7) (104).

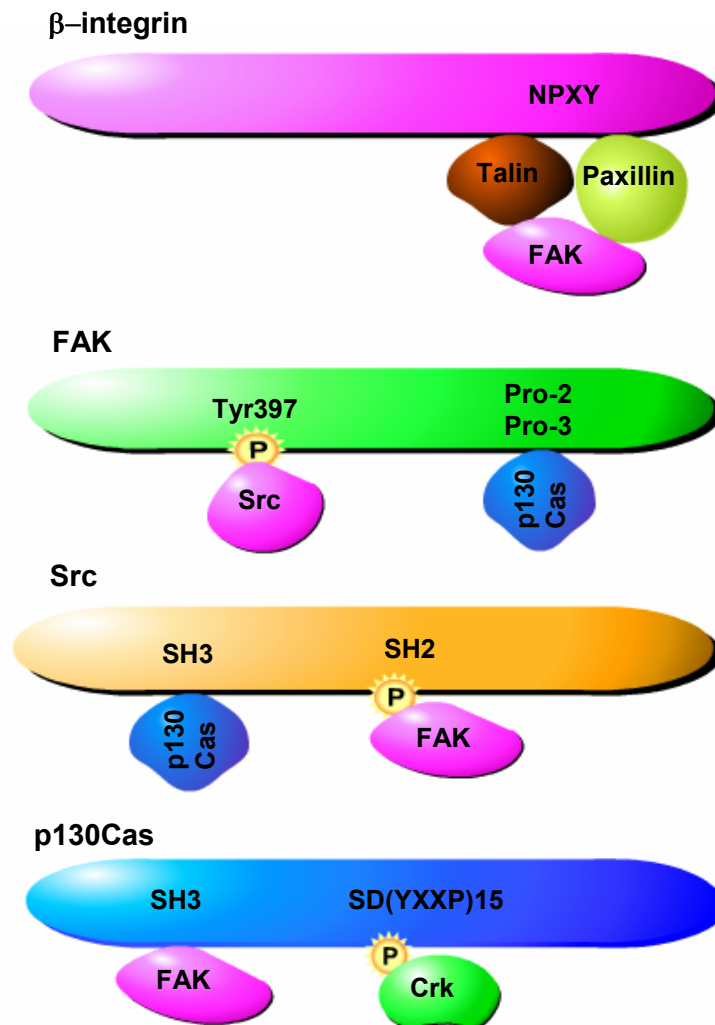


Figure 7. Schematic illustration of binding interactions between β -integrins, FAK, Src and p130Cas proteins. FAK is recruited to the cytoplasmic tail of β -integrin via interactions with integrin-binding proteins talin and paxillin. This results in activation and phosphorylation of FAK at Tyr397, which creates a binding site for SH2-containing protein Src. The FAK–Src complex then promotes tyrosine phosphorylation of p130Cas at YXXP motifs in its substrate domain (SD), enabling it to bind Crk adaptor protein. P130Cas SH3 domain binds to proline domains in the FAK C-terminal.

In addition to autophosphorylation of FAK on Tyr397 residue, FAK can also be phosphorylated by Src at Tyr925 residue, allowing FAK to interact with the adaptor protein growth factor receptor bound protein 2 (Grb2). The SH3 domain of Grb2 binds to son of sevenless (SOS), a guanine nucleotide exchange factor for Ras, which in turn bridges FAK and the integrin-initiated signals to the Ras/MAPK pathway (105, 106).

The binding between Crk adaptor protein and phosphorylated p130Cas is negatively regulated by Abl family tyrosine kinase, a protein that is activated by integrin aggregation and localised at focal adhesions (107). Activated Abl protein phosphorylates Crk at Y221 residue, thereby inducing the intramolecular binding of the Crk SH2 to phosphorylated Y221 in its C-terminal region and preventing Crk from binding to the docking protein p130Cas (108). Disruption of CAS-Crk molecular coupling blocks downstream signals regulating focal adhesion assembly and actin cytoskeleton organisation, thereby decreasing cell motility (Figure 8) (109). Another new protein reported to regulate p130Cas function is Ajuba, which is required to maintain both stabilisation of p130Cas localisation to integrin clustering sites and effective p130Cas–Crk coupling, and results in Rac activation and promoting cell migration (Figure 8) (110).

Integrin-mediated activation of the FAK-Src complex signalling pathway regulates various biological processes and contributes to tumour progression. Previous data has shown that FAK expression resulted in promoting cell survival possibly through enhancing PI3K-mediated activation of the AKT pathway, which in turn increased expression of inhibitor of apoptosis proteins (IAPs) through NF κ B and protected the cells from oxidative-stress induced apoptosis and suppressing p53-mediated apoptosis (Figure 8) (111-113). FAK may limit p53 activity through its N-terminal FERM domain which localised to the nucleus and directly interacted and suppressed transcriptional activation of a number of p53 target genes including p21, Mdm2 and Bax that are important mediators of p53-induced apoptosis, which would propose the anti-apoptotic signal of FAK FERM-domain-initiated pathway (114, 115).

Another way whereby FAK may control cell survival is through association with the FAK interacting protein 200 kDa (FIP200), which localises with integrins at focal adhesions. It has been reported that FIP200 can bind p53, and enhance its half-life and expression. In addition, it can also increase the expression of p21waf, a cell cycle inhibitor, which reduces the activity of cyclin/cyclin-dependent kinase complexes, promoting cell cycle progression, leading to G1-S arrest. Thus, it is possible that FAK may enhance survival signals through FIP200-FAK association, which compete with FIP200-p53 binding, thereby limiting the ability of FIP200 to bind p53 and enhance its activity (116, 117).

Several studies have shown over-expression of FAK in many human tumours and its association with aggressive tumour phenotype (118). As recently revealed, the formation of a FAK–Src signalling complex enhances E-cadherin internalisation during tumour progression, thereby promoting an epithelial-to-mesenchymal transition (EMT) and enhanced cell migration (119-121). In addition, FAK–Src signalling complex formation regulates protease secretion and expression by tumour cells (122). Upon activation, these proteases are localised at the leading edge of migrating tumour cells and promote ECM degradation which can facilitate cell invasion and metastasis (123, 124). The findings that FAK–Src complex can activate endophilin A2 protein, extracellular signal regulated kinase 2 (ERK-2) and JNK pathways, which in turn promote increased gene transcription of target proteins leading to enhanced protease expression, clearly demonstrate that the activated FAK–Src signalling complex may positively regulate tumour growth and spread and lead to an aggressive tumour phenotype (Figure 8) (118, 125, 126).

Previous publications have reported a role of FAK–Src signalling in promoting tumour angiogenesis and this is one likely way by which FAK may enhance tumour growth (127). The binding of FAK with a Grb2-SOS complex leads to Ras small GTPase and Raf kinase activation which phosphorylate mitogen activated protein kinase kinase 1 (MEK1) and ERK2 at S217/S221 and at T185/Y187 residues respectively, thereby activating them. Activated ERK2 in turn enhances transcription of vascular endothelial growth factor (VEGF) gene and thereby promoting tumour growth through stimulating angiogenesis (Figure 8) (128, 129).

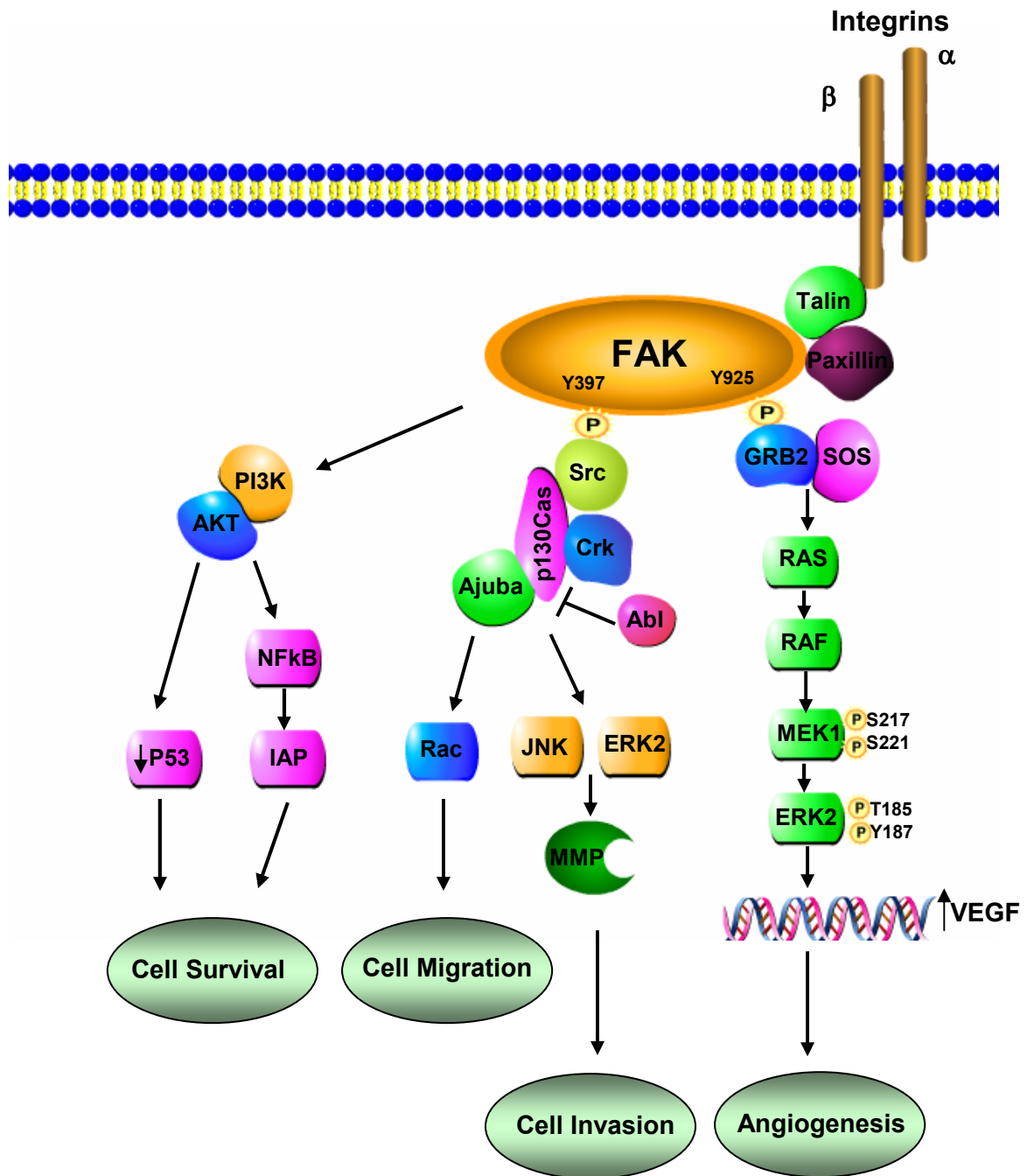


Figure 8. Schematic diagram of FAK downstream signalling pathways. Upon phosphorylation of FAK at Tyr397 by integrins, this result in creation a high-affinity binding site for Src. The FAK-Src complex then triggers multiple downstream pathways to regulate migration, invasion and survival/apoptosis of the cells. FAK can also be phosphorylated by Src at Tyr925 residue, allowing FAK to interact with a Grb2-SOS complex, that lead to MEK1 and ERK2 activation which in turn enhance transcription of VEGF gene and thereby stimulating angiogenesis.

1.3.3 ILK

ILK was identified in a search for proteins present in some integrin-containing focal-adhesion plaques and capable of binding to the cytoplasmic domains of the integrin $\beta 1$ and $\beta 3$ subunits (130, 131). The localisation of ILK at focal adhesions allows it to play an essential role in transduction of many biochemical signals that are initiated by cell-ECM interactions and that regulate various biological cellular events, including cell survival, differentiation, proliferation, migration, invasion and angiogenesis (132, 133).

Previous studies using recombinant ILK and immunoprecipitation kinase assays showed that ILK is an intracellular structural serine/threonine protein kinase capable of phosphorylation of the $\beta 1$ integrin at highly conserved serine/threonine residues, and this appeared crucial in maintaining the stabilisation of $\beta 1$ localisation to focal adhesions (130, 134).

Whereas ILK interacts with integrins via its integrin-binding domain present in its C-terminus, the N-terminus of ILK contains four ankyrin repeats (ANK) which are involved in mediating protein-protein interactions, and which allow ILK to interact with other signalling molecules. Through its ankyrin repeats, ILK can interact with the LIM domain of particularly interesting Cys-His-rich protein (PINCH), which co-localises with integrins at focal adhesions and stabilises the localisation of ILK at focal adhesion sites (135, 136). Furthermore, PINCH can interact with the NCK adaptor protein-2 (Nck2) via its LIM domain and the PINCH-Nck2 complex is recruited to activated EGFR and PDGFR, thereby bridging ILK to growth-factor receptors (Figure 9) (137, 138).

In addition to binding integrins, the C-terminal domain of ILK also interacts with actin-binding adaptor proteins, such as paxillin and parvins, which interact directly with actin networks, allowing ILK to bridge the effects of growth factors and ECM through growth factor receptors and transmembrane integrins to the actin cytoskeleton and regulate cytoskeletal reorganisation and cell migration processes (139-141).

The central pleckstrin homology (PH)-like domain containing phosphoinositide-binding motifs is located between the C-terminal and the N-terminal regions of ILK and is involved in the binding of ILK to Phosphatidylinositol (3, 4, 5)-trisphosphate (PIP3), produced by PI3K, which activate ILK. It has been shown that inhibition/activation of PI3K is associated with decreased/increased activity of ILK respectively, suggesting that ILK is regulated in a PI3K-dependent manner (Figure 9) (142, 143).

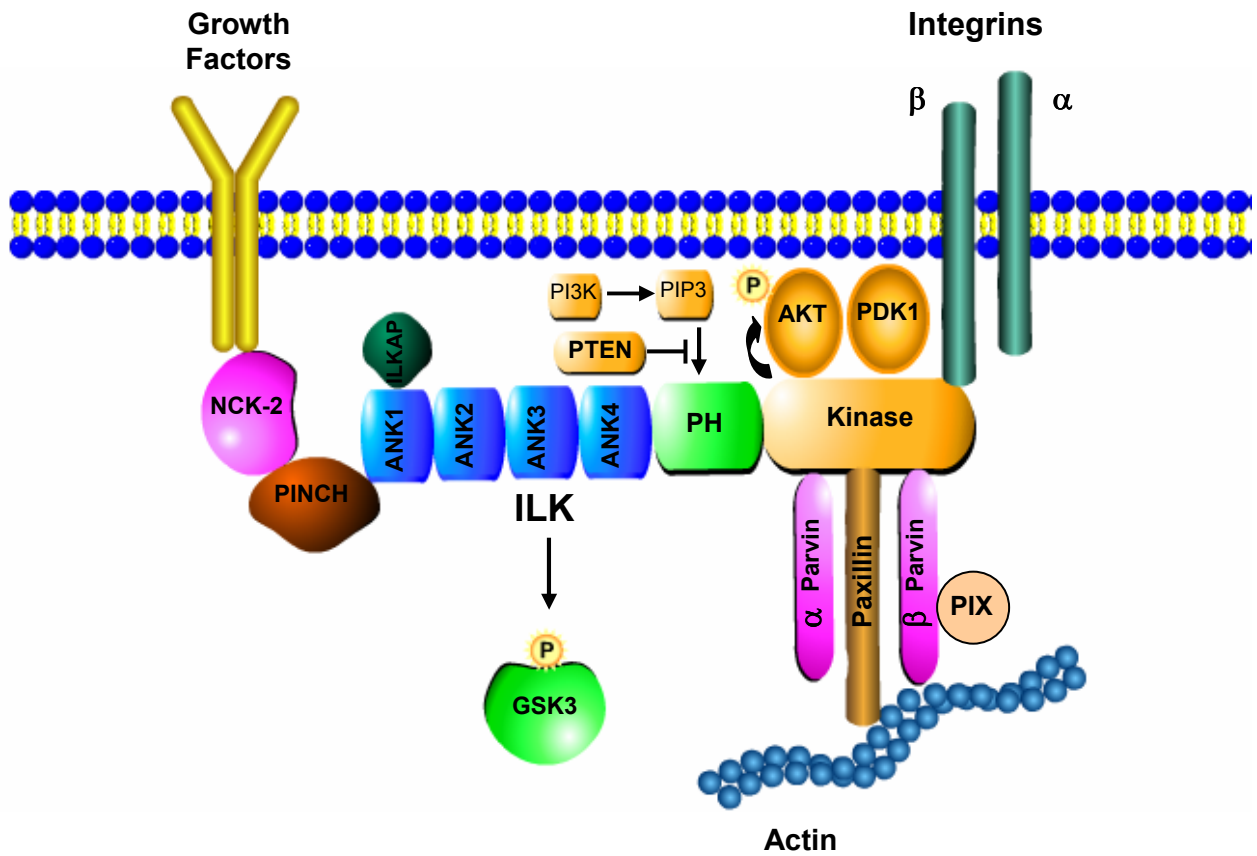


Figure 9. Schematic structure of ILK. ILK consists of three domains, a C-terminal kinase domain, a PH-like domain and ANK at N-terminal. The kinase domain allows ILK to bind with the cytoplasmic tails of β -Integrins, the kinase substrate Akt, the phosphoinositide-dependent kinase-1 (PDK-1) and the actin-binding adaptor proteins, such as paxillin and parvins. β -parvin binds to PAK-interactive exchange factor (PIX), which promotes actin cytoskeletal reorganisation through the GTPases, Rac1 and CDC42. The PH domain of ILK binds to PIP3. The tumour suppressor PTEN dephosphorylates PIP3 to PIP2, resulting in the inhibition of ILK activity. Through its ankyrin repeats, ILK can interact with the LIM domain of PINCH, which binds to the Nck2, thereby coupling growth factor signalling to Integrin signalling through ILK.

The expression and activity of ILK are increased in many human tumours. Although the causes of its over-expression remain to be fully elucidated, several lines of evidence have clearly demonstrated that ILK's oncogenic capacity derives from it regulating a diverse set of downstream effectors and signalling pathways that promote anchorage-dependent cell growth, survival, proliferation, EMT, migration, invasion and tumour angiogenesis (144-148).

It has been shown that ILK phosphorylates PKB/Akt on Ser473 and increases its activity, stimulating signalling pathways which negatively regulate caspase activation and stimulation of nuclear factor B (NF- κ B), leading to the suppression of apoptosis and enhanced cell survival (149-152). In addition, ILK may promote the activity of the β -Catenin/Lef complex and activator protein 1 (AP1) transcription factors, possibly through phosphorylation and inhibition of glycogen synthase kinase 3 (GSK-3), which stimulates expression of the genes encoding cyclin D1 and MMP9 respectively, thereby promoting tumour proliferation and invasion (Figure 10) (153-156).

It has previously been shown that ILK over-expression can modulate cytoskeletal organisation and promotes cell migration via ILK-binding proteins β -parvin and paxillin, which activate PAK-interactive exchange factor (PIX), a guanine-nucleotide exchange factor (GEF) for Rac1 and Cdc42. This indicates a potential link between ILK and these small GTPases which subsequently influence cell motility and spreading. In addition, ILK can phosphorylate myosin light chain (MLC) and myosin phosphatase target subunit, resulting in myosin-mediated contractility and cell motility (Figure 10) (157-159).

Recent evidence has shown that ILK up-regulation can lead to ablation of cellular adhesions in terms of loss of cell–cell or cell–ECM contacts. This appears to be due to a dramatic decrease in E-cadherin expression caused by ILK-induced stimulation of Snail expression, the transcriptional repressor of E-cadherin, and enhanced activity of the transcription factor partner of β -catenin, Lef-1, which in turn promotes transcriptional activity of the β -catenin/Lef complex, consequently result in down-regulation of E-cadherin and loss of cell adhesion (160-165). Taken together with the observations that ILK over-expression in epithelial cells can induce EMT, accompanied by enhanced fibronectin matrix assembly, increased vimentin expression and loss of keratin 14 and 18 expression, these results clearly demonstrate that activated ILK may promote EMT and enhances tumour invasion and metastasis (Figure 10) (166).

Previous studies have implicated a significant role of ILK in tumour angiogenesis. ILK-mediated phosphorylation of AKT has been found to stimulate mammalian target of rapamycin (mTOR) expression, which in turn activates hypoxia inducible factor-1 alpha ($\text{HIF1}\alpha$), thereby enhancing VEGF expression and promoting angiogenesis (Figure 10) (147).

The kinase activity of ILK is negatively regulated by several protein phosphatases, such as ILK-associated protein (ILKAP), a serine/threonine phosphatase which inhibits integrin-mediated phosphorylation of GSK-3, and PTEN which inhibits PI3K-mediated ILK activation, (154, 167-169).

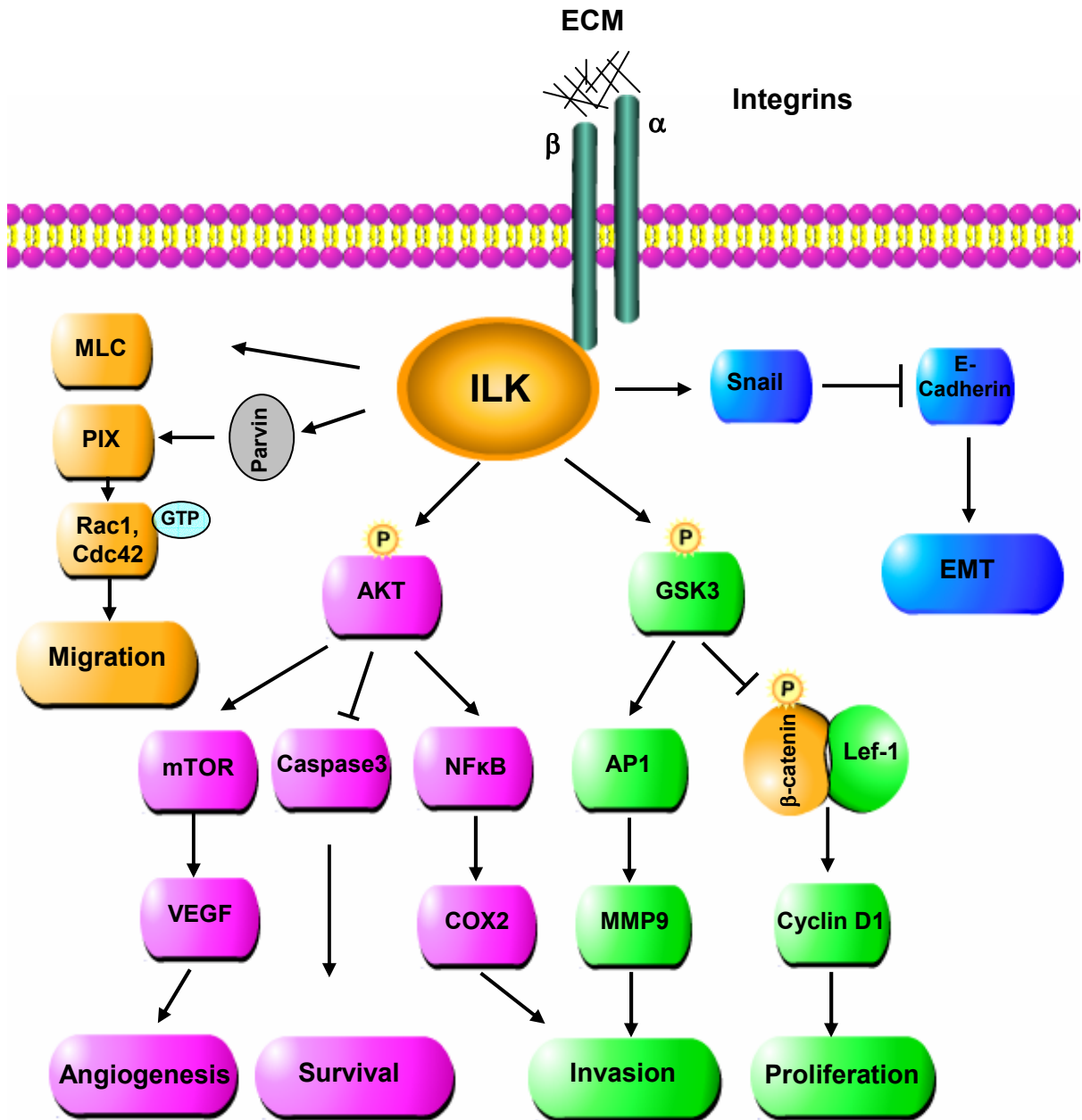


Figure 10. Schematic diagram of ILK downstream signalling pathways. Upon engagement of integrins with ECM, ILK is activated and induces phosphorylation of Akt, which in turn negatively regulate caspase activation and stimulation of NF- κ B, leading to the suppression of apoptosis and enhanced cell survival. P-Akt can also activate mTOR, which in turn enhances VEGF expression and promoting angiogenesis. Activated ILK can also enhance the β -Catenin/Lef complex and AP1 activity, possibly through phosphorylation of GSK-3, which stimulates expression of cyclin D1 and MMP9 respectively, thereby promoting tumour proliferation and invasion. In addition, ILK also induces EMT accompanied with loss of E-cadherin possibly through Snail activation. ILK can also modulates cell motility via activation MLC and PIX proteins.

1.3.4 CD24

CD24 is a small heavily glycosylated mucin-type cell surface protein that is bound to the cell membrane via a glycosylphosphatidylinositol (GPI) anchor. It has a heterogeneous molecular weight ranging from 30 to 70 kDa with a mature protein core of only 27 to 30 amino acids long, suggesting that most of the molecular weight of the protein consists of extensive N- and O-linked glycosylated residues. CD24 is localized in lipid-rafts, which are microdomains that serve as platforms for the regulation of cell adhesion and signalling. Within these rafts, it is closely associated with src-kinases, G-proteins and calcium channels (170).

CD24 is normally expressed on a wide variety of cells including polymorphs, B-lymphocytes, ganglion cells, keratinocytes, renal tubules and adrenal medulla (171, 172). Studies are accumulating to show that CD24 is considered an adhesion molecule, conveys a function in cell-to-cell interaction and regulation of proliferation and adhesion. CD24 has been identified as a ligand of P-selectin, an adhesion receptor on activated endothelial cells and platelets, suggesting the role of CD24 in marginal adhesion and migration of cells under shear forces in the blood stream (173). CD24 can also serve as a ligand of L1, a member of the immunoglobulin superfamily that is expressed on neural and lymphoid cells. CD24-deficient mice displayed an impairment of B cell differentiation suggesting that CD24 expression influences the cell-cell interactions and maturation of B cells (173).

An expanding body of literature revealed the role of CD24 in the regulation of tumour growth, invasion and metastatic tumour progression. CD24 over-expression has been reported not only in haematologic malignancies, but also in several different types of

solid tumours, including non-small cell lung cancers, pancreatic and gastric adenocarcinomas, ovarian cancer and BC and, in general, its over-expression has been associated with poor prognostic outcomes (174-178). In the colon, previous studies have reported patchy focal CD24 expression in the crypt bases in normal mucosa (179). In comparison, CD24 expression is up-regulated in colorectal adenomas and it is thus an early event in colorectal cancer (CRC) carcinogenesis (180). High expression of CD24 is reported in CRC, and this over-expression is associated with poor prognostic outcomes (179). In addition, treatment of CRC cell lines with anti-CD24 antibodies inhibits cell proliferation in a dose- and time-dependent manner in both *in-vitro* and *in-vivo* models (181). Furthermore, forced CD24 expression and knock-down in CRC cell lines expressing low and high levels of CD24 protein is associated with enhanced and suppressed colony forming, transwell migration and invasion abilities respectively, showing the oncogenic role of CD24 in CRC (182).

1.4 Colorectal Cancer

The role of *Cten* in CRC is currently unknown. This is the third most common form of cancer and the second leading cause of cancer-related deaths in the Western world. In the UK, every year around 35,000 individuals are diagnosed with CRC and more than 16,000 will die from this malignancy (183, 184). CRC usually follow a well established pattern of early non-invasive adenomatous growth, succeeded by the ability to invade locally into the adjacent tissues and ultimately by acquisition of metastatic features. The mechanisms by which tumour cells acquire the ability to invade and metastasize are unclear, although many consider that these processes require disruption of cell–cell and cell–matrix adhesion and epithelial–mesenchymal transition (EMT).

The etiology of CRC is not completely understood. However, certain risk factors substantially increase the likelihood of developing CRC. Among these are IBDs (such as Crohn's disease (CD) and ulcerative colitis (UC)) and adenomatous polyps (AP). The association between IBDs and CRC has been confirmed in several studies (185). For instance, 8% of UC patients develop CRC after 20 and 18% after 30 disease-years, respectively (186). Recently, it has been shown that the risk of developing CRC in CD patients is similar to that in patients with UC (186). Moreover, patients with APs have, in general, an increased risk of developing CRC compared to the general population. However, the risk of developing CRC in addition of colonic APs depends mainly on the size and the histological type of adenomas (187, 188).

Most people are treated by surgery which, if undertaken when the tumour is at an early stage, is usually curative. For advanced disease, surgery alone may be insufficient and

adjuvant chemotherapy may be necessary. Administration of adjuvant therapy depends on identification of poor prognostic features in the resection specimen. This however can be prone to variation (189) and there is a need for reliable biomarkers which add to the information obtained by routine pathological analysis.

AIMS OF THE THESIS

Chapter 2. Aims of the thesis

Review of the literature suggests that activity of Cten is probably context-dependent and may vary in tumours of different origin (see chapter 1). In addition, there is no available information concerning Cten expression in CRC. We hypothesized that Cten might contribute to tumour progression in CRC. The overall aim of this thesis is to evaluate the expression and biological role of Cten in the colon, especially during the development of CRC. Studies are also designed to characterise novel Cten-regulated genes and their involvement in CRC.

Specific objectives include:

1. Evaluation of the expression and the role of Cten in benign colorectal diseases, CRC and cancer metastasis using immunohistochemical, quantitative real time PCR (Q-RT-PCR) approaches and *in-vivo* models (chapter 4).
2. Investigating the functional role of Cten in CRC using a dual approach of forced Cten expression and Cten knock-down in CRC cell lines, in order to analyse if modulating levels of Cten expression can influence cellular processes such as cell proliferation, resistance to staurosporine induced apoptosis, cell migration and cell invasion using the appropriate assay (chapter 5).
3. Exploring the potential downstream signalling targets of Cten in CRC through evaluating the relationships between Cten expression and other secondary molecules associated with cancer metastasis, such as CD24, ILK, FAK and phosphorylated FAK (P-FAK) in both CRC cell lines and tissue samples using IHC and Western blot (chapter 6).

5. Evaluating the *Cten* expression in other tumour types such as breast cancer (BC) and pancreatic cancer using IHC on tissue microarray (TMA) platforms and correlate this with prognosis (chapter 7).

MATERIALS AND METHODS

Chapter 3. Materials and methods

3.1 Cell culture and transfection

Twenty-nine well established CRC cell lines (170) were obtained from Molecular and Population Genetics Laboratory, London Research Institute, Cancer Research UK, London and cultured in tissue culture-treated 75cm² flasks (Costar, UK) in growing Dulbecco's Modified Eagle Medium (DMEM) (Invitrogen, UK) supplemented with 10% Foetal Calf Serum (FCS) (Invitrogen, UK) and Penicillin/Streptomycin (Invitrogen, UK) at an atmospheric carbon dioxide content of 5%. Cells were allowed to grow until they reached approximately 90% confluence level and then passaged. Cells were detached from the flasks through washing with Phosphate buffered saline (PBS) (Sigma, USA) followed by incubation for 5 minutes at 37°C incubator in 2ml of trypsin/EDTA (0.5% trypsin, 1 mM EDTA, Sigma, USA). Cells were resuspended in 5ml of DMEM and then plating into new flasks containing 10ml of growing media with 0.1 – 1ml of the cell suspension. The general properties of these cell lines are summarised in Table 1 (Appendix 9.1).

3.2 Gene knock-down

RNA interference (RNAi) is a post-transcriptional gene silencing (PTGS) process in which double stranded RNA (dsRNA) is cleaved by an ATP-dependent ribonuclease (Dicer) into duplexes of 21 or 23 nucleotides short interfering RNAs (siRNAs). Consequently, these siRNAs are incorporated into a second enzyme complex, designated RNA-induced silencing complex (RISC), thereby allowing RISC to recognise and to cleave the target mRNA.

Transfection of cells with siRNA duplexes were carried out using Lipofectamine 2000 according to the manufacturer's protocol. Briefly, 5×10^4 cells were seeded per well in a six well plate (Costar, UK). The following day cells were transfected with 100nM siRNA, 5 μ l lipofectamine 2000 in 500 μ l medium. Six hours post transfection the supernatant was replaced by fresh media. Cells were analysed 72 hours later by Western blot or functional assays. The siRNAs used in this investigation were obtained from (Invitrogen, UK) and include: siCTEN, UUC UCA UUG ACA UGG UGC UCU GGG C, siCont, CCC GUA UAC GAC ACC GAG UAG UCU U, siCD24, CCU ACC CAC GCA GAU UAU UCC AGU and siCont, CCU CAC CGA CGU UUA CUU ACC AAG U. The possibility of scrambled control nucleotide sequence off-target effects were assessed, using the BLAST nucleotide-nucleotide database (NCBI), by comparing the scrambled control nucleotide sequence to the sequence of protein of interest.

3.3 Forced gene expression

Construction of the Green Fluorescent Protein (GFP) tagged Cten (GFP- Cten) expression vector has been previously described (40) and was kindly provided by Dr Su Hao Lo, Department of Biochemistry and Molecular Medicine, University of California- Davis, USA. The expression vector was transfected into cells using Lipofectamine 2000 (Invitrogen, UK) in accordance with the manufacturer's instructions. Briefly, 1×10^5 cells were seeded per well in a six well plate (Costar, UK) and transfected with 4 μ g of GFP-Cten, 10 μ l lipofectamine 2000 in 500 μ l medium. Control cells were transfected with an empty GFP vector (kindly provided from Dr Su Hao Lo, Department of Biochemistry and Molecular Medicine, University of California- Davis, USA). For establishment of stably transfected HCT116, cells

were grown for 4 weeks in selection media containing 800µg/ml G418 (Sigma, USA). For stable transfection of SW480, cells were initially transfected with GFP-Cten as above. After 48 hours, the cells were washed with PBS (Sigma, USA) and then detached by incubating with TE buffer (10 mM Tris-HCl (pH 8), 1 mM EDTA, Sigma, USA) for 5 - 10 minutes. These then underwent fluorescence associated cell sorting (FACS) in an Epics Altra Flow cytometer (Beckman Coulter, Fullerton, CA).

3.4 RNA extraction

Total RNA was extracted from cells using the RNeasy Mini Kit (Stratagene, UK). Approximately 1×10^7 cells were prepared for mRNA extraction. Cell were washed with PBS, 500µl of Detaching Buffer (7µl of Beta-Mercaptoethanol in 1ml of lysis buffer, supplied with kit) was applied to the cells, and then 500µl of the mixture was transferred into RNAase MicroSpin columns placed in Eppendorf tubes and centrifuged at 13,000 rpm for 1 minute. After discarding the supernatant, 500µl of 70% ethanol was added and the mixture was vortexed and centrifuged at 13,000 rpm for 5 minutes. Simultaneously, RNase-Free DNase enzyme was prepared by mixing 50µl of DNase buffer with 5µl of DNase enzyme (supplied with Kit) and incubated with the mixture at 37°C incubator for 15 minutes. The mixture was then washed once in 600µl High Salt Buffer (10mM Tris-HCL(PH7.5), 1mM EDTA, 0.5M NaCl) and twice in 600µl and 300µl Low Salt Buffer (10mM Tris-HCL(PH7.5), 1mM EDTA, 0.1M NaCl) respectively and centrifuged at 13,000 rpm for 1 minute each time. Lastly, the mRNA was eluted by applying 50µl of Elution Buffer and lifted stand for 2 minutes at room temperature and then centrifuged at 13,000 rpm for 1 minute. The final eluted mRNA was stored into fresh sterile tubes in -80°C freezer. Samples of RNA derived from

normal colonic mucosa were obtained following a previous study on IBD undertaken by Prof Ilyas (Division of Pathology, University of Nottingham, UK).

3.5 Complementary DNA (cDNA) preparation and reverse transcriptase

In order to achieve RNA denaturation, 1µg of total RNA was made up to 12.5µl with water and heated at 70°C for 10 minutes. Complementary DNA (cDNA) was then synthesized by incubating 1µg of denatured RNA at 37°C for 60 min in a mixture containing 1 µM of random hexamers (pDN6), 200 units of M-MLV reverse transcriptase (Invitrogen, UK), 10mM DTT (Invitrogen, UK) and 0.5mM each dNTP.

3.6 Q-RT-PCR

Quantitation of *Cten* and E-cadherin expression was performed using the standard curve method. All experiments were conducted in triplicate and *Cten* and *Cadherin-1* (*CDH1*) values were normalised to the housekeeping gene *Homo sapiens hypoxanthine phosphoribosyltransferase* (*HPRT*). For each reaction, 10ng of cDNA template was tested in a final volume of 25µl containing 1x SYBR Green Master Mix (Stratagene, UK) and primers at a final concentration of 250nM. The reaction was allowed to run in a thermal cycler (MX3005P Stratagene, UK) and the cycling conditions were 5 minutes initial denaturation at 95°C followed by 40 cycles of: 30 seconds denaturation at 95°C / 30 seconds annealing (60°C for *CTEN* / 59°C for *HPRT* / 50°C for *CDH1*) / 30 seconds extension at 72°C and a single final extension for 10 minutes. The data for Q-PCR were analysed using the MxPro-QPCR software for Mx3005P QPCR system. All PCR primers were designed using universal probe library software (190) and their specificities were assessed, using the BLAST database, by comparing the primer pairs to the *Homo sapien* genome sequence. The molecular

biology core facilities (MBCF) software (191) was used to determine the melting temperature and the G/C contents for each primer pair and subsequently the primers were ordered from (MWG-Biotech AG, UK). The primers sequences and reaction conditions are summarised in Table 2.

Table 2. Characterisation of PCR primers.

Primer	Sequence	T _m	Binding site	%GC
CTEN Forward	5'-GCGTCTGCTCAGAATCGAC-3'	53°C	1605-1623	58
CTEN Reverse	5'-GATGAGGAAGTGTCGGATGAG-3'	54°C	1664-1644	52
HPRT Forward	5'-TGACCTTGATTTATTTGCATACC-3'	51°C	136-159	33
HPRT Reverse	5'-TGAGGAATAAACACCCTTCCA-3'	51°C	201-180	41
E-Cadherin Forward	5'-TCCCATCAGCTGCCAGAA-3'	54°C	477-496	55
E-Cadherin Reverse	5'-TGACTCCTGTGTTCTGTTA-3'	54°C	976-957	45

3.7 Polymerase chain reaction (PCR)

Since GFP protein is a large protein consisting of over two hundred amino acids, it can possibly cause some functional problems, such as interference in the folding of the target protein or reporting on only a part of the target protein providing false positives or incorrect data. Thus, it was necessary to clone the *Cten* into a small tagged-Myc vector. In order to amplify a full length 2,148 bp product corresponding to *Cten* protein coding sequence, the following primers were designed (using universal probe library software) to introduce a BamH1 and HindIII sites at the 5' and the 3' ends of the PCR product respectively. The primer pairs used were forward primer: 5'-

AT **GGA TCC** TCC CAG GTG ATG TCC AGC CCA CT-3' and reverse primer: 5'-AT **AAG CTT** CTA CAT CCT TTC TGC GTC CTG CAG -3'. The Webcutter 2.0 software (192) was used to ensure that sticky ends are actually created at the 5' and 3' ends of the full length *Cten* PCR product and BamHI and HindIII enzymes do not cut within *Cten* coding sequence. pEGFPC-1 plasmid containing the complete coding sequence of *Cten* was used as a template.

For amplifying a full length 657 bp product corresponding to HPRT protein coding sequence, the following primers were designed using universal probe library software: forward primer: 5'-ATG GCG ACC CGC AGC CCT GGC-3' reverse primer: 5'-TTA GGC TTT GTA TTT TGC TTT-3'. Conventional PCR was done using SW480 CRC cell line cDNA as a template.

The standard reaction was performed in a final volume of 25µl consisting of: 10ng DNA templates, 2x (*Mix Taq*) Master Mix (New England BioLabs, UK), 1.5mM MgCl₂ and *HPRT*, *Cten* full length primers at a final concentration of 250nM. The reaction was allowed to run in a thermal cycler (Perkin Elmer GeneAmp PCR system 2400) for 40 cycles in the following set up, 95°C for 5 minutes (activation), 95°C for 1 minute (denaturation), 60°C for 1 minute (annealing), 72°C for 3 minutes (elongation) and 72°C for 7 minutes (final extension). PCR product was resolved on a 1% agarose gels.

3.8 Agarose gel electrophoresis

100ml of a 1% agarose (Gibco-BR Life Technologies, USA) gel was prepared in 1% Tris Borate EDTA (TBE) buffer (Sigma, USA) and heated in a microwave for ~60

seconds. After the agarose had fully dissolved with intermittent agitation, the mixture was then cooled at room temperature. Once the mixture had cooled, 10 μ l of Sybersafe dye (1000x) (Sigma, USA) was added and the gel was then poured into the gel apparatus and an appropriate comb was inserted. The gel was then left at room temperature to allow the agarose to set. Gels were run using 1x TBE solution as running buffer. 10 μ l PCR product / DNA samples were mixed with 2 μ l loading dye and loaded into the gel wells. Gels were run at ~100 Volts for 45 minutes. Analysis of electrophoresed samples was assessed by viewing on an ultraviolet transilluminator (UVP Inc., USA) and sized according to the 1kb DNA ladder (New England BioLabs, UK). If further band separation was required, the gel was placed in the electrophoresis equipment and electrophoresed for the desired time.

3.9 DNA extraction from agarose gel

Electrophoresed DNA was visualised under ultraviolet light and appropriate bands (2.1kb) were excised from the gel with clean scalpel. The DNA was then isolated from agarose gel using the QIAquick Gel Extraction system (QIAGEN, UK), following the manufacturer's standard protocol. After weighing, the excised gel fragments containing the band of interest were dissolved in 3x volumes of Buffer QG (supplied with the Kit), then incubated at 50°C for 10 minutes. After the gel slice had been dissolved completely, 1x gel volume of isopropanol (Sigma, USA) was added and mixed with the samples which were then washed with 750 μ l of Buffer PE (supplied with the Kit) to remove all traces of agarose and finally the DNA was eluted with 30 μ l of elution buffer. The quantity of the extracted DNA was evaluated by running 1 μ l of the samples on an agarose gel.

3.10 DNA/RNA quantification by spectrophotometry

The final extracted DNA/RNA were quantified on a NanoDrop ND-1000 UV-Vis Spectrophotometer (LabTech International Ltd, Ringmer, UK) (Appendix 9.2). Using a spectrophotometer, a 'blank' measurement was obtained reading sterile water at $\lambda 260\text{nm}$. Samples were analysed at $\lambda 260\text{nm}$ compared to the 'blank' result and all readings were measured by the ratio of $\lambda 260/\lambda 280\text{nm}$ to check the purity of the samples. A ratio of 1.8 – 2 was considered an indication of relative purity.

3.11 TA cloning and ligation of plasmids vectors and inserts

Cloning of HPRT and *Cten* coding sequences into pCR2.1 vector was done in order to use pCR2.1-HPRT and pCR2.1-*Cten* plasmids as templates to monitor their levels quantitatively in CRC cell lines. In addition, a pCR2.1-*Cten* plasmid was used to shuttle the *Cten* coding sequence into pCMVTag3B expression vector. In order to clone HPRT and *Cten* coding sequences in pCR2.1 vector, we follow the manufacturer's instructions applied with the TA Cloning Kit (Invitrogen, UK) which utilises the pCR2.1 vector which has single 3'-thymidine (T) overhangs that facilitates cloning of *Taq* polymerase-amplified PCR products into a plasmid vector. A 10 μl ligation reaction volume was done using 1 μl of pCR2.1 vector, 1 μl 10x Ligation Buffer, 1 μl of T4 DNA Ligase (4 Weiss units) and finally water was added to make a total volume of 10 μl reaction.

The amount of insert (i.e. PCR product needed to ligate with 50ng of pCR2.1 vector) was calculated using the following formula:

$$\text{Xng insert} = \frac{(\text{Y bp PCR product}) (50\text{ng pCR2.1 vector})}{(\text{size in bp of the pCR2.1 vector})}$$

Where Xng is the amount of PCR product of Y base pairs to be ligated for a 1:1 (vector:insert) molar ratio. The reaction mixture was then placed in ice for overnight.

3.12 Plasmid transfection

Plasmid transfection of competent bacterial cells (INV α F') (Invitrogen, UK) was done using the heat shock method. Fifty μ l vial of competent cells which were stored in -80°C freezer, were thawed on ice for 15 minutes. Two μ l of ligation reaction were added to the cells and gently mixed with a pipette tip. The cells were then incubated on ice for 30 minutes. Cells were then heat shocked by placing the tubes in a 42°C water bath for 30 seconds and directly transferred to ice. SOC media (supplied with Kit) was heated to 37°C and 250 μ l were added to the transformed cells which were then placed in a shaking incubator (New Brunswick Scientific Co. Ltd., USA) at 37°C for 1 hour. Between 50 – 250 μ l of the mixture were seeded onto 10cm Petri dishes (Costar, UK) containing 25ml LB agar (Sigma, USA), 25mg/ml ampicillin (Sigma, USA), 25mg/ml 5-bromo-4-chloro-3-indolyl- β -D-galactopyranoside (X-GAL), (Promega, UK) and 25mM Isopropyl β -D-1-thiogalactopyranoside (IPTG), (Promega, UK) for Blue-White screening before picking-up positive colonies. Seeded plates were then incubated at 37°C for overnight.

3.13 Plasmid Miniprep and Midiprep production

In order to generate plasmid DNA, the Gen Elute Plasmid Miniprep and Midiprep Kits were utilised following the standard manufacturer's protocol. For 'Miniprep' preparations, white positive colonies containing the desired plasmid were spiked with pipette tips and used to inoculate 5ml of LB broth (Sigma, USA), containing ampicillin (Sigma, USA) at a final concentration of 5mg/ml. For 'Midiprep', 1ml of the Miniprep growth was added to 500ml growth medium containing 50mg/ml ampicillin. The media was then incubated in the shaking incubator for overnight at 37°C to allow culture of the selected bacteria.

For 'Miniprep' preparations, the culture (3-5ml) was centrifuged for 1 minute at 13,000 rpm and the cell pellet was resuspended in 200µl of resuspension solution. This was then followed by alkaline lysis of the cell pellet through adding 200µl of Lysis solution. Then 350µl of Neutralizing/Binding solution was added to precipitate the cell debris and samples were centrifuged at 13,000rpm for 10 minutes, and then the supernatant was passed through a Gen Elute Miniprep Binding column. The columns were then washed by 750µl of washing solution and the DNA, which binds to the columns, was eluted by 50µl of Elution buffer.

For 'Midiprep' preparations, 100ml of bacterial cultural was used to obtain DNA plasmids using the same solutions used in Minipreps with slightly modified protocol in order to prepare greater volumes of plasmid DNA.

3.14 Glycerol stock preparation of bacterial cultures

LB broth cultures which had been used for generation of plasmid DNA were used to make cell stocks. Seven hundred and fifty µl aliquots of culture were mixed with 250µl

sterile 60% glycerol (Biomatik Corp, USA). Samples were placed in cryovials, labelled and stored at -80°C freezer.

3.15 Enzyme restriction digests

A single enzyme digest of the pCR2.1-Cten plasmid was done for plasmid screening to check for the presence of cloned PCR products. EcoR1 enzyme had been chosen, it cuts twice in the pCR2.1 vector before and after the insert. A 20µl restriction digest reaction volume was done using 2µg DNA, 1µl (EcoR1) restriction enzyme, 2µl enzyme specific 10X reaction buffer, 1µl BSA, and 10µl of sterile water to make a total reaction volume 20µl. The reaction mixture was then incubated at 37°C water bath for 3hours and run on a 1% agarose gel.

3.16 Cloning Cten coding sequence into an expression vector

Sequential 5'-BamH1 and 3'-HindIII enzyme digestion of pCR2.1-Cten plasmid and pCMVTag3B vector was done for shuttling the Cten insert from pCR2.1-Cten plasmid into pCMVTag3B expression vector as well as for creating sticky ends on pCMVTag3B expression vector respectively. The reactions were performed by follow the same protocol used in TA cloning. The corresponding bands were viewed and excised under Ultraviolet light and gel-purified using QIAquick Gel Extraction Kit according to the manufacturer's protocol as described before. The isolated Cten insert was ligated into pCMVTag3B vector at 1:1, 1:3 and 1:5 vector:insert ratios. Two negative controls (vector only and insert only) were also set up to make sure that pCMVTag3B was completely digested and did not religate again. Bacterial

transformation, Purification of pCMVTag3B-Cten plasmid DNA, and Enzyme digest were done according to the manufacturer's protocol as described before.

3.17 Sequencing

In order to know the orientation of the insert within the pCR2.1 vector and detect any mutations, 12µl from pCR2.1-Cten plasmid had been sent for sequencing. Since the size of PCR products using the pCR2.1-Cten plasmid and pCR2.1 vector T7 forward and M13 reverse primers were about 800 base pairs for each and giving that the size of Cten mRNA coding sequence was 2.1 KB, other primers that encode the rest of Cten coding sequence were designed and sent with pCR2.1-Cten plasmid for sequencing. The data for sequencing were analysed using chromas lite program (193).

3.18 Protein extraction and quantitation

Cells were grown to confluence in 75cm² flasks (Costar, UK), washed with cold PBS to remove excess culture medium. The PBS was then removed and the whole cell extraction was prepared in 465µl lysis buffer [(20 mM Tris, pH 7.5, 150 mM NaCl, 1% TritonX-100, 0.5% sodium deoxycholate, 1 mM EDTA, 0.1% SDS, supplemented with 30µl protease and 5µl phosphatase inhibitors (Sigma, UK)]. The mixture was then incubated at an angle in ice for 10 minutes, and then collected together using a cell scraper (Costar, UK), transferred to a 1.5ml eppendorf tubes and centrifuged at 13,000rpm at 4°C for 20 minutes. Finally, the supernatant was collected, aliquoted into 0.5ml eppendorf tubes and store at -20°C.

Protein quantitation reactions were done using BCA Protein Assay Kit (Thermo scientific, UK). A series of bovine serum albumin (BSA) solutions in the concentration range of 25–2000 µg/ml was used as a standard reference range. The buffer solution was used as a blank sample. Ten µl of each sample, standard and blank was pipetted into the 96 microplate wells (Costar, UK) as triplicates. Then 200µl of a 1:50 dilution of Reagent B: Reagent A was added to each well and the plate was shaken for 30 seconds and then incubated at 37°C for 30 minutes. After cooling the plate to room temperature, the absorbance at λ 550nm was measured on SpectraMax microplate reader (Molecular Devices, USA).

3.19 Western Blotting (WB)

The SDS-polyacrylamide gel used in WB consisted of two parts: a lower resolving gel and an upper stacking gel. The lower resolving gel consisted of 10% polyacrylamide (Bio-Rad Laboratories, UK) in buffer solution (1.5M Tris-base (Bio-Rad Laboratories, UK) / 0.4% SDS, pH 8.8). The upper stacking gel consisted of 5% polyacrylamide in buffer solution (0.5M Tris-base / 0.4% SDS, pH 6.8). The gel was then left at room temperature for 30 minutes to be polymerised and then transferred to the electrophoresis unit containing 500ml 1x Tris-Glycine electrophoresis buffer (0.025M Tris base / 0.192M Glycine (Bio-Rad Laboratories, UK) / 0.1% SDS). Thirty µg proteins were prepared by adding an equal volume of 2x SDS loading buffer (100mM Tris-HCl (pH 6.8), 200mM DTT, 4% SDS, 0.2% glycerol and 0.2% bromophenol blue) containing 5% Beta-Mercaptoethanol. The samples were boiled for 5 minutes and then run on an SDS-polyacrylamide gel at 60mA. After electrophoresis, the protein samples were transferred onto PVDF membranes (Stratagene, USA) by the process of semi-dry transfer at 66mA for 2 hours. After blocking in 5% Marvel dried

milk dissolved in 0.1% Tris. Tween. Buffered Saline (20 mM Tris, pH 7.5, 0.1 M NaCl, 0.1 %) (Bio-Rad Laboratories, UK) for 1 hour, membranes were incubated overnight at room temperature with the following primary antibodies. Rabbit anti-Cten (1:1500) (40), rabbit anti-ILK antibody (Abcam, UK, ab2283, 1:500), rabbit anti-FAK antibody (Cell signalling, USA, 1:1000), rabbit anti-phospho-FAK (Cell signalling, USA, 1:1000), mouse anti-E-Cadherin (Abcam, UK, ab1416, 1:500), mouse anti-CD24 SWA11 (a kind gift from Prof. Peter Altevogt, 1:1000) and mouse anti- β -actin (Dako, UK, 1:2000). After three washes in 0.05% Tris. Tween. Buffered Saline, blots were incubated for 1 hour at room temperature with the appropriate horseradish peroxidase-linked secondary antibody. After three further washes, detection was performed using the Enhanced Chemiluminescence Kit (Pierce, USA). Bands were visualised using X-Ray films (Kodak, UK). In order to ensure accurate evaluation of protein loading, whenever possible (i.e. when the molecule of interest was sufficiently separated from the loading control), the membrane was cut in half and each section was blotted probed separately for the molecule of interest and the loading control (usually β -actin). This was performed for E-cadherin, Cten, CD24, ILK and FAK. However, occasionally, the amount of total protein loaded in order to identify the molecule of interest had to be considerable which resulted in the β -actin appearing over-exposed (despite minimum exposure to the x-ray film). This did not affect data interpretation. All experiments to demonstrate changes in expression of specific molecules were performed on at least two separate occasions.

3.20 Epifluorescence Microscopy

Stably transfected HCT116 cells were grown on glass coverslips and then fixed with 3.7% paraformaldehyde (PFA) for 15 minutes at room temperature. Cells were permeabilized with 0.1% Triton X-100 for 10 minutes and then incubated with DAPI (0.04µg/ml, Dako) for 5 minutes. After rinsing with PBS, coverslips were mounted on glass slide using Dako aqueous mountant and fluorescence was visualised with an epifluorescence microscope (Leica microsystems, Switzerland). Images were taken using green fluorescence 590nm emission filter for GFP and blue fluorescence 515nm emission filter for DAPI.

3.21 Proliferation Assay

Proliferation experiments were performed to monitor cell growth over a period of up to 7 days. Each well of a 6 well plate (Costar, UK) was seeded with 1×10^5 cells and cell numbers measured at specific time points using the Methylene Blue assay (194). Cells were firstly fixed in 100µl methanol for 30 minutes. Methanol was then removed and cells air dried for 5minutes followed by addition of 100µl of 1% Methylene Blue (Sigma, USA) for 30 minutes. The methylene blue solution was aspirated and wells washed 4x with distilled water. Finally 100µl of 0.1% HCl in ethanol was added to release the methylene blue and absorbance measured at 620 nm wavelength on a platereader (Labsystems, UK). Each assay was performed in triplicate and repeated in at least two independent experiments.

3.22 Staurosporine induced apoptosis

Staurosporine is commonly used to induce apoptosis in cells and was used to test the resistance to apoptosis conferred by *Cten*. Each well of a 96 well plate (Costar, UK)

was seeded with 5×10^4 cells which were incubated with staurosporine (Sigma, USA) at a final concentration of $6 \mu\text{M}$ for 24 hours. After this period, floating cells were aspirated from each well, spun down, resuspended in $100\mu\text{l}$ of TBS and an equal volume of 0.1% Trypan blue (Sigma, USA) added. Cells showing positive staining for Trypan blue (i.e. apoptotic cells) were counted manually using a haemocytometer (Sigma, USA). Living cells attached to the bottom of the wells were counted using the Methylene Blue assay as described above. The apoptosis assay was performed in triplicate and repeated in at least two independent experiments.

3.23 Cell Migration / Invasion Assays

Cell migration was measured using the transwell migration assay and cell wounding assay. The transwell migration assay used a Boyden chamber containing a polycarbonate filter with an $8 \mu\text{m}$ pore size (Costar, UK). The lower chamber was filled with $200\mu\text{l}$ of DMEM with 20% FCS; the upper chamber was filled with $100\mu\text{l}$ of DMEM with 10% FCS and seeded with 1×10^5 cells. Migration was assessed after 48 hours by fixing the cells attached to the lower surface in 10% methanol for 30 minutes, staining for 30 minutes with Methylene Blue and manually counting the stained cells. Cell invasion was measured in the same way as described for migration except that the upper chamber was prepared by coating the filter with $100\mu\text{l}$ of Matrigel (5mg/ml, BD Biosciences, USA). Cell migration was also measured using a cell wounding assay performed in 6 well plates (Costar, UK). Cells were grown to confluence and then starved for 24 hours in serum free medium. A sterile $200\mu\text{l}$ pipette tip was used to create three separate parallel wounds and migration of the cells across the wound line was assessed after 24 hours. Photographs were taken using a charge coupled device (CCD) camera (Canon, Japan) attached to the inverted phase-contrast

microscope at a power of 40x. In order to statistically analyse cell migration in the wounding assay, images were taken from three separate wounds 24 hours after commencement of the assay. All images were taken at the same magnification and converted into binary images using the ImageJ image analysis program (195) and the area of the wound was measured. Experiments were repeated on two separate occasions. Cell motility assays were performed in triplicate and on two separate occasions.

3.24 Construction of TMA sets

A TMA set had been generated for pancreatic cancer. H&E slides of 64 cases (including 44 cases of pancreatic adenocarcinoma and 20 cases of chronic pancreatitis from (1996-2007) had been reviewed to confirm a histological type of tumour, as well as lymph nodes (LN) metastasis. Normal pancreatic tissue was obtained from the resection specimens in a total of 30 patients. After matching areas on the slides with their corresponding areas on the blocks, marker pen was used to mark those representative areas on the blocks from which the array core will ultimately be taken.

Preparation of recipient blocks was done by pouring paraffin wax into a mould, and placing a histopathological tissue cassette on top, when the wax became cold, the mould was removed. Excess wax was trimmed from the cassette using a microtome to produce a flat surface that made TMA easier and accurate.

Once all donor blocks were marked, and the recipient blocks had been prepared, templates for the array were prepared in order to accommodate 144 samples or cores (12x12) per slide. Samples were done in triplicate and spaced 1.25mm apart to avoid

cracking of the paraffin. The orientation was determined by adding 2 cores of lung tissues at the starting corners.

Before sectioning, the array blocks were placed in a 37°C incubator for 10 minutes. This warmed the paraffin wax thereby promoting adherence of the tissue cores to the walls of the holes in the array blocks, and makes the wax flexible to handle. After that a clean glass microscopic slides were placed on top of the array blocks, and applied even pressure to push all tissue cores level with the top surface of the array. Finally the blocks have been sectioned using standard laboratory microtome techniques.

Another TMA set was also prepared for this study. This contained matched tissue samples from primary colorectal adenocarcinoma and their corresponding liver metastases which collected from 40 patients, diagnosed between 1993 and 2009 and entered into the Nottingham Colorectal Carcinoma Series and prepared as a TMA series.

A BC TMA set, kindly provided by Prof. Ian Ellis (Division of Pathology, University of Nottingham, UK), was available for this study and prepared from a series of 1,409 cases of primary operable invasive breast carcinoma from patients under the age of 70 years, diagnosed between 1987 and 1998 and entered into the Nottingham Tenovus Primary Breast Carcinoma Series. Patients' clinical and pathological data including patients' age, histological tumour type, primary tumour size, LN status, mitotic count, histological grade, Nottingham prognostic index (NPI), vascular invasion (VI), and development of recurrence and distant metastases (DM) were available and maintained on a prospective basis. Survival data including breast cancer specific survival (BCSS) and disease-free interval (DFI) were available. The BCSS is defined as the time (in

months) from the date of the primary surgery to the time of death from breast cancer. DFI is defined as the duration (in months) from the date of the primary surgical treatment to the appearance of first loco-regional or distant metastasis. The data on other biomarkers of known clinical and biological relevance to BC including estrogen receptor (ER), progesterone receptor (PR), androgen receptor (AR), BRCA1, p53, the proliferation marker MIB1, E-cadherin, P-cadherin, EGFR, HER1, HER2, basal and luminal cytokeratins (CKs) (CK5/6, CK14, CK18, CK19) were also available (196-201). The patients' characteristics are summarised in Table 3 (Appendix 9.3).

A CRC TMA set, kindly provided by Prof. Lindy Durrant (Division of Oncology, University of Nottingham, UK), was also prepared from a series of 462 cases of primary operable CRC from patients underwent elective surgery at Nottingham University Hospital between 1994 and 2000 as has been previously described (202). All patients with radical (R0) resected CRC were included. Patients' clinical and pathological data including primary tumour site, TNM stage, histological tumour type, histological grade and the presence of VI were available and maintained on a prospective basis. Adjuvant chemotherapy consisting of 5-fluorouracil and folinic acid was administered to patients with LN metastasis. The UK Office for National Statistics has provided comprehensive disease specific and follow-up data for all cases in the study. The length of follow-up was calculated from the date of surgery, with surviving cases censored for analysis on the 31st December 2003. Disease-specific survival was used as the primary end-point. Ethical review of the study was conducted by the Nottingham Local Research and Ethics Committee, who granted approval for the study as previously described (203). The patients' characteristics are summarised in Table 4 (Appendix 9.4).

3.25 IHC

Slides were immunohistochemically stained using the standard streptavidin–biotin complex method as previously described (204). Water bath-induced method for retrieval of antigen was performed in EDTA buffer, at pH 8.0. Endogenous peroxidase activity was blocked with 0.3% hydrogen peroxide (Dako, UK) for 10 minutes and non-specific antibody binding with normal swine serum (NSS) (Dako, UK) for an additional 10 minutes at room temperature. Then primary antibodies Cten (Abcam, UK, ab57940, 1:75) and P-FAK (Cell signalling, USA, 1:100) were applied for 45 minutes at room temperature. After washing with TBS, biotinylated secondary (C) antibody (Dako, UK) (diluted 1/100 in NSS) was applied and incubated for 30 minutes at room temperature. Slides were then washed with TBS and preformed Strept AB Complex (AB) (Dako, UK) (diluted 1/100 in NSS) was applied for 55 minutes at room temperature. After washing with TBS, slides were incubated using freshly prepared Diaminobenzidine (DAB) (Sigma, USA) solution for 10 minutes at room temperature. After that, copper sulphate (Dako, UK) solution was applied for 10 minutes at room temperature. After immunostaining, slides were counterstained with haematoxylin (Dako, UK). Histochemical score (H-score) was used to assess the intensity and percentage of stained cells across the TMA sets. Only staining of the malignant cells within the tissue cores was considered. Staining intensity was scored from zero to three, (zero equals no staining, one equals weak, 2 equals moderate, three equals strong). The percentage of positive cells was subjectively estimated and scored from 0 to 100%. Percentage staining was multiplied by corresponding intensity with products added representing the H-score ranging from 0-300. Samples were done in triplicate and the average score was taken to represent each patient's tumour score. Sections from normal kidney tissue, which represent an internal positive control for Cten were

used to standardised the intensity of scoring across replicates of the array. Immunostaining was reviewed by two Histopathologists (M. Ilyas, A. Albasri) without prior knowledge of the clinicopathologic data or the patient outcome. This was done independently and the average score was taken. The semi-quantitative system was used for scoring tumour samples on whole tissue sections. This system basically used an ordinal score scale of 0 = no staining, 1 = weak staining, 2 = moderate staining, 3 = intense staining.

3.26 *In vivo* tumourigenesis study

Cells were re-suspended, for *in vivo* administration, in sterile PBS, at pH 7.4 and 1×10^6 cells per mouse was administered by intrasplenic injection in a volume of 500 μ l into male MF1 nude mice (Harlan-Olac). Three groups were used in this study: group 1: HCT116 wild type, group 2: HCT116 GFP control and group 3: HCT116 GFP-*Cten*. The intra-splenic injections were performed by Dr Rajendra Kumari, Division of Pre-Clinical Oncology, Nottingham University.

Mice were maintained in sterile isolators within a barriered unit illuminated by fluorescent lights set to give a 12 hour light-dark cycle (on 07.00, off 19.00) at air temperature range of $23 \pm 2^\circ\text{C}$ as recommended in the United Kingdom Home Office Animals (Scientific Procedures) Act 1986. Mice were housed in social groups during the procedure in plastic cages (Techniplast, UK) with irradiated bedding. Sterile irradiated 2019 rodent diet (Harlan Teckland, UK) and autoclaved water was offered *ad libitum*. An experienced technician checked the condition of the mice daily and weighed the mice weekly. The project was run under Home Office project PPL 40/2962 which was awarded in November 2006 (Watson) following local ethical approval. The study also adhered to the UK Co-ordinating Committee for Cancer

Research (UKCCCR) guidelines.

On day 42 mice were sacrificed by approved S1 method and the spleen, liver and lung were dissected and examined for orthotopic tumors and DM. All tissues were stained with hematoxylin and eosin and slides were scanned at x 20 using the NanoZoomer 2.0 (Hamamatsu Corporation, Japan). The tumour volume was obtained using the NanoZoomer Digital Pathology Image (NDPI) software (Hamamatsu Corporation, Japan).

3.27 Statistical analysis

Statistical analysis was performed using SPSS 16.0 statistical software (SPSS Inc. USA). All evaluations were done using the unpaired two-tailed Student's *t*-test. Association between the *Cten* immunoreactivity expression and different clinicopathological parameters was evaluated using Chi-square test. Determination of the optimal *Cten* cut-off was performed using X-tile bioinformatics software, version 3.6.1, 2003–2005, (Yale University, USA) (205). Survival curves were analysed by the Kaplan–Meier plot with a log rank test to assess significance. Multivariate Cox hazard analysis was used to test the statistical independence and significance of the variables. A p-value of <0.05 was considered significant.

RESULTS

Results

Chapter 4. Evaluation of expression of *Cten* in benign colorectal diseases and CRC

4.1 Introduction

As described earlier in the first chapter, it appears that the function of *Cten* protein is tissue-specific. *Cten* is located on chromosome 17q21, a region often deleted in prostate cancer (8). In addition, previous studies have shown that *cten* is down-regulated in prostate cancers, and it is cleaved by caspase-3 during apoptosis (8, 40). Moreover, *Cten* restores the tumour suppression activity of DLC-1 via recruiting it to focal adhesions, suggesting the tumour suppression function of *Cten* in certain tissues (55). However, it has been found that although *cten* is not normally expressed in some tissues, its expression is up-regulated when these tissues become cancerous. Recently, studies have shown that *cten* might possess an oncogenic activity in certain tissues. *Cten* is up-regulated in thymomas, lung and gastric cancers compared to normal tissues, and in general, its over-expression is associated with poor prognostic outcomes (56, 57, 24). The role of *Cten* in CRC is uncertain and thus, we sought to investigate the *Cten* expression during the development of CRC and ascertain whether this expression has any prognostic implications in CRC.

4.2 Evaluation of expression of *Cten* in non-neoplastic colorectal diseases (normal and IBDs)

In order to evaluate the *Cten* protein expression in non-neoplastic colorectal diseases, ten cases of normal tissue (from tumour edges) and 15 cases of IBDs (7 cases of CD and 8 cases of UC) were analysed immunohistochemically using standard techniques (see chapter 2). Slides were designated positive if >10% cells showed expression of *Cten*.

Evaluation of *Cten* protein expression on whole tissue sections containing both IBDs and normal mucosa revealed a complete lack of the *Cten* expression in normal colonic epithelium apart from weak cytoplasmic staining which was seen in occasional crypts (Figure 11). Similarly, 3/15 (30%) of IBDs cases showed negative *Cten* expression. In contrast, moderate apical cytoplasmic *Cten* immunoreactivity was seen in 12/15 (70%) of IBDs (Figure 12). No cell membrane, nuclear or stromal expression of *Cten* was detected in any of the examined cases.

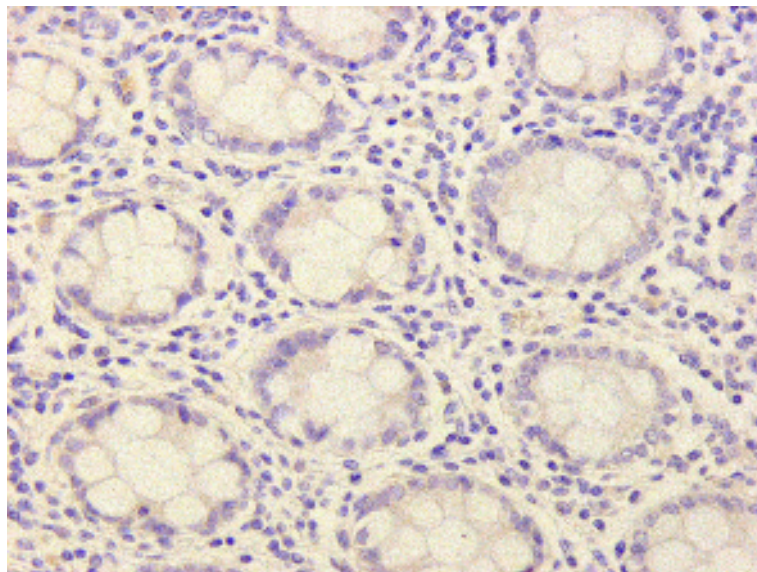


Figure 11. *Cten* immunostaining in normal colonic tissue. Immunohistochemical staining for *Cten* on normal colonic tissue (x200), demonstrating negative staining of *Cten* in normal crypts.

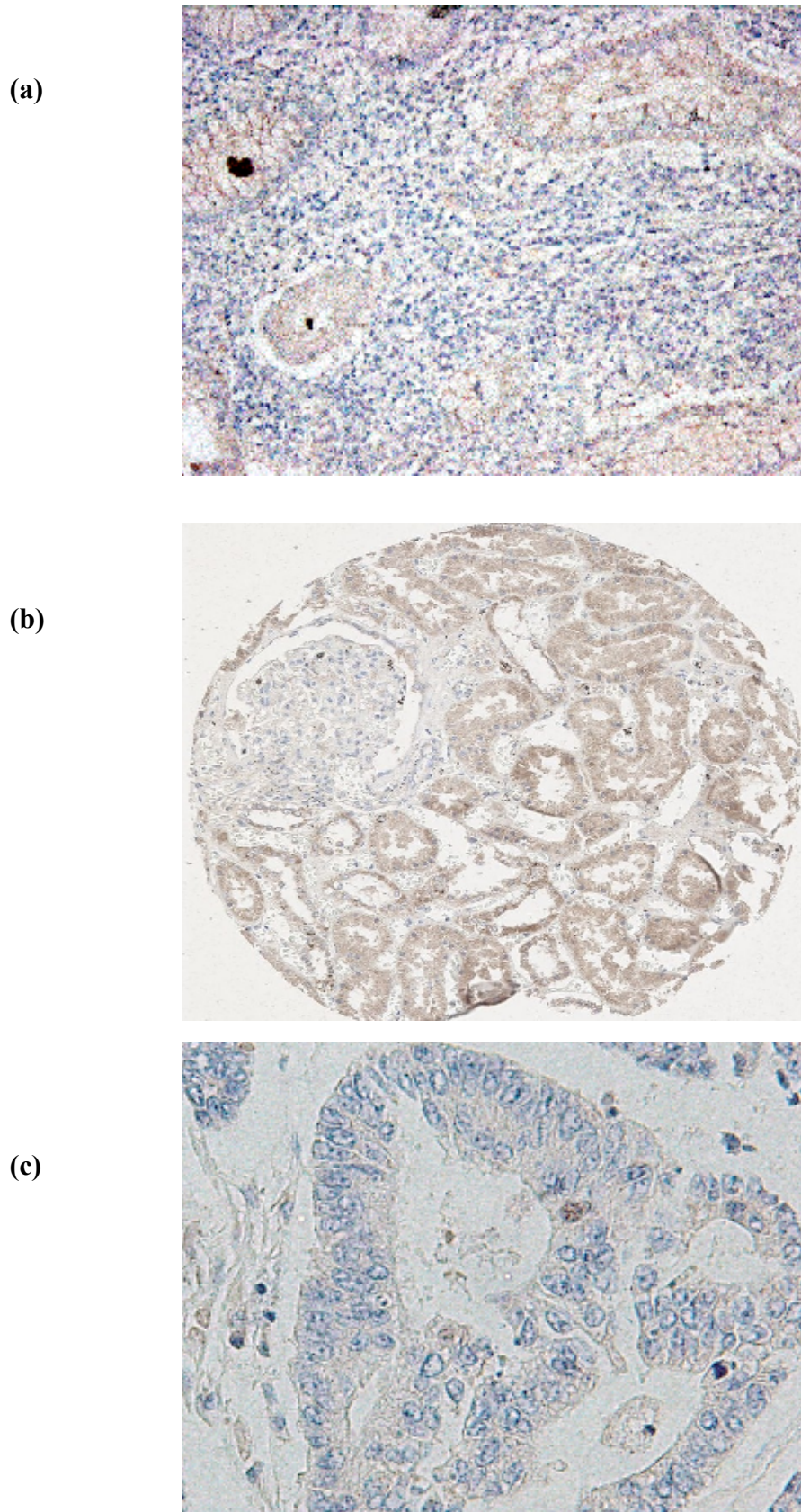


Figure 12. Cten immunostaining in non-neoplastic colorectal diseases. (a, x200), Moderate Cten cytoplasmic staining in IBDs. (b, x100) Sections from normal kidney tissue representing an internal positive control for Cten. (c, x200) Negative control.

4.3 Evaluation of expression of *Cten* in benign colorectal diseases

Cten expression was tested in whole tissue sections containing 20 cases of colorectal adenomas with low grade dysplasia using IHC. Moderate apical cytoplasmic *Cten* expression was seen in 19/20 (95%) of colorectal adenomas (Figure 13). In contrast, no cell membrane, nuclear or stromal expression of *Cten* was detected in any of the examined cases.

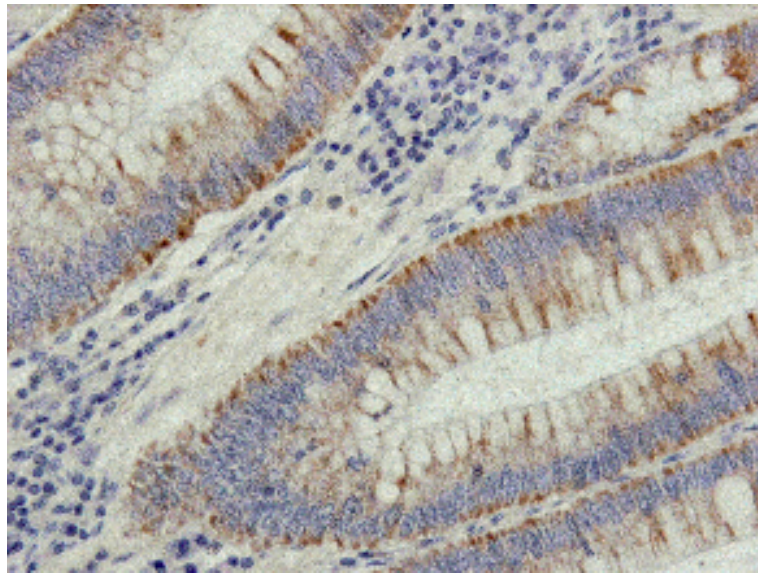


Figure 13. *Cten* immunostaining in colorectal adenomas. Immunohistochemical staining for *Cten* on whole tissue sections of colorectal adenomas (x200), demonstrating moderate apical cytoplasmic *Cten* expression.

4.4 Evaluation of expression and role of Cten in CRC

The up-regulation of Cten protein levels in colorectal adenomas and IBDs prompted us to investigate the level of Cten expression in CRC. We would also correlate that with the prognostic data in order to see if Cten has any prognostic implication in CRC.

4.4.1 Cten expression in CRC

After excluding the uninformative TMA cores (120) from the study, which were either lost, folded, fragmented or did not have invasive tumour tissue, 342 tumours were available for Cten immunostaining assessment. Of these, 25 cases were excluded due to unavailability of survival data for them. The staining pattern for Cten in tumour cells was homogenous cytoplasmic staining (Figure 14). In the whole series, 317/342 (92.6%) of the tumours showed expression for Cten. Patchy focal nuclear staining was seen in 37/342 (10.8%) of cases (Figure 15). In contrast, no tumour cell membrane or stromal expression of Cten was noticed in any of the examined cases. The X-tile bio-informatics software was used to define optimal cut-off points of Cten H-score values (<150, negative/low; \geq 150, moderate/strong expression). This program basically divides the total patient cohort randomly into two separate equal training and validation sets ranked by patients' follow-up time. The optimal cut-points were determined by locating the brightest pixel on the X-tile plot diagram of the training set. Statistical significance was tested by validating the obtained cut-point to the validation set.

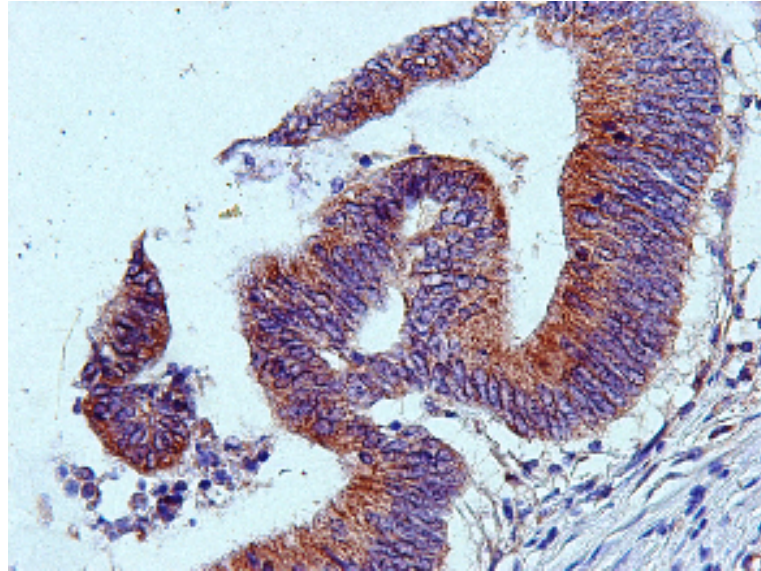


Figure 14. Cten protein expression in CRC. Immunohistochemical staining for Cten on CRC (x200), demonstrating strong cytoplasmic Cten expression.

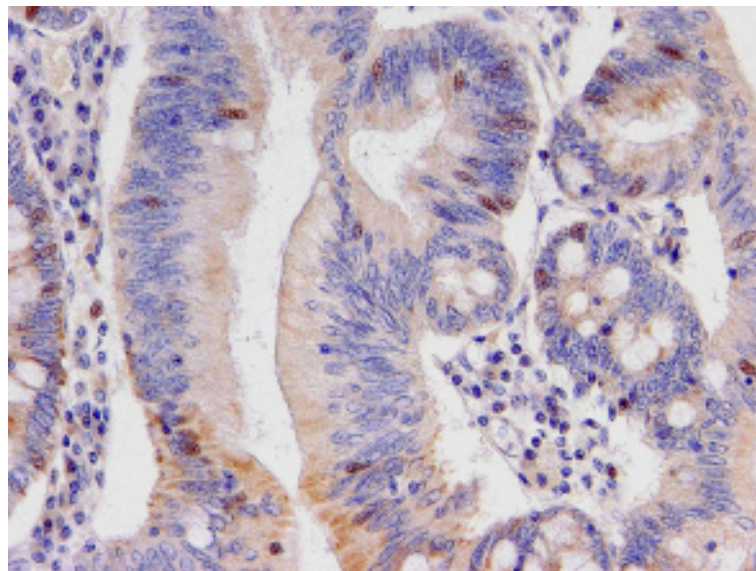


Figure 15. Cten immunostaining in CRC. Immunohistochemical staining for Cten on CRC (x200), demonstrating patchy focal Cten nuclear staining in some cases.

4.4.2 Association of *Cten* cytoplasmic expression with clinicopathological parameters

The association between *Cten* cytoplasmic expression in CRC and clinicopathologic variables is summarised in Table 5. The difference was analysed by the chi-square test, revealing that tumours with high *Cten* expression were associated with advanced Dukes stage, more frequent LN metastasis, extra-mural VI and more prone to metastasis. Firstly, high *Cten* expression was significantly correlated with advanced Dukes stage ($p=0.001$; chi-square test). Three of 62 (4.8%) and 45 of 252 (17.9%) tumours in the high/low *Cten* expression groups had Dukes stage A respectively. In contrast, 15 of 62 (24.3%) in the high *Cten* expression group had Dukes stage D compared with 27 of 252 (10.7%) in low *Cten* expression group. Secondly, regarding LN involvement, the frequency LN metastasis was significantly higher ($p<0.001$; chi-square test) in the high *Cten* expression group with an incidence rate of 35% (20 of 57) compared with a rate of 15.8% (38 of 241) for the low *Cten* expression group. Additionally, the incidence of VI was significantly higher ($p=0.001$; chi-square test) in the high *Cten* expression group (38 of 62 patients, 61.3%) than in the low *Cten* expression group (81 of 249, 32.5%). Finally, the incidence of DM was also significantly higher ($p=0.008$; chi-square test) in the high *Cten* expression group (15 of 62 patients, 24.2%) than in the low *Cten* expression group (26 of 250, 10.4%). There were no significant differences in patients' age, gender, tumour histological type, tumour grade and tumour site between the high and low expression groups.

Table 5. Clinical and pathological correlates of *Cten* expression. High *Cten* expression was associated with advanced disease and poor prognostic features.

Parameter	Low <i>Cten</i>	High <i>Cten</i>	χ^2	p value	Total NO.
Patient age (years)					
< 65	33 (13%)	10 (16.1%)	0.312	0.593	314
65-80	187 (74.3%)	44 (70.9%)			
> 80	32 (12.7%)	8 (13%)			
Gender					
Female	107 (42%)	23 (37%)	0.488	0.485	317
Male	148 (58%)	39 (63%)			
Tumour histological type					
Adenocarcinoma	224 (90%)	52 (85%)	2.450	0.291	310
Non-adenocarcinoma	25 (10%)	9 (15%)			
Tumour grade					
Well differentiated	18 (7.2%)	3 (5%)	0.267	0.872	309
Moderately differentiated	196 (79%)	49 (80.3%)			
Poorly differentiated	34 (13.8%)	9 (14.7%)			
Tumour site					
Colon	121 (53%)	33 (57.9%)	0.806	0.848	285
Rectum	107 (47%)	24 (42.1%)			
Dukes stage					
A	45 (17.9%)	3 (4.8%)	16.318	0.001	314
B	100 (39.7%)	17 (27.4%)			
C	80 (31.7%)	27 (43.5%)			
D	27 (10.7%)	15 (24.3%)			
LN stage					
0	148 (61.4%)	18 (31.7%)	18.536	<0.001	298
1	55 (22.8%)	19 (33.3%)			
2	38 (15.8%)	20 (35%)			
VI					
Negative	168 (67.5%)	24 (38.7%)	11.436	0.001	311
Positive	81 (32.5%)	38 (61.3%)			
DM					
Negative	224 (89.6%)	47 (75.8%)	9.616	0.008	312
Positive	26 (10.4%)	15 (24.2%)			

Note: The analysis has been done in a patient of cohort of 317 cases with CRC. If the total number of cases in a given parameter did not add up to 317, this indicates that there were no data available for the missed cases of each specific factor.

4.4.3 Association of *Cten* cytoplasmic expression with patients' outcome

Kaplan-Meier survival analysis showed that patients with high *Cten* expression had a significantly poorer prognosis than patients with low *Cten* expression. High *Cten* expressing tumours had shorter DFS than those with low *Cten* expression ($p < 0.001$; log-rank test, Figure 16). However, multivariate Cox proportional hazard analysis including tumour size, LN status and DM occurrence (TNM) stage, VI and *Cten* expression revealed that there was a trend towards *Cten* expression as an independent predictor of DFS in CRC (hazard ratio 1.559, 95% CI 0.963–2.526, $p = 0.071$, Table 6).

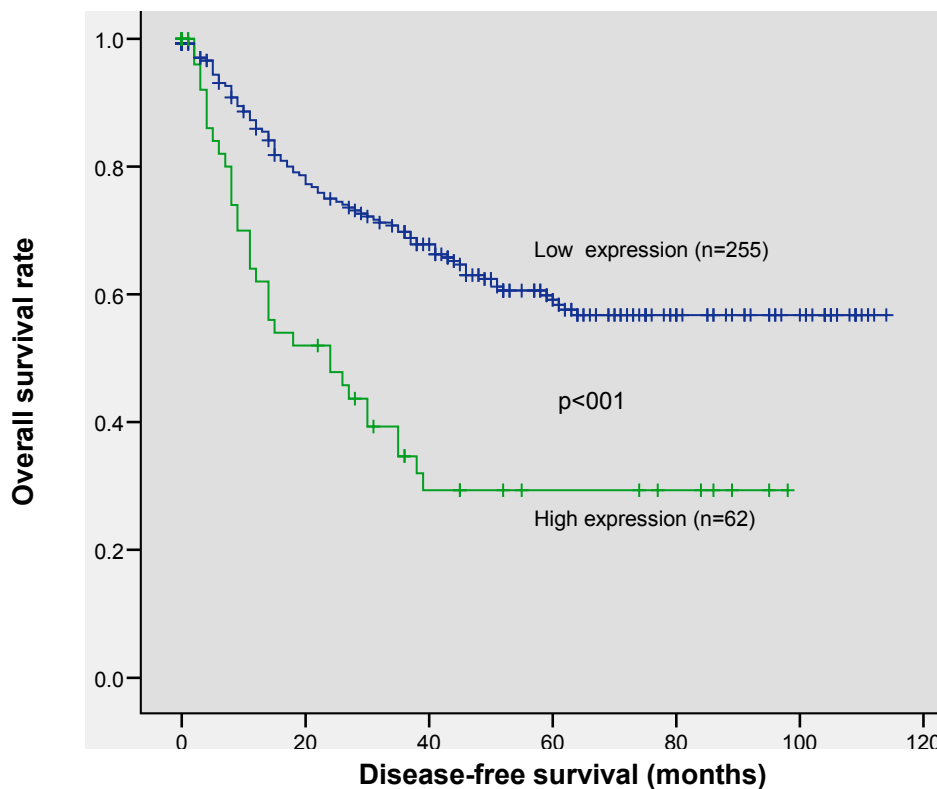


Figure 16. Kaplan-Meier plot for DFS in relation to expression of cytoplasmic *Cten*. Patients with high *Cten* expression had a significantly shorter DFS than patients with low *Cten* expression ($p < 0.001$; log-rank test). The data were right censored at 120 months and so all cases had 120 months follow up. The two survival lines are not the same length because none of the high *Cten* cases lived beyond 100 months. Only the Stage III tumours (Dukes' C) had chemotherapy and so this was not included in the analysis.

Table 6. Cox-proportional hazard analysis for predictors of DFS and *Cten* expression. Multivariate Cox hazard analysis including TNM, VI and *Cten* expression shows a trend towards *Cten* expression as an independent predictor of DFS in CRC (hazard ratio 1.559, 95% CI 0.963–2.526, p=0.071).

Parameter	Hazard ratio	95% CI	p value
Disease-free survival			
TNM	0.061	0.025–1.493	< 0.001
VI	1.985	1.275–3.091	0.002
<i>Cten</i> expression	1.559	0.963–2.526	0.071

4.4.4 Association of *Cten* nuclear expression with clinicopathological parameters and patient outcome

On further analysis 37/342 (10.8%) of cases showed *Cten* nuclear staining. There was no significant association between any level of *Cten* nuclear expression and known clinicopathological parameters, including patients' age ($p=0.741$; chi-square test), gender ($p=0.411$; chi-square test), tumour histological type ($p=0.597$; chi-square test), tumour grade ($p=0.777$; chi-square test), tumour site ($p=0.761$; chi-square test), Dukes stage ($p=0.565$; chi-square test), LN metastasis ($p=0.997$; chi-square test) and DM ($p=0.437$; chi-square test). Furthermore, on Kaplan-Meier analysis, no significant association was found between *Cten* nuclear expression and DFS ($p=0.878$; log-rank test, Figure 17).

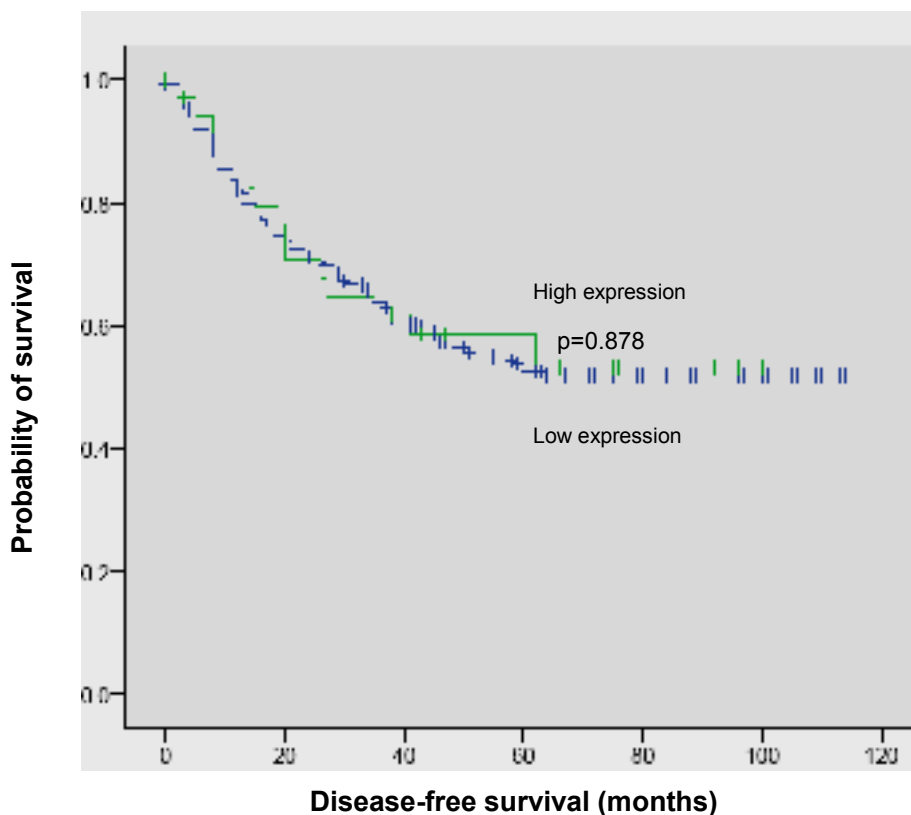


Figure 17. Kaplan-Meier plot for DFS in relation to expression of nuclear *Cten*. Kaplan-Meier graph showing no significant association between *Cten* nuclear expression and DFS ($p=0.878$; log-rank test) in CRC.

4.5 Evaluation of expression of Cten in metastatic tumours

Tumours with high Cten expression were associated with poor prognostic features such as advanced Dukes stage, more frequent LN metastasis, and extra-mural VI. Multivariate analysis however showed that high Cten expression was an independent prognostic factor. There was also an association of high Cten expression with distant metastasis and to further investigate this, another independent series of 40 cases of paired primary CRC and corresponding hepatic metastasis deposits was tested for Cten expression by IHC. Cten cytoplasmic staining was scored using the H-score system. Samples were done in triplicate and the average score was taken to represent each patient's tumour score. Both primary and metastatic tumours showed similar levels of cytoplasmic staining. However, metastatic deposits were significantly associated with a shift of Cten expression to the nucleus ($p=0.002$; Fisher's exact test, Figure 18 a, b).

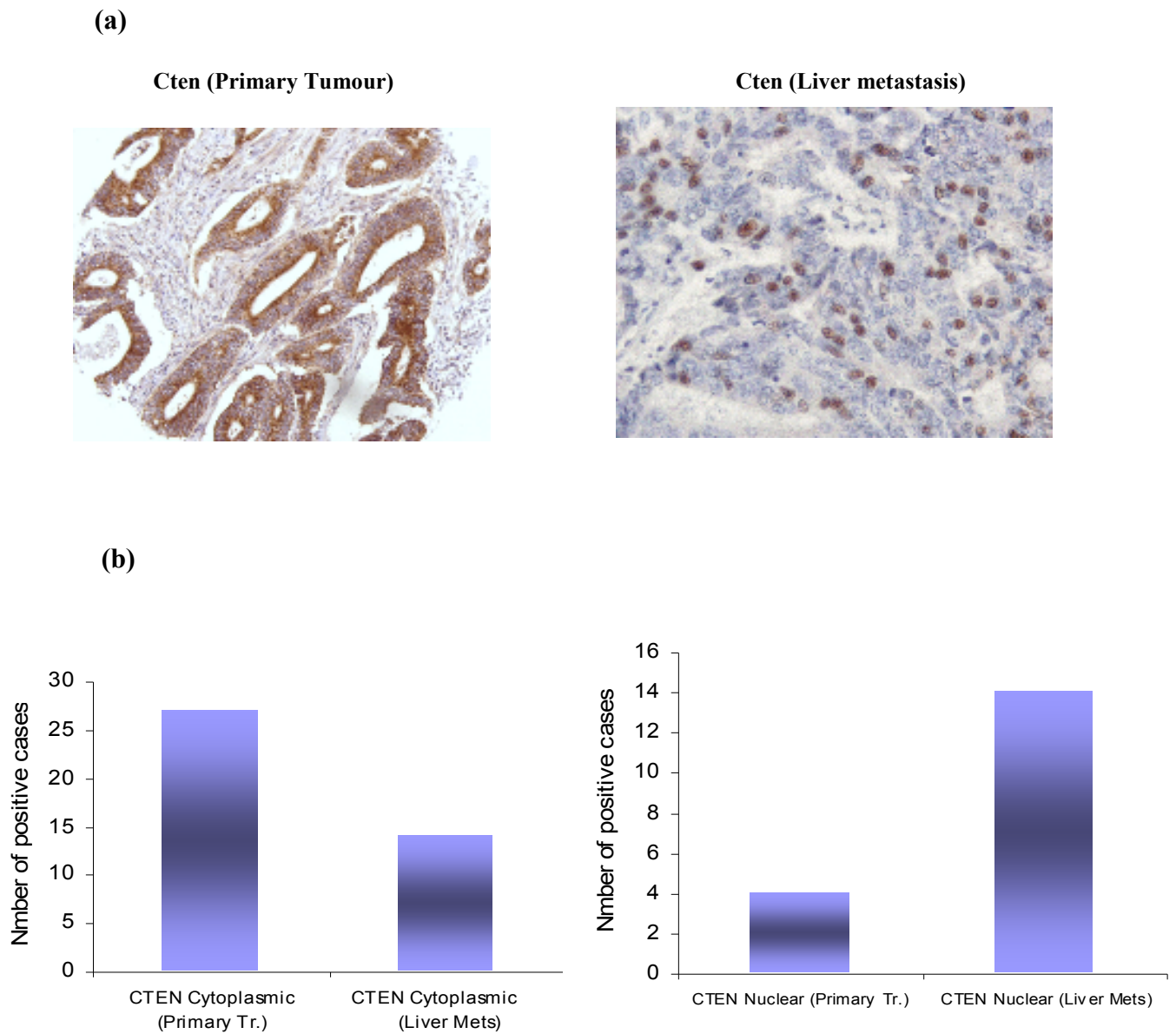


Figure 18. Cten protein expression in primary tumour samples and their corresponding liver metastasis. A. Cten immunostaining showing cytoplasmic Cten expression in primary tumours (x100) and nuclear Cten expression in metastatic tumours (x200). B. Positively stained TMAs showed that there was no significant difference between the primary tumour samples and the liver metastases regarding cytoplasmic Cten levels ($p=0.138$; Fisher's exact test), but interestingly, we found a highly significant difference in nuclear localisation of Cten between these TMA samples ($p=0.002$; Fisher's exact test).

4.6 Discussion

Our study involved evaluation of immunohistochemical staining of *Cten* in AP as well as in CRC. We detected a consistent up-regulation of *Cten* in 90% of colorectal adenoma with low grade dysplasia. Our findings are in agreement with previous studies reporting a 4.8-fold increase of *Cten* mRNA in colorectal adenomas compared with normal mucosa tissue (206). In addition, we have reported that normal colonic mucosa showed very low or almost negative *Cten* expression at protein levels. Taken together, this confirms that *Cten* is dramatically up-regulated in the early stages of colorectal tumour development.

IBD, in the form of CD and UC, is generally characterised by repeated episodes of extensive intestinal ulcerations and in each episode the inflammation is succeeded, eventually, by tissue healing whereby there is repair of the damaged mucosa or remodeling of the epithelium with, in some cases, restitution to near-normal original architecture (182). In order to achieve this, certain cellular processes must be activated. These involve an increase in cell numbers to replace the lost tissue, restitution by migration of epithelial cells from the wound margins and eventual filling and remodeling of the damaged area by proliferating epithelial and connective tissue cells to restore normal appearances (182). In this study we provide the first report of *Cten* up-regulation in regenerative mucosa in 70% of IBDs, indicating that *Cten* may play a role in regulating the regenerative process in colorectal diseases. It is possible that up-regulation of *Cten* in regenerating tissue is related to some of its other proposed functions, such as control of adhesion and migration. Our data from our forced expression and knock-down experiments concurred and showed that *Cten* appears to stimulate cell migration in both transwell migration assays and cell wounding assays

(see the next chapter for details). Enhanced cell migration may be important in wound healing by allowing epithelial cells to migrate to areas where epithelium has been lost (182).

In this study, we have also evaluated the expression of Cten protein using IHC in a large well-characterised cohort of CRC cases. This is the largest study to date pertaining to Cten protein expression in CRC and we found that around 90% of tumours expressed some level of Cten in the cytoplasm. Our series could be dichotomised into those with low Cten expression (H score <150) and high Cten (H score >150). We found that high cytoplasmic Cten expression was significantly associated with poor prognostic clinico-pathologic variables, including advanced Duke's stage, lymph node metastasis, extra-mural VI and DM. In addition, high Cten expressing tumours had shorter DFS than those with low Cten expression. However, multivariate Cox proportional hazard analysis including tumour size, LN status and DM occurrence (TNM) stage, VI and Cten expression showed that Cten expression was of borderline significance as an independent predictor of DFS in CRC. Recently published data have demonstrated that the C-terminal of the tensin family proteins contains an SH2 domain, allowing them to interact with certain tyrosine-phosphorylated proteins, such as PI3K, FAK and P130Cas, thereby regulating cell motility and migration (3, 8, 209). As Cten shares extensive homology with other tensin members at its C-terminus, it has been suggested that Cten may possibly affect diverse biological activities including cell motility and migration in a manner similar to that of the other tensin proteins. The high frequency of expression of Cten in adenomas has showed that up-regulation is an early event in the development of colorectal tumours. Taken together with the biological data on Cten, we may

conjecture that *Cten* is a motility associated molecule and may be involved in driving tumour progression and metastasis and could therefore represent a therapeutic target as well as a prognostic factor in patients with CRC.

Nuclear expression of *Cten* in CRC has been described in other studies and was confirmed in our study. However, the number of cases showing nuclear expression was small (10% of the total study group) and it was not associated with the known clinicopathological parameters of CRC. Only very small numbers of cases were available and thus it is likely that only strong effects will have been identified. The study was significantly underpowered to pick up moderate or weak associations. This study also revealed that nuclear *Cten* expression was significantly greater in the metastatic deposits than the primary tumours although there was no significant difference between the primary tumour samples and the liver metastases regarding cytoplasmic *Cten* levels. The functional implication of nuclear localisation of *Cten* has been investigated in a previous study (207). In this study *Cten* has been reported to interact with beta-catenin, a critical player in the canonical Wnt pathway. This interaction is critical for *Cten*-mediated effects on colony formation, anchorage-independent growth, and invasiveness of colon cancer cells (207).

Chapter 5. Evaluation of the function of Cten in CRC

5.1 Introduction

Our immunohistochemical analysis showed that there is up-regulation of Cten in colorectal adenomas and IBD and high expression of Cten in the primary colorectal tumour. Its expression is associated with advanced disease and poor prognostic outcomes in CRC. Therefore, we decided to study the function of Cten in CRC through examination of a series of CRC cell lines for expression of *Cten* in order to identify cell lines with high and low expression of the gene. This was to be followed by functional analysis of Cten using a dual approach of forced Cten expression in cell lines with low expression and Cten knock-down in the cell lines with high expression. This approach would allow us to analyse if modulating levels of Cten expression can influence cellular processes such as cell proliferation, resistance to staurosporine induced apoptosis, cell migration and cell invasion using the appropriate assay. Finally, the effect of Cten on tumour cells was tested *in-vivo* by injecting cells stably transfected with GFP tagged Cten into mice and compared that with GFP-injected mice in order to test the role of Cten in inducing metastasis.

5.2 Quantification of *Cten* in CRC cell lines

5.2.1 Cloning of HPRT into pCR2.1 vector

Cloning of HPRT and *Cten* coding sequences into pCR2.1 vector was done in order to use pCR2.1-HPRT and pCR2.1-*Cten* plasmids as templates to monitor their levels quantitatively in CRC cell lines. This allows absolute quantification of *Cten* in CRC cell lines. In addition, it provides a tool to study the effects of exogenous *Cten* on cell signalling and cell behaviour.

The cloning of HPRT into pCR2.1 vector requires a prior addition of adenosine (A) residue to the 3' ends of the double stranded PCR product through adding *Taq* polymerase enzyme to the PCR. This enabled the direct cloning into a linearised pCR2.1 vector which has single 3'-thymidine (T) overhangs within the vector tails.

Conventional PCR using 10ng cDNA of SW480 CRC cell line as a template and the HPRT full length coding sequence primers amplified a product of the expected size (675bp) (Figure 19). After that, the PCR product was purified and ligated into pCR2.1 vector using a ratio of 1:1 (vector: insert). The ligation mix was transformed into competent bacteria, colonies were picked, mini-preps grown and plasmid DNA (pCR2.1-HPRT) extracted. Real time PCR was performed using pCR2.1-HPRT as a template in combination with HPRT primers (see chapter 3 for primer sequences). This showed a single and specific peak comparable for all samples tested and corresponded to a positive control SW480 cell line's HPRT peak (Figure 20). In-frame cloning of HPRT was confirmed by sequence analysis (Appendix 9.5).

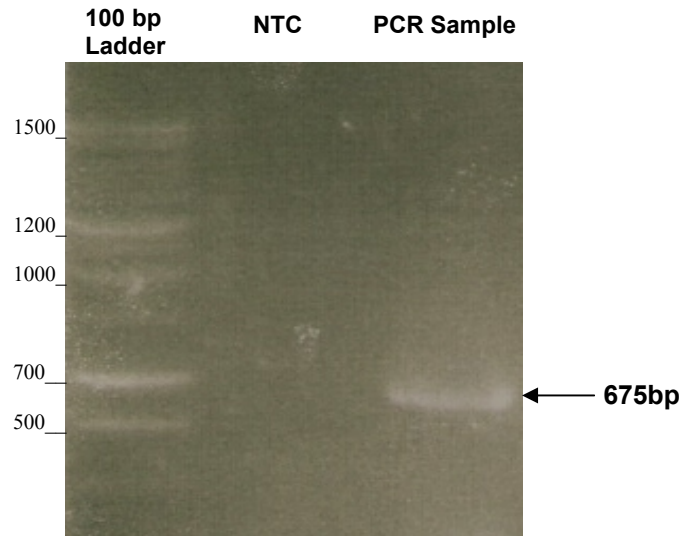


Figure 19. HPRT PCR product amplification for cloning into pCR2.1 vector. Following amplification, the PCR product was purified on a 1% gel and sized according to the 100bp DNA ladder, NTC:negative control.

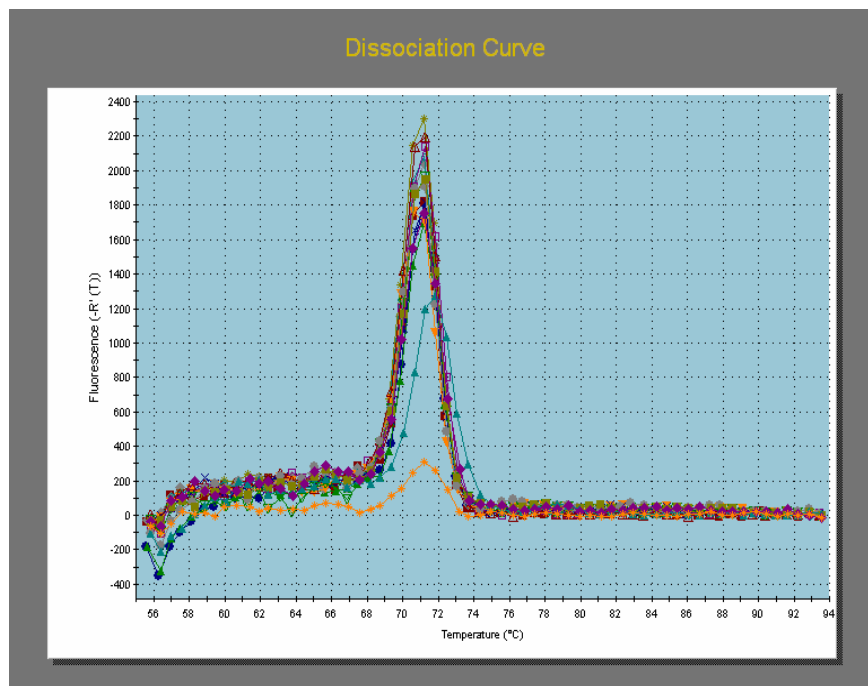


Figure 20. Real time PCR dissociation curves of pCR2.1-HPRT cloning samples. Real time PCR was performed using pCR2.1-HPRT cloning samples as templates in combination with HPRT primers showed a single and specific peak comparable for all samples tested and corresponded to a positive control SW480 cell line's HPRT peak.

5.2.2 Cloning of *Cten* into pCR2.1 vector

In order to clone *Cten* into pCR2.1 vector, a PCR was performed using the pEGFPC-1 plasmid containing the complete coding sequence of *Cten* as a template and *Cten* primers which create BamHI and HindIII overhangs at the 5' and at the 3' termini of the PCR product as described in chapter 3. Conventional PCR of the pEGFPC-1 plasmid using the above primers amplified a product of the expected size (2,148bp) (Figure 21). This PCR product was then gel purified and cloned into pCR2.1 vector following the same TA cloning principle and conditions used in the previous section.

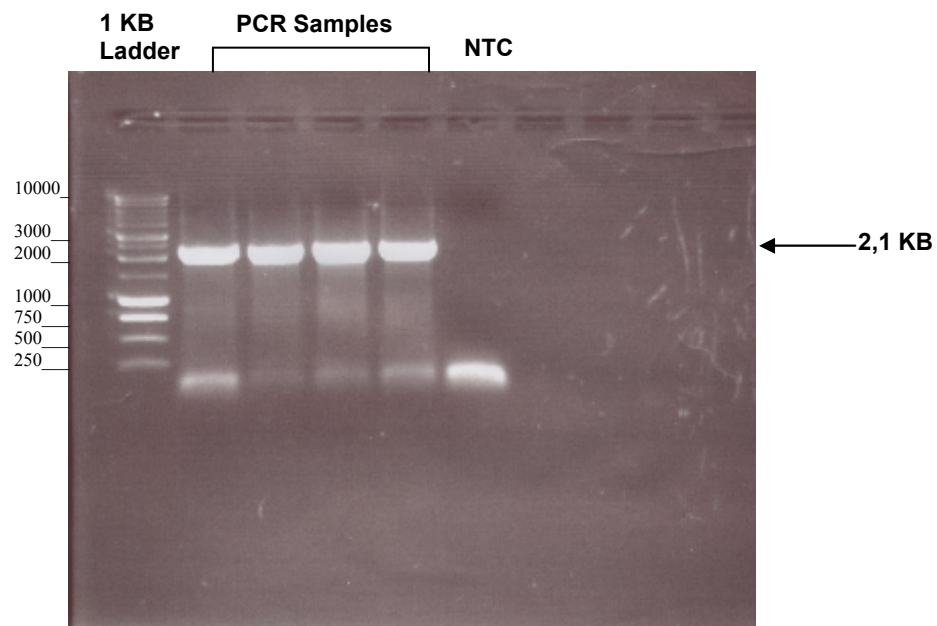


Figure 21. *Cten* PCR product amplification for cloning into pCR2.1 vector. Following amplification, the *Cten* PCR product (2,148bp) was purified on a 1% gel and sized according to the 1KB DNA ladder, NTC:negative control.

An analytical digest of putative pCR2.1-*Cten* was carried out using EcoRI an enzyme which cuts twice in the pCR2.1 vector (Figure 22), but not in the *Cten* PCR insert as has been checked by using the Webcutter 2.0 software. The digestion results confirmed the presence of *Cten* insert within the pCR2.1 vector (Figure 23).

For further evaluation pCR2.1-Cten plasmid, an ordinary PCR was undertaken using the *Cten* primers used in TA cloning. This showed a single and specific band for Cten coding sequence corresponded to pEGFPC1-Cten plasmid positive control (Figure 24). We sent 12µl of pCR2.1-Cten plasmid for sequencing, and the results showed that Cten was inserted into pCR2.1 vector in reverse (HindIII to BamHI) orientation (Appendix 9.6, 9.7). This is because the TA vector cloning system allows the ligation of an insert in both 5'-3' and 3'-5' orientations.

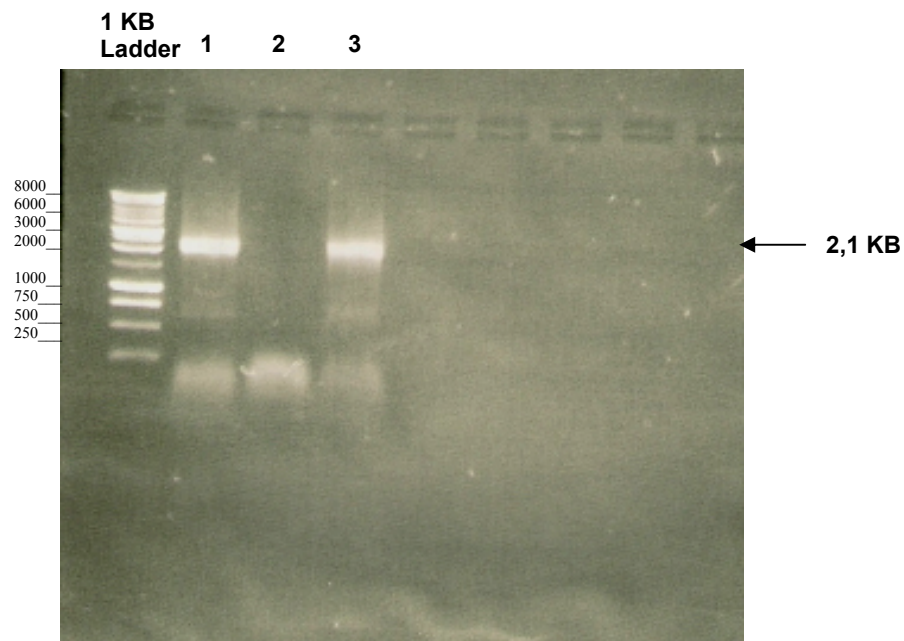


Figure 24. Cten PCR product amplification using pCR2.1-Cten plasmid. A PCR showed a band corresponded to Cten coding sequence and confirming the cloning of Cten into pCR2.1 vector. 1 (pCR2.1-Cten sample), 2 (negative control), 3 (pEGFPC1-Cten plasmid positive control).

5.2.3 Evaluating the *HPRT* mRNA expression in CRC cell lines

Expression of *HPRT* mRNA was evaluated by Q-RT-PCR using *HPRT* primers in 29 CRC cell lines (Figures 25-28, see chapter 3 for primer sequences). Data was analysed using the standard curve method (whereby a reference sample is serially diluted and the Ct values at each dilution are plotted on a graph) with cloned *HPRT* in pCR2.1 used to generate the standard curve.

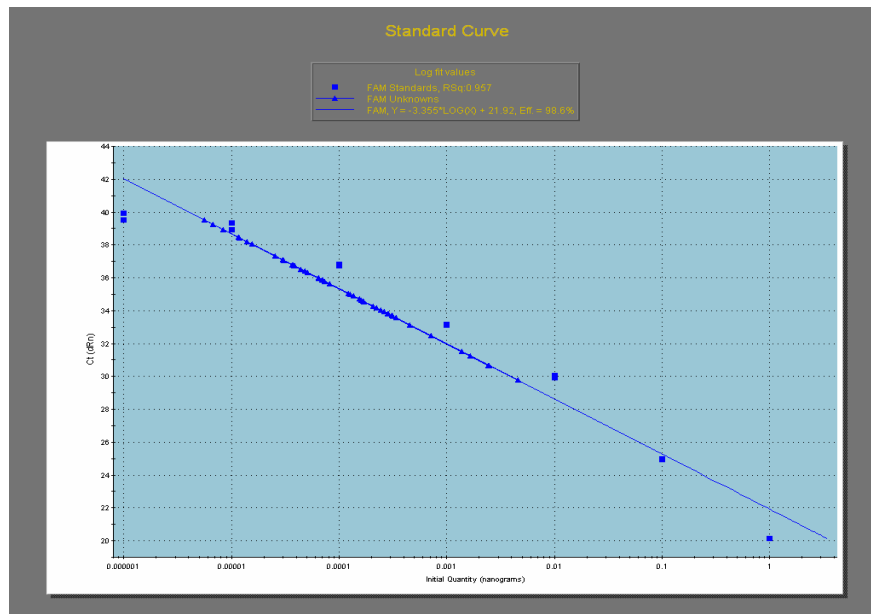


Figure 25. *HPRT* Q-RT-PCR standard curve of 29 human CRC cell lines. The Q-RT-PCR was carried out in triplicates and showed 98.6% efficiency.

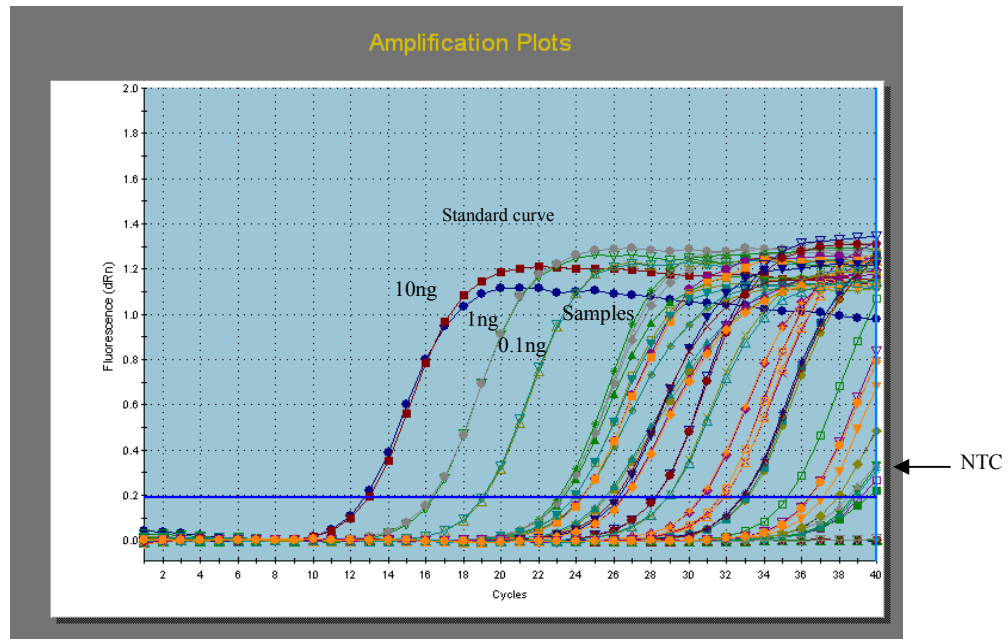


Figure 26. *HPRT* Q-RT-PCR amplification plots of 16 human CRC cell lines. Serial dilutions for *HPRT* standard curve were prepared in decreasing 10-fold increments starting from 10ng. As depicted above, *HPRT* message in CRC cell lines can be clearly detected all of the way down from 0.1ng standard curve dilution. NTC were came-up after 35 cycles. The Q-RT-PCR was carried out in triplicates.

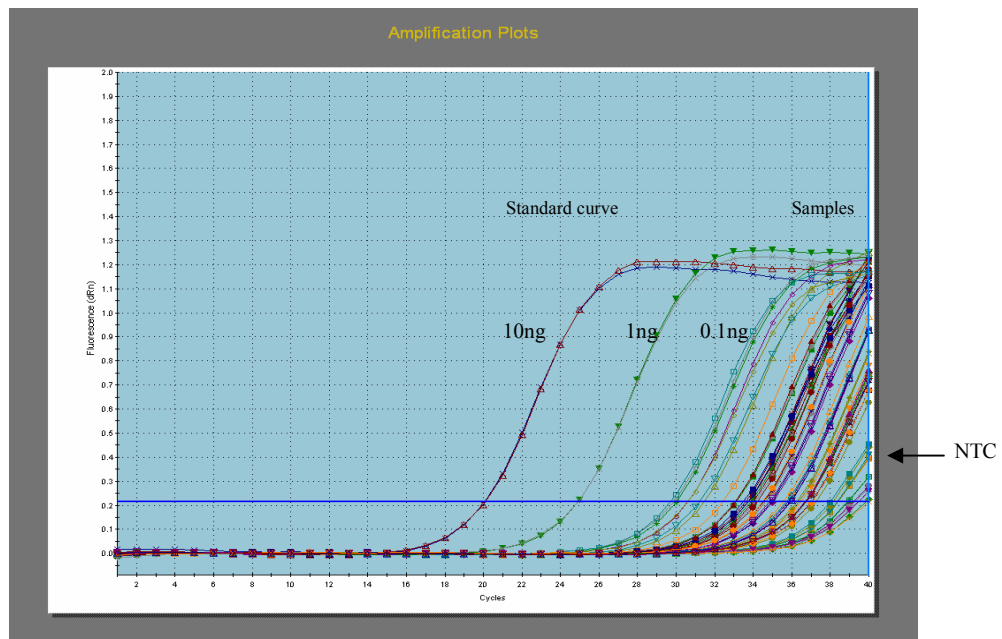


Figure 27. *HPRT* Q-RT-PCR amplification plots of 13 human CRC cell lines. *HPRT* message in CRC cell lines can be clearly detected all of the way down from 0.1ng standard curve dilution. NTC were came-up after 36 cycles. The Q-RT-PCR was carried out in triplicates.

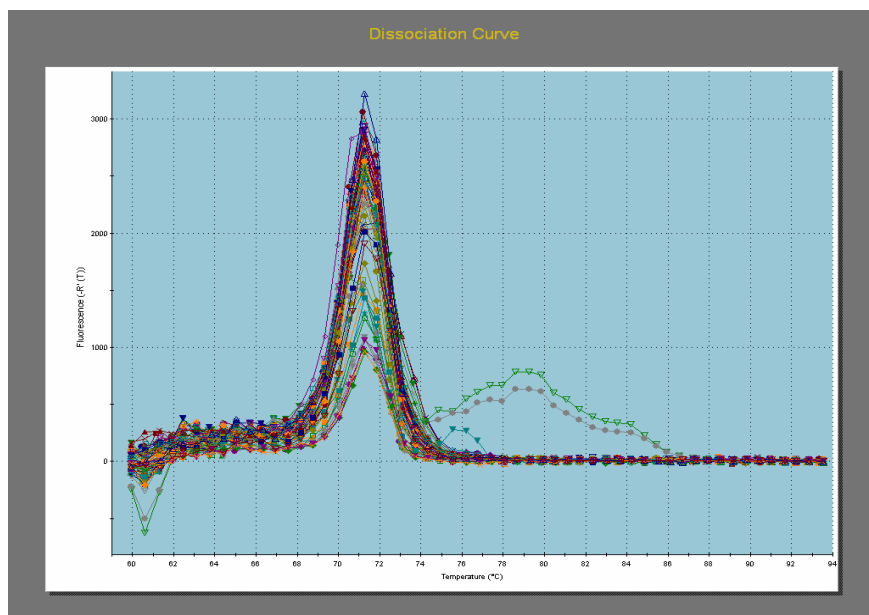


Figure 28. *HPRT* Q-RT-PCR dissociation curves of 29 human CRC cell lines. Dissociation curves of *HPRT* in CRC cell lines showed a single and specific peak comparable for all samples.

5.2.4 Evaluating the *Cten* mRNA expression in CRC cell lines

Expression of *Cten* mRNA was evaluated by Q-RT-PCR using *Cten* primers in 29 CRC cell lines (Figures 29-32, see chapter 3 for primer sequences). Data was evaluated using the standard curve method with cloned *Cten* in pCR2.1 used to generate the standard curve. Analysis was performed in triplicate for each sample and data was normalised to cloned HPRT in pCR2.1 vector to obtain absolute *Cten* mRNA levels for the cell lines tested.

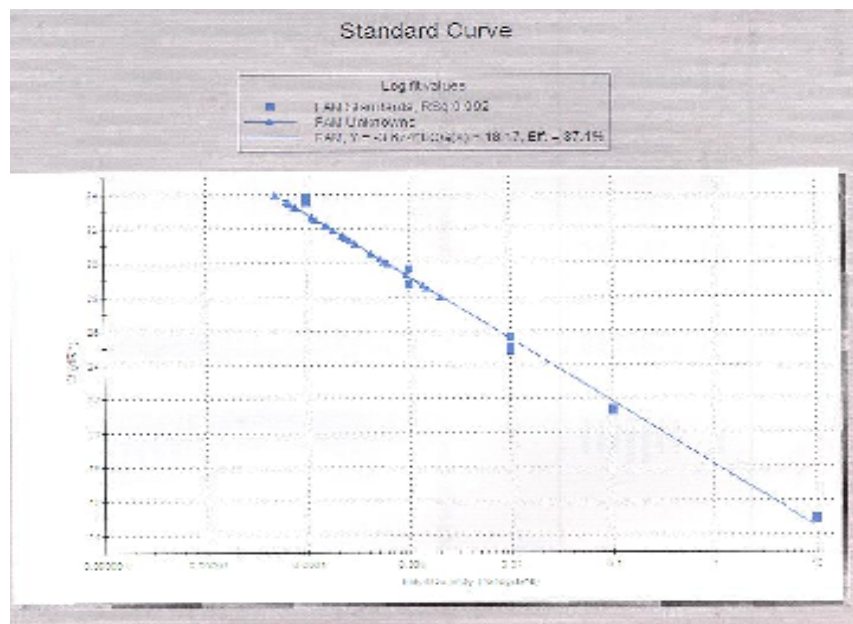


Figure 29. *Cten* Q-RT-PCR standard curve of 29 human CRC cell lines. The Q-RT-PCR was carried out in triplicates and showed 87.1% efficiency.

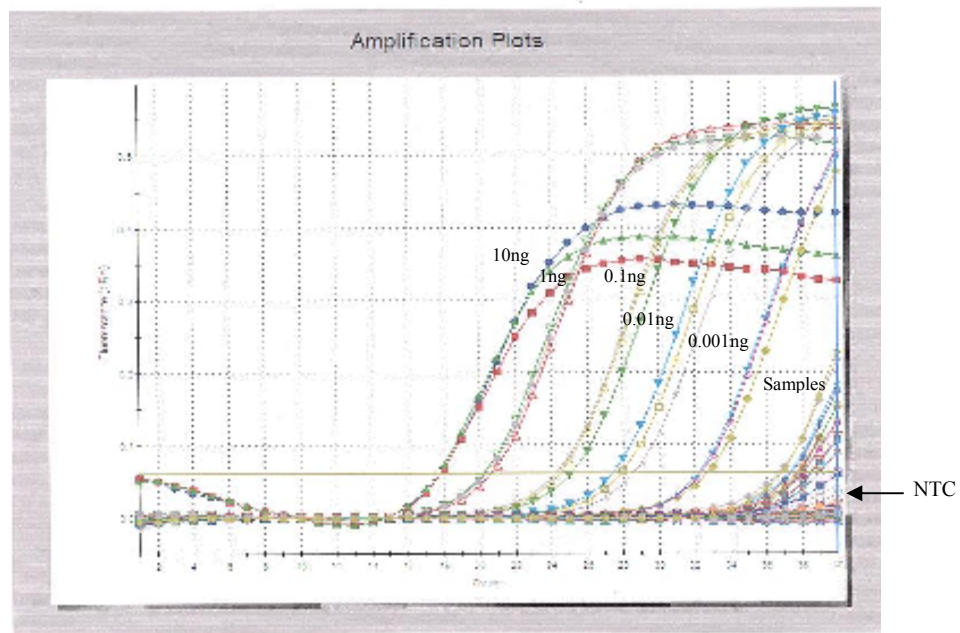


Figure 30. *Cten* Q-RT-PCR amplification plots of 9 human CRC cell lines. *Cten* message in CRC cell lines can be clearly detected all of the way down from 0.001ng standard curve dilution. NTC were came-up after 38 cycles. The Q-RT-PCR was carried out in triplicates.

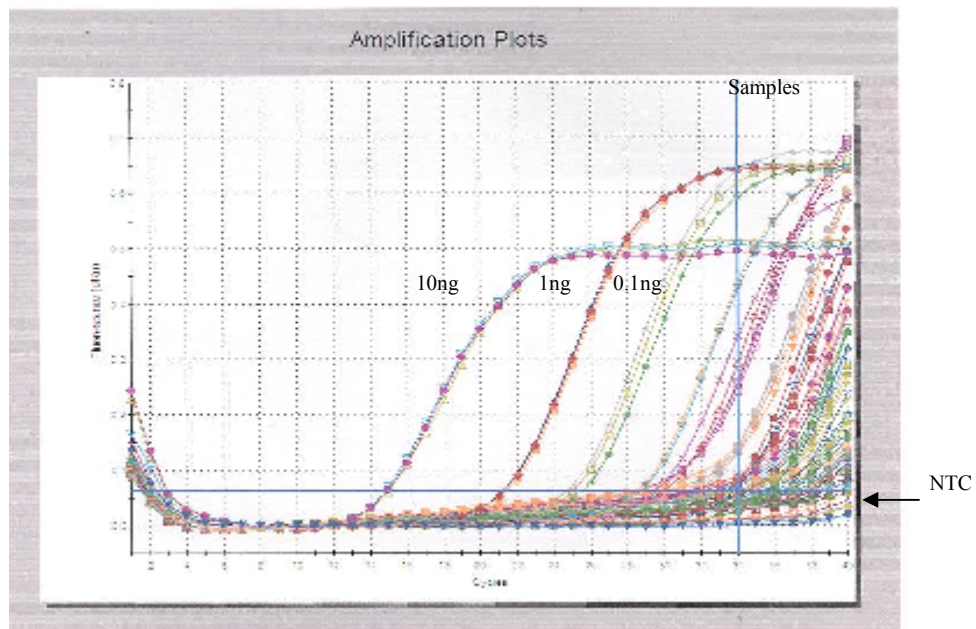


Figure 31. *Cten* Q-RT-PCR amplification plots of 20 human CRC cell lines. *Cten* message in CRC cell lines can be clearly detected all of the way down from 0.1ng standard curve dilution. NTC were came-up after 38 cycles. The Q-RT-PCR was carried out in triplicates.

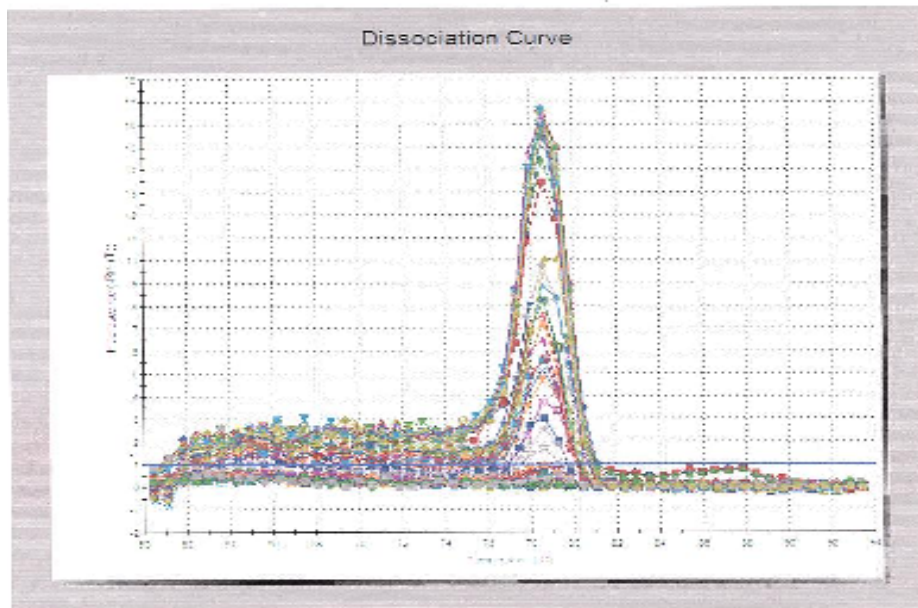


Figure 32. *Cten* Q-RT-PCR dissociation curves of 29 human CRC cell lines. Dissociation curves of *Cten* in CRC cell lines showed a single and specific peak comparable for all samples.

Normalised *Cten* mRNA expression in CRC cell lines showed that 18/29 (62%) cell lines showed up-regulation of *Cten* mRNA levels and they differ in their level of expression up to 50 fold. The cell lines showing up-regulation appeared to fall into two groups, with 13 showing a two- to eight-fold increase and five showing over a 35-fold increase. These results are summarised in Table 7 and Figure 33.

HCT116 and SW480 are both well-described cell lines which were found to have little expression of *Cten* at the mRNA level. These were thus chosen for *Cten* forced expression experiments. In contrast, following the Q-RT-PCR analysis, SW620 was found to have high expression of *Cten* at the mRNA level and thus was most suitable for gene knock-down experiments.

Table 7. Expression of *Cten* in CRC cell lines assessed by Q-RT-PCR. The normalised *Cten* mRNA was found to be over-expressed in several CRC cell lines at varying levels.

Cell line	Fold difference
DLD1	57.1
COLO205	51.4
LOVO	48.6
SW620	48.6
COLO201	35.7
C80	7.1
GP2D	7.1
VACO10MS	7.1
C32	4.3
C84	4.3
HCA46	4.3
SW1116	4.3
VACO5	4.3
C125	3.6
LS1034	3.6
SW122	3.6
SW480	3.6
SW948	2.9
C106	0.7
COLO320DM	0.7
HT29	0.7
HT55	0.7
RKO	0.7
HCA7	0.6
HCT116	0.6
HUTU80	0.6
HRA19	0.3
CACO2	0.2
SW837	0.2

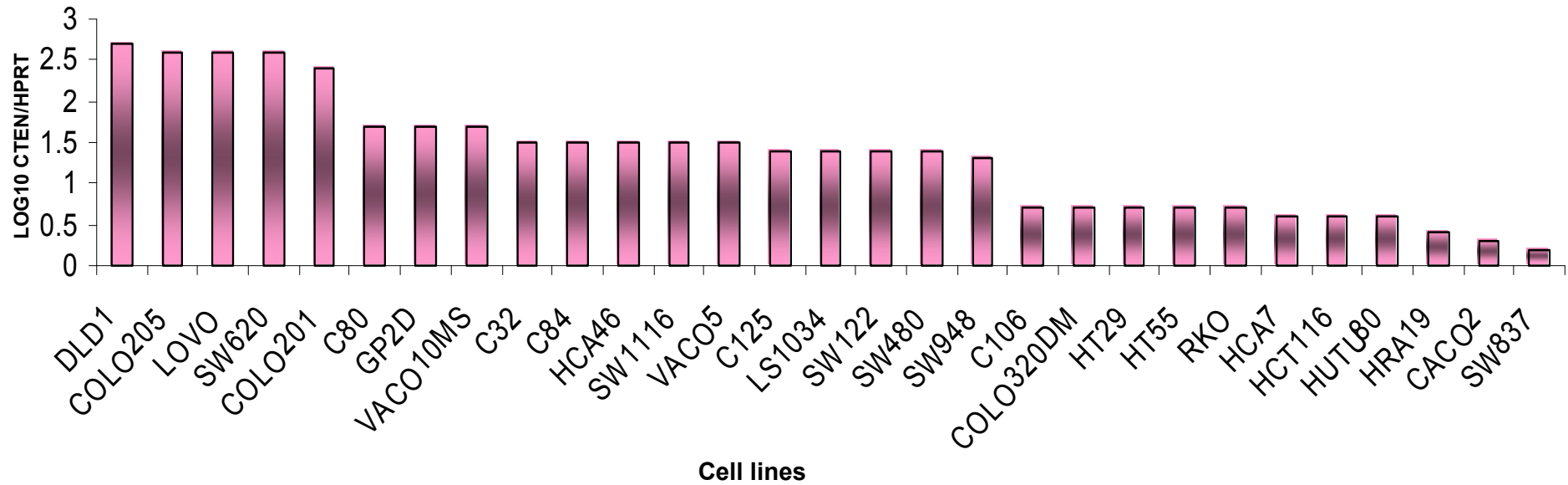


Figure 33. Bar chart of *Cten* levels in CRC cell lines as measured by Q-RT-PCR. *Cten* values were normalised to the housekeeping gene *HPRT* and up-regulated in CRC cell lines at varying levels. 18/29 (62%) of CRC cell lines showed up-regulation of message expression (i.e. >2 fold) with a 5 fold increase seen in DLD1.

5.3 Establishment of stable *Cten*-stably expressing cell lines

HCT116 and SW480 are both well described cell lines. Their identities were confirmed by mutation screening analysis done by our group using the high resolution melting curve analysis of DNA/cDNA (208). These cell lines were found to have little expression of *Cten* at the message level and no detectable *Cten* protein by Western blot. Thus, these were chosen for studies of *Cten* function. HCT116 was stably transfected with an expression vector containing GFP-tagged *Cten* or with empty GFP vector (as control) followed by prolonged growth in G418 selection media. Full-length protein expression in the stable cell lines obtained was confirmed by western blotting. Whole cell lysates were blotted with anti-*Cten* antibody and a band of 110 kDa (representing the GFP-*Cten* protein) was present in HCT116 cell line transfected with GFP-*Cten* plasmid whilst there was no evidence of *Cten* in HCT116 cell line transfected with GFP vector control. β -actin was used as a loading control (Figure 34). Evaluation of the *Cten* protein in the stably transfected cell lines showed levels which were equivalent to those present in the cell line SW620 (Figures 34). This is derived from a metastatic deposit and shows high endogenous *Cten* mRNA and protein levels. For SW480 a slightly different strategy was used and the transfected cells were FACS-sorted 24 hours after transfection. Transfection efficiencies were unexpectedly low with only 11% efficiency in the GFP-*Cten* transfections versus 32% in the GFP vector controls (Figure 35). After sorting, cells were grown in G418 selection media to produce stably transfected colonies.

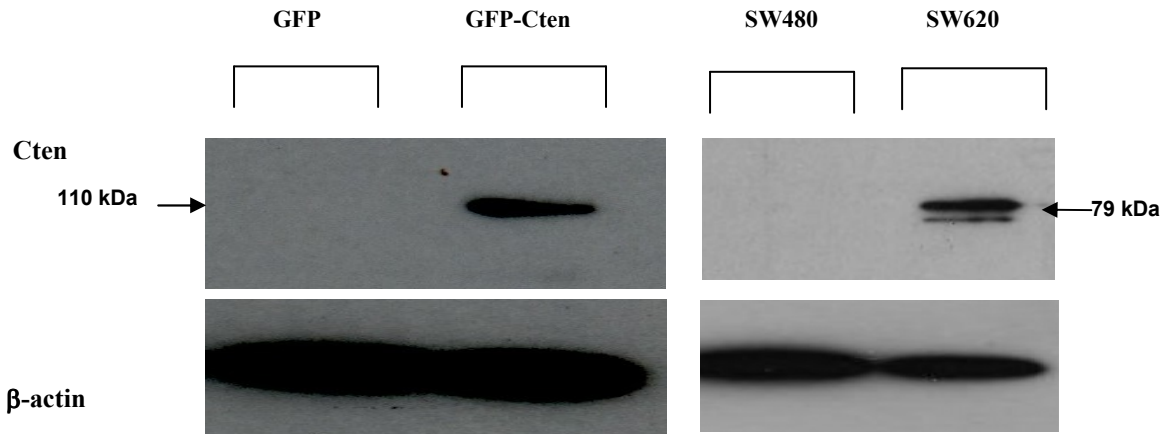


Figure 34. Immunoblotting for Cten using whole cell extracts from HCT116-GFP or HCT116-GFP-Cten. HCT116 was stably transfected with GFP-Cten through prolonged growth in selection G418 selection. Evaluation of the Cten protein in the stably transfected cell lines showed levels which were equivalent to those present in the cell line SW620. β -actin is shown as a loading control. Please note that β -actin western is overexposed and this is true for most of the blots in this study. The reason for that is because we load a lot of protein (30 ug) to detect Cten protein and other proteins of interest and the loading control is tested on the same samples.

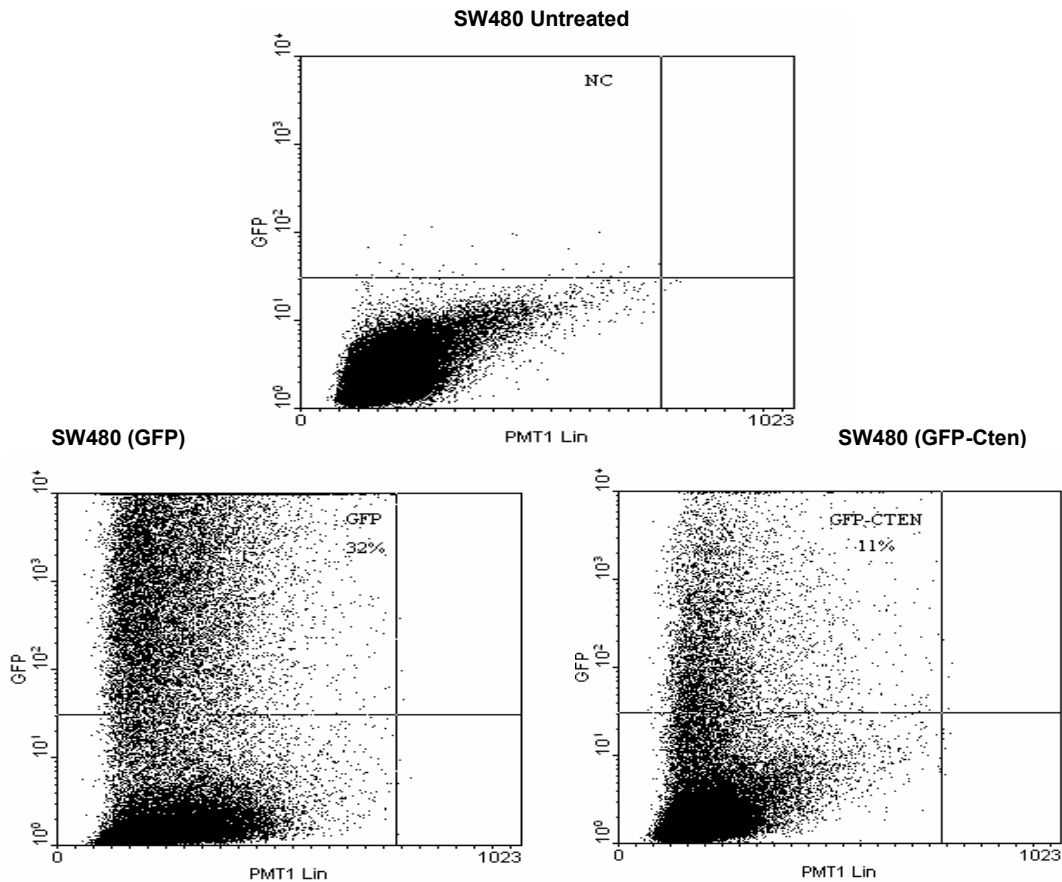


Figure 35. SW480 cell line FACS sorting. Non-transfected cells were used to set the gating levels. Cells transfected with GFP-Cten or empty vector were then sorted on the basis of fluorescence.

5.4 Role of Cten in regulating cell proliferation

The effects of Cten expression on proliferation were tested in both HCT116 and SW480 cells using a time course experiment conducted over a period of 7 days. This showed that when compared with empty vector controls; forced expression of Cten does not have an effect of proliferation in either cell line (Figure 36).

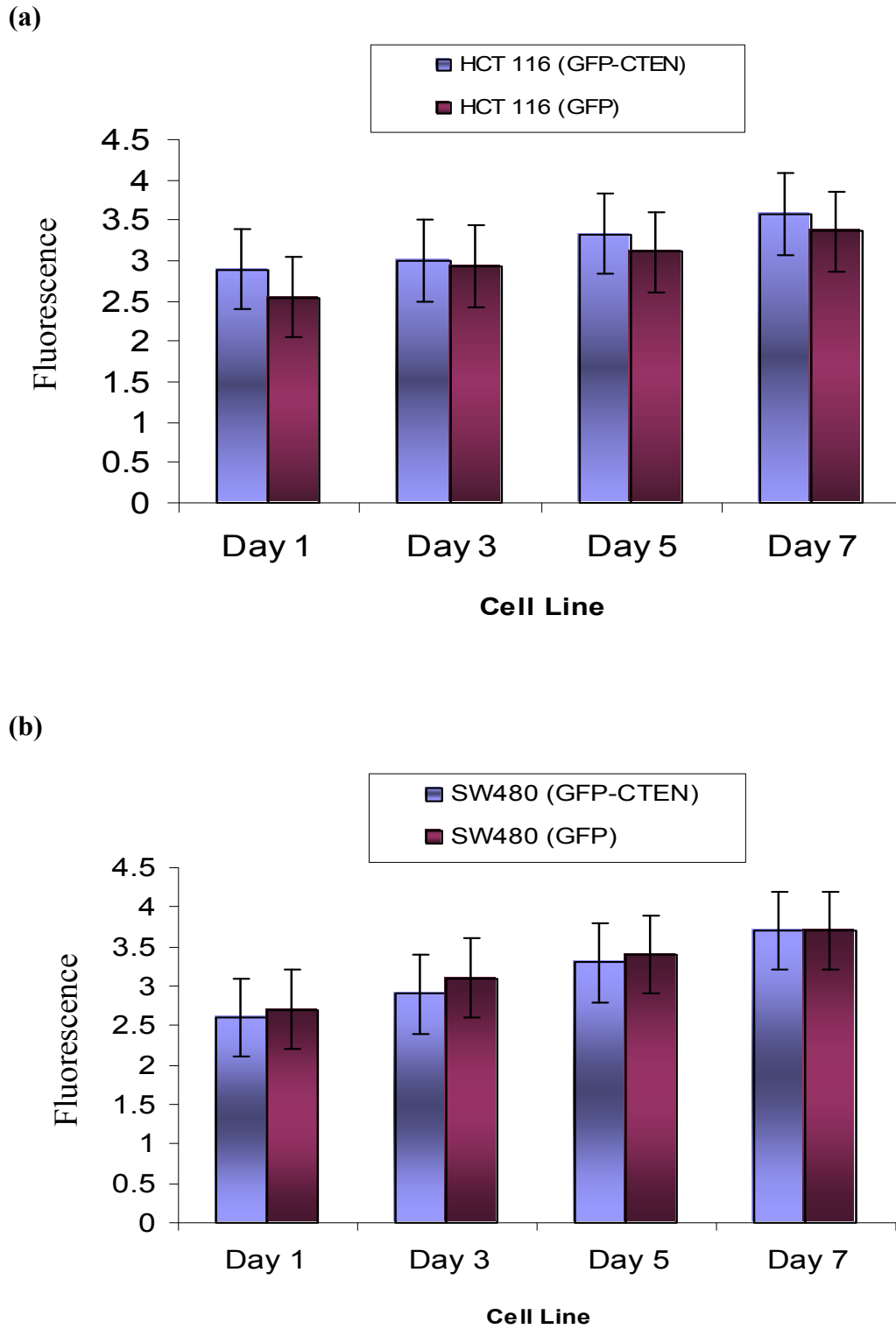


Figure 36. Effect of *Cten* forced expression on cell proliferation. A time course analysis of cell proliferation over seven days in (a) HCT116 and (b) SW480 cell lines showed that forced expression of *Cten* had little effect on cell numbers compared to controls. Error bars show standard deviation.

5.5 Role of Cten in resisting apoptotic stress

Having shown that Cten forced expression does not have an effect on cell number in CRC cell lines, we next tested whether Cten could cause resistance to staurosporine-induced apoptotic stress. Staurosporine is commonly used to induce apoptosis in cells and was used to test the resistance to apoptosis conferred by Cten. After 24 hours incubation with 6 μ M staurosporine, more living (i.e. adherent.) cells and fewer dead cells (as determined by uptake of trypan-blue) were observed in wells containing Cten transfected cells than in wells containing GFP-transfected controls ($p < 0.001$ for both; Student's t-test, Figure 37).

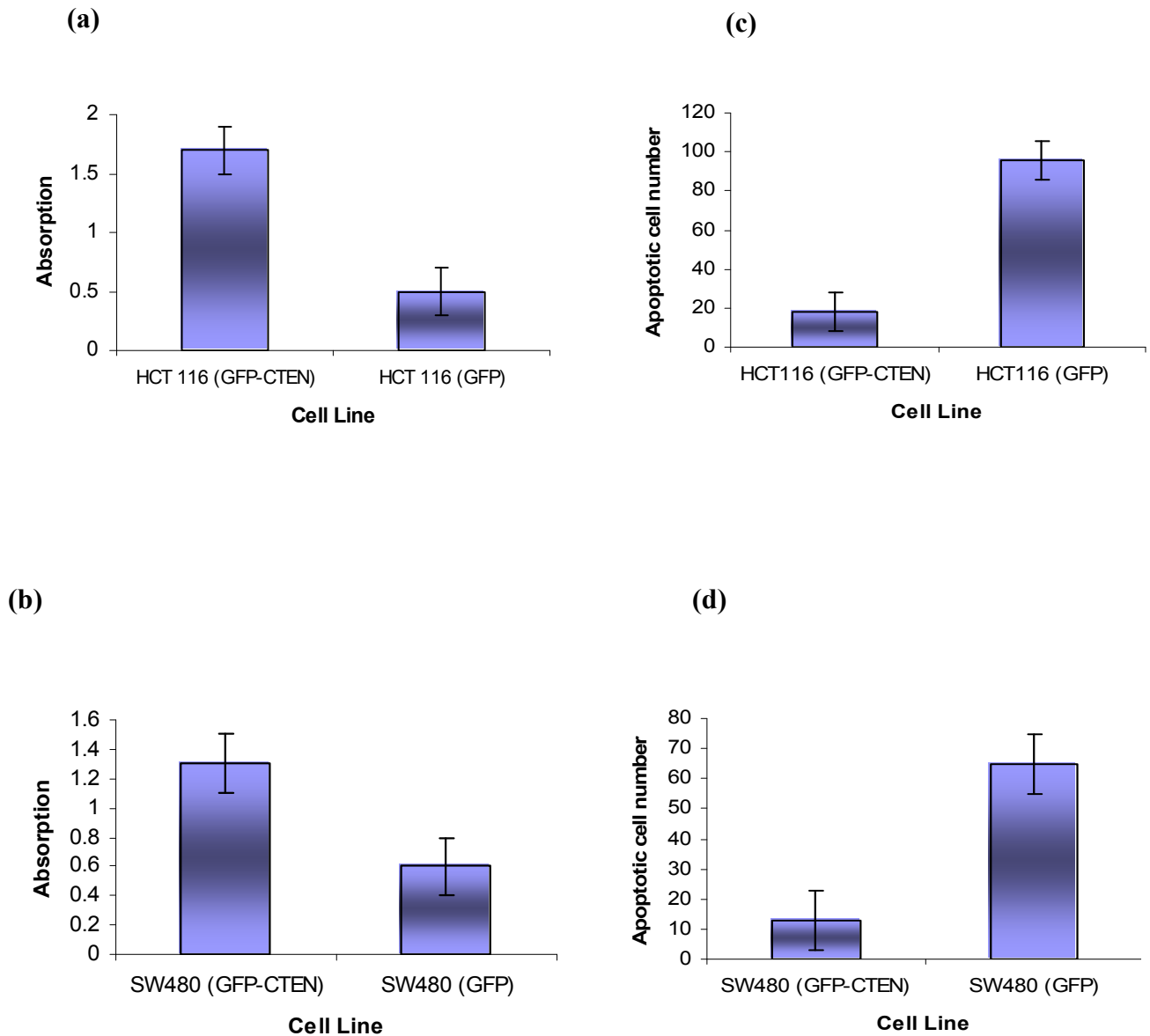


Figure 37. Cten conferred resistance to staurosporine-induced apoptosis in both SW480 and HCT116 cells. Induction of apoptosis was quantified by two methods: number of adherent cells (measured by the methylene blue assay) (a,b) and number of floating cells taking up trypan blue (measured by manual counting) (c, d). For both methods of assessment and in both cell lines, there was a significant difference ($p < 0.005$ for each condition; Student's t-test).

5.6 Role of Cten in regulating cell motility

5.6.1 Effects of Cten forced expression on cell migration and invasion

Although forced expression of Cten had no effect on proliferation in HCT116 cells, it altered their cellular morphology. Examination by epifluorescence microscopy showed that cells transfected with GFP-Cten adopted an elongated spindle-like shape whilst those transfected with GFP control plasmid retained an epithelioid appearance (Figure 38).

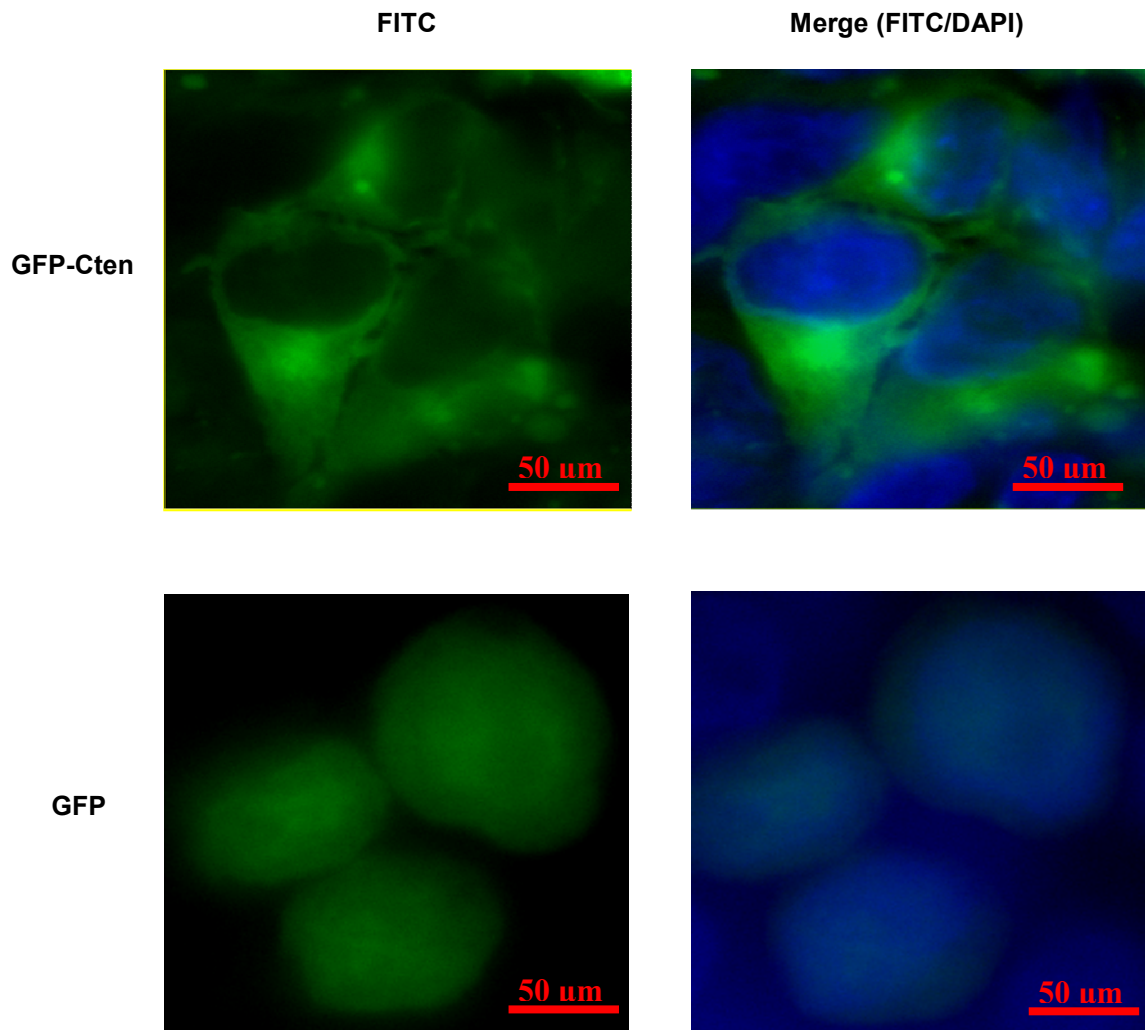


Figure 38. Epifluorescence microscopy to assess the localisation of GFP and Cten in transfected cells. Cells transfected with GFP empty vector had a rounded phenotype with GFP present both within the nucleus and the cytoplasm. Cells transfected with GFP-Cten showed a more spindle like morphology with fluorescence seen only in the cytoplasm.

Having shown that forced expression of *Cten* induced a change in appearance of the cells, manifested as an acquisition of an elongated spindle-like appearance, consistent with EMT, this was an unexpected observation and prompted us to evaluate the effect of *Cten* on cell migration and invasion. Transwell migration assays, using SW480 and HCT116 cell lines resulted in markedly increased cellular migration ($p < 0.001$ for each cell line; Student's t-test, Figure 39) of cells containing *Cten* versus control cells. In order to validate the transwell migration assay, a cell wounding assay was performed using HCT116 GFP- and HCT116 GFP-*Cten*-transfectants. Cells expressing *Cten* showed a more rapid migration across the wound than controls ($p = 0.03$; Student's t-test, Figure 40) and thereby confirmed our transwell migration assay findings. Cell invasion was tested using the Boyden chamber assay containing a thin layer of Matrigel (5mg/ml) on the upper side of the filter. In both HCT116 and SW480 cells, forced expression of *Cten* stimulated invasion compared to GFP control cells ($p < 0.001$ for each cell line; Student's t-test, Figure 41).

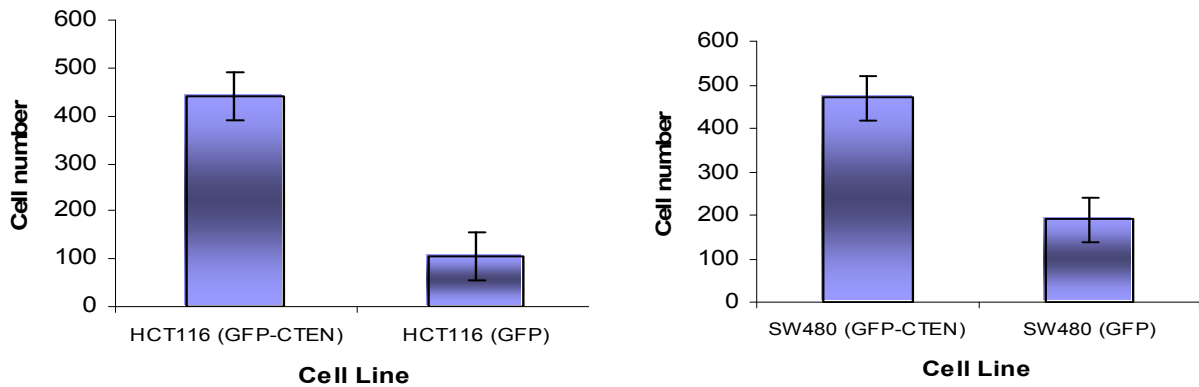


Figure 39. Effect of *Cten* forced expression on cell migration using a transwell migration assay. In both HCT116 and SW480 cell lines, transwell migration assays showed that greater numbers of cell migrated through the filter when transfected with GFP-*Cten* compared to control empty GFP vector ($p < 0.001$ for both cell lines; Student's t-test). Data shown are representative of experiments performed in triplicate (and replicated in independent experiments). Error bars show standard deviation.

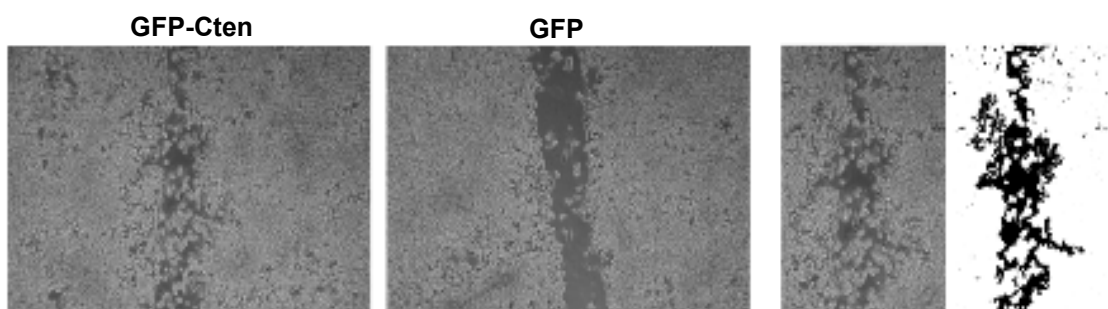


Figure 40. Effect of *Cten* forced expression on cell migration using a cell wounding assay. The assay in HCT116 showed greater migration across the wound in cells transfected with GFP-*Cten* than empty vector controls. The area of the wound was measured using ImageJ and showed that the wound was significantly smaller in cells transfected with GFP-*Cten* than controls ($p = 0.03$; Student's t-test).

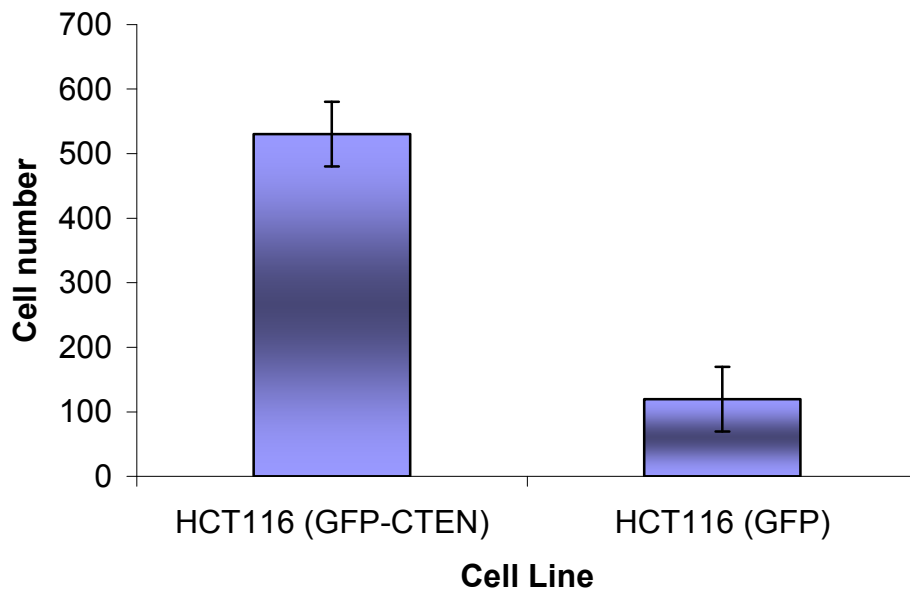
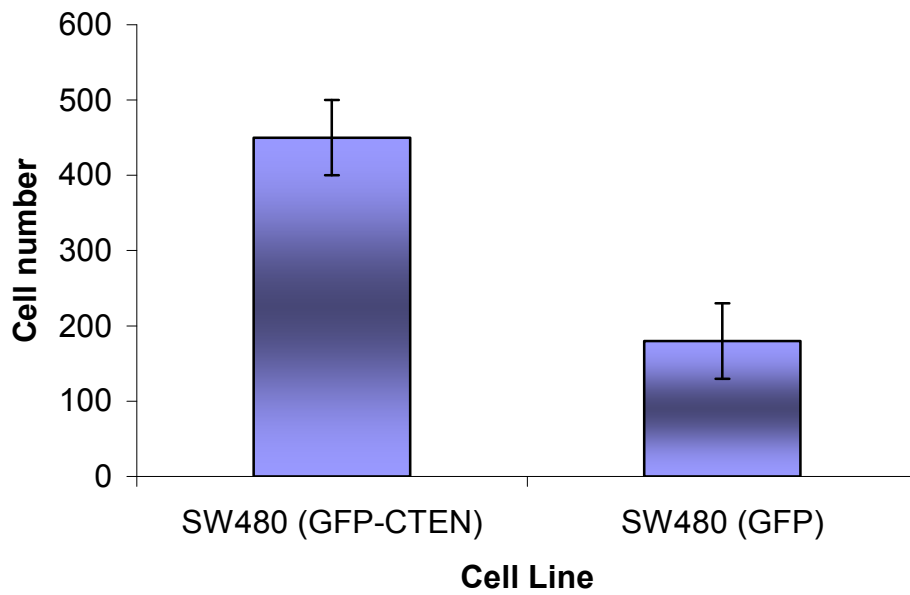


Figure 41. Effect of *Cten* forced expression on cell invasion. In both SW480 and HCT116 cell lines, invasion assays showed that *Cten* stimulated invasion through matrigel ($p < 0.001$ for both cell lines; Student's *t*-test). Data shown are representative of experiments performed in triplicate (and replicated in independent experiments). Error bars show standard deviation.

5.6.2 Effects of *Cten* knock-down on cell migration and invasion

Having shown that forced expression of *Cten* in HCT116 and SW480 CRC cell lines promotes cell motility, we used the reciprocal approach of knock-down of endogenously over-expressed *Cten* in order to validate our findings. SW620 cells, which endogenously express high levels of *Cten*, underwent gene knock-down by RNAi. Cells were transfected with specific *Cten* siRNA or non-targeting scrambled control. First, we confirmed the efficacy of *Cten* siRNA knock-down by q-RT-PCR and western blotting. We detected a 70% decrease in *Cten* mRNA levels, which was reflected also at protein levels (Figure 42 a, b).

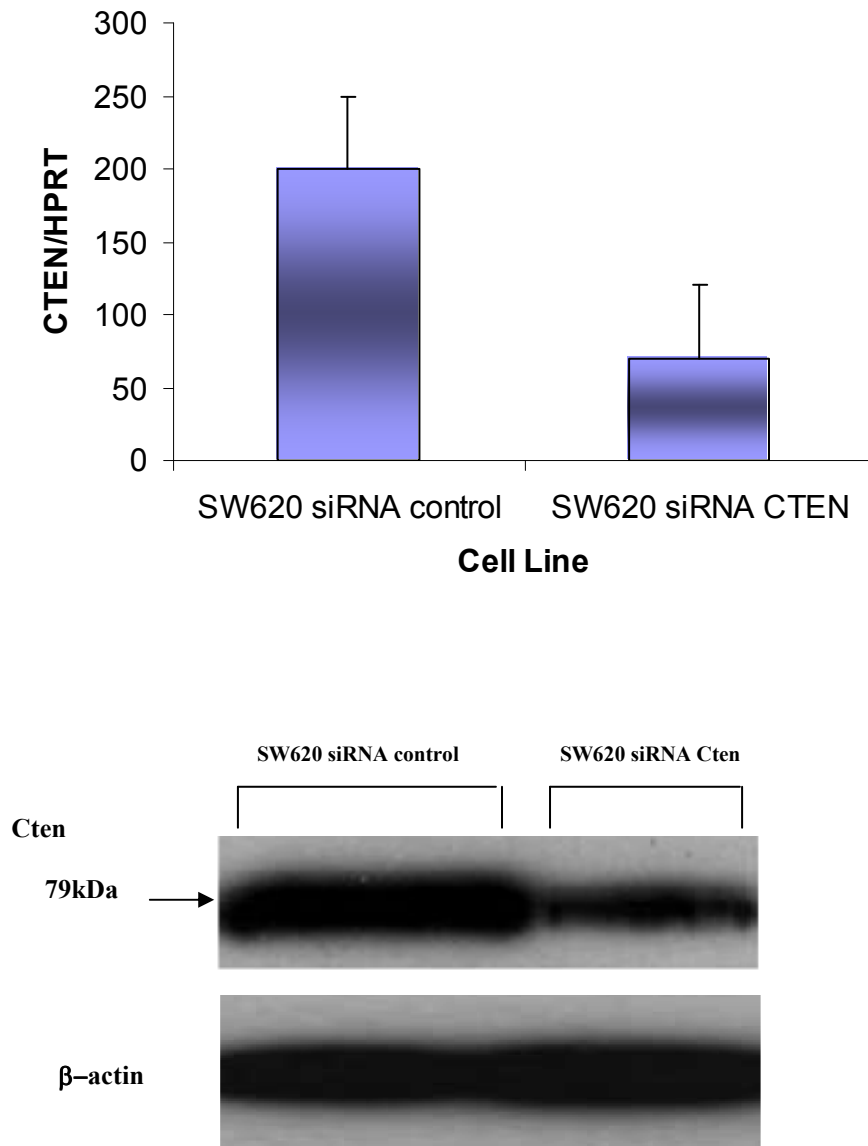


Figure 42. Cten knock-down in SW620 cells. Cten knock-down using Cten siRNA was confirmed by Q-RT-PCR (a) and western blotting (b). A 70% decrease in *Cten* mRNA levels (a), was also reflected at protein levels (b). β -actin was used as a loading control. Error bars show standard deviation.

Experiments were repeated following *Cten* knock-down. Cell migration assays using the Boyden chamber showed a marked decrease in cellular migration when *Cten* levels were depleted compared with siRNA control transfected cells ($p < 0.001$; Student's t-test, Figure 43). Effect of *Cten* knock-down on cell invasion showed a statistically significant decrease in cellular invasion capability, when high endogenous *Cten* levels were decreased ($p < 0.001$; Student's t-test, Figure 44).

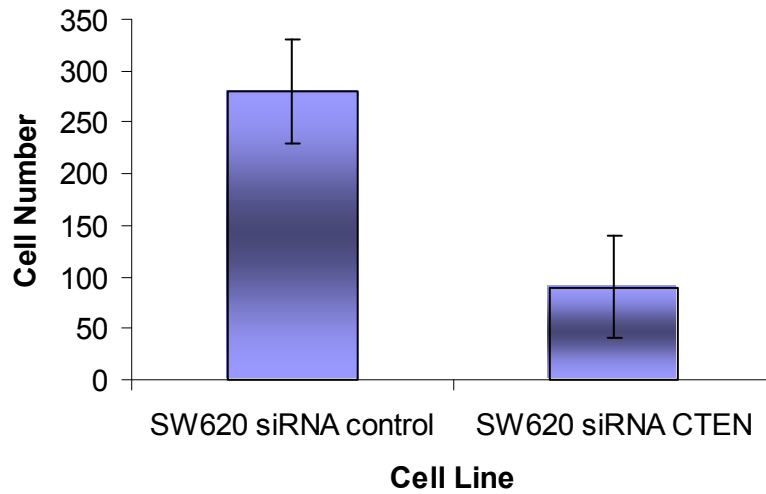


Figure 43. Effect of *Cten* knock-down on cell migration. Transwell migration assay showed a significant decrease in cellular migration of cells transfected with *Cten* siRNA compared with siRNA control transfected cells ($p < 0.001$; Student's *t*-test). Data shown are representative of experiments performed in triplicate (and replicated in independent experiments). Error bars show standard deviation.

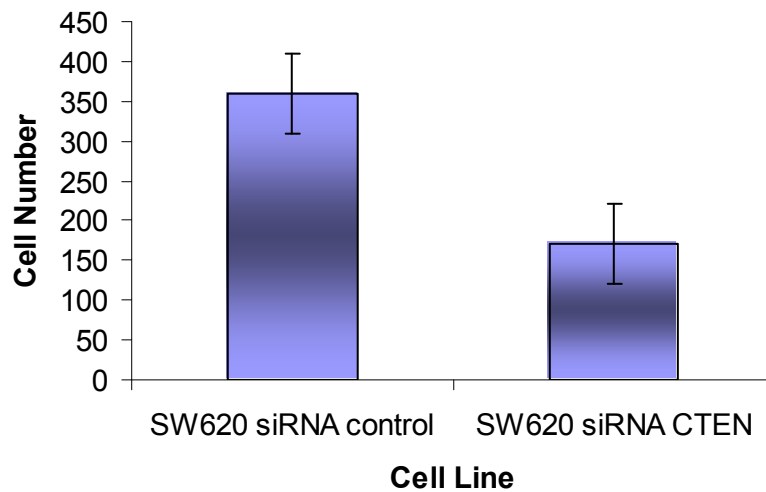


Figure 44. Effect of *Cten* knock-down on cell invasion. Invasion assay showed a significant decrease in cellular invasion of cells transfected with *Cten* siRNA compared with siRNA control transfected cells ($p < 0.001$; Student's *t*-test). Data shown are representative of experiments performed in triplicate (and replicated in independent experiments). Error bars show standard deviation.

5.7 Role of *Cten* in metastasis

Our current data show unequivocally that *Cten* plays a role in stimulating cell motility in CRC. Acquisition of cell motility may be important in tumour metastasis and thus we tested whether *Cten* could enhance the metastatic properties of HCT116. For this purpose *in-vivo* models of tumour metastasis in mice were used. Cells were stably transfected with either GFP-*Cten* or GFP alone (as controls) and injected into the spleens of nude mice. Compared to the controls, mice injected with cells expression GFP-*Cten* developed a significantly greater total tumour burden in the spleen (average intra-splenic tumour volume for mice injected with cells expression HCT116 GFP-*Cten* and HCT116 GFP were 4.3mm^3 and 1.2mm^3 respectively, $p=0.03$; Mann-Whitney U test, Figure 45). The number of discrete tumour deposits in the liver was similar in both groups but the size of the deposits was greater in mice injected with cells expression HCT116 GFP-*Cten* leading to a greater tumour burden (average intra-hepatic tumour volume for mice injected with cells expression HCT116 GFP-*Cten* and HCT116 GFP were 3.5mm^3 and 1.4mm^3 respectively ($p=0.05$; Mann Whitney U test, Figure 46). There were no significant differences in overall survival between the mice injected with cells expression HCT116 GFP-*Cten* and HCT116 GFP ($p=0.214$; log-rank test, Figure 47).

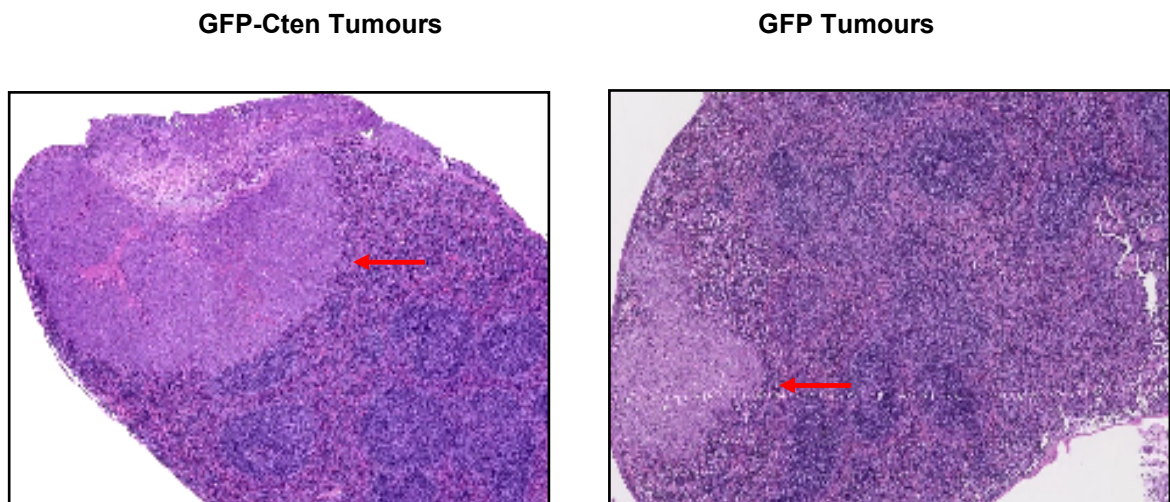
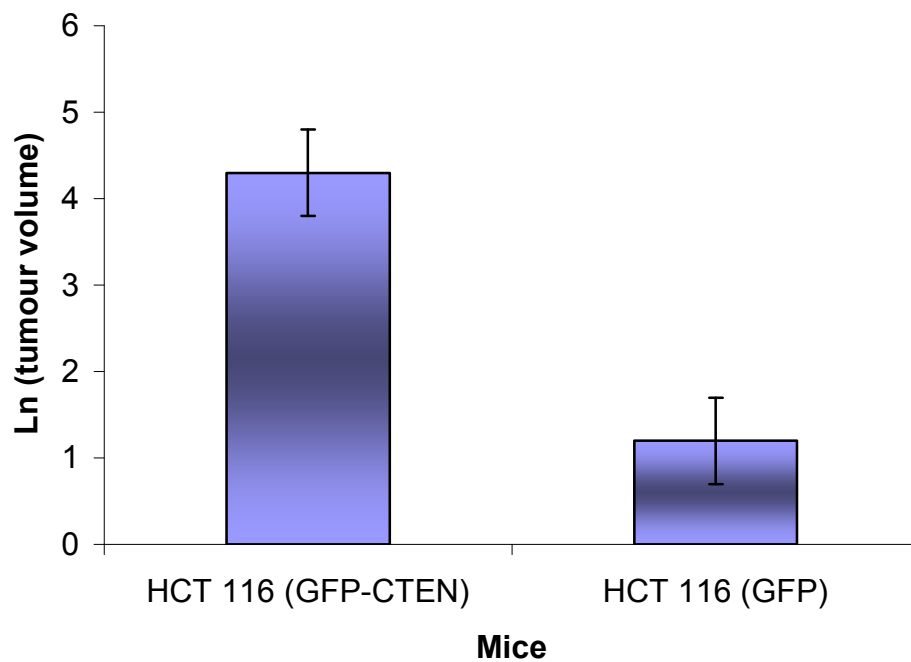


Figure 45. Average intra-splenic tumour volume from the mice injected with HCT116-GFP or HCT116-GFP-Cten cells. Compared to the controls, mice injected with cells expression GFP-Cten developed a significantly greater total tumour burden in the spleen ($p=0.03$; Mann Whitney U test). The tumour volume was measured using the NDPI software. Arrows show intra-splenic tumour. Error bars represented standard deviations.

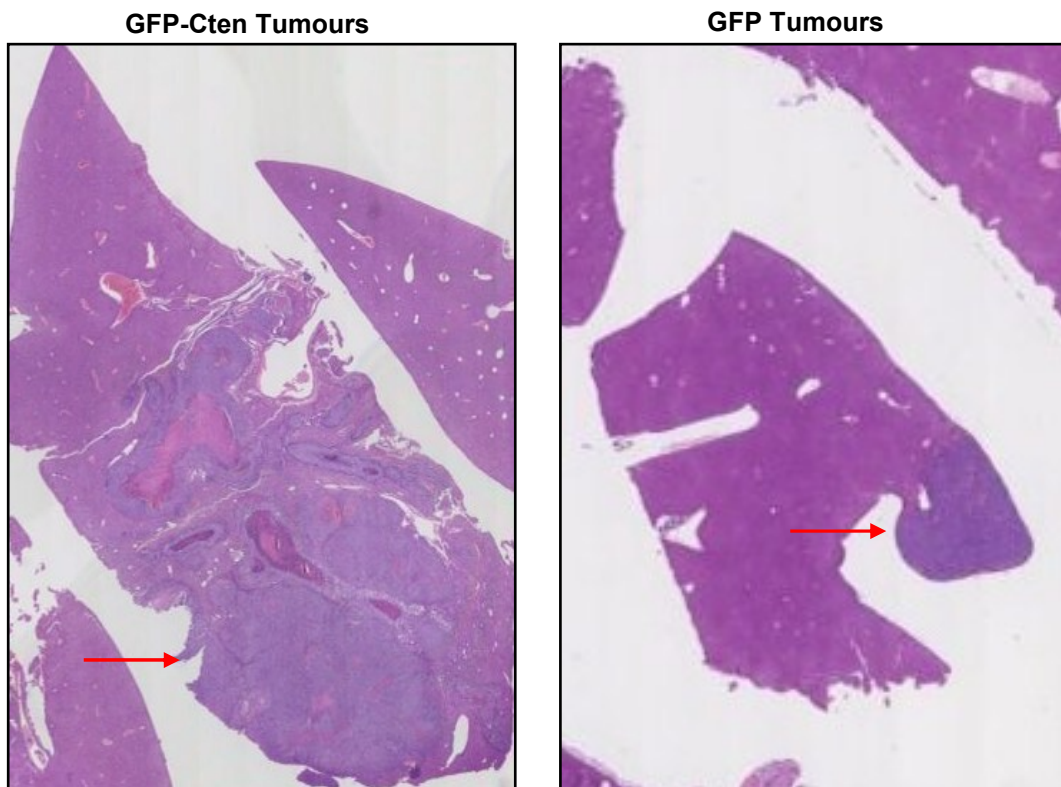
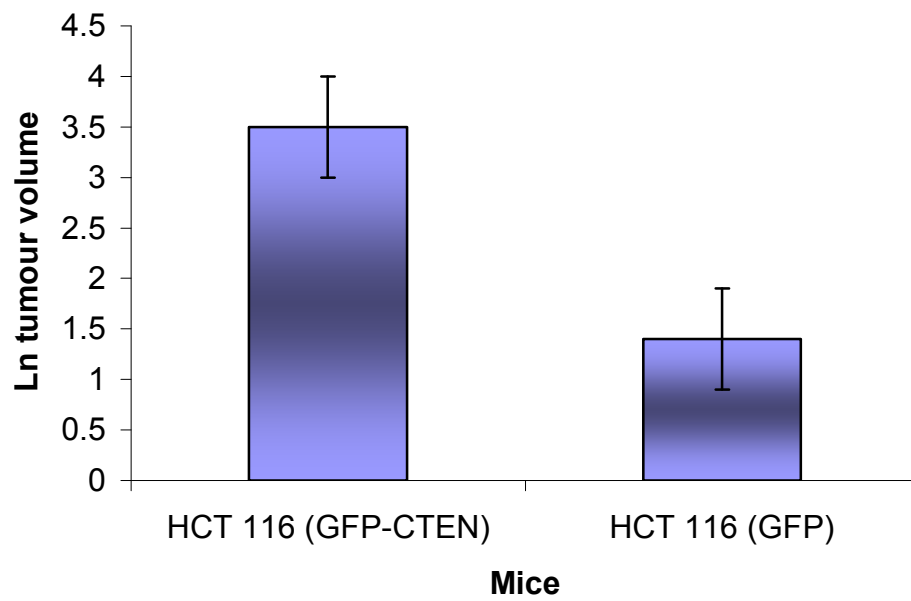


Figure 46. Average liver tumour volume from the mice injected with HCT116-GFP or HCT116-GFP-Cten cells. Compared to the controls, mice injected with cells expression GFP-Cten developed a significantly greater total tumour burden in the liver ($p=0.05$; Mann Whitney U test). Arrows show liver tumour. Error bars represented standard deviations

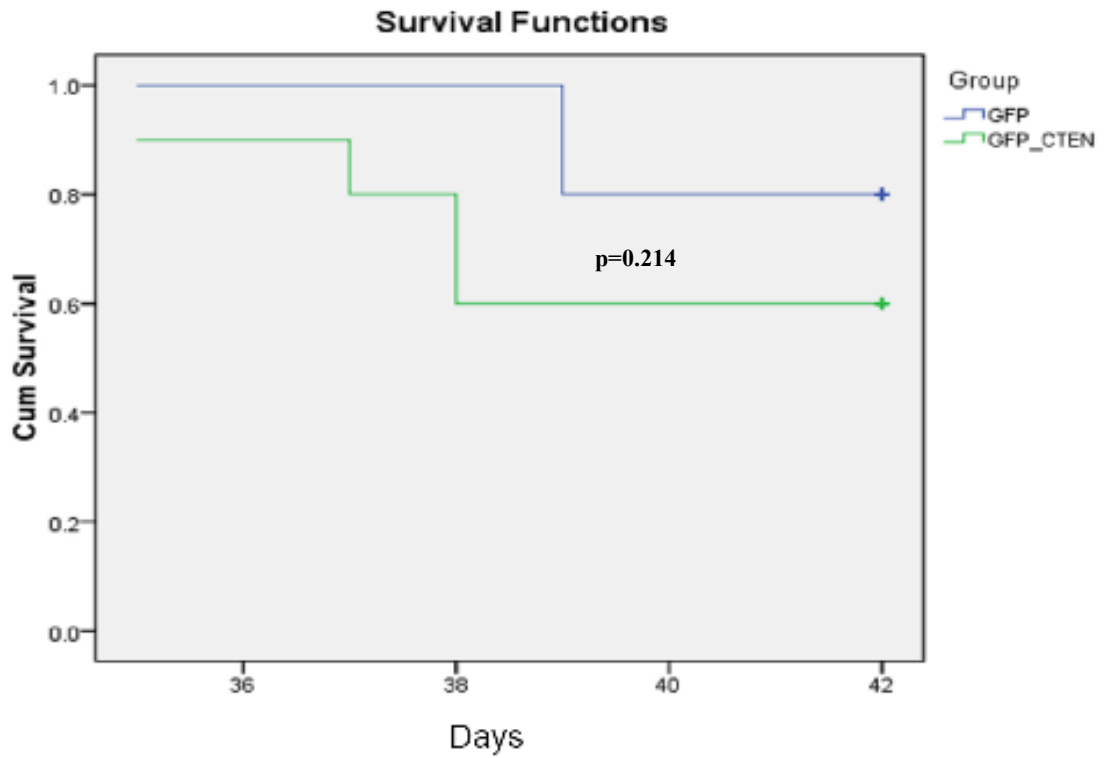


Figure 47. Kaplan–Meier plot for survival in mice injected with HCT116-GFP or HCT116-GFP-Cten cells. Analysis of the Kaplan–Meier showed no significant differences in overall survival between the mice injected with cells expression HCT116 GFP-Cten and HCT116 GFP ($p=0.214$; log-rank test).

5.8 Discussion

The Q-RT-PCR for *Cten* showed high efficiency and a wide dynamic range (i.e. the standard curve performed for the *Cten* PCR was able to detect *Cten* cDNA template at concentrations ranging over 5 orders of magnitude. *Cten* mRNA was detected in 62% cell lines although they differed in their level of expression up to 57 fold - well within the dynamic range of the PCR thus confirming the reliability of the quantification). The wide range of expression of *Cten* in the cell lines reflects the heterogeneity in the cell lines in the same way that tumours are heterogeneous for expression of many different types of genes. Given the small numbers of cell lines, the interpretation has to be cautious, although it is of interest that three of five cell lines with very high expression (COLO205, SW620 and COLO201) were derived from metastatic deposits, suggesting the close association between *Cten* expression and cancer metastasis in CRC. The Q-RT-PCR was only done once – this was because it was about identifying cell lines with high and low expression and then confirming this with Westerns. HCT116 and SW480 are both well-described cell lines which were found to have little expression of *Cten* at the mRNA level and little detectable *Cten* protein by western blot. These were thus chosen for studies of *Cten* forced expression experiments. In comparison, SW620 cell line was found to have high *Cten* expression at both mRNA and protein levels. Therefore, it was chosen for *Cten* gene knock-down experiments.

The C-terminal of tensin protein contains a SH2 domain, allowing tensin to interact with certain tyrosine-phosphorylated proteins, such as PI3K, FAK and P130Cas. This binding is critical for tensin-mediated effects on cell motility, migration and cell survival, suggesting that tensin is not only a structural protein but also plays a key role in mediating signalling transduction at focal adhesions (3, 8, 209). As *Cten* shares

extensive homology with other tensin members at its C-terminus, it has been proposed that *Cten* may possibly affect diverse biological activities including cell motility, migration and cell survival in a manner similar to that of the other tensin proteins. In addition, studies in breast cell lines show that *Cten* protein stimulates cell motility through displacement of TNS3 at focal adhesions and consequent dissociation between the cytoplasmic tails of integrin molecules and actin fibres (30). Our data showed that forced expression of *Cten* in CRC cell lines could induce EMT and this would be suggestive of a role in controlling cell motility in CRC. This was confirmed by experiments showing that *Cten* could stimulate cell migration and cell invasion in both HCT116 and SW480 cell lines. In order to further evaluate the role of *Cten* in modulating cell motility, we used RNAi to knock-down *Cten* in the CRC cell line SW620. This cell line expresses high levels of endogenous *Cten* and knock-down of *Cten* resulted in inhibition of cell migration and invasion. Our data are in agreement with those of Liao *et al*, who reported that forced *Cten* expression and knock-down in CRC cell lines expressing low and high levels of *Cten* protein is associated with enhanced and suppressed transwell migration and invasion abilities respectively (207).

This implies that *Cten* may be a gene that promotes tumour metastasis. We can speculate further that the observed resistance to staurosporine-induced apoptosis may reflect an ability to survive in hostile environments such as sites of metastasis. Our data support *Cten*'s role as an oncogene and, furthermore, suggest that its role may be in supporting tumour metastasis rather than tumour growth.

Our current data show that compared with control mice (injected with cells transfected with GFP empty vector), mice injected with cell expressing *Cten* developed a greater

tumour burden both locally within the spleen and within the liver metastases. These data clearly demonstrate the significant association of *Cten* with cancer metastasis in both *in-vitro* and *in-vivo* models and would support our own data and other published data showing the association between high *Cten* expression and advanced disease stage in lung, thymic and gastric tumours (56, 57, 24). Our data also show no significant differences in overall survival between the mice injected with cells expression HCT116 GFP-*Cten* and HCT116 GFP. This is not unexpected, due to small numbers of mice used in the study. Given this, any attempt to identify associations was underpowered significantly.

Chapter 6. Evaluation of Cten targets in CRC

6.1 Introduction

Previous studies had shown that ectopic expression of Cten protein in CRC cell lines caused changes in cell morphology and increased cell motility (both migration and invasion). These data were validated in another testing system. RNAi was used to knock down Cten in the CRC cell line SW620 which resulted in inhibition of both cell migration and invasion. Furthermore, high levels of Cten expression were significantly associated with advanced disease/metastasis in human CRC. In addition, Cten expression was capable of enhancing metastasis in an *in-vivo* model. Therefore, we sought to clarify the mechanistic basis of Cten-mediated changes in cell motility in CRC.

6.2 Cloning of *Cten* into an expression vector

In order to validate our previous *Cten* functional results using the GFP tagged *Cten* plasmid and to test whether the GFP would cause a functional problem, it was necessary to shuttle the *Cten* coding sequence into a Myc tagged vector and to engineer a pCMVTag3B-*Cten* expression construct. To achieve that, sequential BamHI and HindIII restriction digests were employed for both pCR2.1-*Cten* plasmid and pCMVTag3B vector in order to isolate the *Cten* insert from pCR2.1 vector and shuttle into pCMVTag3B expression vector.

The pCR2.1-*Cten* plasmid BamHI and HindIII restriction digests confirmed the sequencing results and showed that *Cten* was inserted into pCR2.1 vector in reverse (HindIII to BamHI) orientation. The digestion results showed the linearisation of pCR2.1-*Cten* plasmid after HindIII digestion and releasing the *Cten* insert from the pCR2.1 vector after BamHI digestion (Figure 48, 49).

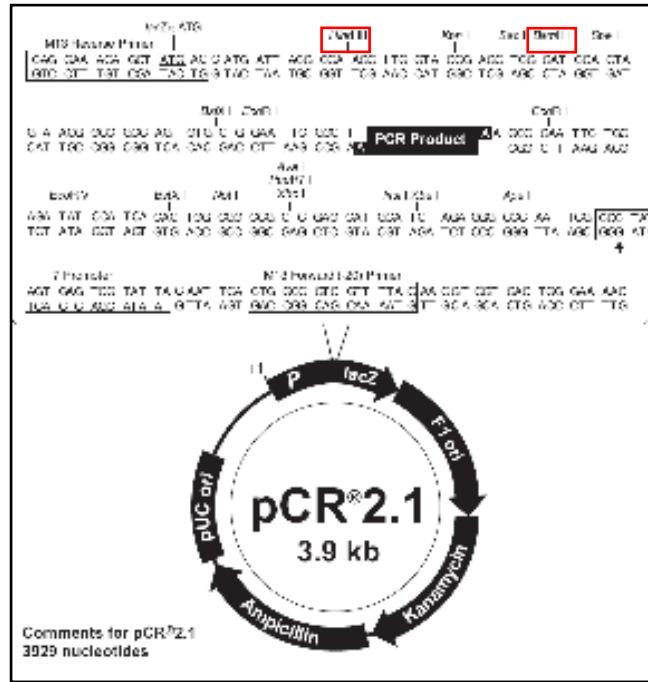


Figure 48. pCR2.1 vector map. Red boxes show BamHI and HindIII enzymes restriction sites.

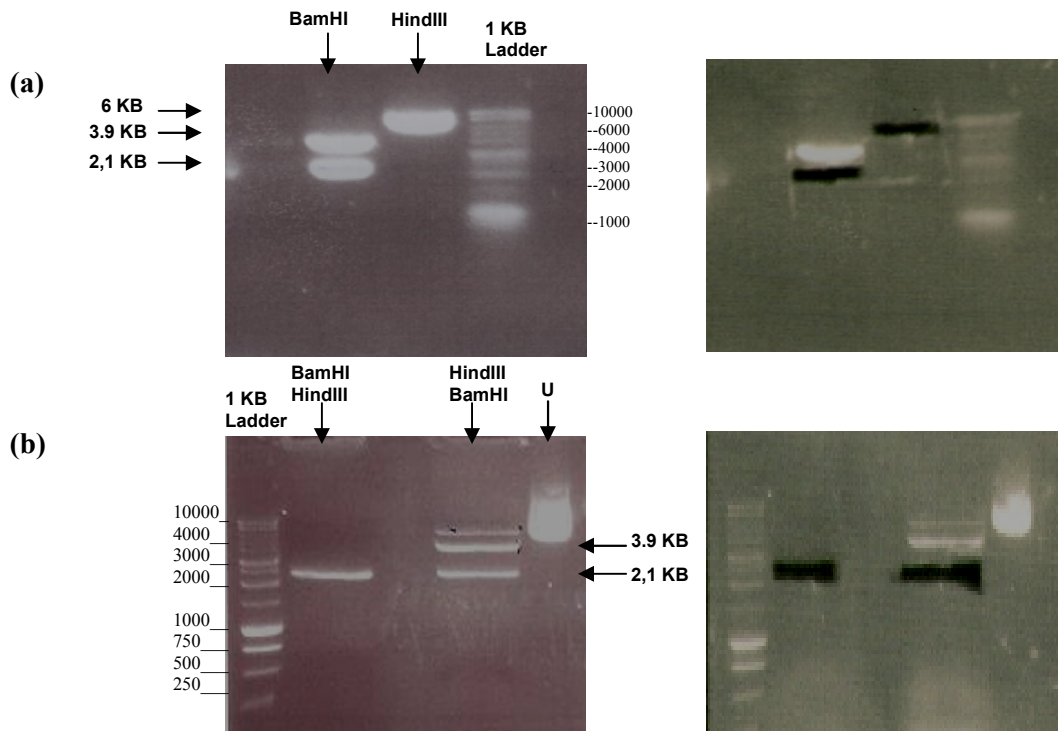


Figure 49. Gel purification and sequential digestion of pCR2.1-Cten plasmid. The sequential digestion was done with one enzyme (a) then with both enzymes (b). The digestion results showed the linearisation of pCR2.1-Cten plasmid (6 KB) after HindIII digestion and releasing the Cten insert (2.1 KB) from the pCR2.1 vector (3.9 KB) after BamHI digestion. There are two BamHI site: in the vector upstream of the multiple cloning site and in the upstream primer of Cten. If the insert goes in reverse orientation, even a single BamHI digest will release the insert thus giving two bands.

The gel purified BamHI/HindIII *Cten* insert was then ligated into a BamHI/HindIII digested pCMVTag3B vector (Figure 50, 51) at ratio of 1:1. Another 2 ligation reactions were also set up as negative controls. These contained all the reaction components except the purified insert in the first one and the vector in the second one (no colonies were seen in the negative control plates). The ligation mix was transformed into competent bacteria, colonies were picked, mini-preps grown and plasmid DNA extracted.

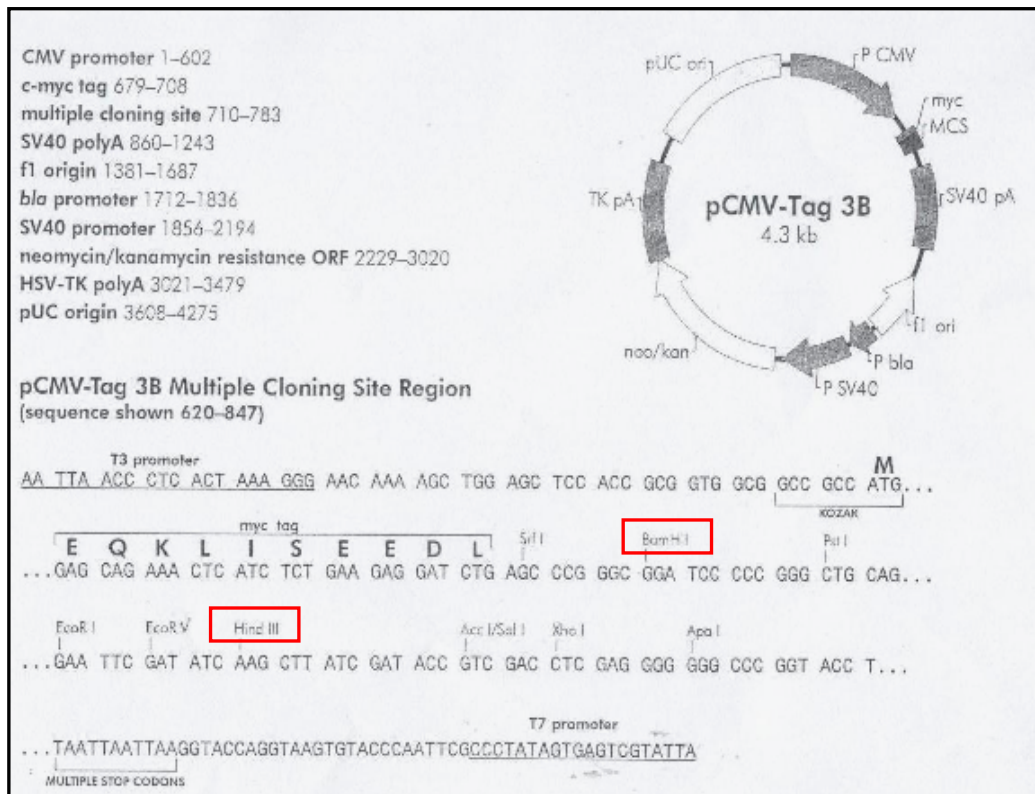


Figure 50. pCMV-Tag3B expression vector map. Red boxes show BamHI and HindIII enzymes restriction sites.

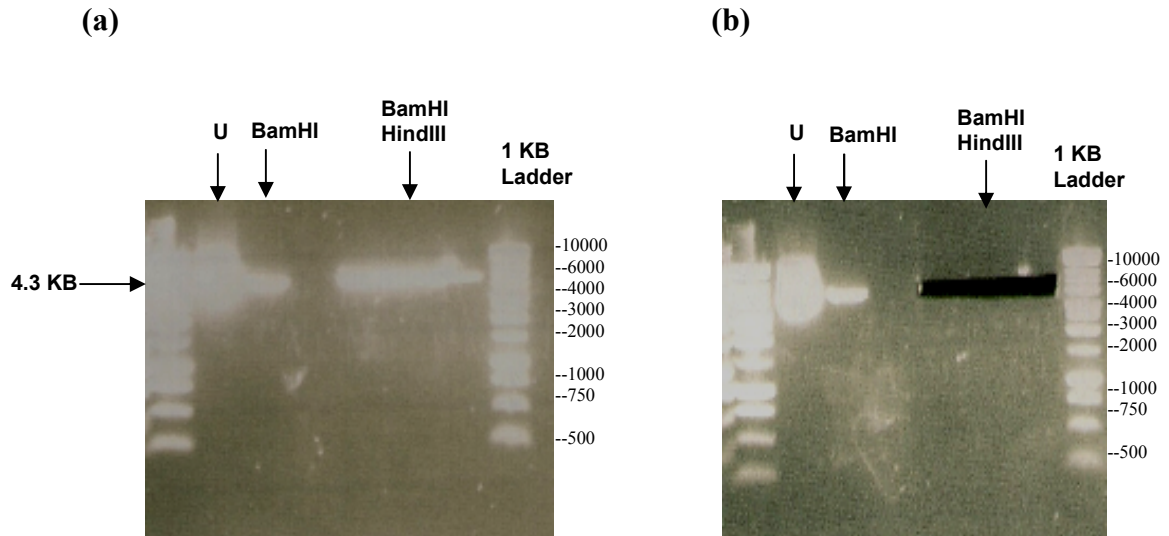


Figure 51. Gel purification and sequential digestion of pCMV-Tag3B vector. The vector was digested with BamHI restriction enzyme, tube purified and sequentially digested with HindIII restriction enzyme (a). Electrophoresed DNA was visualised under ultraviolet light and appropriate band (4.3 KB) was excised from the gel with clean scalpel in order to isolate the DNA from agarose gel using the Gel Extraction system, following the manufacturer's standard protocol. Figure (b) shows that the band has been correctly excised. U: Undigested.

Analytical digestion using XhoI and SacI of potential pCMVTag3B-Cten plasmid from positive colonies were performed to verify the presence of the insert within the vector. XhoI enzyme cuts once in both the Cten insert as well as in the pCMVTag3B vector, releasing two bands of expected size of 1,428bp and 5,020bp respectively. In comparison, SacI enzyme cuts once in the Cten insert, linearising the pCMVTag3B-Cten plasmid with a band of expected size of 6,448bp (Figure 52). However, none of the analytical digestion results showed bands specific for pCMVTag3B-Cten plasmid. We only found empty pCMVTag3B vectors (Figure 53). This means that either pCMVTag3B vector was re-ligated and not completely double digested, or the ligation reaction was not efficient.

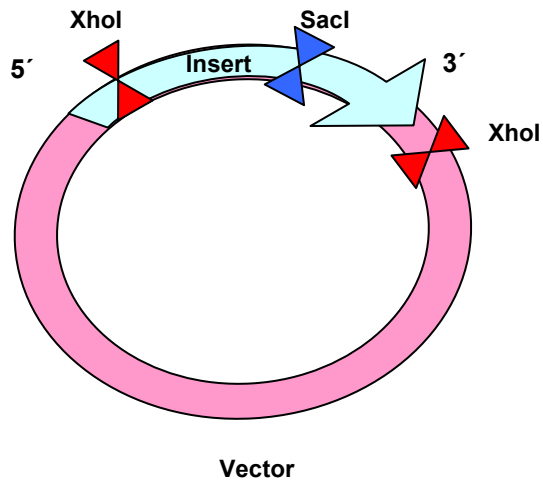


Figure 52. Diagram shows *XhoI* and *SacI* enzymes restriction sites in pCMVTag3B-Cten plasmid. *XhoI* enzyme cuts once in both the *Cten* insert at 720bp away from the 5' end and in the pCMVTag3B vector just 18bp after the *Cten* insert 3' end, releasing two bands of expected size of 1,428bp and 5,020bp. In comparison, *SacI* enzyme cuts once in the *Cten* insert at 1761bp away from the 3' end, linearising the pCMVTag3B-Cten plasmid with a band of expected size of 6,448bp.

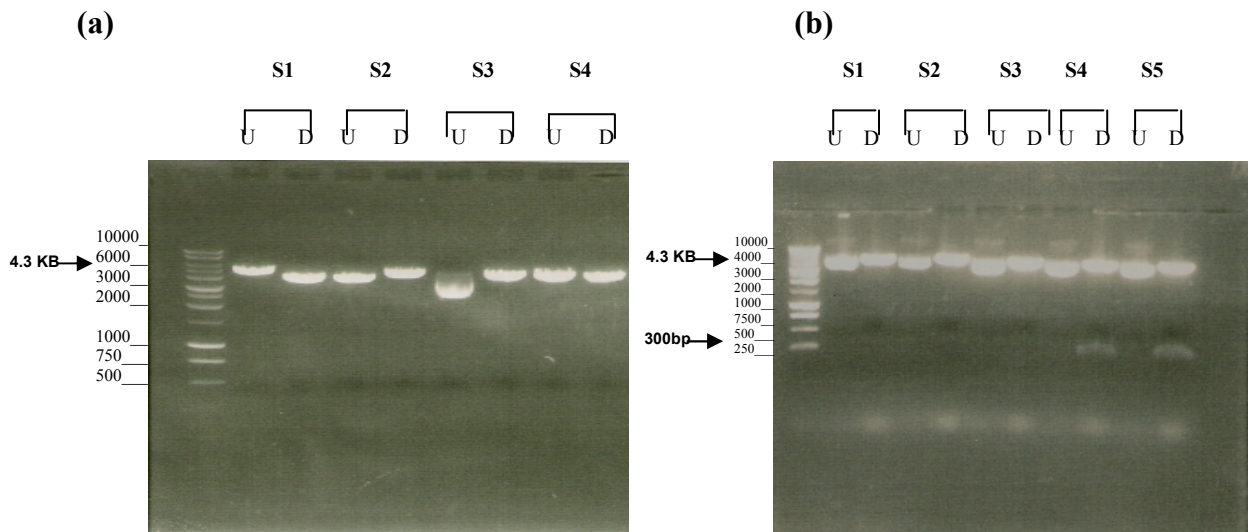
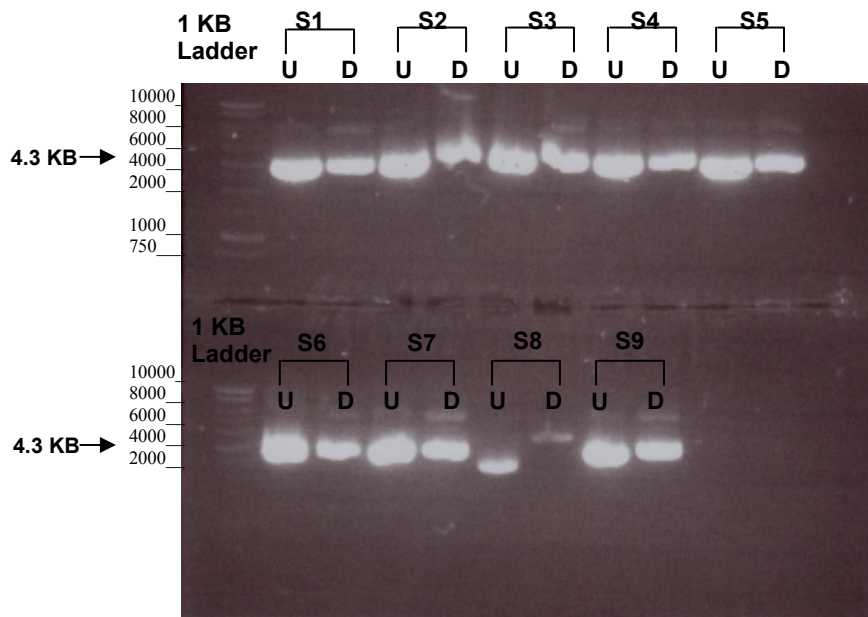


Figure 53. Agarose gel of potential pCMVTag3B-Cten clones after analytical enzyme digestions. The digestion with (a) *SacI* and (b) *XhoI* enzymes show empty vectors (4.3 KB) in most of the test samples. Samples 4 and 5 digested with *XhoI* enzyme show additional non-specific bands (300bp), suggesting a partially digested samples. S: Sample, U: Undigested, D: Digested.

To overcome these problems, a new sequential digestion and gel purification of pCR2.1-Cten plasmid and pCMVTag3B vector were done, and at this time an additional washing step, during gel purification using QG buffer (750µl) according to the manufacturer's protocol, was performed to avoid vector self-ligation. This was followed by ligation reactions at ratio of 3:1 and 5:1 (vector: insert) to achieve a better ligation efficiency. Again, no colonies were seen in the negative control plates. Analytical digest using XhoI and SacI of potential pCMVTag3B-Cten plasmids were carried out, only empty pCMVTag3B vectors were detected (Figure 54 a, b).

All attempts to shuttle the Cten gene from pCR2.1-Cten vector into a mammalian expression plasmid pCMVTag3B failed. Therefore, all transfections and functional analyses of Cten were carried out using GFP-Cten plasmid, which was kindly provided from (Dr Su Hao Lo, Department of Biochemistry and Molecular Medicine, University of California- Davis, USA)

(a)



(b)

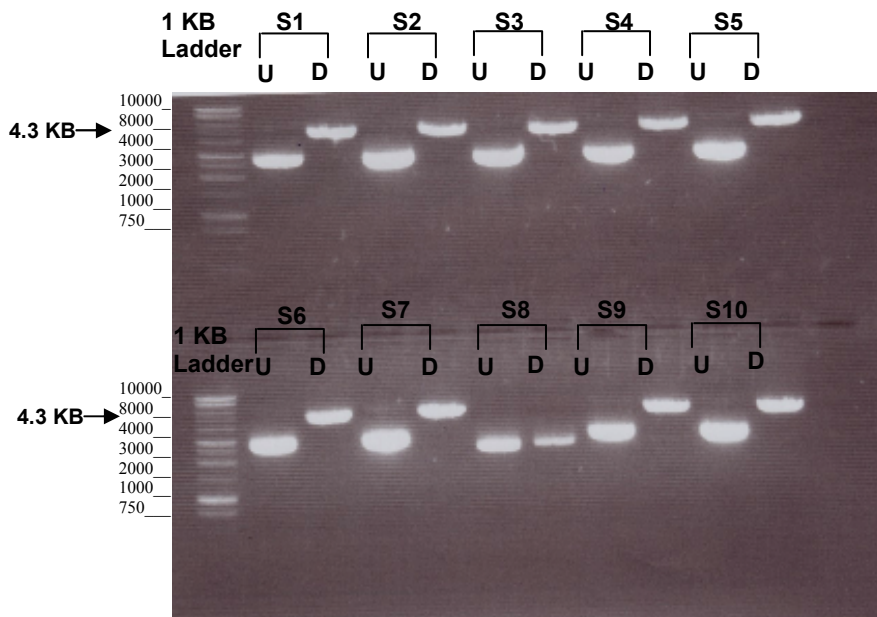


Figure 54. Agarose gel of potential pCMVTag3B-Cten clones after analytical digestion with (a) *SacI* and (b) *XhoI* enzymes. The digestion results show empty vectors (4.3 KB) in most of the test samples. S: Sample, U: Undigested, D: Digested.

6.3 Cten and E-cadherin expression

Given the effects of forced Cten expression on cell morphology and cell motility, we next sought to investigate possible mechanisms for these effects. Cten localises at focal adhesions and has been shown to disrupt integrin function. However, epithelial cells also have intercellular adhesion which is mediated via *adherens junctions* and, in particular, through the adhesion molecule E-cadherin. Disruption of *adherens junctions* through loss of E-cadherin function can stimulate cell motility (210). Western blot analysis of cells transfected with GFP-Cten showed decreased levels of E-cadherin protein - when compared with empty vector control cells in both HCT116 and SW480 (Figure 55). This suggests that the effects of Cten are mediated via an E-cadherin-dependent mechanism. In order to investigate whether reduction of E-cadherin protein was due to reduced gene transcription or enhanced protein degradation, Q-RT-PCR analysis of *CDH1* mRNA levels was performed. In both cell lines there was no change in message in cell lines transfected with Cten as compared to controls (Figure 56). This suggests that Cten causes reduction of E-cadherin protein at the posttranslational level.

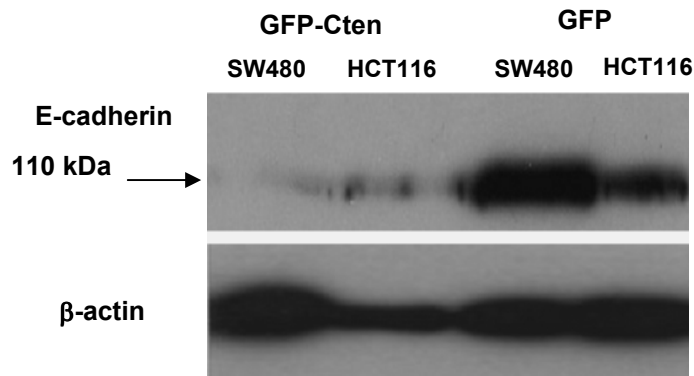


Figure 55. Cten and E-cadherin protein expression. Western Blot for E-cadherin shows that, in both HCT116 and SW480 cell lines, the E-cadherin protein is markedly decreased in cells transfected with GFP-Cten compared with empty vector control. The β -actin control is performed from the same sample used for E-cadherin Western blotting. The bands may seem overexposed due to the high quantity of protein loaded in order to detect E-cadherin (see materials and methods)

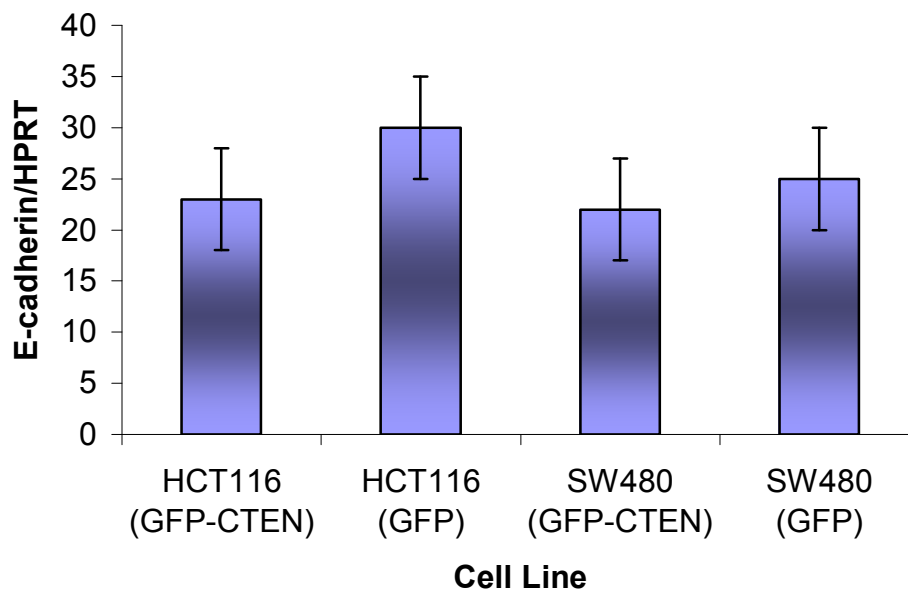


Figure 56. Cten and *CDH1* mRNA expression. Analysis of *CDH1* expression levels by Q-RT-PCR showed that there is no change in mRNA levels following forced Cten expression.

Having shown that forced expression of *Cten* in HCT116 and SW480 CRC cell lines correlates with decreased E-Cadherin protein levels, we used the reciprocal approach of knock-down of endogenously over-expressed *Cten* in order to validate our previous findings. SW620 cells, which endogenously express high levels of *Cten*, were transfected with specific *Cten* siRNA or non-targeting scrambled control. The knock-down of *Cten* in SW620 cells lead to increased E-cadherin levels (Figure 57), confirming our previous findings of an inverse relationship between *Cten* and E-cadherin levels in CRC.

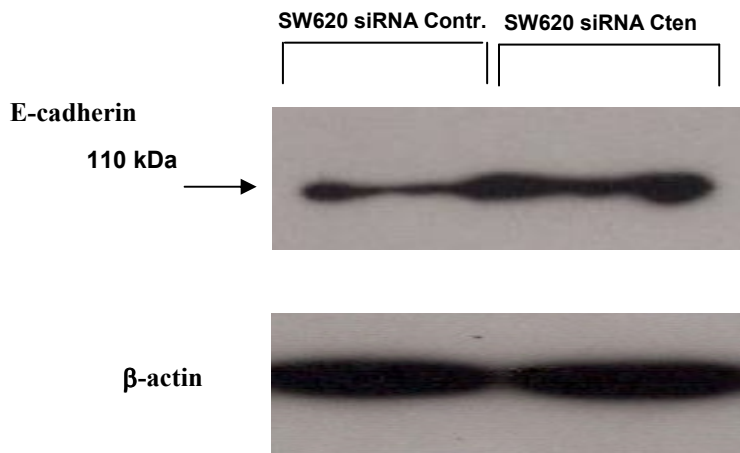
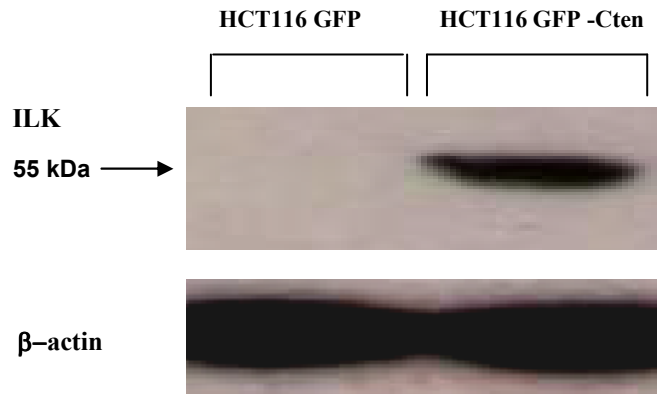


Figure 57. Effect of *Cten* knock-down on E-cadherin protein expression. Immunoblotting showed that *Cten* knock-down in SW620 cells leads to increased E-cadherin levels. β -actin was used as a loading control. Overexposure of the β -actin control is due to the same reason highlighted in the previous figure. Data shown are representative of experiments performed in duplicate (and replicated in independent experiments).

6.4 Cten and ILK expression

The close localisation of ILK with Cten at cytoplasmic site of integrin molecules together with the reports that ILK can cause down-regulation of E-cadherin raises the possibility of that part of the Cten-mediated effect on cell migration and E-cadherin expression may occur via ILK. We tested this hypothesis using a dual approach of forced Cten expression and Cten knock-down in cell lines respectively expressing low and high levels of Cten protein. Forced expression of GFP-Cten in the CRC cell line HT116 cells resulted in up-regulation of ILK (Figure 58 a). In agreement with these results, the reciprocal Cten knock-down experiments in SW620 cells resulted in down-regulation of ILK (Figure 58 b).

(a)



(b)

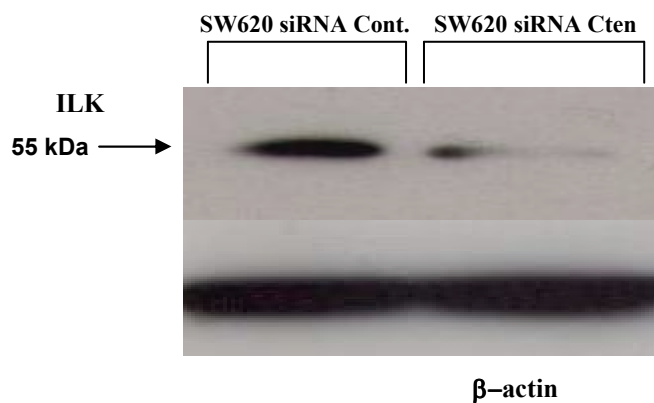


Figure 58. Effect of Cten forced expression and knock-down on ILK protein expression. Western blots showed that forced expression and knock-down of Cten in HCT116 (a) and SW620 (b) cells, resulted in up-regulation and down-regulation of ILK protein level respectively. β -actin was used as a loading control. The reason for β -actin control being overexposed is because we load a lot of protein (30 ug) to detect ILK protein and the loading control is tested on the same samples. Data shown are representative of experiments performed in duplicate (and replicated in independent experiments).

6.5 *Cten* and FAK expression

6.5.1 Evaluation of expression and role of FAK in CRC

FAK is a 125-kDa non-receptor and non-membrane associated PTK which localises to focal adhesions. These are sites where integrin molecules mediate attachment between the cell and the ECM (87, 88, 211). FAK has been shown to act as an early modulator in the integrin signalling cascade and facilitates "outside-in" signalling to downstream targets such as extracellular signal-regulated kinase 2 or c-Jun-N-terminal kinase (212). FAK has been found to be highly expressed in a variety of tumours, including head and neck, ovarian, thyroid, and colon carcinomas (213-217). Forced FAK expression in ovarian cells has been reported to enhance G1 to S phase transition, suggesting a role for FAK in the promotion of cell proliferation (218). Conversely, knock-down of FAK protein or treatment of cancer cells with anti-FAK antibodies can induce apoptosis (219, 220). In addition, isolated fibroblasts from FAK-KO mice have been shown to migrate significantly more slowly than their normal counterparts (221) suggesting that FAK also promotes cell migration.

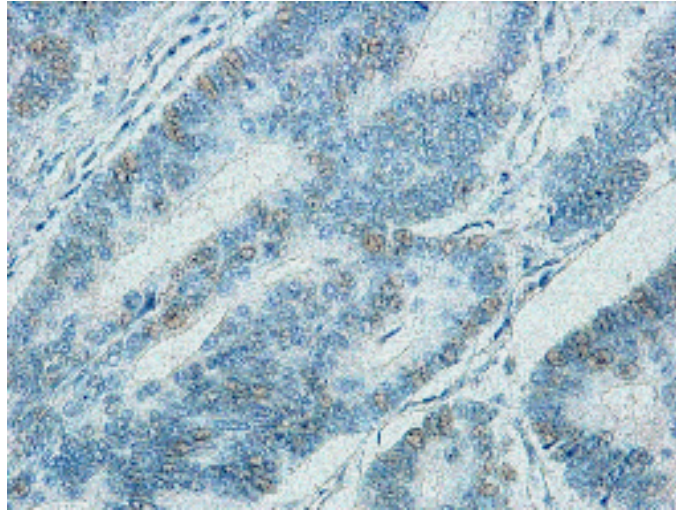
For full activation, FAK requires phosphorylation of the amino acid residue Tyrosine 397. This creates binding sites for SH2 domain-containing proteins thereby triggering multiple signalling pathways (222). The binding of Src to FAK can also phosphorylate FAK at Y925, an additional amino acid residue known to be associated with integrin adhesion dynamics and E-cadherin de-regulation during Src-induced EMT (223, 224).

In the present study, we evaluated P-FAK protein expression in a large well-characterised series CRC cases (n=462) with a long term follow-up using IHC and TMA to test if P-FAK has a prognostic significance in patients with CRC.

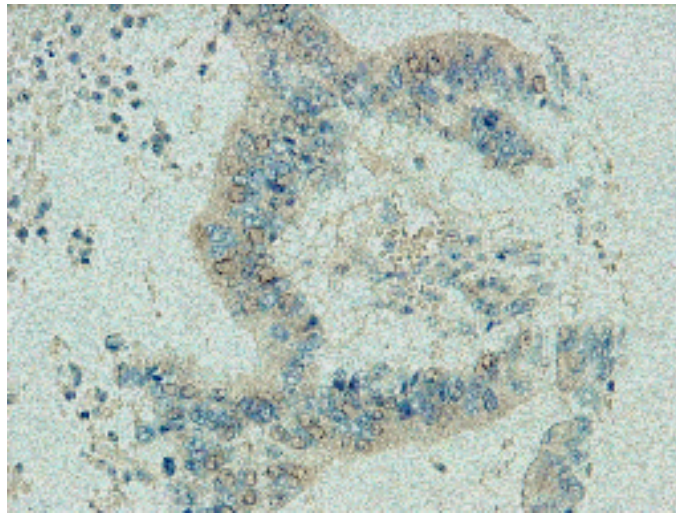
6.5.1.1 P-FAK expression in CRC cases

After excluding the uninformative TMA cores (109) from the study, which were either lost, folded, fragmented or did not have invasive tumour tissue, 353 tumours were available for P-FAK immunostaining assessment by the H-score method. Expression of P-FAK was predominantly nuclear and was seen in 155/353 (44%) of cases (Figure 59 a). Cytoplasmic expression of P-FAK was inversely correlated with nuclear expression of P-FAK and noticed in 79/353 (22%) of cases (Figure 59 b). In contrast, no tumour cell membrane or stromal expression of P-FAK was noticed in any of the examined cases. The X-tile bio-informatics software (Yale University, USA) was used to define optimal cut-off points of P-FAK H-score. This program basically divides the total patient cohort randomly into two separate equal training and validation sets ranked by patients' follow-up time. The optimal cut-points were determined by locating the brightest pixel on the X-tile plot diagram of the training set and dichotomised the scoring into "low P-FAK" (H score <30) and "high P-FAK" (H score >30). Statistical significance was tested, using the chi-square test, by validating the obtained cut-point to the validation set.

(a)



(b)



(c)

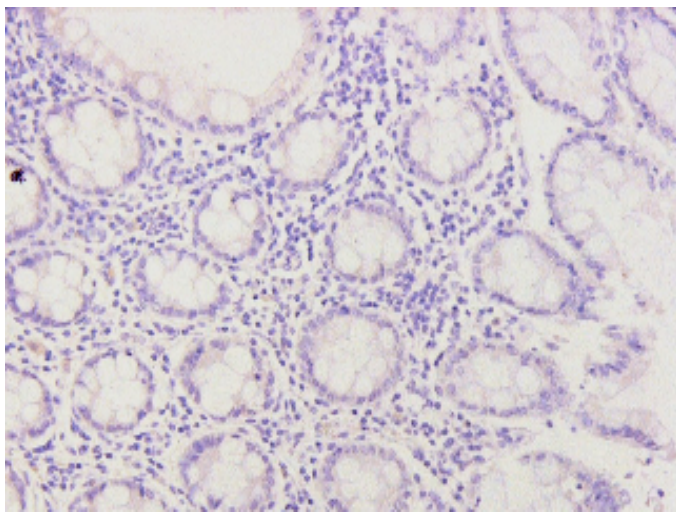


Figure 59. P-FAK protein expression in CRC. Immunohistochemical staining for P-FAK on TMA sections of CRC (x200), demonstrating (a) moderate P-FAK nuclear staining and (b) moderate cytoplasmic and nuclear staining. (c) Negative control.

6.5.1.2 Association of P-FAK expression with clinicopathological parameters

Analysis of positively stained P-FAK cases revealed that there was no significant association between the level of P-FAK nuclear expression and known clinicopathological variables, including tumour histological type, tumour grade, tumour site, TNM staging, LN metastasis, VI and DM (Table 8). In contrast, P-FAK cytoplasmic expression within the malignant tumours, was significantly associated with DM ($p=0.02$; chi-square test) and showed an inverse association with a trend toward TNM staging ($p=0.05$; chi-square test), LN metastasis ($p=0.07$; chi-square test) and VI ($p=0.09$; chi-square test). However, no significant association was noticed between P-FAK cytoplasmic expression and tumour histological type, tumour grade and tumour site (Table 8).

Table 8. Association of P-FAK cytoplasmic and nuclear expressions with clinicopathological features. No significant association was found between P-FAK nuclear expression and known clinicopathological variables. In contrast, high P-FAK cytoplasmic expression was significantly associated with DM and showed an inverse association with a trend toward TNM, LN metastasis and VI.

Parameter	Low P-FAK Nuclear	High P-FAK Nuclear	X ²	p	Total No.	Low P-FAK Cytoplasmic	High P-FAK Cytoplasmic	X ²	p	Total No.
Tumour histological type										
Adenocarcinoma	74 (86%)	57 (88%)	2.450	0.351	151	14 (82.4%)	48 (84.2%)	4.540	0.102	74
Non-adenocarcinoma	12 (14%)	8 (12%)				3 (17.6%)	9 (15.8%)			
Tumour grade										
Well differentiated	4 (4.9%)	6 (9%)	3.867	0.137	148	1 (5.8%)	7 (12.3%)	3.874	0.126	74
Moderately differentiated	65 (79.3%)	51 (77.3%)				14 (82.4%)	43 (75.4%)			
Poorly differentiated	13 (15.8%)	9 (13.7%)				2 (11.8%)	7 (12.3%)			
Tumour site										
Colon	41 (52.5%)	34 (55%)	0.806	0.852	140	11 (65%)	27 (50%)	2.463	0.348	71
Rectum	37 (47.5%)	28 (45%)				6 (35%)	27 (50%)			
TNM stage										
0 (T _{is})	1 (1.2%)	0 (0%)	1.318	0.574	148	2 (10%)	13 (22%)	7.847	0.057	78
1	13 (15.8%)	10 (15%)				6 (30%)	25 (43.7%)			
2	34 (41.5%)	23 (35%)				6 (30%)	15 (25.8%)			
3	26 (31.7%)	23 (35%)				4 (20%)	4 (6.8%)			
4	8 (9.8%)	10 (15%)				2 (10%)	1 (1.7%)			
LN stage										
0	49 (63%)	34 (53.2%)	4.536	0.104	142	8 (47%)	39 (71%)	6.819	0.071	72
1	17 (21.7%)	15 (23.4%)				4 (23.5%)	8 (14.5%)			
2	12 (15.3%)	15 (23.4%)				5 (29.5%)	8 (14.5%)			
VI										
Negative	55 (65%)	43 (65.2%)	0.730	0.871	151	11 (58%)	44 (73.3%)	5.382	0.096	79
Positive	30 (35%)	23 (34.8%)				8 (42%)	16 (26.7%)			
DM										
Negative	77 (90.6%)	56 (85%)	2.936	0.235	151	18 (69.3%)	27 (51%)	9.165	0.021	79
Positive	8 (9.4%)	10 (15%)				8 (30.7%)	26 (49%)			

Note: If the total number of cases in a given parameter did not add up to 155 (nuclear P-FAK) or 79 (cytoplasmic P-FAK), this indicates that there were no data available for the missed cases of each specific factor.

6.5.1.3 Association of P-FAK expression with patients' outcome

Univariate survival analyses showed that patients with high P-FAK nuclear expression had shorter DFS than those with low P-FAK nuclear expression ($p=0.005$; log-rank test, Figure 60 a). In addition, multivariate Cox proportional hazard analysis revealed that P-FAK nuclear positivity was a predictor of shorter DFS ($p=0.016$; log-rank test, Table 9) independent of TNM staging and vascular invasion. Unexpectedly, Kaplan-Meier analyses showed that patients with high P-FAK cytoplasmic expression had better survival than those with low P-FAK cytoplasmic expression ($p=0.001$; log-rank test, Figure 60 b).

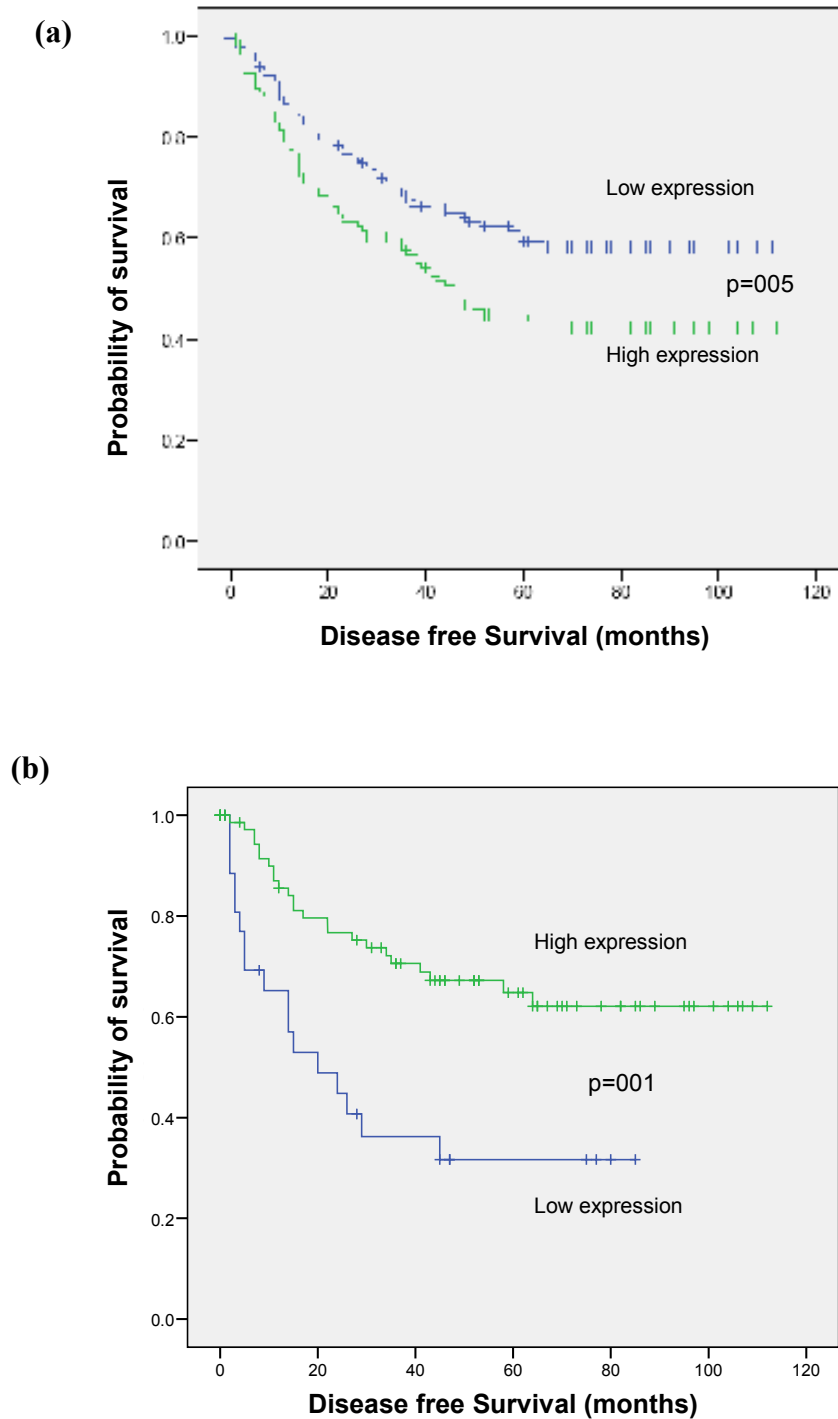


Figure 60. Kaplan-Meier plot for DFS in relation to expression of nuclear and cytoplasmic P-FAK. (a) Patients with high nuclear P-FAK have a significantly shorter DFS than patients with low nuclear P-FAK ($p=0.005$, log-rank test). In contrast, (b) patients with high P-FAK cytoplasmic expression had better survival than those with low P-FAK cytoplasmic expression ($p=0.001$, log-rank test).

Table 9. Cox-proportional hazard analysis for predictors of DFS and P-FAK cytoplasmic and nuclear expression. Multivariate Cox hazard analysis including TNM, VI and P-FAK cytoplasmic and nuclear expressions shows that P-FAK nuclear expression was an independent predictor of DFS in CRC (hazard ratio 1.129, 95% CI 0.763–2.126, p=0.016).

Parameter	Hazard ratio	95% CI	p value
Disease free Survival			
TNM stage	1.839	1.582–2.251	< 0.001
VI	1.431	1.043–2.152	0.002
P-FAK nuclear expression	1.129	0.763–2.126	0.016
P-FAK cytoplasmic expression	1.024	0.524–2.011	0.804

6.5.2 Cten and FAK interaction

Since tensin family proteins interact with FAK, we focused on FAK as another potential downstream signalling molecule for Cten in CRC. Therefore, the effect of Cten on FAK level was examined. Forced expression of Cten in HCT116 cells resulted in an increase of FAK and P-FAK levels (Figure 61). Knock-down of Cten in SW620 cells confirmed the results obtained by over-expression studies. Western blot analysis from SW620 cells transfected with control siRNA showed high FAK and P-FAK levels in comparisons to cells transfected with Cten siRNA (Figure 62).

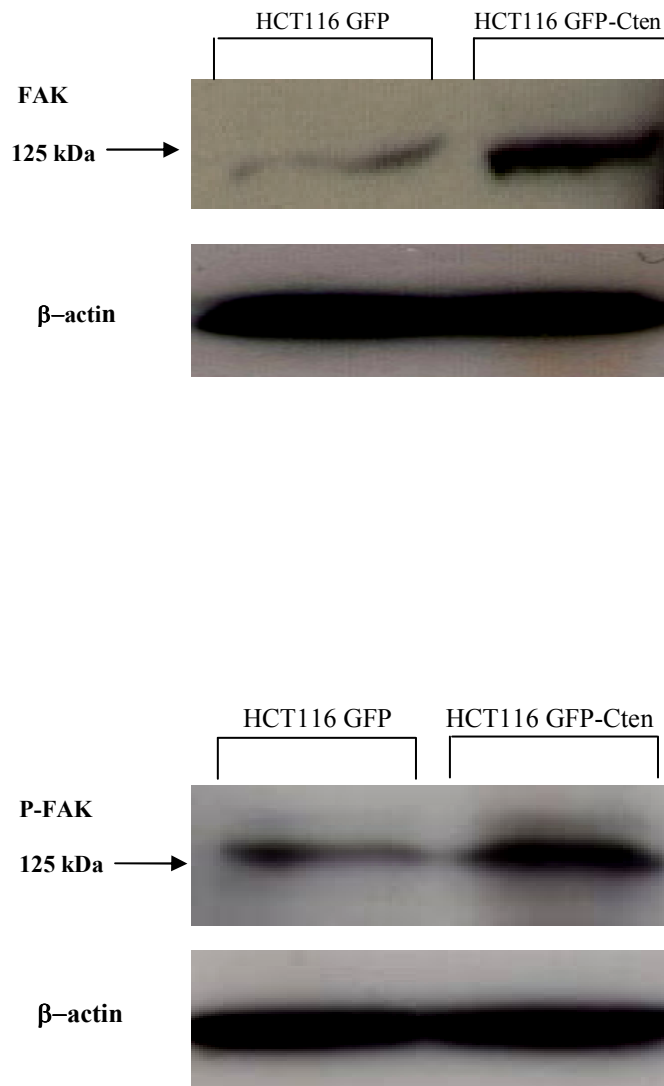


Figure 61. Effect of *Cten* forced expression on FAK and P-FAK protein expression levels. Western blots showed that forced expression of *Cten* in HCT116 cells resulted in an increase expression of FAK and P-FAK proteins. β -actin was used as a loading control.

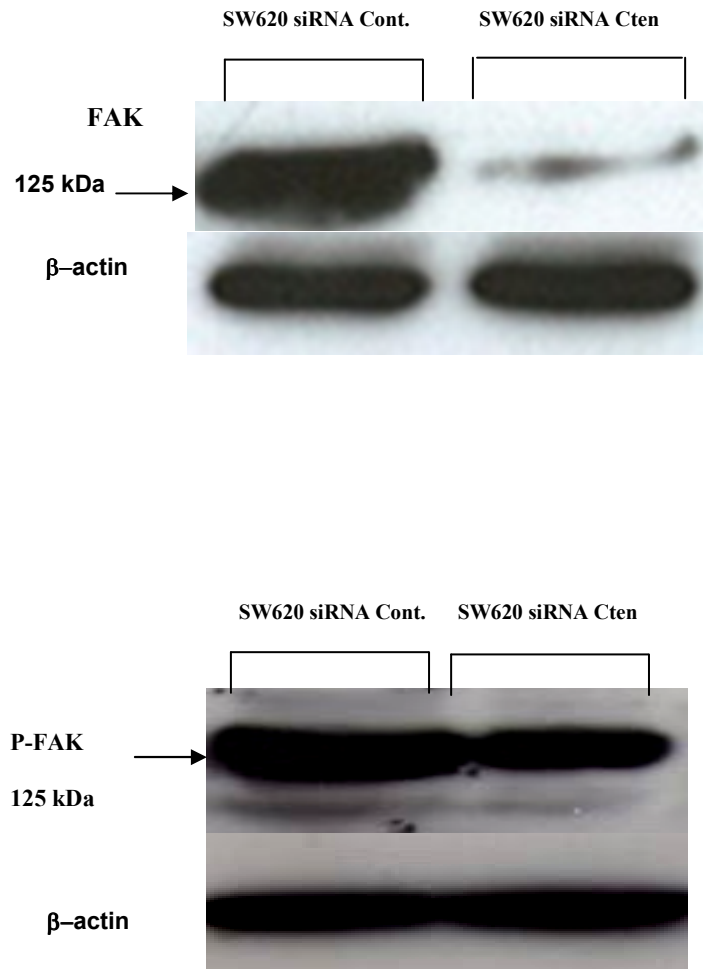


Figure 62. Effect of Cten knock-down on FAK and P-FAK protein expression levels. Knock-down of Cten in SW620 cells, showed high FAK and P-FAK levels in control SW620 cells compared to cells transfected with Cten siRNA. β -actin was used as a loading control.

6.6 *Cten* and CD24 expression

CD24 is a small 80 amino acids-spanning heavily glycosylated mucin-like glycosyl-phosphatidylinositol (GPI)-linked cell surface protein. Previous studies have been reported CD24 to be over-expressed in a wide variety of tumours, including non-small cell lung cancers, pancreatic and gastric adenocarcinomas, ovarian cancer, CRC and BC and, in general, its over-expression has been associated with poor prognostic outcomes (174-178). It has been reported that CD24 has regulatory and recruitment effects on $\beta 1$ integrin proteins, as it induces the lateral localisation of $\beta 1$ integrins into lipid raft domains (225), hinting that CD24-mediated effects on cell motility may depend on the $\beta 1$ integrin subunit. The close localisation of *Cten* at the cytoplasmic tail of $\beta 1$ integrin prompted us to investigate the relationship between CD24 and *Cten*. Western blot analysis of the HCT116 cell line (expressing low levels of both CD24 and *Cten*) stably transfected with pCDN6-CD24 (182) showed no effect on *Cten* expression in comparison to HCT116 cells (Figure 63 a). However, western blot analysis of HCT116 cells stably transfected with GFP-*Cten*, showed increased levels of CD24 compared to GFP vector control cells (Figure 63 b). Moreover, SW620 cells transfected with *Cten* siRNA contained lower CD24 levels than siRNA scrambled control cells (Figure 63 b).

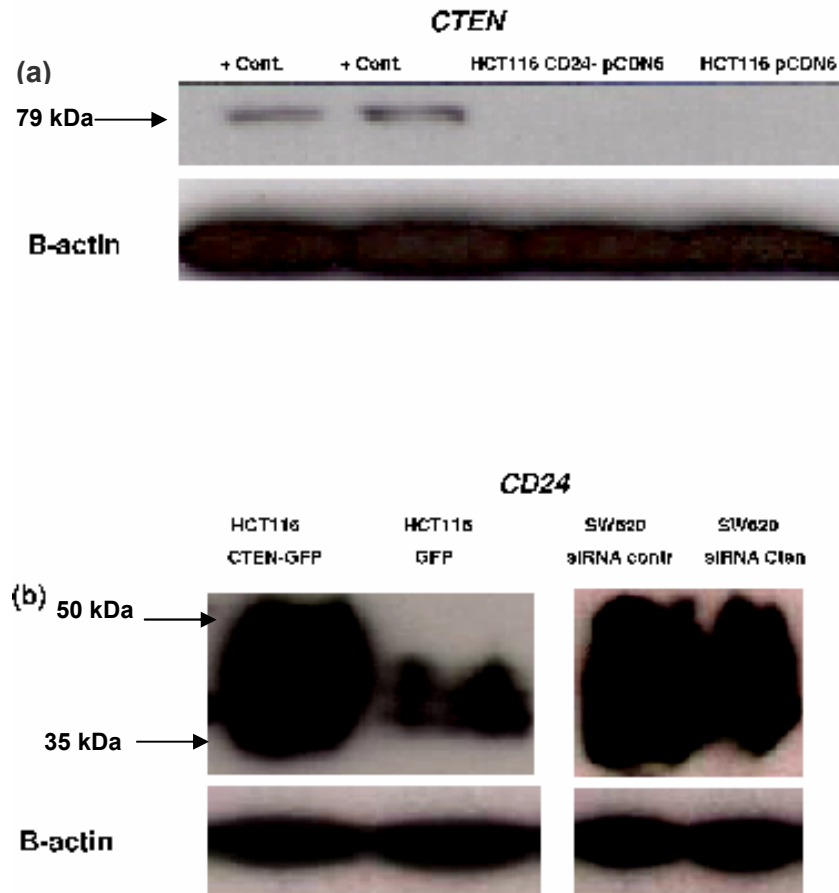
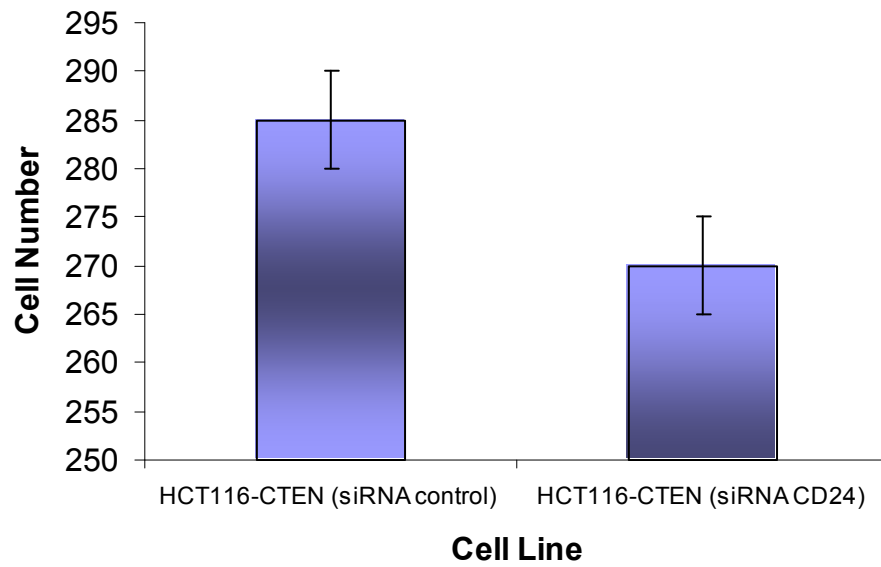


Figure 63. Cten and CD24 protein expression. Western Blot for Cten and CD24 proteins shows that, in the same cell lines, forced expression of Cten was associated with up-regulation of CD24 (glycosylated pattern) but not the vice versa. In addition, Cten knocked-down in SW620 cell line resulted in down-regulation of CD24 compared to siRNA scramble control. Positive controls shown in the top panel represent HCT116 and SW480 cells transfected with GFP-Cten. β -actin was used as a loading control. The bands may seem overexposed due to the high quantity of protein loaded in order to detect CD24 (see materials and methods)

Given the CD24-regulatory effect on the $\beta 1$ integrin subunit where ILK and FAK are localised as well as the induction effect of *Cten* on CD24 levels, we hypothesised that *Cten* may function through CD24 signalling. To test this hypothesis, knock-down of CD24 in HCT116 cell line stably transfected with GFP-*Cten* was carried out and a significant decrease regarding both cell migration and invasion was observed in the absence of *Cten* in comparison to control cells ($p < 0.001$ for both; Student's t-test, Figure 64 a, b). Furthermore, Western Blot analysis showed that CD24 knock-down was associated with up-regulation of E-cadherin and down-regulation of ILK and FAK proteins, indicating that CD24 lies downstream of *Cten* in CRC and that *Cten*-mediated effects on cell motility and E-cadherin, ILK and FAK levels may be CD24-dependent (Figure 65).

(a)



(b)

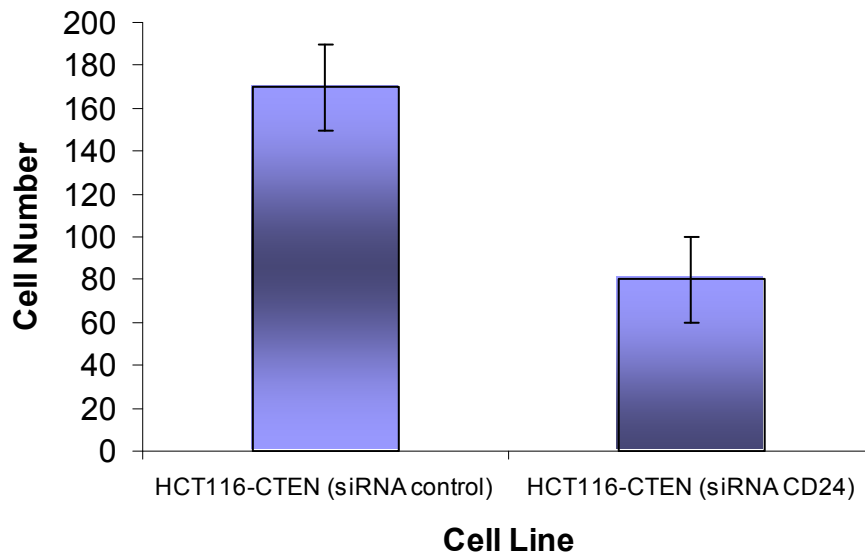


Figure 64. Cten functional relationship with CD24 protein. Knock-down of CD24 in HCT116 cell line stably transfected with GFP-Cten showed a significant decrease in both (a) cell migration and (b) invasion assays ($p < 0.001$; Student's t-test).

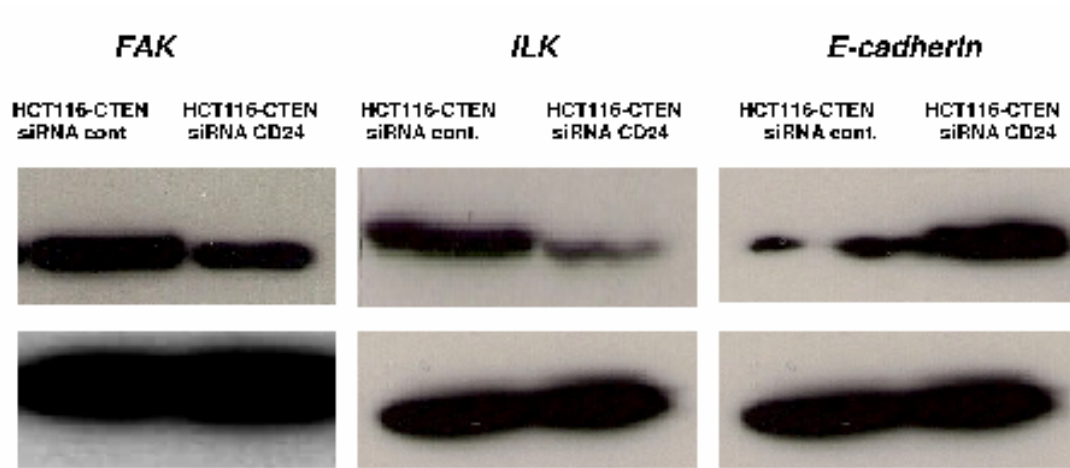


Figure 65. CD24 involvement in Cten signalling pathway. Western Blot analysis showed that CD24 knock-down in Cten stably transfected HCT116 cells was associated with up-regulation of E-cadherin and down-regulation of ILK and FAK proteins. β -actin was used as a loading control. The bands may seem overexposed due to the high quantity of protein loaded in order to detect FAK, ILK and E-cadherin proteins (see materials and methods)

6.7 Analysis of Cten and P-FAK expression in metastatic CRC

The data from the *in-vitro* experiments led us believe that ILK and P-FAK were downstream targets of Cten. We sought to validate this by examining the expression levels of these proteins in tissue samples by IHC. Attempts of IHC with the commercially available antibodies for ILK were unsuccessful. Immunohistochemical expression of Cten and P-FAK was examined in a series of 40 matched samples of primary colorectal adenocarcinomas and corresponding liver metastases arrayed as tissue microarrays (provided by our group). The level of staining was evaluated using the H-score system. The tissue microarrays showing no or weak staining (H-score <30) were classed as negative, those showing moderate or strong staining (H-score >30) were counted as positive. Evaluation of all the cases (i.e. both primary tumours and metastases) revealed a highly significant difference between levels of P-FAK expression in the primary and metastatic cases ($p=0.001$; chi-square test). There was no significant association between Cten expression and P-FAK expression in primary tumours ($p=0.491$; chi-square test), but interestingly, we found a highly significant association between nuclear Cten expression and P-FAK expression in hepatic metastases cases ($p<0.001$; chi-square test). One of 14 (2%) in the negative P-FAK expression group showed Cten positive immunoreactivity. In comparison, 14 of 26 (98%) in the positive P-FAK expression group had Cten positive immunoreactivity (Figure 66, Table 10).

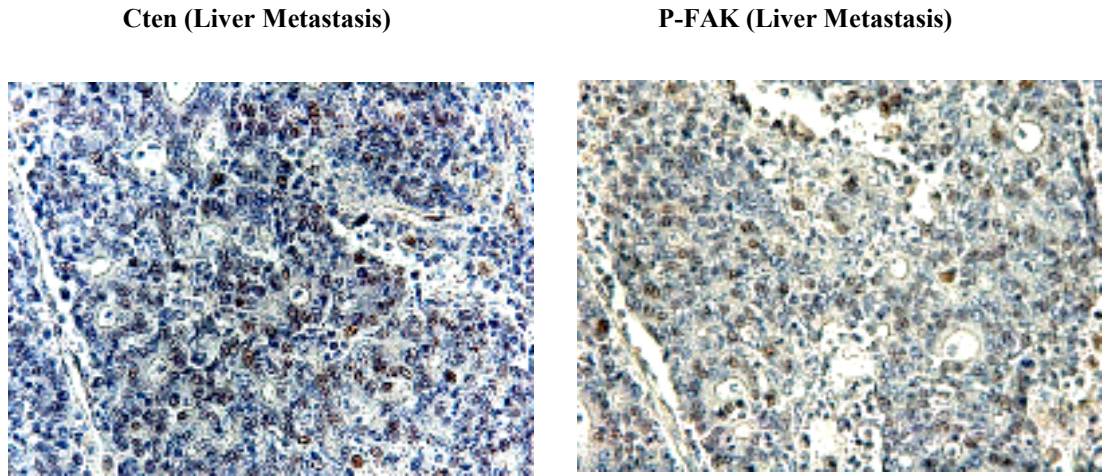


Figure 66. P-FAK protein expression in primary tumour samples and their corresponding liver metastasis. Positively stained tissue microarrays from the same sections showed a positive correlation between *Cten* expression and P-FAK expression in hepatic metastases cases.

Table 10. Association between *Cten* expression and P-FAK expression in hepatic metastases cases. Positive significant association was found between nuclear *Cten* expression and P-FAK expression in hepatic metastases cases ($p < 0.001$; chi-square test).

Parameter	Cten -ve	Cten +ve	χ^2	p value
P-FAK expression				
P- FAK -ve	13 (52.0%)	1 (2%)	11.556	0.001
P-FAK +ve	12(48.0%)	14(98.0%)		

6.8 Discussion

The molecular basis of *Cten*-mediated effects on cell migration and EMT is still under investigation. In the current study, we have shown that, in both CRC cell lines, *Cten* forced expression and knock-down was associated with down-regulation and up-regulation of E-cadherin protein expression, respectively. This suggests that *Cten* is important in the regulation of cell motility through E-cadherin-dependent mechanisms. A growing body of evidence has reported loss of E-cadherin expression in advanced CRC (226) and interestingly, experiments used to silence the expression of E-cadherin not only showed a morphological shift from an epithelial to mesenchymal phenotype, characteristic of EMT, but also a concomitant increase in invasive cell behaviour (227).

The close localisation of ILK with *Cten* at the cytoplasmic site of integrin molecules raises the possibility that the *Cten*-mediated effect on cell migration and E-cadherin expression signals via this molecule. It has been shown that ILK expression is elevated in a variety of cancers including CRC and the levels of expression were significantly higher in invasive than non-invasive lesions (228). Over-expression of ILK in normal breast epithelial cells results in down-regulation of E-cadherin expression, possibly through activation of the E-cadherin repressor Snail. In correlation with that, the ILK-over-expressing cells also become invasive, reorganise cortical actin into cytoplasmic stress fibers, and switch from an epithelial cytokeratin positive to a mesenchymal vimentin intermediate filament phenotype, suggestive of a role for ILK in EMT, which is a hallmark of cancer progression to an increasingly malignant phenotype (163). The present study has shown that *Cten*-forced expression and knock-down in CRC cell lines resulted in up-regulation and down-regulation of ILK respectively, indicating that

Cten-mediated effect on cell migration and E-cadherin expression may signal directly or indirectly via ILK. Attempts of IHC with the commercially available antibody for ILK (ab2283, Abcam, UK) were unsuccessful. Two different immunohistochemical antibody detection Kits (ABC and EnVision kits, kindly provided by Prof. Ian Ellis, Division of Pathology, University of Nottingham, UK) were used and in each one we tried different dilutions of ILK antibody in order to optimise the optimal condition for ILK antibody to work. However, each time we found non-specific background staining masking the ILK cytoplasmic staining.

The expression and phosphorylation of the non-receptor tyrosine kinase FAK has been shown to correlate with epithelial to mesenchymal changes occurring in tumours during their progression to an invasive phenotype (229). In addition, FAK influences the sensitivity of tumour cells to chemotherapy, and combination of antisense oligonucleotide inhibitors of FAK with cytotoxic agents might be a promising anti-cancer therapy (230). Given that, we sought to investigate the utility of P-FAK as a prognostic marker in CRC in a large and well-characterised cohort of CRC cases. Using IHC we were able to detect the expression of P-FAK protein in the nucleus in 44% of tumours. This is similar to published data which have found 45% CRCs showing positive P-FAK expression (231). In the current study population nuclear P-FAK expression was not related to any of the clinicopathological parameters examined. However, univariate and multivariate analysis of our population showed that high expression of nuclear P-FAK in CRC had a poor prognostic impact on patients' outcome. Nuclear expression of P-FAK has also been reported in other studies and Ssang-Taek *et al* found that FAK may limit p53 activity through the FAK N-terminal FERM domain through directly interacting and suppressing transcriptional

activation of a number of p53 target genes including p21, Mdm2 and Bax. The latter molecules are important mediators of p53-induced apoptosis, which would propose an anti-apoptotic effect of nuclear FAK through a FERM-domain-initiated pathway (114).

Cten co-localises with paxillin in focal adhesions and is involved in mediating the metastatic potential of mammary tumours (30). *Cten* contains a SH2 and PTB domains, both of which have been shown to be involved in protein-protein interactions (5, 11, 14). FAK has also been reported to localise to focal adhesions via its interaction with paxillin (91) thus some interaction between *Cten* and P-FAK may be expected. We have shown earlier that *Cten* regulates cell migration and invasion and our data here show that *Cten* also appears to regulate FAK and P-FAK in CRC cell lines. This suggests that *Cten* may mediate cell motility through FAK. In order to test whether this may occur in tumour tissue, we evaluated *Cten* and P-FAK proteins expression in a series of paired primary CRC and hepatic metastases. In agreement with previous studies we found similar levels of P-FAK in primary and metastatic deposits (232, 233). Comparison of the *Cten* and P-FAK immunostaining showed that they were highly correlated thereby supporting the observations we have made in the cell lines.

It has been shown in a previous study that CD24 promotes cell motility in a β 1 integrin-dependent manner. Analysis of the results of cell migration and invasion assays in A125 and MDA-MB-435S cells, stably transfected with CD24 or an empty pcDNA3.1 vector demonstrated that cells expressing CD24 migrated and invaded across an endothelial monolayer significantly faster than the control cells. In addition antibody-mediated blocking of β 1 integrin interaction significantly reduced the migration of the CD24-transfectants, while it had no effect on the motility of the

CD24-negative control cells (225). Given that and the finding that CD24 can induce the lateral localisation of $\beta 1$ integrins into lipid raft domains where it regulates its function and activity, we hypothesised that CD24 may be involved in the Cten signalling pathway and Cten-mediated effects on cell motility may rely on CD24. The present study has shown that Cten-forced expression and knock-down in CRC cell lines resulted in up-regulation and down-regulation of CD24 respectively and inhibition of CD24 abrogated the effects of Cten on cell motility indicating a functional relationship between these two proteins. In agreement with this, knock-down of CD24 was associated with up-regulation of E-cadherin and down-regulation of ILK and FAK proteins, again indicating that CD24 lies downstream of Cten and the Cten-mediated effects on cell motility and E-cadherin, ILK, and FAK levels depend on CD24. These data are summarised in Figure 69.

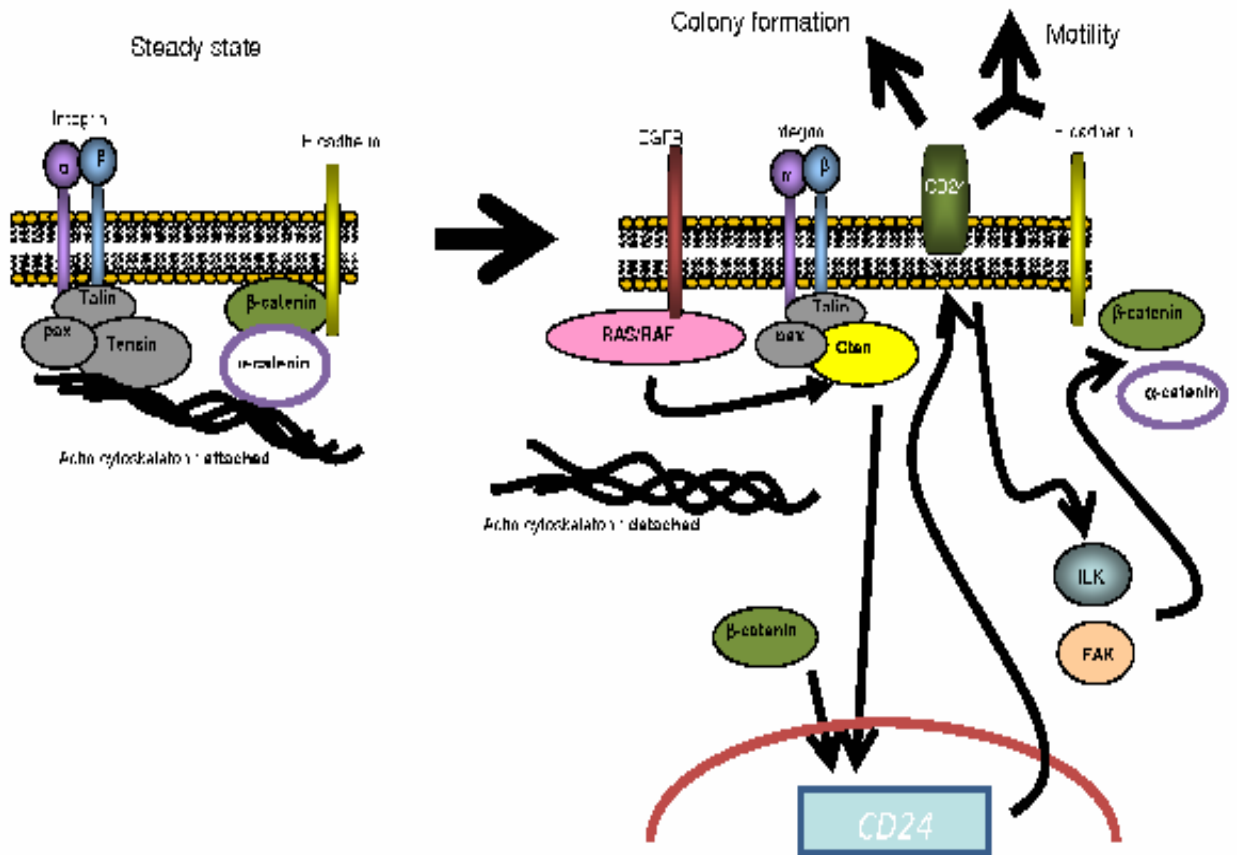


Figure 67. A model representing the role of Cten in cancer metastasis. Having shown that manipulation of Cten protein in CRC cell lines was mirrored by similar changes in CD24 protein expression and inhibition of CD24 abrogated the effects of Cten on cell motility and E-cadherin, ILK, and FAK protein levels, we designed the following model suggesting the functional interaction between Cten and CD24 at focal adhesion and their role in cancer metastasis. In steady state, focal adhesion complex is stabilised and cells are attached to actin cytoskeleton through tensin. Following EGF stimulation, Cten is up-regulated, leads to induction of CD24 protein. Upon up-regulation, CD24 will lead to initiation of cell migration and colony formation by it self or it will activate ILK and FAK which lead to repression of E-cadherin and consequently EMT and cell migration.

Chapter 7. *Cten* expression in other tumour types

7.1 Introduction

The studies so far have shown the oncogenic role of *Cten* in CRC. It has been demonstrated that in CRC cell lines, *Cten* confers resistance to staurosporine-induced apoptosis, stimulates EMT together with migration and invasion. In addition, *Cten* up-regulation in CRC patients is associated with advanced disease and poor prognosis. However, since *Cten* is a recently described gene, data about its regulation are sparse. In BC, *Cten* is positively regulated by c-Erb-B2 protein (30) – this is over-expressed in a specific subset of breast cancers due to gene amplification and is a part of the EGFR signalling pathway. The EGFR pathway signals through Kirsten rat sarcoma viral oncogene homolog (K-Ras) and although EGFR/c-Erb-B2 amplifications are rare in CRC, gain-of-function mutations in K-Ras are extremely common and are seen in up to 60% of tumours (208, 234). The K-Ras gene encodes a 21-kDa small protein that is activated in response to several factors, such as extracellular hormones, growth factors and cytokines and serves as a molecular switch converting signals from receptor and non-receptor tyrosine kinases to downstream cytoplasmic or nuclear events. These chemical signals lead to protein synthesis and regulation of various cellular processes, such as cell adhesion, survival, proliferation, apoptosis and differentiation (235). This prompted investigation of *Cten* expression in BC and correlation of that with the prognostic criteria. Since pancreatic cancer is characterised by a K-Ras mutation frequency of around 80% (236), it was decided to investigate this tumour too.

7.2 Evaluating the expression and the role of Cten in BC

7.2.1 Cten expression in BC

After excluding the uninformative TMA cores (220) from the study, which were either lost, folded, fragmented or did not have invasive tumour tissue, 1,500 tumours were available for Cten immunostaining assessment. The staining pattern for Cten in breast tumour cells was homogenous cytoplasmic staining (Figure 68). In the whole series, 1,409/1,500 (93%) of the tumours showed expression for Cten. In contrast, no nuclear, cell membrane or stromal expression of Cten was detected in any tumour specimen. Normal breast epithelium entrapped in some cores did not show any Cten staining (Figure 68). The X-tile bio-informatics software was used to define optimal cut-off points of Cten H-score values (<85 , negative/low; ≥ 85 , moderate/strong expression) as described earlier in chapter 4.

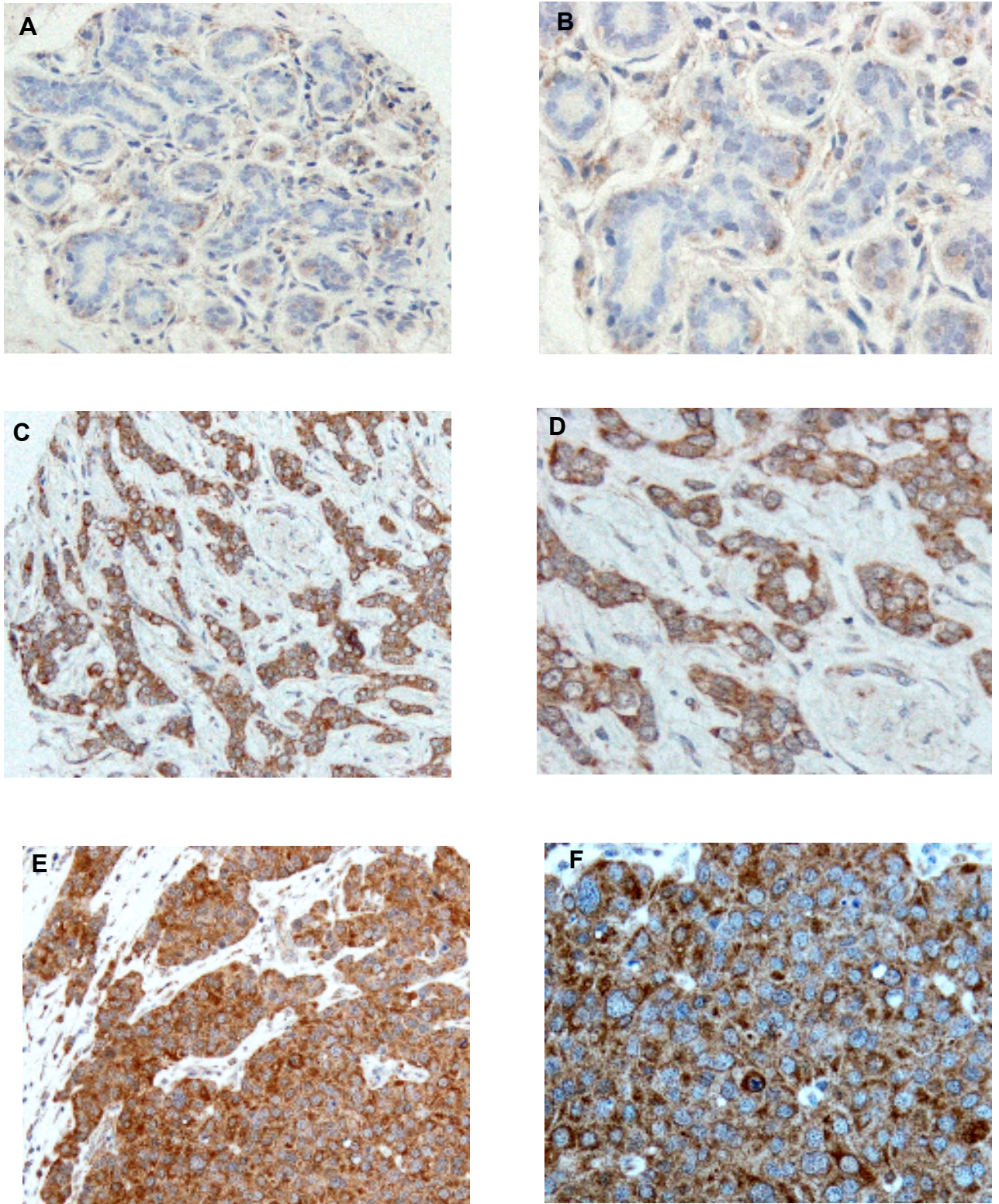


Figure 68. Cten protein expression in normal and BC TMA cores: (A, x100 and B, x200) normal breast showing negative Cten expression. (C, x100 and D, x200) low grade invasive ductal carcinoma with moderate Cten expression. (E, x100 and F, x200) high grade invasive ductal carcinoma showing strong Cten expression.

7.2.2 Correlation between *Cten* expression and clinicopathological parameters

Table 11 summarises the associations between *Cten* expression and clinicopathological parameters. *Cten* expression was significantly associated with larger tumour size ($p=0.035$; chi-square test), higher tumour grade ($p=0.023$; chi-square test), axillary LN metastasis ($p=0.016$; chi-square test) and higher NPI ($p=0.023$; chi-square test). A significant association ($p=0.017$; chi-square test) was found between *Cten* expression and the histological tumour type with frequent expression in invasive ductal carcinoma of no special type, and lobular carcinoma showing high levels of *Cten* expression (98% and 100%, respectively). Furthermore, there was a significant association between increased *Cten* expression and phosphorylated-Akt (P-Akt), PIK3CA and N-cadherin ($p<0.001$; chi-square test). However, *Cten* expression was not significantly associated with patients' age, menopausal status, VI, p53, human epidermal growth factor receptor 2 (HER2), EGFR, ER, Mindbomb homolog 1 (MIB1) and breast cancer1, early onset (BRCA1) expression or any of Nielson's group subtypes (Table 12).

Table 11. Correlations between *Cten* expression and clinicopathological parameters. High *Cten* expression was associated with advanced disease and poor prognostic features.

Parameter	Low <i>Cten</i> No.(%)	High <i>Cten</i> No. (%)	X^2	p value
Age				
<50	47 (9.4%)	451 (90.6%)	2.047	0.152
>50	66 (7.3%)	842 (92.7%)		
Menopausal status				
Premenopausal	52 (9.9%)	475 (90.1%)	3.820	0.064
Postmenopausal	61 (6.9%)	818 (93.1%)		
Tumour size				
<1.5 cm	80 (9.2%)	791 (90.8%)	4.254	0.044
>1.5 cm	29 (5.1%)	501 (94.9%)		
Lymph Node stage				
1 (Negative)	82 (9.8%)	787 (90.2%)	5.842	0.035
2/3 (Definite)	21 (4.6%)	602 (96.4%)		
Grade				
1	30 (12.2%)	215 (87.8%)	7.555	0.019
2	38 (7.9%)	445 (92.1%)		
3	45 (6.7%)	629 (93.3%)		
NPI				
Good (<3.4)	45 (10.1%)	402 (89.9%)	7.578	0.016
Moderate (3.41–5.4)	59 (8.1%)	671 (91.9%)		
Poor (4.41–5)	9 (4%)	218 (96%)		
VI				
Negative	81 (10%)	722 (90%)	1.185	0.286
Definite	42 (9.2%)	411 (90.8%)		
Local recurrence				
Negative	49 (12.1%)	381 (87.9%)	5.211	0.039
Positive	75 (9.1%)	822 (90.9%)		
Regional recurrence				
Negative	45 (10.1%)	442 (90.8%)	4.778	0.042
Positive	35 (6.7%)	769 (93.3%)		
DM				
Negative	80 (9.4%)	791 (90.6%)	4.780	0.041
Positive	36 (5.2%)	499 (94.8%)		
Histological type				
Ductal/NST	55 (7%)	735 (93%)	7.634	0.012
Lobular	10 (7.4%)	148(92.6%)		
Tubular mixed	21 (11.3%)	229 (88.7%)		
Medullary	5 (13.2%)	33 (86.8%)		
Other special types	14 (20%)	56 (80%)		

Table 12. Correlations between *Cten* expression and other biomarkers. High *Cten* expression was significantly associated with PR (p=0.016; chi-square test), P-Akt, PIK3CA and N-cadherin proteins (p<0.001; chi-square test) and showed a trend toward P-cadherin (p=0.085; chi-square test).

Parameter	Low <i>Cten</i> No.(%)	High <i>Cten</i> No. (%)	χ^2	p value
ER				
Negative	24 (7.0%)	319 (93.0%)	0.650	0.477
Positive	68 (8.4%)	741 (91.6%)		
PR				
Negative	32 (5.7%)	525 (94.3%)	6.119	0.016
Positive	70 (9.5%)	668 (90.5%)		
AR				
Negative	27 (8.0%)	315 (91.0%)	0.669	0.457
Positive	58 (7.4%)	731 (93.6%)		
HER2				
Negative	99 (8.4%)	1,084 (91.6%)	1.623	0.654
Positive	11 (5.9%)	174 (94.1%)		
EGFR				
Negative	70 (7.6%)	855 (92.4%)	0.022	0.890
Positive	18 (7.9%)	211 (92.1%)		
P53				
Negative	74 (7.7%)	889 (92.3%)	0.092	0.814
Positive	25 (7.2%)	323 (92.8%)		
E-cadherin				
Negative	35 (6.9%)	471 (93.1%)	0.124	0.345
Positive	69 (8.5%)	739 (91.5%)		
P-cadherin				
Negative	47 (9.2%)	465 (90.8%)	5.147	0.058
Positive	37 (6.3%)	548 (93.7%)		
N-cadherin				
Negative	72 (11.1%)	578 (88.9%)	26.91	<0.001
Positive	11 (2.5%)	424 (97.5%)		
PIK3				
Negative	46 (14.2 %)	278 (85.8%)	37.22	<0.001
Positive	41 (4.3 %)	911 (95.7 %)		
P-Akt				
Negative	55 (10.2%)	551 (87%)	27.23	<0.001
Positive	14 (2.5%)	427 (97.5%)		
MIB1				
Low proliferative	38 (9.8%)	348 (90.2%)	2.567	0.131
High proliferative	51 (7.1%)	668 (92.9%)		
Nielsen groups				
Luminal	74 (8.4%)	804 (91.6%)	2.053	0.562
HER2	12 (6.2%)	183 (93.8%)		
Basle-like	3 (4.8%)	60 (95.2%)		

7.2.3 Correlation between *Cten* expression and patients' outcome

Kaplan-Meier plotting demonstrated that patients with high *Cten* expression had significantly poorer prognosis than those with low *Cten* expression. Moreover, *Cten* expression was associated with an increased likelihood to develop DM ($p=0.041$; chi-square test), but this was not significantly associated with any particular metastatic site. Univariate survival analyses showed that patients with tumours positive for *Cten* had shorter BCSS ($p=0.004$; log-rank test, Figure 69). Positive expression of *Cten* also showed association with a shorter DFI ($p=0.041$; log-rank test, Figure 69). However, multivariate Cox proportional hazard analysis including tumour size, histological grade, LN stage, adjuvant hormonal, chemotherapy and *Cten* expression showed that *Cten* expression was not an independent predictor of BCSS and DFI ($p=0.213$, $p=0.874$ respectively) (Table 13).

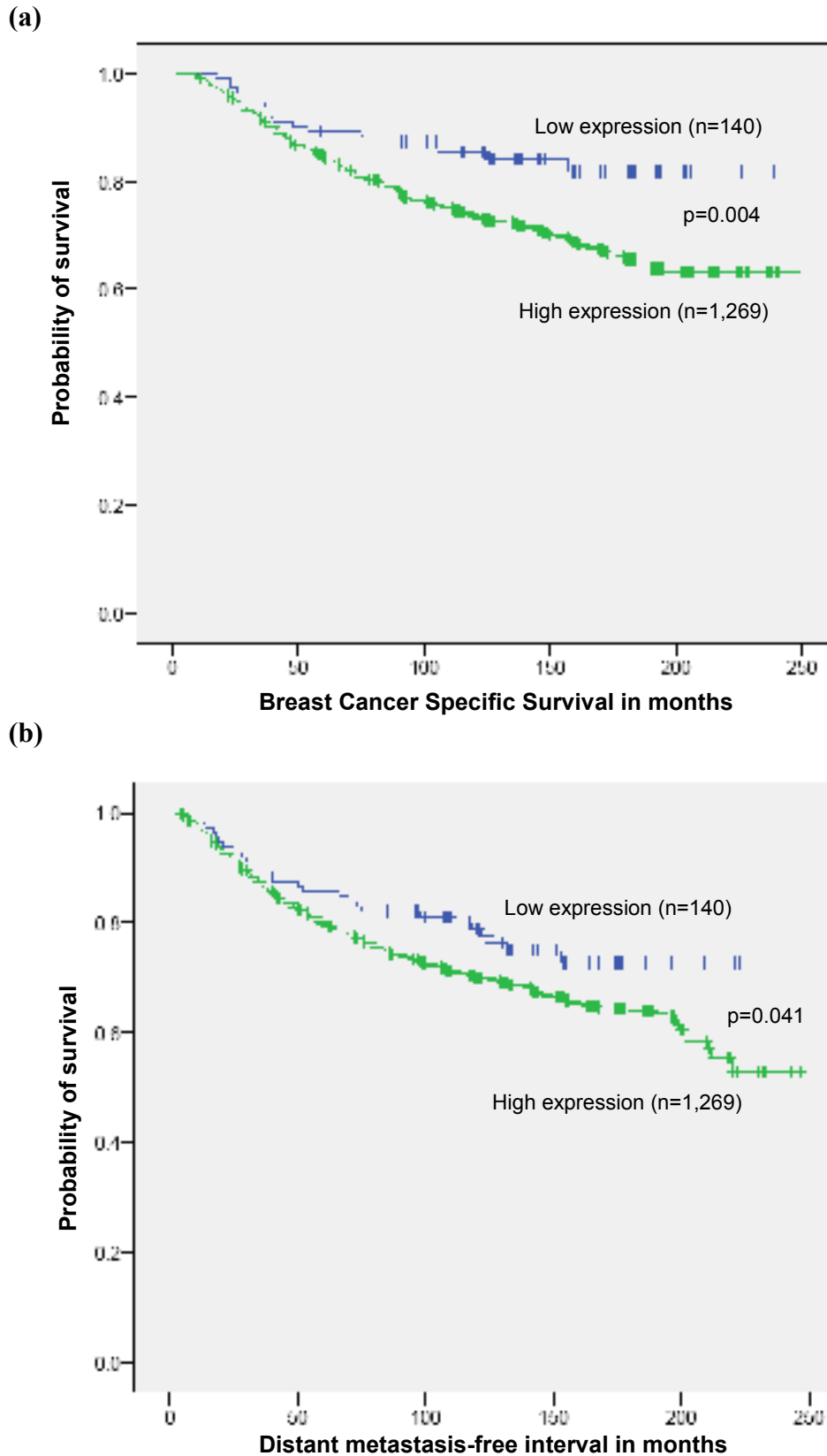


Figure 69. Kaplan-Meier plot for BCSS and DFI in relation to expression of cytoplasmic *Cten*. Kaplan–Meier plots showed that patients with tumours positive for *Cten* had shorter (a) BCSS ($p=0.004$) and (b) shorter DFI ($p=0.041$). All surviving patients were censored after 250 months follow-up

Table 13. Cox-proportional hazard analysis for predictors of BCSS, DFI and Cten expression. Multivariate Cox hazard analysis including tumour grade, size, LN stage and Cten expression shows that Cten expression was not an independent predictor of BCSS and DFI in BC (p=0.213; hazard ratio 1.379, 95% CI 0.832–2.287, p=0.874; hazard ratio 1.034, 95% CI 0.681–1.571, respectively).

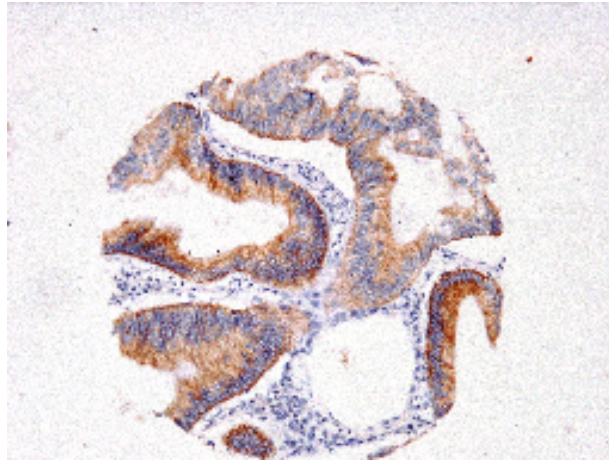
Parameter	Hazard ratio	95% CI	p value
BCSS			
Tumour size	1.328	1.181–1.493	<0.001
Nodal stage	1.874	1.600–2.196	<0.001
Tumour grade	2.106	1.745–2.542	<0.001
Chemotherapy	0.679	0.511–0.901	0.007
Endocrine therapy	0.924	0.845–1.011	0.084
Cten expression	1.379	0.832–2.287	0.213
DM-free interval			
Tumour size	1.408	1.254–1.581	<0.001
Nodal stage	1.899	1.633–2.208	<0.001
Tumour grade	1.682	1.425–1.987	<0.001
Chemotherapy	0.673	0.513–0.883	0.004
Endocrine therapy	0.931	0.856–1.012	0.093
Cten expression	1.034	0.681–1.571	0.874

7.3 Evaluating the expression of *Cten* in pancreatic cancer

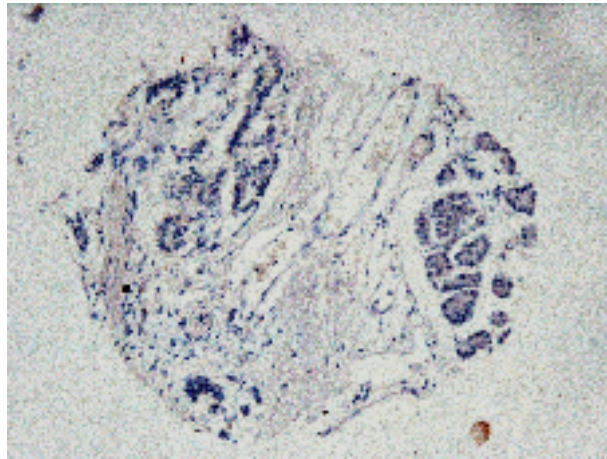
It has been shown that in BC, *Cten* is a downstream target of EGFR signalling and these studies shown that other EGFR downstream targets, P-Akt and PIK3CA, are significantly associated with increased *Cten* expression. Since these molecules are up-regulated in pancreatic cancer (237, 238), this prompted us to evaluate the expression of *Cten* using IHC in a large well-characterised pancreatic cancer series, containing normal, benign and malignant pancreatic tissues in order to explore *Cten*'s biological significance in pancreatic cancer.

Our study showed that 31/44 (65%) of tumours expressed moderate-strong levels of *Cten* in the cytoplasm (Figure 70 a). In contrast, no tumour cell membrane, nuclear or stromal expression of *Cten* was noticed in any of the examined cases. Similarly, chronic pancreatitis and normal pancreatic tissues were also showed complete lack of the *Cten* expression (Figure 70 b, c). These data clearly suggested that *Cten* may play a role during pancreatic carcinogenesis.

(a)



(b)



(c)

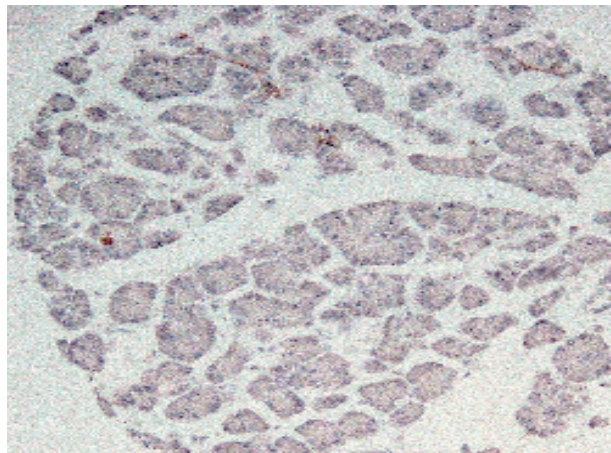


Figure 70. Cten immunostaining non-neoplastic pancreatic diseases and pancreatic cancer. Immunohistochemical staining for Cten on TMA sections demonstrating a strong expression in (a, x100) pancreatic ductal adenocarcinoma and a complete lack of staining in chronic pancreatitis (b, x100) and normal pancreatic epithelium (c, x100).

7.4 Discussion

In breast tissue, *Cten* is regulated by the EGFR and appears to exist in a relationship of mutual exclusivity with TNS3 at focal adhesions. Treatment of the normal human mammary cell line MCF10A with EGF appears to induce expression of *Cten*, thereby causing a switch from TNS3 to *Cten* at focal adhesions. This stimulates migration through disruption of the link between integrins and cortical actin fibres (30). As an increase in motility and migration are indispensable components of tumour growth and metastatic spread (239), this prompted us to investigate the level of *Cten* expression in BC and correlate that with the prognostic criteria, in order to evaluate if *Cten* has any prognostic implication in BC.

In this study, the expression of *Cten* protein was assessed using IHC in a large, well-characterised cohort of BC cases, to evaluate its potential biological and prognostic relevance. We found that *Cten* expression was significantly associated with poor prognostic clinicopathologic parameters, including larger tumour size, higher tumour grade, axillary LN metastasis and poor NPI. Moreover, our data showed that *Cten* was more frequently over-expressed in invasive duct carcinoma NST and invasive lobular carcinoma, histological types known to be associated with poor prognosis (240).

In agreement with our findings in CRC that *Cten* changed cell morphology and increased cell motility through repression of E-cadherin protein, we have found a significant association, in the BC study, between *Cten* expression and lobular carcinoma that is known to be associated with loss of E-cadherin expression (241). Although, *Cten* expression did not show a significant association with E-cadherin protein expression in this series, there was a significant association with N-cadherin

and a trend of positive association with P-cadherin expression; markers which have been reported to be frequently over-expressed in high-grade invasive breast carcinomas, conferring an increased motility of BC cells and being associated with tumour aggressiveness (242, 243). A growing body of evidence has shown that decreased expression of E-cadherin does not necessarily lead to induced cell motility in BC cells. In addition, forced expression of E-cadherin in invasive, N-cadherin-expressing MDA-MB-435 cells does not reduce their motility or invasive capacity. However, forced expression of N-cadherin in non-invasive, E-cadherin-positive BT-20 cells confers the capacity to invade, even though they continued to express high levels of E-cadherin (244). Taken together, these data demonstrate that BC invasiveness might be correlated with N-cadherin expression rather than lack of E-cadherin expression as reported in CRC (244).

Our findings are in agreement with previous studies showing association between *Cten* and both high tumour grade and the ability to metastasise to axillary LN (30). Moreover, we showed that patients with *Cten* over-expressing tumours had shorter BCSS and distant metastasis-free interval, supporting the oncogenic role of *Cten* in BC. However, our data showed that *Cten* expression was not significantly associated with increased expression of HER2, EGFR and ER as shown previously (30). This discrepancy may be due to the variations in the number of cases involved in both studies. They investigated a relatively small cohort (n=272) of primary breast tumours compared to the number of cases (n=1,409) assessed in this study.

Having shown that *Cten* is a downstream target of EGFR signalling in BC and, since the EGFR and its downstream targets P-Akt and PIK3CA and up-regulated in

pancreatic cancer (237, 238), we hypothesised that *Cten* may have a role in pancreatic cancer. To test this hypothesis, *Cten* protein expression was evaluated using IHC in a large well-characterised pancreatic cancer TMA series, containing normal, benign and malignant pancreatic tissues in order to evaluate *Cten*'s biological significance in pancreatic cancer.

Our study showed that 65% of tumours showed positive *Cten* cytoplasmic expression. In contrast, no tumour cell membrane, nuclear or stromal expression of *Cten* was noticed in any of the examined cases. Similarly, chronic pancreatitis and normal pancreatic tissues were also showed complete lack of the *Cten* expression. These data clearly suggest that *Cten* may play a role during pancreatic carcinogenesis. Recently, we have reported that *Cten* is expressed in certain pancreatic cell lines. Forced expression of *Cten* in Panc-1 (a pancreatic cancer cell line with low *Cten* expression) and knockdown in PSN-1 (a pancreatic cancer cell line showing high *Cten* expression) did not alter cell proliferation but were associated with enhanced and suppressed colony forming, transwell migration and invasion abilities respectively. Both of these observations were consistent with findings in CRC (data submitted for publication).

GENERAL DISCUSSION

&

FUTURE OUTLOOK

Chapter 8. General discussion and future outlook

In this thesis, we have characterised the expression and biological role of Cten in the colon, especially during the development of CRC. Expression of Cten was tested by IHC whilst the biological role of Cten was tested in CRC using both *in-vivo* and *in-vitro* models. For functional studies, a dual approach was used in order to avoid inaccurate conclusions from “off target” effects of gene knock-down and non-specific effects of forced expression. Concordance of the data using these two different methodologies was taken to signify a credible result. The potential downstream signalling targets for Cten were explored through evaluating the relationships between Cten expression and other secondary molecules associated with cancer metastasis, such as CD24, ILK, FAK and P-FAK in both CRC cell lines and tissue samples. Finally, having found it to be functionally important in CRC, we were prompted to look in other organs. We investigated the level of Cten expression in BC and pancreatic cancer and correlated that with the prognostic criteria in order to explore the biological and signalling implications of Cten expression in those organs.

Published data would suggest that the activity of Cten is probably context-dependent and may vary in tumours of different origin. The role of Cten in CRC is currently unknown. Tumours usually follow a well established pattern of early non-invasive adenomatous growth, succeeded by the ability to invade locally into the adjacent tissues and ultimately by acquisition of metastatic features. The mechanisms by which tumour cells acquire the ability to invade and metastasize are unclear, although many consider that these processes require disruption of cell–cell and cell–matrix adhesion and EMT.

Cten has no actin binding domain and thus when it is present it breaks the connection between the integrins and the actin cytoskeleton. It could therefore be expected to increase motility and this is what we found. Our data showed that in HCT116 and SW480 (cell lines shown to have low *Cten* expression), *Cten* ectopic expression significantly promotes both cell migration and invasion. The *Cten*-mediated effects on cell motility were further tested using RNA interference to knock down *Cten* in the CRC cell line SW620. This cell line expresses high levels of endogenous *Cten* and knock-down of *Cten* resulted in inhibition of cell migration. Since *Cten* has no effect on tumour growth, these data clearly suggest that, when acting as an oncogene in CRC, *Cten*'s role may lie more in positively regulating both cell migration and invasion rather than tumour growth. Our data are in agreement with studies by Liao *et al*, who found that MDA-MB-468 human mammary cells stably transfected with GFP and GFP-*Cten* plasmids grew at the same rate, suggesting that forced expression of *Cten* did not appear to alter cell proliferation (40). In addition, he reported that, in CRC cell lines, forced *Cten* expression and knock-down was associated with enhanced and suppressed transwell cell migration and invasion abilities respectively (207). Thus *Cten* is a motility associated molecule, its up-regulation in IBDs may aid the gut healing process and epithelial restitution.

Physiologically perhaps *Cten* helps to integrate events in integrin and cadherin mediated adhesion to allow cell motility to occur. It certainly connects the two different types of adhesion molecules and both types of junctions (focal adhesions and adherens junctions) need to be broken down for motility. In cancer, *Cten* gives these properties to facilitate invasion and metastasis as our experiments have shown. In fact, the current study, evaluating the immunohistochemical expression of *Cten* in CRC,

indicated that high *Cten* expression was significantly associated with biological aggressiveness observed, including advanced Duke's stage, LN metastasis, extra-mural VI and DM. Kaplan–Meier survival analysis demonstrated that patients with high *Cten* expression had significantly shorter DFS than those with low-*Cten* expression. In addition, we also have shown that high *Cten* expression in BC was significantly associated with poor prognostic variables including larger tumour size, higher histological grade, axillary nodal involvement and poor NPI. Our data showed that *Cten* was more frequently over-expressed in invasive duct carcinoma and invasive lobular carcinoma, histologic types known to be associated with aggressiveness and poor prognosis. Furthermore, *Cten* expression was significantly associated with up-regulation of N-cadherin and there was a trend of positive association with P-cadherin expression; markers which have been reported to over-express frequently in high-grade invasive breast carcinomas, conferring an increased motility of BC cells and being associated with tumour aggressiveness. Kaplan-Meier survival analysis demonstrated that patients with high *Cten* expression had significantly shorter BCSS and metastasis-free survival than those with low-*Cten* expression. Given the very low levels of *Cten* protein we reported in normal colonic and breast tissue epithelia, these data clearly confirm the dramatic up-regulation of *Cten* in cancer and this is associated with biological aggressiveness and poor prognostic outcomes. Our data showed that *Cten* expression in BC was not significantly associated with increased expression of HER2, EGFR and ER. These, however, contradict those of Katz *et al*, who reported a significant association between increased *Cten* expression and up-regulation of HER2, EGFR and ER proteins (30). We are uncertain of the cause for this discrepancy although this may be due to the variations in the number of cases involved in both studies (they investigated a relatively small cohort (n=272) of primary breast tumours

compared to our number of cases (n=1,409)) and it is of interest that, in agreement with our study, they found a significant association between *Cten* expression and both high tumour grade and the ability to metastasise to axillary LN (30).

The data from the *in-vitro* were further confirmed by *in-vivo* experiment. Our results showed that compared to the controls, mice injected with cells expression GFP-*Cten* developed a significantly greater total tumour burden in the spleen. The number of discrete tumour deposits in the liver was similar in both groups but the size of the deposits was greater in mice injected with cells expression HCT116 GFP-*Cten* leading to a greater tumour burden. The data from the *in-vitro* and *in-vivo* experiments suggest that the motility inducing effects of *Cten* may contribute to tumour metastasis.

The data from the *in-vitro* and *in-vivo* experiments led us to further investigate this association of *Cten* with tumour metastasis, through evaluating the *Cten* expression in a series of 40 cases of paired primary CRC and corresponding hepatic metastasis by IHC. Both primary and metastatic tumours showed similar levels of cytoplasmic staining. However, metastatic deposits were significantly associated with a shift of *Cten* expression to the nucleus, suggesting the functional implication of nuclear localisation of *Cten* and its association with tumour metastasis. The significance of nuclear localisation of *Cten* to the metastatic process is uncertain. Within the nucleus, it can be found in complex with β -catenin and it may thus be a modulator of Wnt signalling or regulate the β -catenin/T-cell factor transcriptional activity (207). Others have reported that *Cten* enhances colony formation in CRC cell lines (207) and thus we can conjecture that *Cten* mediated Wnt signalling may support stem cells in a foreign environment during tumour metastasis.

Although the above data suggest that *Cten* plays a role in advanced CRC, it wasn't clear when *Cten* was up-regulated in the adenoma-carcinoma sequence. Thus we investigated *Cten* expression in tissue sections containing colorectal adenoma. Our data showed a consistent up-regulation of *Cten* in 90% of colorectal adenoma with low grade dysplasia, and this confirms that *Cten* is dramatically up-regulated in the early stages of colorectal tumour development. Up-regulated *Cten* in adenomas may seem bizarre at first glance since adenomas are not invasive and thus is no obvious selective advantage. However, adenomas can frequently be seen migrating into non-neoplastic crypts and this probably represents a method of adenoma growth. It may be the selective advantage of *Cten* up-regulation in the early stages of tumourigenesis.

In agreement with our data, it has been reported that in thymomas and lung tumours, *Cten* functions as an oncogene with progressive up-regulation correlating with advanced tumour stage (56, 57). Moreover, evaluation of the expression of *Cten* in gastric cancer cases using IHC revealed that high *Cten* expression was significantly associated with poorer tumour grade, deeper invasion into the serosal layer, peritoneal dissemination and LN metastasis. Kaplan–Meier survival analysis demonstrated that patients with high *Cten* expression tended to show shorter survival than those with low-*Cten* expression (24).

Our data show that *Cten* has an oncogenic behaviour in CRC, BC and pancreas whilst others have shown a similar role in thymomas, lung and gastric cancers. This is however contradictory to data published by other groups showing that *Cten* may have tumour suppressor activity in certain types of tumours. The *Cten* gene is localised at chromosome 17q21, a region frequently deleted in prostate cancer and its expression is

down-regulated in prostate cancer compared to normal prostate (8). In addition, previous studies using coimmunoprecipitation assay, show that Cten is able to interact, via its SH2 domain, with DLC1 protein, and may therefore enable its appropriate focal adhesion localisation, that is essential for DLC1's tumour suppression activity. DLC1 is identified as a candidate tumour suppressor, that regulates actin stress fibers and cell adhesion and inhibits tumour cell growth and migration (55). Its expression is down-regulated in various cancers, including liver, breast, lung, brain, stomach, colon, and prostate cancers. Therefore, these data indicate that down-regulation or loss of Cten expression may be advantageous to the development or spread of certain types of tumours (55). On the other hand, recruiting DLC1 to focal adhesions may not be the only function for cten. It is known that caspase-3 is able to cleave Cten at the DSTD⁵⁷⁰S sequence, thereby releasing a fragment, Cten 571–715, which contains the PTB domain and is able to reduce cell growth by inducing apoptosis through binding to the β integrin tails and disruption of the link between integrins and cortical actin fibres. In this case, the loss of cten expression may lead to uncontrolled cell growth and result in cell transformation (40). Thus, all together these findings strongly support the idea that the activity of Cten is probably context-dependent and may vary in tumours of different origin.

The observed EMT and the altered cell motility following forced Cten expression prompted us to examine whether these changes could be caused through alteration of *CDHI* expression. Western blot analysis of proteins extracted from HCT116 and SW480 cells transfected with GFP-Cten plasmid and SW620 cells transfected with Cten siRNA showed that forced Cten expression and knock-down were associated with down-regulation and up-regulation of E-cadherin protein levels respectively,

suggesting that *Cten*-mediated effects on cell motility and EMT in an E-cadherin-dependent manner.

The mechanism by which *Cten* may cause down-regulation of E-cadherin protein is uncertain. The association of *Cten* with integrin molecules raises the possibility of an effect via ILK. Forced expression of *Cten* in the CRC cell line HT116 cells resulted in up-regulation of ILK. In agreement with these results, the reciprocal *Cten* knock-down experiments in SW620 cells resulted in down-regulation of ILK. Activation of ILK has been reported to inhibit transcription of *CDHI* through induction of the repressor *SNAIL*. However, we found that there was no change in *CDHI* mRNA levels following *Cten* expression, suggesting that reduction in E-cadherin protein was probably due to post-transcriptional regulation. Thus if *Cten* is responsible for down-regulation of E-cadherin through ILK, it is probably not through the *SNAIL* pathway.

It is likely that *Cten* activates other downstream targets in addition to ILK. FAK is a 125 kDa non-receptor and non-membrane associated PTK, which also localises at focal adhesions and is involved in many critical cellular events including adhesion, migration, proliferation and survival. Upon clustering of integrins, FAK is recruited to focal adhesions and this leads to phosphorylation of FAK at Tyr397, which creates a high-affinity binding site recognised by the SH2 domain of PI3K triggering the PI3K/Akt signalling pathway, which in turn controls cell spreading, cell movement and cell survival. The binding of Src to FAK can also phosphorylate FAK at Y925, an amino acid residue known to be associated with integrin adhesion dynamics and E-cadherin de-regulation during Src-induced EMT (223, 224).

Cten co-localises with paxillin in focal adhesions and is involved in mediating the metastatic potential of mammary tumours (30). Cten contains a SH2 and a PTB domain, both of which have been shown to be involved in protein-protein interactions (5, 11, 14). FAK has also been reported to localise to focal adhesions via its interaction with paxillin (91) thereby providing a theoretical mechanism for interaction. Therefore, we focused on FAK as a potential downstream signalling molecule for Cten. Our data have shown that Cten also appears to regulate FAK and P-FAK in CRC cell lines. This suggests that Cten may also mediate cell motility through FAK. In order to test whether this may occur in tumour tissue, we evaluated Cten and P-FAK proteins expression in a series of paired primary CRC and hepatic metastases. Using IHC we found that P-FAK is predominantly a nuclear protein. This is, however, contrary to previously published data that confirmed the autophosphorylated and active form of FAK (FAK Y397) is localised to the cytoplasm (247). We have no explanation for this discrepancy other than the differences in the tissue samples examined and the methodology used (such as differences in the source of the antibodies used for P-FAK immunodetection). Comparison of the Cten and P-FAK immunostaining showed that they were highly correlated thereby supporting the observations we have made in the cell lines. In addition, we have reported in BC the significant associations between increased Cten expression and up-regulation of P-Akt and PI3K proteins. Taken together, this data strongly indicated that Cten may be considered as a key target in FAK–PI3K–Akt signalling pathway.

Nuclear expressions of FAK and P-FAK have been described in other studies and were confirmed in our study. Ssang-Taek *et al* described the functional implication of these and found that FAK may limit p53 activity through FAK N-terminal FERM domain

which localises to the nucleus and directly interacts and suppresses transcriptional activation of a number of p53 target genes including p21, Mdm2 and Bax that are important mediators of p53-induced apoptosis, which would propose the anti-apoptotic signal of FAK FERM-domain-initiated pathway (114).

CD24 is a small 80 amino acids-spanning heavily glycosylated mucin-like GPI-linked cell surface protein. CD24 expression is up-regulated in colorectal adenomas and it is thus an early event in CRC carcinogenesis (180). High expression of CD24 is reported in CRC, and this over-expression is associated with poor prognostic parameters (179). In addition, forced CD24 expression in CRC cell lines is associated with enhanced colony forming, transwell migration and invasion abilities (182). Conversely, knock-down of CD24 reduced cell migration in both transwell migration assays and cell wounding assays (182). It has been shown in a previous study that CD24 promotes cell motility in a $\beta 1$ integrin-dependent manner. Antibody-mediated blocking of $\beta 1$ integrin interaction significantly reduced the migration of the CD24-transfectants, while it had no effect on the motility of the CD24-negative control cells (225). Given that and the finding that CD24 can induce the lateral localisation of $\beta 1$ integrins into lipid raft domains where it regulates its function and activity, we hypothesised that *Cten* may function through CD24 signalling. We tested this hypothesis using, again, our dual approach of forced *Cten* expression and *Cten* knock-down in cell lines respectively expressing low and high levels of *Cten* protein. Forced expression of *Cten* in the CRC cell line HT116 (a cell line shown to have low *Cten*/CD24 expression) resulted in up-regulation of CD24. In agreement with these results, the reciprocal *Cten* knock-down experiments in SW620 (a cell line shown to have high *Cten*/CD24 expression) resulted in down-regulation of CD24. Having thus demonstrated that *Cten*

regulates expression of CD24, we tested whether *Cten* induces cell motility through CD24. To test this hypothesis, knock-down of CD24 in HCT116 cell line stably transfected with GFP-*Cten* was carried out and resulted in abrogation of the effect of *Cten* on cell migration and invasion, suggesting a functional relationship between *Cten* and CD24 molecules. Moreover, Western Blot analysis showed that CD24 knock-down was associated with up-regulation of E-cadherin and down-regulation of ILK and FAK proteins. These data show that CD24 probably lies downstream of *Cten* and is involved in *Cten* induced cell motility. Moreover, it has been reported that CD24 lies upstream effector of PI3K–Akt signalling pathway in CRC (245). Taken together, this data strongly suggest that *Cten* probably also signals through PI3K–Akt signalling pathway at focal adhesions.

It has been reported in previous studies that *Cten* is regulated by EGFR signalling in BC. This is of interest since EGFR signals through K-Ras and the EGFR/K-Ras signalling pathway is up-regulated in CRC and many other cancers (208, 234). For example, lung cancers commonly have K-Ras or EGFR mutation and *Cten* expression is also up-regulated in these (246). This is supported by increased *Cten* expression in pancreatic cancers (which have high frequency of K-Ras mutation) (236). These data clearly show that *Cten* probably mediates signals for EGFR-K-Ras signalling. However there are other mechanisms also regulating *Cten* expression since, in both CRC and pancreatic cancer, there are occasional cell lines containing K-Ras mutation which do not express *Cten*.

In summary, we have shown that *Cten* is up-regulated in CRC and BC and that this is associated with poor prognostic variables and shorter disease free survival. The high

frequency of expression of *Cten* in adenomas shows that up-regulation is an early event in the development of colorectal tumours. Our study has also shown that ectopic expression of *Cten* in the HCT116 CRC cell line causes changes in cell morphology and increased cell motility (both migration and invasion). Conversely, the reciprocal *Cten* knock-down experiments in SW620 results in inhibition of both cell migration and invasion. Furthermore, high levels of *Cten* expression are significantly associated with advanced disease/metastasis in human CRC. In addition, *Cten* expression is capable of enhancing metastasis in an *in-vivo* model. The current study has clarified the mechanistic basis of *Cten*-mediated changes in cell motility. This may depend on ILK, FAK and CD24 focal adhesions signalling molecules and suggests that *Cten* may signal through PI3K–Akt signalling pathway. We have also shown that increased *Cten* expression is associated with up-regulation and down-regulation of N-cadherin and E-cadherin proteins respectively suggesting the role of *Cten* in N-cadherin/E-cadherin switch and EMT process. This may therefore represent a novel method of E-cadherin control and provides further proof of integrin–cadherin crosstalk.

Future directions for work may include further study of *Cten* and tensin regulation. Since *Cten* shares an extensive homology with other tensin members at its C-terminal, the promoter sequence of *Cten* could be compared with that of the promoters of other tensin genes. Areas of high sequence conservation could be identified and analysed for the presence of transcription factor binding sites in order to explore mechanisms of control of expression. The activity of the *Cten* promoter region could be tested in colorectal carcinoma cell lines and possibly pancreatic cancer cell lines. The function of conserved putative transcription factor binding sites can be tested by mutating these using site directed mutagenesis and testing activity with single and combined

mutations. In addition, it would be of interest to further explore, using immunoprecipitation (IP), proteomics, two-dimensional gel electrophoresis (2D PAGE) and yeast-2 hybrid assays, other binding partners of cten, map the regions responsible for the binding on cten and demonstrate if this interaction has any prognostic implication in tumourigenesis.

REFERENCES

References

1. Lo SH, An Q, Bao SD, Wong WK, Liu Y, Janmey PA, et al. Molecular-cloning of chick cardiac-muscle tensin - full-length cdna sequence, expression, and characterization. *Journal of Biological Chemistry*. 1994;269(35):22310-9.
2. Chuang JZ, Lin DC, Lin S. Molecular-cloning, expression, and mapping of the high-affinity actin-capping domain of chicken cardiac tensin. *Journal of Cell Biology*. 1995;128(6):1095-109.
3. Lo SH, Janmey PA, Hartwig JH, Chen LB. Interactions of tensin with actin and identification of its three distinct actin-binding domains. *J Cell Biol*. 1994 Jun;125(5):1067-75.
4. Bockholt SM, Burridge K. Cell spreading on extracellular-matrix proteins induces tyrosine phosphorylation of tensin. *Journal of Biological Chemistry*. 1993;268(20):14565-7.
5. Davis S, Lu ML, Lo SH, Lin S, Butler JA, Druker BJ, et al. Presence of an SH2 domain in the actin-binding protein tensin. *Science*. 1991 May 3;252(5006):712-5.
6. Ishida T, Ishida M, Suero J, Takahashi M, Berk BC. Agonist-stimulated cytoskeletal reorganization and signal transduction at focal adhesions in vascular smooth muscle cells require c-Src. *Journal of Clinical Investigation*. 1999;103(6):789-97.
7. Jiang B, Yamamura S, Nelson PR, Mureebe L, Kent KC. Differential effects of PDGFisotypes on human smooth muscle cell proliferation and migration are mediated by distinct signaling pathways. *Surgery*. 1996;120(2):427-32.
8. Lo SH, Bin Lo T. *Cten*, a COOH-terminal tensin-like protein with prostate restricted expression, is down-regulated in prostate cancer. *Cancer Research*. 2002;62(15):4217-21.
9. Lo SH, Weisberg E, Chen LB. Tensin - a potential link between the cytoskeleton and signal-transduction. *Bioessays*. 1994;16(11):817-23.
10. Chen HY, Duncan IC, Bozorgehami H, Lo SH. TNS1 and a previously undocumented family member, TNS2, positively regulate cell migration. *Proceedings of the National Academy of Sciences of the United States of America*. 2002;99(2):733-8.
11. Cui YM, Liao YC, Lo SH. Epidermal growth factor modulates tyrosine phosphorylation of a novel tensin family member, TNS3. *Molecular Cancer Research*. 2004;2(4):225-32.
12. Auger KR, Songyang Z, Lo SH, Roberts TM, Chen LB. Platelet-derived growth factor-induced formation of tensin and phosphoinositide 3-kinase complexes. *J Biol Chem*. 1996 Sep 20;271(38):23452-7.
13. Chen H, Lo SH. Regulation of tensin-promoted cell migration by its focal adhesion binding and Src homology domain 2. *Biochem J*. 2003 Mar 15;370(Pt 3):1039-45.
14. Calderwood DA, Fujioka Y, de Pereda JM, Garcia-Alvarez B, Nakamoto T, Margolis B, et al. Integrin beta cytoplasmic domain interactions with PTBdomains: A

structural prototype for diversity in integrin signaling. *Proceedings of the National Academy of Sciences of the United States of America*. 2003;100(5):2272-7.

15. Chen H, Rossier C, Morris MA, Scott HS, Gos A, Bairoch A, et al. A testis-specific gene, TPTE, encodes a putative transmembrane tyrosine phosphatase and maps to the pericentromeric region of human chromosomes 21 and 13, and to chromosomes 15, 22, and Y. *Hum Genet*. 1999 Nov;105(5):399-409.

16. Kanaoka Y, Kimura SH, Okazaki I, Ikeda M, Nojima H. GAK: A cyclin G associated kinase contains a tensin/auxilin-like domain. *Febs Letters*. 1997;402(1):73-80.

17. Li J, Yen C, Liaw D, Podsypanina K, Bose S, Wang SI, et al. PTEN, a putative protein tyrosine phosphatase gene mutated in human brain, breast, and prostate cancer. *Science*. 1997;275(5308):1943-7.

18. Schroder S, Morris SA, Knorr R, Plessmann U, Weber K, Vinh NG, et al. Primary structure of the neuronal clathrin-associated protein auxilin and its expression in bacteria. *European Journal of Biochemistry*. 1995;228(2):297-304.

19. Steck PA, Pershouse MA, Jasser SA, Yung WKA, Lin H, Ligon AH, et al. Identification of a candidate tumour suppressor gene, MMAC1, at chromosome 10q23.3 that is mutated in multiple advanced cancers. *Nature Genetics*. 1997;15(4):356-62.

20. Lo SH. Tensin. *Int J Biochem Cell Biol*. 2004 Jan;36(1):31-4.

21. Kay BK, Williamson MP, Sudol P. The importance of being proline: the interaction of proline-rich motifs in signaling proteins with their cognate domains. *Faseb Journal*. 2000;14(2):231-41.

22. Chen HY, Ishii A, Wong WK, Chen LB, Lo SH. Molecular characterization of human tensin. *Biochemical Journal*. 2000;351:403-11.

23. Maeda I, Yamada H, Takano T, Nishihara E, Ito Y, Matsuzuka F, et al. Increased Expression Levels of TNS3 mRNA in Thyroid Functional Adenomas as Compared to Non-functioning Adenomas. *Experimental and Clinical Endocrinology & Diabetes*. 2009;117(4):191-3.

24. Sakashita K, Mimori K, Tanaka F, Kamohara Y, Inoue H, Sawada T, et al. Prognostic relevance of Tensin4 expression in human gastric cancer. *Annals of Surgical Oncology*. 2008;15(9):2606-13.

25. Chiang MK, Liao YC, Kuwabara Y, Lo SH. Inactivation of TNS3 in mice results in growth retardation and postnatal lethality. *Developmental Biology*. 2005;279(2):368-77.

26. Lo SH, Yu QC, Degenstein L, Chen LB, Fuchs E. Progressive kidney degeneration in mice lacking tensin. *Journal of Cell Biology*. 1997;136(6):1349-61.

27. Cho AR, Uchio-Yamada K, Torigai T, Miyamoto T, Miyoshi I, Matsuda J, et al. Deficiency of the TNS2 gene in the ICGN mouse: an animal model for congenital nephrotic syndrome. *Mammalian Genome*. 2006;17(5):407-16.

28. Chen HY, Lo SH. Regulation of tensin-promoted cell migration by its focal adhesion binding and Src homology domain 2. *Biochemical Journal*. 2003;370:1039-45.

29. Martuszevska D, Ljungberg B, Johansson M, Landberg G, Oslakovic C, Dahlback B, et al. TNS3 is a negative regulator of cell migration and all four Tensin family members are downregulated in human kidney cancer. *PLoS One*. 2009;4(2):e4350.
30. Katz M, Amit I, Citri A, Shay T, Carvalho S, Lavi S, et al. A reciprocal tensin-3-cten switch mediates EGF-driven mammary cell migration. *Nature Cell Biology*. 2007;9(8):961-U124.
31. Zamir E, Geiger B. Molecular complexity and dynamics of cell-matrix adhesions. *Journal of Cell Science*. 2001;114(20):3583-90.
32. Pankov R, Cukierman E, Katz BZ, Matsumoto K, Lin DC, Lin S, et al. Integrin dynamics and matrix assembly: Tensin-dependent translocation of alpha(5)beta(1) integrins promotes early fibronectin fibrillogenesis. *Journal of Cell Biology*. 2000;148(5):1075-90.
33. Pankov R, Momchilova A. Fluorescent Labeling Techniques for Investigation of Fibronectin Fibrillogenesis (Labeling Fibronectin Fibrillogenesis). *Methods in Molecular Biology*. 2009:261-74.
34. Bockholt SM, Otey CA, Glenney JR, Burridge K. Localization of a 215-kDa tyrosine-phosphorylated protein that cross-reacts with tensin antibodies. *Experimental Cell Research*. 1992;203(1):39-46.
35. North AJ, Galazkiewicz B, Byers TJ, Glenney JR, Small JV. Complementary distributions of vinculin and dystrophin define 2 distinct sarcolemma domains in smooth-muscle. *Journal of Cell Biology*. 1993;120(5):1159-67.
36. Ishii A, Lo SH. A role of tensin in skeletal-muscle regeneration. *Biochemical Journal*. 2001;356:737-45.
37. Beckerle MC, Burridge K, Demartino GN, Croall DE. Colocalization of calcium-dependent protease-ii and one of its substrates at sites of cell-adhesion. *Cell*. 1987;51(4):569-77.
38. Rock MT, Brooks WH, Roszman TL. Calcium-dependent signaling pathways in T cells - Potential role of calpain, protein tyrosine phosphatase 1B, and p130(Cas) in integrin-mediated signaling events. *Journal of Biological Chemistry*. 1997;272(52):33377-83.
39. Kook S, Kim DH, Shim SR, Kim W, Chun JS, Song WK. Caspase-dependent cleavage of tensin induces disruption of actin cytoskeleton during apoptosis. *Biochemical and Biophysical Research Communications*. 2003;303(1):37-45.
40. Lo SS, Lo SH. Cleavage of cten by caspase-3 during apoptosis. *Oncogene*. 2005;24(26):4311-4.
41. Katz BZ, Zohar M, Teramoto H, Matsumoto K, Gutkind JS, Lin DC, et al. Tensin can induce JNK and p38 activation. *Biochemical and Biophysical Research Communications*. 2000;272(3):717-20.
42. Guan M, Zhou XL, Soultz N, Spandidos DA, Popescu NC. Aberrant methylation and deacetylation of deleted in liver cancer-1 gene in prostate cancer: Potential clinical applications. *Clinical Cancer Research*. 2006;12(5):1412-9.
43. Healy KD, Hodgson L, Kim TY, Shutes A, Maddileti S, Juliano RL, et al. DLC-1 suppresses non-small cell lung cancer growth and invasion by RhoGAP-

- dependent and independent mechanisms. *Molecular Carcinogenesis*. 2008;47(5):326-37.
44. Kim TY, Jong HS, Song SH, Dimtchev A, Jeong SJ, Lee JW, et al. Transcriptional silencing of the DLC-1 tumor suppressor gene by epigenetic mechanism in gastric cancer cells. *Oncogene*. 2003;22(25):3943-51.
45. Kim TY, Lee JW, Kim HP, Jong HS, Jung MR, Bang YJ. DLC-1, a GTPase-activating protein for Rho, is associated with cell proliferation, morphology, and migration in human hepatocellular carcinoma. *Biochemical and Biophysical Research Communications*. 2007;355(1):72-7.
46. Ng IOL, Liang ZD, Cao L, Lee TKW. DLC-1 is deleted in primary HCC and exerts inhibitory effects on the proliferation of hepatoma cell lines with deleted DLC-1. *Cancer Research*. 2000;60(23):6581-4.
47. Seng TJ, Low JSW, Li H, Cui Y, Goh HK, Wong MLY, et al. The major 8p22 tumor suppressor DLC1 is frequently silenced by methylation in both endemic and sporadic nasopharyngeal, esophageal, and cervical carcinomas, and inhibits tumor cell colony formation. *Oncogene*. 2007;26(6):934-44.
48. Ullmannova V, Popescu NC. Expression profile of the tumor suppressor genes DLC-1 and DLC-2 in solid tumors. *International Journal of Oncology*. 2006;29(5):1127-32.
49. Yuan BZ, Durkin ME, Popescu NC. Promoter hypermethylation of DLC-1, a candidate tumor suppressor gene, in several common human cancers. *Cancer Genetics and Cytogenetics*. 2003;140(2):113-7.
50. Yuan BZ, Jefferson AM, Baldwin KT, Thorgeirsson SS, Popescu NC, Reynolds SH. DLC-1 operates as a tumor suppressor gene in human non-small cell lung carcinomas. *Oncogene*. 2004;23(7):1405-11.
51. Yuan BZ, Miller MJ, Keck CL, Zimonjic DB, Thorgeirsson SS, Popescu NC. Cloning, characterization, and chromosomal localization of a gene frequently deleted in human liver cancer (DLC-1) homologous to rat RhoGAP. *Cancer Research*. 1998;58(10):2196-9.
52. Yam JWP, Ko FCF, Chan CY, Jin DY, Ng IOL. Interaction of DLC1 with TNS2 in Caveolae and implications in tumor suppression. *Cancer Research*. 2006;66(17):8367-72.
53. Yam JWP, Ko FCF, Chan CY, Yau TO, Tung EKK, Leung THY, et al. TNS2 variant 3 is associated with aggressive tumor behavior in human hepatocellular carcinoma. *Hepatology*. 2006;44(4):881-90.
54. Maeda I, Takano T, Yoshida H, Matsuzuka F, Amino N, Miyauchi A. TNS3 is a novel thyroid-specific gene. *Journal of Molecular Endocrinology*. 2006;36(1):R1-R8.
55. Liao YC, Si LZ, White RWD, Lo SH. The phosphotyrosine-independent interaction of DLC-1 and the SH2 domain of cten regulates focal adhesion localization and growth suppression activity of DLC-1. *Journal of Cell Biology*. 2007;176(1):43-9.
56. Sasaki H, Moriyama S, Mizuno K, Yukiue H, Konishi A, Yano M, et al. Cten mRNA expression was correlated with tumor progression in lung cancers. *Lung Cancer*. 2003;40(2):151-5.

57. Sasaki H, Yukiue H, Kobayashi Y, Fukai I, Fujii Y. Cten mRNA expression is correlated with tumor progression in thymoma. *Tumor Biology*. 2003;24(5):271-4.
58. Allred DC, Clark GM, Tandon AK, Molina R, Tormey DC, Osborne CK, et al. HER-2/NEU in node-negative breast-cancer - prognostic-significance of overexpression influenced by the presence of insitu carcinoma. *Journal of Clinical Oncology*. 1992;10(4):599-605.
59. Wu M, Merajver SD. Molecular biology of inflammatory breast cancer: applications to diagnosis, prognosis, and therapy. *Breast Dis*. 2005;22:25-34.
60. Li YQ, Mizokami A, Izumi K, Narimoto K, Shima T, Zhang J, et al. CTEN/Tensin 4 Expression Induces Sensitivity to Paclitaxel in Prostate Cancer. *Prostate*. 70(1):48-60.
61. Hynes RO. Integrins: Bidirectional, allosteric signaling machines. *Cell*. 2002;110(6):673-87.
62. Schwartz MA, Schaller MD, Ginsberg MH. Integrins: Emerging paradigms of signal transduction. *Annual Review of Cell and Developmental Biology*. 1995;11:549-99.
63. Jockusch BM, Bubeck P, Giehl K, Kroemker M, Moschner J, Rothkegel M, et al. The molecular architecture of focal adhesions. *Annual Review of Cell and Developmental Biology*. 1995;11:379-416.
64. Yamada KM, Geiger B. Molecular interactions in cell adhesion complexes. *Current Opinion in Cell Biology*. 1997;9(1):76-85.
65. Clark EA, Brugge JS. Integrins and signal-transduction pathways - the road taken. *Science*. 1995;268(5208):233-9.
66. Giancotti FG, Ruoslahti E. Transduction - Integrin signaling. *Science*. 1999;285(5430):1028-32.
67. Howe A, Aplin AE, Alahari SK, Juliano RL. Integrin signaling and cell growth control. *Current Opinion in Cell Biology*. 1998;10(2):220-31.
68. Geiger B, Bershadsky A. Assembly and mechanosensory function of focal contacts. *Current Opinion in Cell Biology*. 2001;13(5):584-92.
69. Lock JG, Wehrle-Haller B, Stromblad S. Cell-matrix adhesion complexes: master control machinery of cell migration. *Semin Cancer Biol*. 2008 Feb;18(1):65-76.
70. Small JV, Stradal T, Vignat E, Rottner K. The lamellipodium: where motility begins. *Trends in Cell Biology*. 2002;12(3):112-20.
71. Borisy GG, Svitkina TM. Actin machinery: pushing the envelope. *Current Opinion in Cell Biology*. 2000;12(1):104-12.
72. Ballestrem C, Hinz B, Imhof BA, Wehrle-Haller B. Marching at the front and dragging behind: differential alpha-V beta 3-integrin turnover regulates focal adhesion behavior. *Journal of Cell Biology*. 2001;155(7):1319-32.
73. Wehrle-Haller B, Imhof BA. The inner lives of focal adhesions. *Trends in Cell Biology*. 2002;12(8):382-9.
74. Wehrle-Haller B, Imhof BA. Actin, microtubules and focal adhesion dynamics during cell migration. *International Journal of Biochemistry & Cell Biology*. 2003;35(1):39-50.

75. Hynes RO. The emergence of integrins: a personal and historical perspective. *Matrix Biology*. 2004;23(6):333-40.
76. Petruzzelli L, Takami M, Humes HD. Structure and function of cell adhesion molecules. *American Journal of Medicine*. 1999;106(4):467-76.
77. Puklin-Faucher E, Sheetz MP. The mechanical integrin cycle (vol 122, pg 179, 2009). *Journal of Cell Science*. 2009;122(4):575-.
78. Schwartz MA. Integrin signaling revisited. *Trends in Cell Biology*. 2001;11(12):466-70.
79. Moro L, Venturino M, Bozzo C, Silengo L, Altruda F, Beguinot L, et al. Integrins induce activation of EGF receptor: role in MAP kinase induction and adhesion-dependent cell survival. *Embo Journal*. 1998;17(22):6622-32.
80. Soldi R, Mitola S, Strasly M, Defilippi P, Tarone G, Bussolino F. Role of alpha(v)beta(3) integrin in the activation of vascular endothelial growth factor receptor-2. *Embo Journal*. 1999;18(4):882-92.
81. Barja-Fidalgo C, De Freitas MS, Coelho ALJ, Mariano-Oliveira A, Helal E, Marcinkiewicz C, et al. Disintegrins: integrin selective ligands able to activate integrin-coupled signaling and to modulate leukocyte functions. *Inflammation Research*. 2005;54:S97-S.
82. Hannigan GE, Dedhar S. Protein kinase mediators of integrin signal transduction. *Journal of Molecular Medicine-Jmm*. 1997;75(1):35-44.
83. Kinbara K, Goldfinger LE, Hansen M, Chou FL, Ginsberg MH. Ras GTPASES: Integrins' friends or foes? (vol 4, pg 767, 2003). *Nature Reviews Molecular Cell Biology*. 2004;5(1):75-.
84. Stupack DG, Cheresh DA. Get a ligand, get a life: integrins, signaling and cell survival. *Journal of Cell Science*. 2002;115(19):3729-38.
85. Vuori K. Integrin signaling: Tyrosine phosphorylation events in focal adhesions. *Journal of Membrane Biology*. 1998;165(3):191-9.
86. Hao HF, Naomoto Y, Bao XH, Watanabe N, Sakurama K, Noma K, et al. Progress in researches about FAK in gastrointestinal tract. *World Journal of Gastroenterology*. 2009;15(47):5916-23.
87. Schaller MD. Biochemical signals and biological responses elicited by the FAK. *Biochimica Et Biophysica Acta-Molecular Cell Research*. 2001;1540(1):1-21.
88. Schlaepfer DD, Hauck CR, Sieg DJ. Signaling through FAK. *Progress in Biophysics & Molecular Biology*. 1999;71(3-4):435-78.
89. Sieg DJ, Hauck CR, Ilic D, Klingbeil CK, Schaefer E, Damsky CH, et al. FAK integrates growth-factor and integrin signals to promote cell migration. *Nature Cell Biology*. 2000;2(5):249-56.
90. Mitra SK, Hanson DA, Schlaepfer DD. FAK: In command and control of cell motility. *Nature Reviews Molecular Cell Biology*. 2005;6(1):56-68.
91. Scheswohl DM, Harrell JR, Rajfur Z, Gao G, Campbell SL, Schaller MD. Multiple paxillin binding sites regulate FAK function. *J Mol Signal*. 2008;3:1.
92. Schaller MD. Cellular functions of FAK kinases: insight into molecular mechanisms and novel functions. *Journal of Cell Science*. 123(7):1007-13.

93. Hildebrand JD, Taylor JM, Parsons JT. An SH3 domain-containing GTPase-activating protein for Rho and Cdc42 associates with FAK. *Molecular and Cellular Biology*. 1996;16(6):3169-78.
94. Liu YH, Loijens JC, Martin KH, Karginov AV, Parsons JT. The association of ASAP1, an ADP ribosylation factor-GTPase activating protein, with FAK contributes to the process of focal adhesion assembly. *Molecular Biology of the Cell*. 2002;13(6):2147-56.
95. Medley QG, Buchbinder EG, Tachibana K, Ngo H, Serra-Pages C, Streuli M. Signaling between FAK and trio. *Journal of Biological Chemistry*. 2003;278(15):13265-70.
96. Polte TR, Hanks SK. Interaction between FAK and crk-associated tyrosine kinase substrate p130(Cas). *Proceedings of the National Academy of Sciences of the United States of America*. 1995;92(23):10678-82.
97. Mitra SK, Schlaepfer DD. Integrin-regulated FAK-Src signaling in normal and cancer cells. *Curr Opin Cell Biol*. 2006 Oct;18(5):516-23.
98. Chen HC, Appeddu PA, Isoda H, Guan JL. Phosphorylation of tyrosine 397 in FAK is required for binding phosphatidylinositol 3-kinase. *Journal of Biological Chemistry*. 1996;271(42):26329-34.
99. Chen HC, Guan JL. Association of FAK with its potential substrate phosphatidylinositol 3-kinase. *Proceedings of the National Academy of Sciences of the United States of America*. 1994;91(21):10148-52.
100. Han DC, Guan JL. Association of FAK with Grb7 and its role in cell migration. *Journal of Biological Chemistry*. 1999;274(34):24425-30.
101. Playford MP, Schaller MD. The interplay between Src and integrins in normal and tumor biology. *Oncogene*. 2004;23(48):7928-46.
102. Toutant M, Costa A, Studler JM, Kadare G, Carnaud M, Girault JA. Alternative splicing controls the mechanisms of FAK autophosphorylation. *Molecular and Cellular Biology*. 2002;22(22):7731-43.
103. Iwahara T, Akagi T, Fujitsuka Y, Hanafusa H. Crkl1 regulates FAK activation by making a complex with Crk-associated substrate, p130(Cas). *Proceedings of the National Academy of Sciences of the United States of America*. 2004;101(51):17693-8.
104. Brabek J, Constancio BS, Shin NY, Pozzi A, Weaver AM, Hanks SK. CAS promotes invasiveness of Src-transformed cells. *Oncogene*. 2004;23(44):7406-15.
105. Cary LA, Guan J-L. FAK in integrin-mediated signaling. *Frontiers in Bioscience*. 1999;4(CITED JAN. 19, 1999):D102-13.
106. Schlaepfer DD, Hanks SK, Hunter T, Vandergeer P. Integrin-mediated signal-transduction linked to Ras pathway by Grb2 binding to FAK. *Nature*. 1994;372(6508):786-91.
107. Lewis JM, Baskaran R, Taagepera S, Schwartz MA, Wang JYJ. Integrin regulation of c-Abl tyrosine kinase activity and cytoplasmic-nuclear transport. *Proceedings of the National Academy of Sciences of the United States of America*. 1996;93(26):15174-9.

108. Holcomb M, Rufini A, Barila D, Klemke RL. Deregulation of proteasome function induces Abl-mediated cell death by uncoupling p130(CAS) and c-CrkII. *Journal of Biological Chemistry*. 2006;281(5):2430-40.
109. Cho SY, Klemke RL. Extracellular-regulated kinase activation and CAS/Crk coupling regulate cell migration and suppress apoptosis during invasion of the extracellular matrix. *Journal of Cell Biology*. 2000;149(1):223-36.
110. Pratt SJ, Epple H, Ward M, Feng YF, Braga VM, Longmore GD. The LIM protein Ajuba influences p130Cas localization and Rac1 activity during cell migration. *Journal of Cell Biology*. 2005;168(5):813-24.
111. Golubovskaya VM, Finch R, Cance WG. Direct interaction of the N-terminal domain of FAK with the N-terminal transactivation domain of p53. *Journal of Biological Chemistry*. 2005;280(26):25008-21.
112. Schlaepfer DD, Mitra SK, Ilic D. Control of motile and invasive cell phenotypes by FAK. *Biochimica Et Biophysica Acta-Molecular Cell Research*. 2004;1692(2-3):77-102.
113. Sonoda Y, Matsumoto Y, Funakoshi M, Yamamoto D, Hanks SK, Kasahara T. Anti-apoptotic role of FAK (FAK): Induction of inhibitor-of-apoptosis proteins and apoptosis suppression by the overexpression of FAK in a human leukemic cell line, HL-60. *Biochemical Society Transactions*. 2000;28(5):A383.
114. Lim ST, Chen XL, Lim Y, Hanson DA, Vo TT, Howerton K, et al. Nuclear FAK promotes cell proliferation and survival through FERM-enhanced p53 degradation. *Molecular Cell*. 2008;29(1):9-22.
115. Zhao J, Guan JL. Signal transduction by FAK in cancer. *Cancer and Metastasis Reviews*. 2009;28(1-2):35-49.
116. Cohen LA, Guan JL. Mechanisms of FAK regulation. *Current Cancer Drug Targets*. 2005;5(8):629-43.
117. Melkounian ZK, Peng X, Gan BY, Wu YY, Guan JL. Mechanism of cell cycle regulation by FIP200 in human BCcells. *Cancer Research*. 2005;65(15):6676-84.
118. Hsia DA, Mitra SK, Hauck CR, Streblov D, Nelson JA, Ilic D, et al. Differential regulation of cell motility and invasion by FAK. *Journal of Cell Biology*. 2003;160(5):753-67.
119. Avizienyte E, Frame MC. Src and FAK signalling controls adhesion fate and the epithelial-to-mesenchymal transition. *Current Opinion in Cell Biology*. 2005;17(5):542-7.
120. Irby RB, Yeatman TJ. Increased Src activity disrupts cadherin/catenin-mediated homotypic adhesion in human colon cancer and transformed rodent cells. *Cancer Research*. 2002;62(9):2669-74.
121. Thiery JP, Sleeman JP. Complex networks orchestrate epithelial-mesenchymal transitions. *Nature Reviews Molecular Cell Biology*. 2006;7(2):131-42.
122. Mitra SK, Lim ST, Chi A, Schlaepfer DD. Intrinsic FAK activity controls orthotopic breast carcinoma metastasis via the regulation of urokinase plasminogen activator expression in a syngeneic tumor model. *Oncogene*. 2006;25(32):4429-40.
123. Liotta LA. Tumor invasion and metastases role of the extracellular-matrix - rhoads memorial award lecture. *Cancer Research*. 1986;46(1):1-7.

124. Woessner JF. Matrix metalloproteinases and their inhibitors in connective-tissue remodeling. *Faseb Journal*. 1991;5(8):2145-54.
125. Hu B, Jarzynka MJ, Guo P, Imanishi Y, Schlaepfer DD, Cheng SY. Angiopoietin 2 induces glioma cell invasion by stimulating matrix metalloprotease 2 expression through the alpha(v)beta(1) integrin and FAK signaling pathway. *Cancer Research*. 2006;66(2):775-83.
126. Wu XY, Gan BY, Yoo Y, Guan JL. FAK-mediated Src phosphorylation of endophilin A2 inhibits endocytosis of MT1-MMP and promotes ECM degradation. *Developmental Cell*. 2005;9(2):185-96.
127. Renshaw MW, Price LS, Schwartz MA. FAK mediates the integrin signaling requirement for growth factor activation of MAP kinase. *Journal of Cell Biology*. 1999;147(3):611-8.
128. Giubellino A, Burke TR, Bottaro DP. Grb2 signaling in cell motility and cancer. *Expert Opinion on Therapeutic Targets*. 2008;12(8):1021-33.
129. Mitra SK, Mikolon D, Molina JE, Hsia DA, Hanson DA, Chi A, et al. Intrinsic FAK activity and Y925 phosphorylation facilitate an angiogenic switch in tumors. *Oncogene*. 2006;25(44):5969-84.
130. Hannigan GE, LeungHagesteijn C, FitzGibbon L, Coppolino MG, Radeva G, Filmus J, et al. Regulation of cell adhesion and anchorage-dependent growth by a new beta(1)-integrin-linked protein kinase. *Nature*. 1996;379(6560):91-6.
131. Li F, Zhang Y, Wu C. ILK is localized to cell-matrix focal adhesions but not cell-cell adhesion sites and the focal adhesion localization of ILK is regulated by the PINCH-binding ANK repeats. *J Cell Sci*. 1999 Dec;112 (Pt 24):4589-99.
132. Hannigan G, Troussard AA, Dedhar S. ILK: A cancer therapeutic target unique among its ILK. *Nature Reviews Cancer*. 2005;5(1):51-63.
133. McDonald PC, Fielding AB, Dedhar S. ILK - essential roles in physiology and cancer biology. *Journal of Cell Science*. 2008;121(19):3121-32.
134. Barreuther MF, Grabel LB. The role of phosphorylation in modulating beta(1) integrin localization. *Experimental Cell Research*. 1996;222(1):10-5.
135. Tu YZ, Li FG, Goicoechea S, Wu CY. The LIM-only protein PINCH directly interacts with ILK and is recruited to integrin-rich sites in spreading cells. *Molecular and Cellular Biology*. 1999;19(3):2425-34.
136. Yoganathan N, Yee A, Zhang Z, Leung D, Yan J, Fazli L, et al. ILK, a promising cancer therapeutic target: biochemical and biological properties. *Pharmacology & Therapeutics*. 2002;93(2-3):233-42.
137. Braverman LE, Quilliam LA. Identification of Grb4/Nck beta, a Src homology 2 and 3 domain-containing adapter protein having similar binding and biological properties to Nck. *Journal of Biological Chemistry*. 1999;274(9):5542-9.
138. Tu YZ, Li FG, Wu CY. Nck-2, a novel Src homology2/3-containing adaptor protein that interacts with the LIM-only protein PINCH and components of growth factor receptor kinase-signaling pathways. *Molecular Biology of the Cell*. 1998;9(12):3367-82.
139. Hannigan GE, Coles JG, Dedhar S. ILK at the heart of cardiac contractility, repair, and disease. *Circulation Research*. 2007;100(10):1408-14.

140. Legate KR, Montanez E, Kudlacek O, Fassler R. ILK, PINCH and parvin: the tIPP of integrin signalling. *Nature Reviews Molecular Cell Biology*. 2006;7(1):20-31.
141. Nikolopoulos SN, Turner CE. ILK (ILK) binding to paxillin LD1 motif regulates ILK localization to focal adhesions. *Journal of Biological Chemistry*. 2001;276(26):23499-505.
142. Delcommenne M, Tan C, Gray V, Rue L, Woodgett J, Dedhar S. Phosphoinositide-3-OH kinase-dependent regulation of glycogen synthase kinase 3 and protein kinase B/AKT by the ILK. *Proceedings of the National Academy of Sciences of the United States of America*. 1998;95(19):11211-6.
143. Shaw G. The pleckstrin homology domain: An intriguing multifunctional protein module. *Bioessays*. 1996;18(1):35-46.
144. Kaneko Y, Kitazato K, Basaki Y. ILK regulates vascular morphogenesis induced by vascular endothelial growth factor. *Journal of Cell Science*. 2004;117(3):407-15.
145. Oloumi A, McPhee T, Dedhar S. Regulation of E-cadherin expression and beta-catenin/Tcf transcriptional activity by the ILK. *Biochimica Et Biophysica Acta-Molecular Cell Research*. 2004;1691(1):1-15.
146. Persad S, Dedhar S. The role of ILK (ILK) in cancer progression. *Cancer and Metastasis Reviews*. 2003;22(4):375-84.
147. Tan C, Cruet-Hennequart S, Troussard A, Fazli L, Costello P, Sutton K, et al. Regulation of tumor angiogenesis by ILK (ILK). *Cancer Cell*. 2004;5(1):79-90.
148. Wu CY, Dedhar S. ILK (ILK) and its interactors: a new paradigm for the coupling of ECM to actin cytoskeleton and signaling complexes. *Journal of Cell Biology*. 2001;155(4):505-10.
149. Delcommenne M, Tan C, Gray V, Rue L, Woodgett J, Dedhar S. Phosphoinositide-3-OH kinase-dependent regulation of glycogen synthase kinase 3 and protein kinase B/AKT by the ILK. *Proc Natl Acad Sci U S A*. 1998 Sep 15;95(19):11211-6.
150. Lynch DK, Ellis CA, Edwards PAW, Hiles ID. ILK regulates phosphorylation of serine 473 of protein kinase B by an indirect mechanism. *Oncogene*. 1999;18(56):8024-32.
151. Ozes ON, Mayo LD, Gustin JA, Pfeffer SR, Pfeffer LM, Donner DB. NF-kappaB activation by tumour necrosis factor requires the Akt serine-threonine kinase. *Nature*. 1999 Sep 2;401(6748):82-5.
152. Romashkova JA, Makarov SS. NF-kappa B is a target of AKT in anti-apoptotic PDGF signalling. *Nature*. 1999;401(6748):86-90.
153. D'Amico M, Hulit J, Amanatullah DF, Zafonte BT, Albanese C, Bouzahzah B, et al. The ILK regulates the cyclin D1 gene through glycogen synthase kinase 3beta and cAMP-responsive element-binding protein-dependent pathways. *J Biol Chem*. 2000 Oct 20;275(42):32649-57.
154. Persad S, Troussard AA, McPhee TR, Mulholland DJ, Dedhar S. Tumor suppressor PTEN inhibits nuclear accumulation of beta-catenin and T cell/lymphoid enhancer factor 1-mediated transcriptional activation. *Journal of Cell Biology*. 2001;153(6):1161-73.

155. Troussard AA, Costello P, Yoganathan TN, Kumagai S, Roskelley CD, Dedhar S. The integrin linked kinase (ILK) induces an invasive phenotype via AP-1 transcription factor-dependent upregulation of matrix metalloproteinase 9 (MMP-9). *Oncogene*. 2000 Nov 16;19(48):5444-52.
156. Troussard AA, Tan C, Yoganathan TN, Dedhar S. Cell-ECM interactions stimulate the AP-1 transcription factor in an ILK- and glycogen synthase kinase 3-dependent manner. *Molecular and Cellular Biology*. 1999;19(11):7420-7.
157. Deng JT, Van Lierop JE, Sutherland C, Walsh MP. Ca²⁺-independent smooth muscle contraction - A novel function for ILK. *Journal of Biological Chemistry*. [Article]. 2001 May;276(19):16365-73.
158. Muranyi A, MacDonald JA, Deng JT, Wilson DP, Haystead TAJ, Walsh MP, et al. Phosphorylation of the myosin phosphatase target subunit by ILK. *Biochemical Journal*. 2002;366:211-6.
159. Rosenberger G, Jantke I, Gal A, Kutsche K. Interaction of alpha PIX (ARHGEF6) with beta-parvin (PARVB) suggests an involvement of alpha PIX in integrin-mediated signaling. *Human Molecular Genetics*. 2003;12(2):155-67.
160. Barbera MJ, Puig I, Dominguez D, Julien-Grille S, Guaita-Esteruelas S, Peiro S, et al. Regulation of Snail transcription during epithelial to mesenchymal transition of tumor cells. *Oncogene*. 2004;23(44):7345-54.
161. Li YJ, Yang JW, Dai CS, Wu CY, Liu YH. Role for ILK in mediating tubular epithelial to mesenchymal transition and renal interstitial fibrogenesis. *Journal of Clinical Investigation*. 2003;112(4):503-16.
162. Novak A, Hsu SC, Leung-Hagesteijn C, Radeva G, Papkoff J, Montesano R, et al. Cell adhesion and the ILK regulate the LEF-1 and beta-catenin signaling pathways. *Proceedings of the National Academy of Sciences of the United States of America*. 1998;95(8):4374-9.
163. Somasiri A, Howarth A, Goswami D, Dedhar S, Roskelley CD. Overexpression of the ILK mesenchymally transforms mammary epithelial cells. *Journal of Cell Science*. 2001;114(6):1125-36.
164. Tan C, Costello P, Sanghera J, Dominguez D, Baulida J, de Herreros AG, et al. Inhibition of integrin linked kinase (ILK) suppresses beta-catenin-Lef/Tcf-dependent transcription and expression of the E-cadherin repressor, snail, in APC^{-/-} human colon carcinoma cells. *Oncogene*. 2001 Jan 4;20(1):133-40.
165. Wu CY, Keightley SY, Leung-Hagesteijn C, Radeva G, Coppolino M, Goicoechea S, et al. Integrin-induced protein kinase regulates fibronectin matrix assembly, E-cadherin expression, and tumorigenicity. *Journal of Biological Chemistry*. 1998;273(1):528-36.
166. Menke A, Philippi C, Vogelmann R, Seidel B, Lutz MP, Adler G, et al. Down-regulation of E-cadherin gene expression by collagen type I and type III in pancreatic cancer cell lines. *Cancer Research*. 2001;61(8):3508-17.
167. Kumar AS, Naruszewicz I, Wang P, Leung-Hagesteijn C, Hannigan GE. ILKAP regulates ILK signaling and inhibits anchorage-independent growth. *Oncogene*. 2004;23(19):3454-61.
168. Leslie NR, Downes CP. PTEN: The down side of PI 3-kinase signalling. *Cellular Signalling*. 2002;14(4):285-95.

169. Persad S, Attwell S, Gray V, Delcommenne M, Troussard A, Sanghera J, et al. Inhibition of ILK (ILK) suppresses activation of protein kinase B/Akt and induces cell cycle arrest and apoptosis of PTEN-mutant prostate cancer cells. *Proceedings of the National Academy of Sciences of the United States of America*. 2000;97(7):3207-12.
170. Lu LW, Smithson G, Kincade PW, Osmond DG. Two models of murine B lymphopoiesis: a correlation. *European Journal of Immunology*. 1998;28(6):1755-61.
171. Poncet C, Frances V, Gristina R, Scheiner C, Pellissier JF, FigarellaBranger D. CD24, a glycosylphosphatidylinositol-anchored molecule, is transiently expressed during the development of human central nervous system and is a marker of human neural cell lineage tumors. *Acta Neuropathologica*. 1996;91(4):400-8.
172. Aigner S, Ramos CL, Hafezi-Moghadam A, Lawrence MB, Friederichs J, Altevogt P, et al. CD24 mediates rolling of breast carcinoma cells on P-selectin. *Faseb Journal*. 1998;12(12):1241-51.
173. Signer S, Stoeber ZM, Fogel M, Weber E, Zarn J, Ruppert M, et al. CD24, a mucin-type glycoprotein, is a ligand for P-selectin on human tumor cells. *Blood*. 1997;89(9):3385-95.
174. Chou YY, Jeng YM, Lee TT, Hu FC, Kao HL, Lin WC, et al. Cytoplasmic CD24 expression is a novel prognostic factor in diffuse-type gastric adenocarcinoma. *Annals of Surgical Oncology*. 2007;14:2748-58.
175. Jacob J, Bellach J, Grutzmann R, Alldinger I, Pilarsky C, Dietel M, et al. Expression of CD24 in adenocarcinomas of the pancreas correlates with higher tumor grades. *Pancreatology*. 2004;4(5):454-60.
176. Kristiansen G, Denkert C, Schluns K, Dahl E, Pilarsky C, Hauptmann S. CD24 is expressed in ovarian cancer and is a new independent prognostic marker of patient survival. *American Journal of Pathology*. 2002;161(4):1215-21.
177. Kristiansen G, Schluns K, Yongwei Y, Denkert C, Dietel M, Petersen I. CD24 is an independent prognostic marker of survival in nonsmall cell lung cancer patients. *British Journal of Cancer*. 2003;88(2):231-6.
178. Kristiansen G, Winzer KJ, Mayordomo E, Bellach J, Schluns K, Denkert C, et al. CD24 expression is a new prognostic marker in breast cancer. *Clinical Cancer Research*. 2003;9(13):4906-13.
179. Weichert W, Denkert C, Burkhardt M, Gansukh T, Bellach J, Altevogt P, et al. Cytoplasmic CD24 expression in CRC independently correlates with shortened patient survival. *Clinical Cancer Research*. 2005;11(18):6574-81.
180. Ahmed MA, Al-Attar A, Kim J, Watson NF, Scholefield JH, Durrant LG, et al. CD24 shows early upregulation and nuclear expression but is not a prognostic marker in CRC. *J Clin Pathol*. 2009 Dec;62(12):1117-22.
181. Sagiv E, Memeo L, Karin A, Kazanov D, Jacob-Hirsch J, Mansukhani M, et al. CD24 is a new oncogene, early at the multistep process-of CRC carcinogenesis. *Gastroenterology*. 2006;131(2):630-9.
182. Mohamed A.H. Ahmed, Darryl Jackson, Rashmi Seth, Adrian Robins, Dileep N. Lobo, Mohammad Ilyas, et al. CD24 is Upregulated in Inflammatory Bowel Disease and Stimulates Cell Motility and Colony Formation. *Inflamm Bowel Dis*. 2010;16:795–803.

183. Sengupta N, Gill KA, MacFie TS, Lai CS, Suraweera N, McDonald S, et al. Management of CRC: a role for genetics in prevention and treatment? *Pathol Res Pract.* 2008;204(7):469-77.
184. Swaroop VS, Larson MV. Colonoscopy as a screening test for CRC in average-risk individuals. *Mayo Clin Proc.* 2002 Sep;77(9):951-6.
185. Herszenyi L, Miheller P, Tulassay Z. Carcinogenesis in inflammatory bowel disease. *Digestive Diseases.* 2007;25(3):267-9.
186. Choi PM, Zelig MP. Similarity of colorectal-cancer in crohns-disease and ulcerative-colitis - implications for carcinogenesis and prevention. *Gut.* 1994;35(7):950-4.
187. Eaden JA, Abrams KR, Mayberry JF. The risk of CRC in ulcerative colitis: a meta-analysis. *Gut.* 2001;48(4):526-35.
188. Muto T, Bussey HJR, Morson BC. Evolution of cancer of colon and rectum. *Cancer.* 1975;36(6):2251-70.
189. Morris EJ, Maughan NJ, Forman D, Quirke P. Who to treat with adjuvant therapy in Dukes B/stage II CRC? The need for high quality pathology. *Gut.* 2007 Oct;56(10):1419-25.
190. Universal ProbeLibrary Roche Diagnostics Ltd. 2010 [Online] (updated 12 January 2010) Available from: <https://www.roche-applied-science.com/servlet/RCConfigureUser?URL=StoreFramesetView&storeId=10305&catalogId=10304&langId=-1&countryId=uk>.
191. Molecular Biology Core Facilites. 2009 [Online] (updated 22 June 2009) Available from: [https:// www.mbcf.dfci.harvard.edu/docs/oligocalc.html](https://www.mbcf.dfci.harvard.edu/docs/oligocalc.html)
192. Carolina Biological Supply Company. 2007 [Online] (updated 6 May 2007) Available from: <http://www.carolina.com/>.
193. Chromas. Technelysium Pty Ltd. 2009 [Online] (updated 19 June 2010) Available from: <http://www.technelysium.com.au/chromas.html>.
194. Oliver MH, Harrison NK, Bishop JE, Cole PJ, Laurent GJ. A rapid and convenient assay for counting cells cultured in microwell plates - application for assessment of growth-factors. *Journal of Cell Science.* 1989;92:513-8.
195. Immage Processing and Analysis in Java 2010 [Online] (updated 24 June 2010) Available from: <http://rsbweb.nih.gov/ij/index.html>
196. Abd El-Rehim DM, Ball G, Pinder SE, Rakha E, Paish C, Robertson JFR, et al. High-throughput protein expression analysis using TMA technology of a large well-characterised series identifies biologically distinct classes of BC confirming recent cDNA expression analyses. *International Journal of Cancer.* 2005;116(3):340-50.
197. Abd El-Rehim DM, Pinder SE, Paish CE, Bell JA, Rampaul RS, Blamey RW, et al. Expression and co-expression of the members of the epidermal growth factor receptor (EGFR) family in invasive breast carcinoma. *British Journal of Cancer.* 2004;91(8):1532-42.
198. Aleskandarany MA, Green AR, Rakha EA, Mohammed RA, Elsheikh SE, Powe DG, et al. Growth fraction as a predictor of response to chemotherapy in node-negative breast cancer. *Int J Cancer.* 2010;126(7):1761-9.

199. Aleskandarany MA, Rakha EA, Ahmed MA, Powe DG, Paish EC, Macmillan RD, et al. PIK3CA expression in invasive breast cancer: a biomarker of poor prognosis. *BCRes Treat*. 2009 Aug 22.
200. Rakha EA, El-Rehim DA, Paish C, Green AR, Lee AHS, Robertson JF, et al. Basal phenotype identifies a poor prognostic subgroup of BC of clinical importance. *European Journal of Cancer*. 2006;42(18):3149-56.
201. Rakha EA, El-Sayed ME, Green AR, Lee AHS, Robertson JF, Ellis IO. Prognostic markers in triple-negative breast cancer. *Cancer*. 2007;109(1):25-32.
202. Ullenhag GJ, Mukherjee A, Watson NFS, Ai-Attar AH, Scholefield JH, Durrant LG. Overexpression of FLIPL is an independent marker of poor prognosis in CRC patients. *Clinical Cancer Research*. 2007;13(17):5070-5.
203. Watson NFS, Durrant LG, Scholefield JH, Madjd Z, Scrimgeour D, Spendlove I, et al. Cytoplasmic expression of p27(kip1) is associated with a favourable prognosis in CRC patients. *World Journal of Gastroenterology*. 2006;12(39):6299-304.
204. McCarty KS, Miller LS, Cox EB, Konrath J, McCarty KS. Estrogen-Receptor Analyses - Correlation of Biochemical and Immunohistochemical Methods Using Monoclonal Antireceptor Antibodies. *Archives of Pathology & Laboratory Medicine*. 1985;109(8):716-21.
205. Camp RL, Dolled-Filhart M, Rimm DL. X-tile: A new bio-informatics tool for biomarker assessment and outcome-based cut-point optimization. *Clinical Cancer Research*. 2004;10(21):7252-9.
206. Sabates-Bellver J, Van der Flier LG, de Palo M, Cattaneo E, Maake C, Rehrauer H, et al. Transcriptome profile of human colorectal adenomas. *Mol Cancer Res*. 2007 Dec;5(12):1263-75.
207. Liao YC, Chen NT, Shih YP, Dong Y, Lo SH. Up-regulation of Cten Molecule Promotes the Tumorigenicity of Colon Cancer through beta-Catenin. *Cancer Research*. 2009;69(11):4563-6.
208. Seth R, Crook S, Ibrahim S, Fadhil W, Jackson D, Ilyas M. Concomitant mutations and splice variants in KRAS and BRAF demonstrate complex perturbation of the Ras/Raf signalling pathway in advanced CRC. *Gut*. 2009 Sep;58(9):1234-41.
209. Davis S, Lu ML, Lo SH, Lin S, Butler JA, Druker BJ, et al. Presence of an SH2 domain in the actin-binding protein tensin. *Science*. 1991;252(5006):712-5.
210. Shtutman M, Levina E, Ohouo P, Baig M, Roninson IB. Cell adhesion molecule L1 disrupts E-cadherin-containing adherens junctions and increases scattering and motility of MCF7 breast carcinoma cells. *Cancer Research*. 2006;66(23):11370-80.
211. Schaller MD, Borgman CA, Cobb BS, Vines RR, Reynolds AB, Parsons JT. P125FAK, a structurally distinctive protein-tyrosine kinase associated with focal adhesions. *Proceedings of the National Academy of Sciences of the United States of America*. 1992;89(11):5192-6.
212. Tilghman RW, Slack-Davis JK, Sergina N, Martin KH, Iwanicki M, Hershey ED, et al. FAK is required for the spatial organization of the leading edge in migrating cells. *Journal of Cell Science*. 2005;118(12):2613-23.

213. Cance WG, Harris JE, Iacocca MV, Roche E, Yang XH, Chang JL, et al. Immunohistochemical analyses of FAK expression in benign and malignant human breast and colon tissues: Correlation with preinvasive and invasive phenotypes. *Clinical Cancer Research*. 2000;6(6):2417-23.
214. Han NM, Fleming RYD, Curley SA, Gallick GE. Overexpression of FAK (p125(FAK)) in human colorectal carcinoma liver metastases: Independence from c-src or c-yes activation. *Annals of Surgical Oncology*. 1997;4(3):264-8.
215. Judson PL, He XP, Cance WG, Van Le L. Overexpression of FAK, a protein tyrosine kinase, in ovarian carcinoma. *Cancer*. 1999;86(8):1551-6.
216. Kornberg LJ. FAK and its potential involvement in tumor invasion and metastasis. *Head and Neck-Journal for the Sciences and Specialties of the Head and Neck*. 1998;20(8):745-52.
217. Owens LV, Xu LH, Craven RJ, Dent GA, Weiner TM, Kornberg L, et al. Overexpression of the FAK (p125(fak)) in invasive human tumors. *Cancer Research*. 1995;55(13):2752-5.
218. Zhao JH, Reiske H, Guan JL. Regulation of the cell cycle by FAK. *Journal of Cell Biology*. 1998;143(7):1997-2008.
219. Xu L, Owens LV, Sturge GC, Yang X, Liu ET, Craven RJ, et al. Attenuation of the expression of the FAK induces apoptosis in tumor cells. *Proceedings of the American Association for Cancer Research Annual Meeting*. 1996;37(0):19.
220. Xu LH, Yang XH, Craven RJ, Cance WG. The COOH-terminal domain of the FAK induces loss of adhesion and cell death in human tumor cells. *Cell Growth & Differentiation*. 1998;9(12):999-1005.
221. McKean DM, Sisbarro L, Ilic D, Kaplan-Albuquerque N, Nemenoff R, Weiser-Evans M, et al. FAK induces expression of Prx1 to promote tenascin-C-dependent fibroblast migration. *Journal of Cell Biology*. 2003;161(2):393-402.
222. McLean GW, Fincham VJ, Frame MC. v-Src induces tyrosine phosphorylation of FAK independently of tyrosine 347 and formation of a complex with Src. *Journal of Biological Chemistry*. 2000;275(30):23333-9.
223. Avizienyte E, Wyke AW, Jones RJ, McLean GW, Westhoff MA, Brunton VG, et al. Src-induced de-regulation of E-cadherin in colon cancer cells requires integrin signalling. *Nature Cell Biology*. 2002;4(8):632-8.
224. Brunton VG, Avizienyte E, Fincham VJ, Serrels B, Metcalf CA, 3rd, Sawyer TK, et al. Identification of Src-specific phosphorylation site on FAK: dissection of the role of Src SH2 and catalytic functions and their consequences for tumor cell behavior. *Cancer Res*. 2005 Feb 15;65(4):1335-42.
225. Runz S, Mierke CT, Joumaa S, Behrens J, Fabry B, Altevogt P. CD24 induces localization of beta 1 integrin to lipid raft domains. *Biochemical and Biophysical Research Communications*. 2008;365(1):35-41.
226. Gofuku J, Shiozaki H, Tsujinaka T, Inoue M, Tamura S, Doki Y, et al. Expression of E-cadherin and alpha-catenin in patients with colorectal carcinoma - Correlation with cancer invasion and metastasis. *American Journal of Clinical Pathology*. 1999;111(1):29-37.

227. Hennig G, Behrens J, Truss M, Frisch S, Reichmann E, Birchmeier W. Progression of carcinoma-cells is associated with alterations in chromatin structure and factor-binding at the e-cadherin promoter in-vivo. *Oncogene*. 1995;11(3):475-84.
228. Bravou V, Klironomos G, Papadaki E, Stefanou D, Varakis J. ILK (ILK) expression in human colon cancer. *British Journal of Cancer*. 2003;89(12):2340-1.
229. McLean GW, Carragher NO, Avizienyte E, Evans J, Brunton VG, Frame MC. The role of focal-adhesion kinase in cancer - a new therapeutic opportunity. *Nat Rev Cancer*. 2005 Jul;5(7):505-15.
230. Smith CS, Golubovskaya VM, Peck E, Xu LH, Monia BP, Yang XH, et al. Effect of FAK (FAK) downregulation with FAK antisense oligonucleotides and 5-fluorouracil on the viability of melanoma cell lines. *Melanoma Research*. 2005;15(5):357-62.
231. YuYing Chen KC, Feng Pan, Li Yang, JianJun Li, LiuXin Xiang, JianMing He, HouJie Liang. Expressions of FAK, FAK pY397, Akt and NF- κ B in colorectal carcinomas and study on their correlation. *Chinese Clinical Oncology*. 2009;14(3):199-202
232. Basson MD, Sanders MA, Gomez R, Hatfield J, VanderHeide R, Thamilselvan V, et al. FAK protein levels in gut epithelial motility. *American Journal of Physiology-Gastrointestinal and Liver Physiology*. 2006;291(3):G491-G9.
233. Lark AL, Livasy CA, Calvo B, Caskey L, Moore DT, Yang XH, et al. Overexpression of FAK in primary colorectal carcinomas and colorectal liver metastases: IHC and real-time PCR analyses. *Clinical Cancer Research*. 2003;9(1):215-22.
234. Fadhil W, Ibrahim S, Seth R, Ilyas M. Quick-multiplex-consensus (QMC)-PCR followed by high-resolution melting: a simple and robust method for mutation detection in formalin-fixed paraffin-embedded tissue. *J Clin Pathol*. 2010 Feb;63(2):134-40.
235. Alex A. Adjei. Blocking Oncogenic Ras Signaling for Cancer Therapy. *J Natl Cancer Inst*. 2001;93 (14): 1062-1074.
236. Moore PS, Beghelli S, Zamboni G, Scarpa A. Genetic abnormalities in pancreatic cancer. *Mol Cancer*. 2003 Jan 7;2:7.
237. Bloomston M, Bhardwaj A, Ellison EC, Frankel WL. Epidermal growth factor receptor expression in pancreatic carcinoma using TMA technique. *Digestive Surgery*. 2006;23(1-2):74-9.
238. Yamamoto S, Tomita Y, Hoshida Y, Morooka T, Nagano H, Dono K, et al. Prognostic significance of activated Akt expression in pancreatic ductal adenocarcinoma. *Clinical Cancer Research*. 2004;10(8):2846-50.
239. Liotta LA, Kohn EC. The microenvironment of the tumour-host interface. *Nature*. 2001;411(6835):375-9.
240. Turashvili G, Bouchal J, Baumforth K, Wei W, Dziechciarkova M, Ehrmann J, et al. Novel markers for differentiation of lobular and ductal invasive breast carcinomas by laser microdissection and microarray analysis. *BMC Cancer*. 2007;7:55.

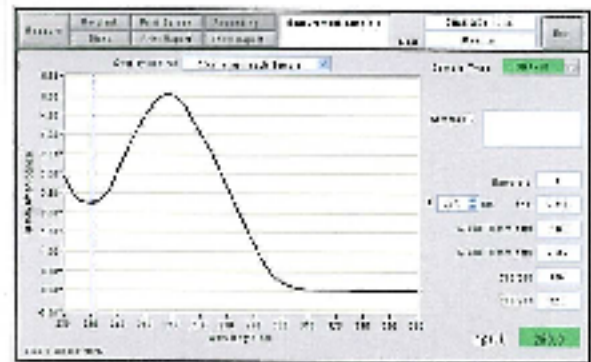
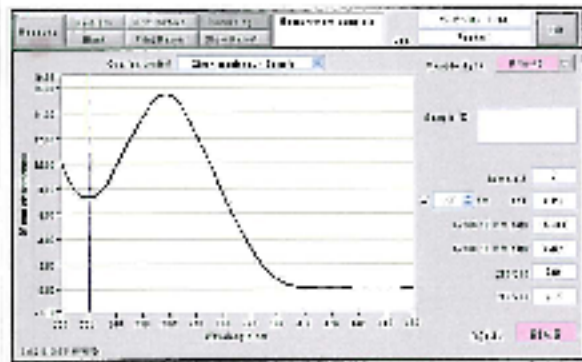
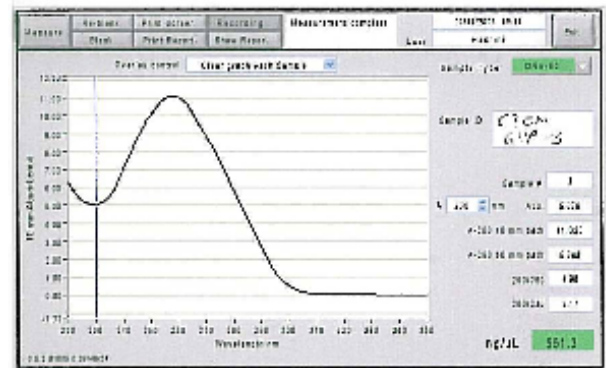
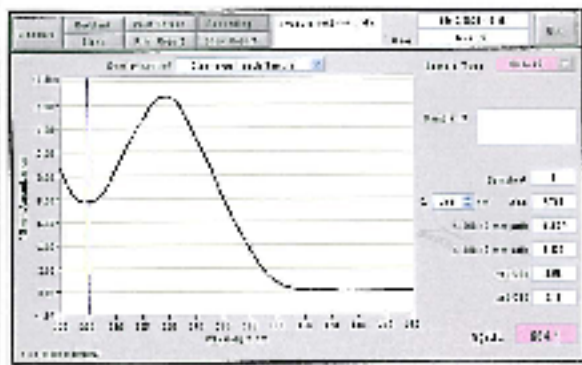
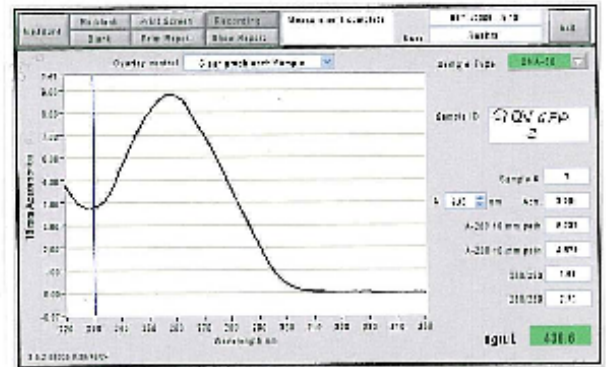
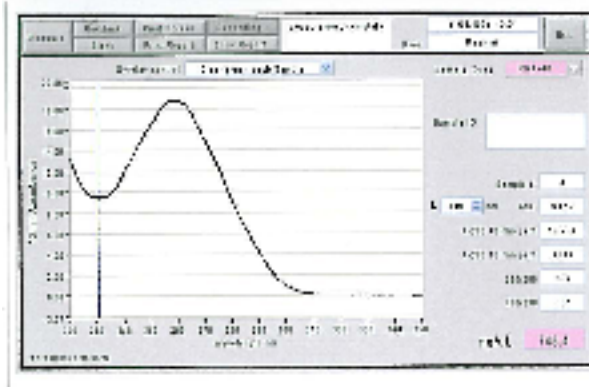
241. Moll R, Mitze M, Frixen UH, Birchmeier W. Differential Loss of E-Cadherin Expression in Infiltrating Ductal and Lobular Breast Carcinomas. *American Journal of Pathology*. 1993;143(6):1731-42.
242. Nagi C, Guttman M, Jaffer S, Qiao R, Keren R, Triana A, et al. N-cadherin expression in breast cancer: correlation with an aggressive histologic variant--invasive micropapillary carcinoma. *BCRes Treat*. 2005 Dec;94(3):225-35.
243. Rasbridge SA, Gillett CE, Sampson SA, Walsh FS, Millis RR. Epithelial (E-) and Placental (P-) Cadherin Cell-Adhesion Molecule Expression in Breast-Carcinoma. *Journal of Pathology*. 1993;169(2):245-50.
244. Nieman MT, Prudoff RS, Kim JB, Johnson KR, Wheelock MJ. N-cadherin promotes motility in human breast cancer cells regardless of their E-cadherin expression. *Molecular Biology of the Cell*. 1999;10:696.
245. I. Naumov SK, D. Kazanov, S. Shapira, E. Sagiv, N. Arber. Role of the PI3K-AKT pathway as a downstream effector of CD24. In ASCO (American Society of Clinical Oncology) Role of the PI3K-AKT pathway as a downstream effector of CD24 Florida, USA 22-24 January 2010. 2010.
246. Riely GJ, Marks J, Pao W. KRAS mutations in non-small cell lung cancer. *Proc Am Thorac Soc*. 2009 Apr 15;6(2):201-5.
247. Aronsohn, M.S., Brown, H.M., Hauptman, G., Kornberg, L.J. Expression of focal adhesion kinase and phosphorylated focal adhesion kinase in squamous cellcarcinoma of the larynx. *Laryngoscope*. 2003;113:1944-1948.

APPENDIX

Chapter 9. Appendix**Appendix 9.1 Table 1. CRC cell lines and their characteristics.**

Cell line	Age	Sex	Duck Stage	Differentiation	Site
C106	78	F	A	Moderate	Lower Rectum
C125	66	F	A	Moderate	Colon
C32	64	F	C	Well	Colon
C80	69	M	C	Poor	Rectum
C84	67	M	C	Poor	Caecum
Caco2	72	M	A	Well	Colon
COLO201	70	M	D	Poor	Colon-Ascites
COLO205	70	M	D	Poor	Colon-Ascites
COLO320DM	55	F	C	Moderate	Sigmoid Colon
DLD1	70	M	C	Moderate	Colon
GP2D	71	F	B	Poor	Recurrence Colon
HCA46	53	F	C	Poor	Sigmoid Colon
HCA7	58	F	B	Moderate	Hepatic Flexur
HCT116	64	M	D	Well	Colon
HRA-19	66	F	B	Well	Colon
HT29	44	F	A	Moderate	Colon
HT55	54	F	C	Moderate	Rectum
HuTu80	53	M	A	Well	Duodenum
LoVo	56	M	D	Poor	Colon, distant lymph node
LS1034	54	M	C	Poor	Caecum
RKO	64	F	C	Moderate	Colon
SW1116	73	M	A	Moderate	Colon
SW1222	44	M	C	Moderate	Colon
SW480	50	M	B	Moderate	Colon
SW620	51	M	C	Moderate	Colon lymph node
SW837	53	M	B	Well	Rectum
SW948	81	F	C	Moderate	Colon
VACO10MS	72	F	D	Moderate	Colon Omentum
VACO5	78	F	C	Poor	Caecum

Appendix 9.2



Appendix 9.3

Table 3. BC patient and tumour characteristics (n = 1,409)

Parameter	Number (%)
Age	
<40	40 (5)
40-50	600 (39)
51-60	346 (25)
>60	410 (31)
Tumour size	
<1.5 cm	530 (35)
>1.5 cm	760 (65)
LN stage	
1 (negative)	461 (28)
2 (1-3 LN)	558 (39)
3 (>3 LN)	472 (33)
Grade	
1	448 (31)
2	316 (21)
3	625 (48)
NPI	
Poor	296 (14)
Moderate	877 (54)
Good	316 (32)
DM	
Negative	796 (59)
Positive	694 (41)
Recurrence	
Negative	603 (42)
Positive	788 (58)
Vascular invasion	
Negative	
Positive	571 (39)
	828 (61)

Appendix 9.4

Table 4. CRC patient and tumour characteristics (n = 462)

Parameter	Category	Number (%)
Age (years)	Median	72
	Range	57-89
Sex	Male	257 (57%)
	Female	192 (43%)
Status	Alive	167 (37%)
	Dead (cancer related)	221 (49%)
	Dead (unrelated causes)	60 (13%)
	Unknown	1
Histological type	Adenocarcinoma	382 (85%)
	Mucinous adenocarcinoma	49 (11%)
	Columnar adenocarcinoma	4 (1%)
	Signet ring mucinous adenocarcinoma	6 (1%)
	Unknown	8 (2%)
Histological grade	Well differentiated	28 (6%)
	Moderately differentiated	345 (77%)
	Poorly differentiated	67 (15%)
	Unknown	9 (2%)
Tumour site	Colon	230 (52%)
	Rectal	177 (39%)
	Unknown	42 (9%)
Duke's stage	A	66 (15%)
	B	175 (39%)
	C1	133 (30%)
	C2	20 (4%)
	D	52 (11%)
	Unknown	3 (1%)
TNM stage	0 (T _{is})	3 (1%)
	1	67 (15%)
	2	172 (38%)
	3	149 (33%)
	4	51 (11%)
	Unknown	7 (2%)
Extramural vascular invasion	Negative	219 (49%)
	Positive	121 (27%)
	Unknown	109 (24%)

Appendix 9.5 Sequencing of pCR2.1-HPRT plasmid. Sequencing results confirmed the presence of HPRT insert in pCR2.1

pCR2.1-HPRT M13 Reverse

